PB86-174018

BARRIERS IN CONSTRUCTION ZONES
VOLUME 3

U.S. Department of Transportation
Federal Highway Administration

Research, Development, and Technology
Turner-Fairbank Highway Research Center
6300 Georgetown Pike
McLean, Virginia 22101

Report No.
FHWA/RD-86/094

Final Report
April 1986

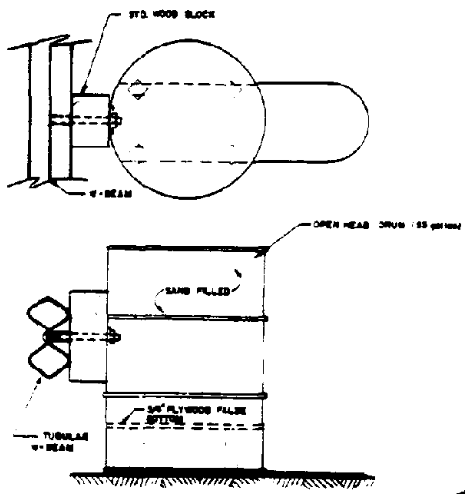

TEXAS TRANSPORTATION INSTITUTE

BARRIERS IN CONSTRUCTION ZONES

Volume 3: Appendices B, C, D, E and F

Theoretical and Economic Analysis

Prepared for
Contract DOT-FH-11-9458
Office of Research

Federal Highway Administration

U. S. Department of Transportation

Appendix B
by
Don L. Ivey

Appendix C
by
Kenneth C. Walker
and
H. E. Ross, Jr.

Appendix D
by
W. Lynn Beason

Appendix E
by
Roger J. Koppa

Appendix F
by
Project Staff

Texas A&M Research Foundation

Texas Transportation Institute

The Texas A&M University System

April 1985

METRIC CONVERSION FACTORS

APPROXIMATE CONVERSIONS FROM METRIC MEASURES

SYMBOL	WHEN YOU KNOW	MULTIPLY BY	TO FIND	SYMBOL
	LENGTH			
in	inches	2.5	centimeters	cm
ft	feet	30	centimeters	cm
yd	yards	0.9	meters	m
mi	miles	1.6	kilometers	km
	AREA			
in^2	square inches	6.5	square centimeters	cm^2
ft^2	square feet	0.09	square meters	m^2
yd^2	square yards	0.6	square meters	m^2
mi^2	square miles	2.6	square kilometers	km^2
	acres	0.4	hectares	ha
	MASS (weight)			
oz	ounces	28	grams	g
lb	pounds	0.45	kilograms	kg
	short tons (2000 lb)	0.9	tonnes	t
	VOLUME			
tsp	teaspoons	5	milliliters	ml
tbsp	tablespoons	15	milliliters	ml
fl oz	fluid ounces	30	milliliters	ml
c	cups	0.24	liters	l
pt	pints	0.47	liters	l
qt	quarts	0.95	liters	l
gal	gallons	3.8	liters	l
ft^3	cubic feet	0.03	cubic meters	m^3
yd^3	cubic yards	0.76	cubic meters	m^3
	TEMPERATURE (exact)			
°F	Fahrenheit temperature	5/9 (after subtracting 32)	Celsius temperature	°C

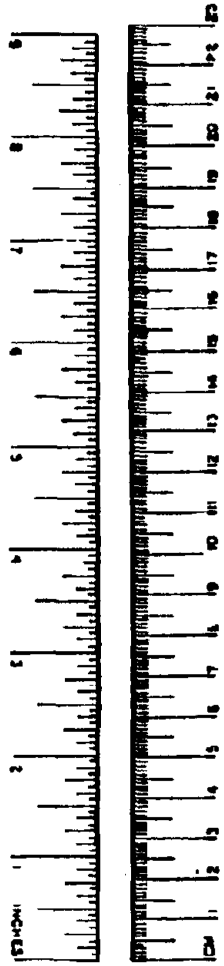

APPROXIMATE CONVERSIONS FROM METRIC MEASURES

SYMBOL	WHEN YOU KNOW	MULTIPLY BY	TO FIND	SYMBOL
	LENGTH			
mm	millimeters	0.04	inches	in
cm	centimeters	0.4	inches	in
m	meters	3.3	feet	ft
m	meters	1.1	yards	yd
km	kilometers	0.6	miles	mi
	AREA			
cm^2	square centimeters	0.16	square inches	in^2
m^2	square meters	1.2	square yards	yd^2
km^2	square kilometers	0.4	square miles	mi^2
ha	hectares (10,000 m^2)	2.5	acres	
	MASS (weight)			
g	grams	0.035	ounces	oz
kg	kilograms	2.2	pounds	lb
t	tonnes (1000 kg)	1.1	short tons	
	VOLUME			
ml	milliliters	0.03	fluid ounces	fl oz
l	liters	2.1	pints	pt
l	liters	1.06	quarts	qt
l	liters	0.26	gallons	gal
m^3	cubic meters	36	cubic feet	ft^3
m^3	cubic meters	1.3	cubic yards	yd^3
	TEMPERATURE (exact)			
°C	Celsius temperature	9/5 (then add 32)	Fahrenheit temperature	°F

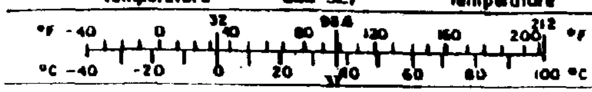

TABLE OF CONTENTS

LIST OF FIGURES

LIST OF TABLES

BARRIERS IN CONSTRUCTION ZONES

APPENDIX B

Simplified Energy Analysis

Prepared for
Contract DOT-FH-11-9458
Office of Research

Federal Highway Administration

U. S. Department of Transportation

by

Don L. Ivey
Research Engineer

Texas A&M Research Foundation

Texas Transportation Institute

The Texas A&M University System

April 1985

Energy Analysis of CMB

A portable CMB subjected to a vehicle impact at or near one of the joints between segments can be analyzed using the energy method. The analysis is subject to a number of simplifying assumptions. The positions of barrier segments before and after vehicle impact are shown in Figure 1 from an overhead view.

The major simplifying assumptions are:

- Only two segments of the barrier move.
- The amount of vehicle kinetic energy associated with the lateral component of vehicle velocity is expended in work on the barrier and the vehicle.
- The complex development of moment in a barrier joint can be approximated as shown in Figure 2.
- Static and sliding friction between the barrier base and the support media can be approximated as shown by Figure 3.
- The work done in deforming vehicle structure can be approximated by the equation derived from Figure 4.

The basic energy balance equation to be used is

$$E_\ell = Em_t + E_\mu + E_c \tag{1}$$

where

E_ℓ = that amount of kinetic energy associated with the lateral component of vehicle velocity, kip-ft. If one assumes that the vehicle velocity component parallel to the barrier is not affected by the impact then E_ℓ represents the change in vehicle kinetic energy due to the impact period between first contact and the time when the vehicle is parallel to the barrier.

Em_t = the total of Em_1, Em_2, and Em_3, the total work done in rotating barrier joints, kip-ft.

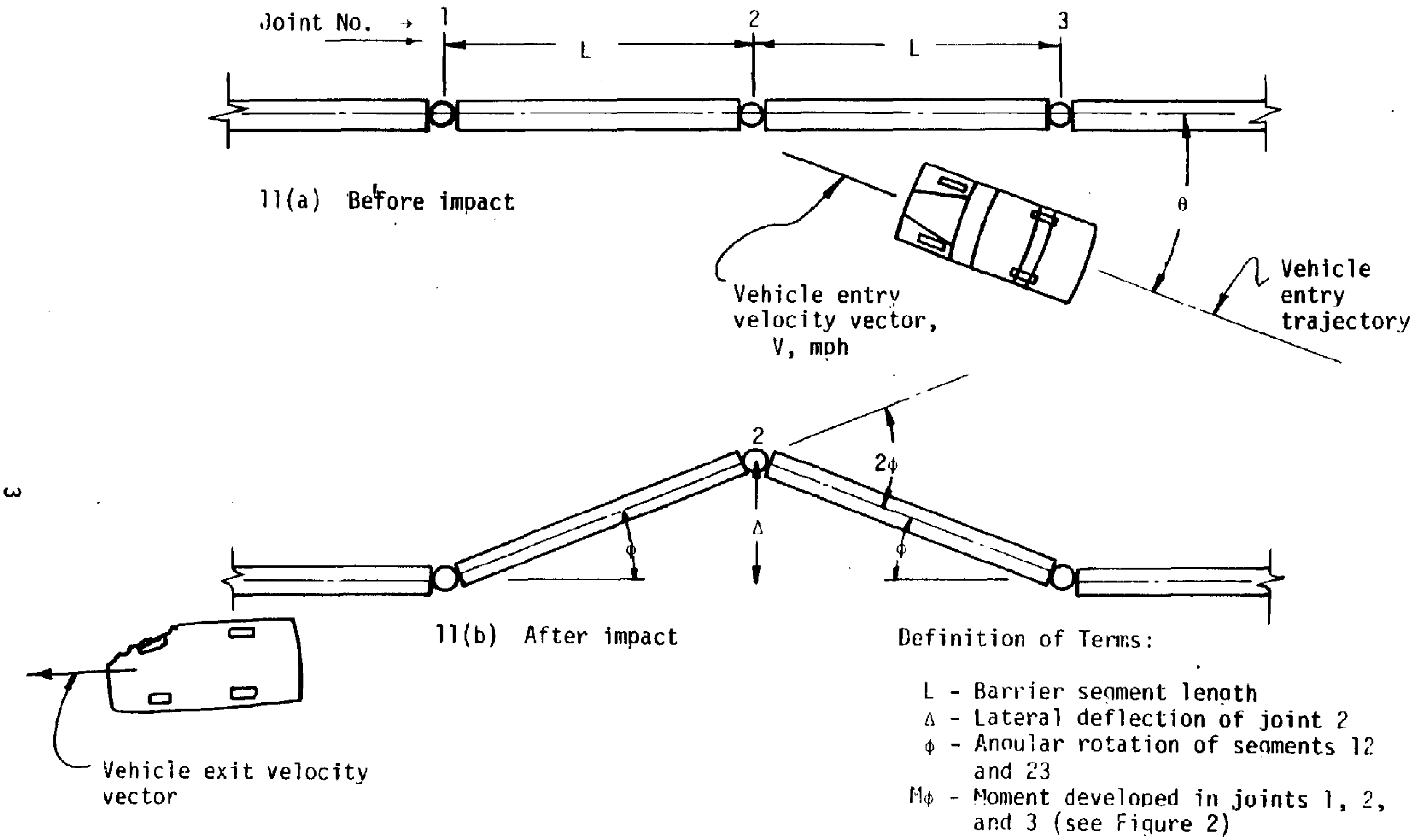

Figure 1. Idealized barrier segment positions before and after impact.

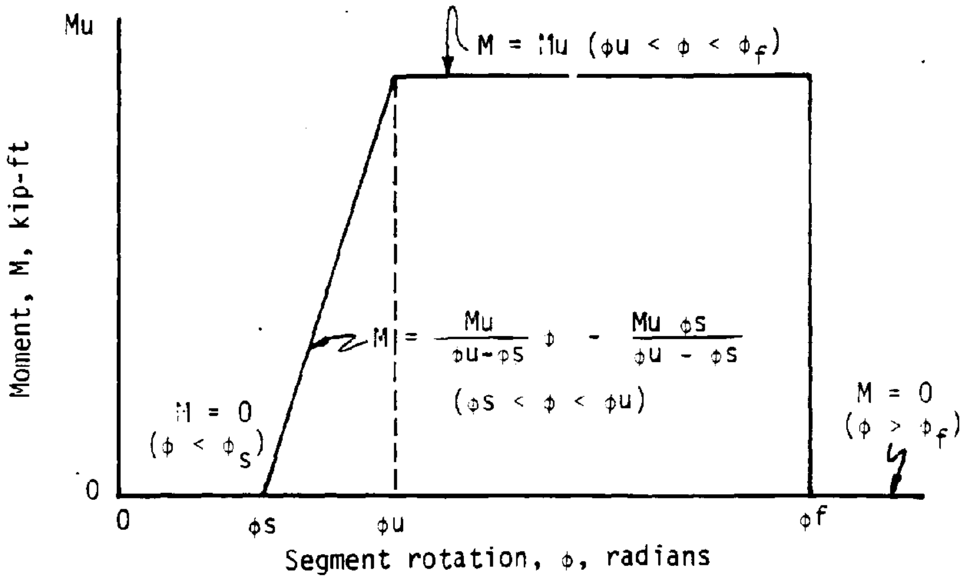

Figure 2. Joint moment as a function of rotation.

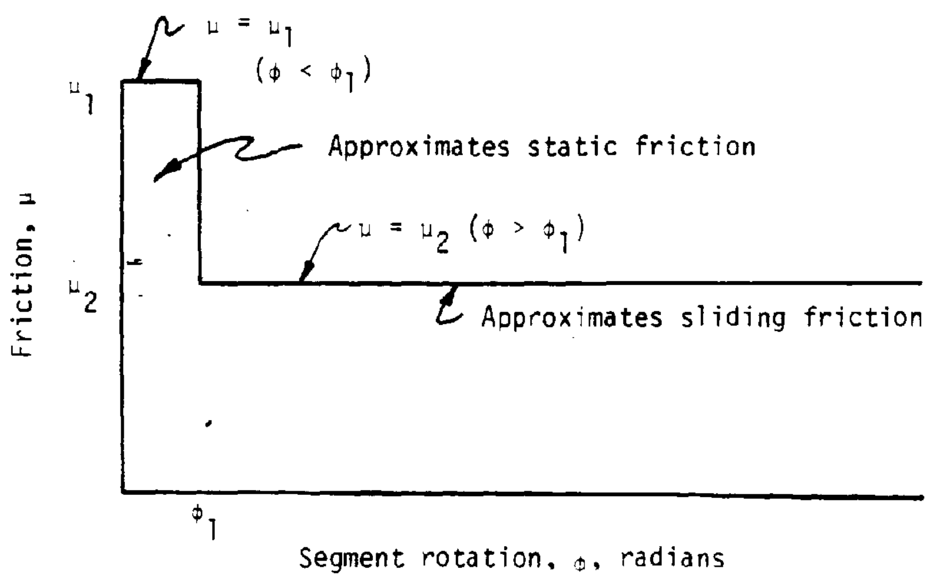

Figure 3. Barrier-support media friction as a function of barrier segment rotation, ϕ.

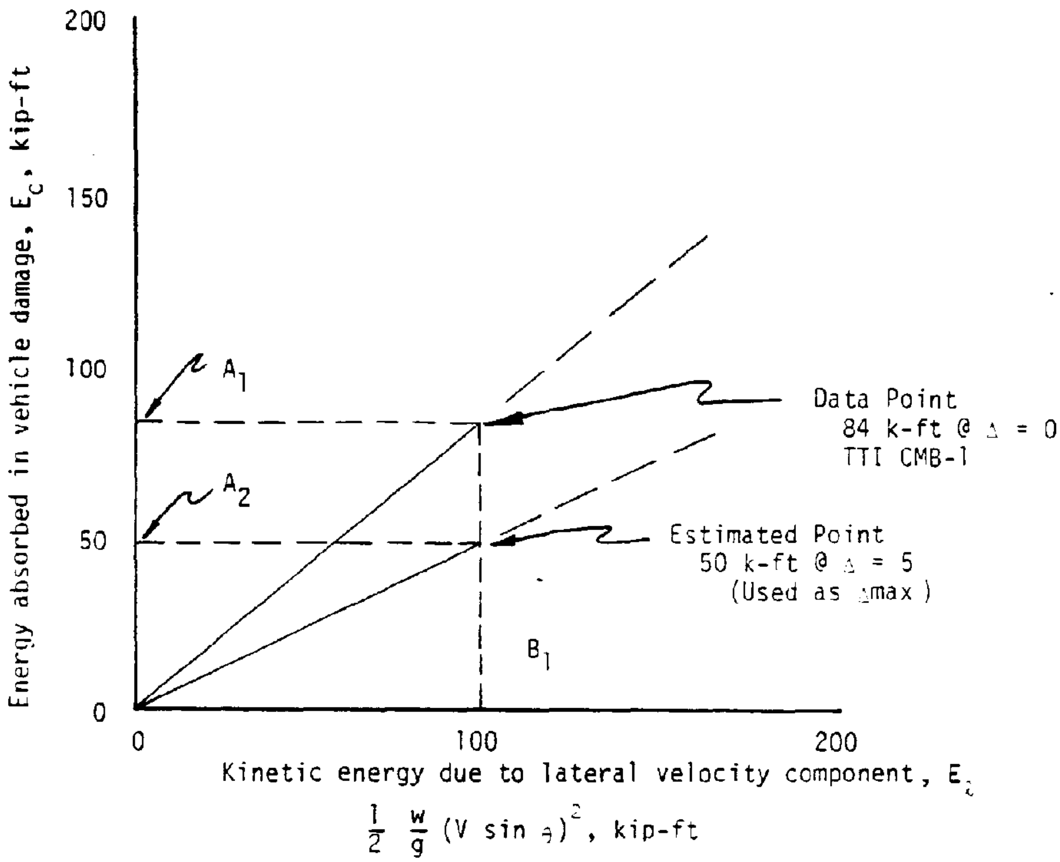

Note:

$$E_{c_{\Delta=0}} = \frac{A_1}{B_1} E_\ell$$

$$E_{c_{\Delta=\Delta max}} = \frac{A_2}{B_1} E_\ell$$

$$E_{c_\Delta} = \frac{A_\Delta}{B_1} E_\ell \qquad (1)$$

Now A_Δ can be proportioned from A_2 to A_1 for different levels of deflection by the equation

$$A_\Delta = A_1 - (A_1 - A_2)\,\frac{\Delta}{\Delta max} \qquad (2)$$

and

$$\Delta = L \sin \theta \qquad (3)$$

By substituting A_Δ and Δ into equation (1) we find

$$E_c = \frac{\left(A_1 - \frac{(A_1 - A_2)}{\Delta max} L \sin \theta\right) \quad E_\ell}{B_1}$$

Figure 4. Illustration of estimating work done in deforming vehicle structure.

$E\mu$ = the work done in sliding two barrier segments through the angle ϕ, kip-ft.

E_c = the work done in deforming the vehicle structure during impact, kip-ft. (See Figure 4)

Note, $$Em_t = Em_1 + Em_2 + Em_3 \tag{2}$$

where

Em_1 = the work done in rotating joint 1 through the angle ϕ, kip-ft. (See Figure 2)

Em_2 = the work done in rotating joint 2 through the angle 2ϕ, kip-ft. (See Figure 2)

Em_3 = the work done in rotating joint 3 through the angle ϕ, kip-ft. (See Figure 2)

The values of Em_1 and Em_2 can be determined from the following integrals (or numerically from Figure 2).

$$Em_1 = \int_0^{\phi} M \, d\phi \, , \; Em_2 = \int_0^{2\phi} M \, d\phi \, , \; Em_3 = \int_0^{\phi} M \, d\phi \tag{3}$$

From Figure 1 it is seen that joints 1 and 3 go through an angular deformation of ϕ while joint 2 goes through 2ϕ.

ϕ = the maximum rotation due to impact of segment 1-2 and 2-3.

M = the moment developed by a joint when subjected to an angular deformation of ϕ.

The work done in sliding the barrier segments can be computed by multiplying barrier segment weight by the amount of friction developed in any interval of sliding movement and summing all these differential portions of work. This value is approximated by Equation 4, which can be solved numerically by referring to Figure 3.

$$E\mu = Wi \, L^2 \int_0^{\phi} \mu \, d\phi \tag{4}$$

where

Wi = the weight per unit length of the barrier, kip-ft.

μ = the coefficient of friction associated with any movement of the barrier (See Figure 3), dimensionless.

L = the length of a barrier segment, ft.

The work done in deforming the automobile structure, E_c, is approximated by Equation 5.

$$E_c = \frac{E\ell}{B_1} \left(A_1 - \frac{(A_1 - A_2)\, L \sin \phi}{\Delta \max} \right) \qquad (5)$$

where

A_1 = constant used in determining Ec, kip-ft. (See Figure 4)

A_2 = constant used in determing Ec, kip-ft. (See Figure 4)

B_1 = constant used in determining Ec, kip-ft. (See Figure 4)

Δ max = maximum functional barrier deflection, ft. (This is simply the maximum deflection that can be produced and the barrier still be considered to be geometrically continuous. It is taken to be five feet.

Wi = weight per unit length of barrier, kip-ft

L = barrier segment length, ft.

ϕ = the angular movement of one of the two moving barrier segments, radians.

By substituting the values of Em_t, $E\mu$ and Ec into Equation 1 the following equation results:

$$E\ell = \frac{2 \int_0^{\phi} M \, d\phi + \int_0^{2\phi} M \, d\phi + W_i L^2 \int_0^{\phi} \mu \, d\phi}{1 - \frac{1}{B_1} \left(A_1 - \frac{(A_1 - A_2)\, L \sin \phi}{\Delta \max} \right)} \qquad (6)$$

The control value of $E\ell$ is calculated from the equation

$$E\ell = \frac{1}{2} \frac{W}{g} (V \sin \theta)^2 \qquad (7)$$

where

W = vehicle weight, kips

g = acceleration of gravity, ft/sec^2

v = vehicle velocity, ft/sec

and θ = vehicle impact angle, degrees

The solution of Equation 6 can be quickly achieved by the method of finite differences; assuming a value of ϕ, calculating the value of the right side of the equation and comparing the calculated value with the known value of $E\ell$ from Equation 7 as shown in Figure 5. If $E\ell$ from Equation 6 is greater than $E\ell$ from Equation 7 the value of ϕ is too large. Therefore, a smaller value should be estimated and the procedure repeated. If $E\ell$ (Eq. 6) is less than $E\ell$ (Eq. 7) the value of ϕ is too small and a larger value should be chosen for the next trial. The correct value of ϕ (i.e. the one necessary to balance the equation) will be defined within 1% accuracy within ten interations if a reasonable first estimate of ϕ is chosen.

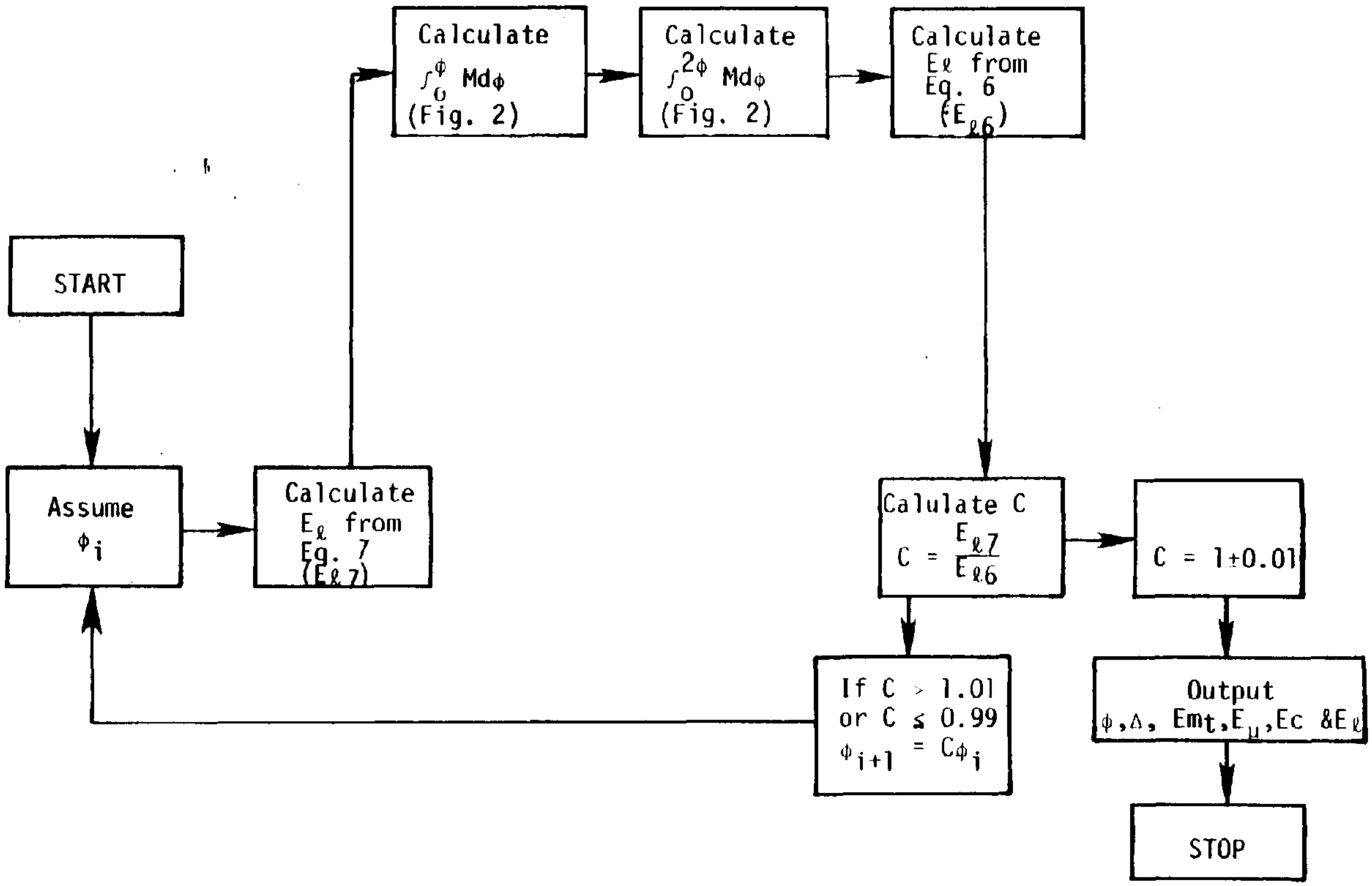

Figure 5. Flow diagram to solve Equation 6.

NOTATION

C_r - Rotational friction force reduction coefficient

C_t - Translational friction force reduction coefficient

F_{fx_i} - Friction force in X_i direction on segment i

F_{fy_i} - Friction force in Y_i direction on segment i

F_{sk} - Generalized force due to potential in k-th direction

$F_{X'}$ - External applied force in X' direction

$F_{Y'}$ - External applied force in Y' direction

K_e - Elastic spring stiffness

K_l - Spring stiffness in lock-up

K_p - Plastic spring stiffness

L_i - Length of segment i

M_{fi} - Mass of segment i

M_i - Moment due to friction forces on segment i

M_u - Spring force (moment) due to deformation

n - Number of segments in system

Q_{ek} - Generalized force due to applied loads

Q_{fk} - Generalized force due to applied friction

Q_{frk} - Generalized force due to rotational friction

Q_{ftk} - Generalized force due to translational friction

Q_k - Sum of generalized forces acting in k-th direction

q_k - Generalized displacement

$\dot{q}_k$ - Generalized velocity

$\ddot{q}_k$ - Generalized acceleration

R_{Fi} - Resultant friction force on segment i

$\dot{R}_i$ - Resultant velocity on segment i

r_{XAi} - Local coordinate of point of external force application for segment i

t - Time

U - Kinetic energy

V - Potential energy

W_i - Weight of segment i

X', Y' - Global coordinate axes

X_i, Y_i - Local coordinate axes for segment i

X'_{Ai}, Y'_{Ai} - Global coordinates for location of external force application

X'_F - Global location where external force is applied

X'_i, Y'_i - Global coordinates of segment i center of mass

$\dot{X}'_i$, $\dot{Y}'_i$ - Global velocity of segment i center of mass

X'_{iR} - Global coordinate of reference end of segment of which external force is applied

X'_{iT} - Global coordinate of terminal end of segment on which external force is applied

X'_R, Y'_R - Global coordinates of reference end of barrier system

$\Delta\phi_i$ - Differential rotation of spring i

δ_{q_k} - Generalized virtual displacement

δW - Virtual work

$\delta X'_{Ai}$ - Virtual displacement of external force in the X' direction

$\delta Y'_{Ai}$ - Virtual displacement of external force in the Y' direction

$\dot{\varepsilon}_R$ - Rotational velocity check for friction adjustment

$\dot{\varepsilon}_T$ - Translational velocity check for friction adjustment

μ_i - Friction coefficient for segment i

ρ_i - Distance from reference end to center of mass for segment i

ϕ_e - End of elastic deformation in joint spring

ϕ_f - Failure deformation in spring

ϕ_i - Rotation of segment i

$\dot{\phi}_i$ - Rotational velocity of segment i

ϕ_p - End of plastic range for deformation in joint spring

ϕ_s - Rotational slack in joint spring

ω_i - Rotational velocity of segment i

DEVELOPMENT OF SIMULATION PROGRAM

System Characterization

A free-standing, segmental concrete median barrier (CMB) system can be modeled as a series of "n" articulated rigid segments. The geometry is defined in the global coordinate system with the X' and Y' axes. The i-th segment has its own local coordinate system given by the X_i and Y_i axes. Each link is characterized by four variables: length, L_i; distance from reference end to the center of mass, ρ_i; mass of segment, M_i; and friction coefficient with the roadway, μ_i. The spatial relationship is defined by the generalized coordinates given in the global system. These are: the distance from the global origin to the reference end of segment 1, X_R', and Y_R'; and the global rotational angle of each segment, ϕ_1 to ϕ_n. This gives n+2 degrees of freedom. The idealized model is shown in Figure 6.

Segment Center of Mass Location

The relationship between segment fixed coordinates (X_i, Y_i) and space-fixed coordinates (X',Y') is given as:

$$X' = X_i \operatorname{Cos}\phi_i - Y_i \operatorname{Sin}\phi_i; \text{ and} \quad \ldots \ldots \quad (8)$$

$$Y' = X_i \operatorname{Sin}\phi_i - Y_i \operatorname{Cos}\phi_i \quad \ldots \ldots \quad (9)$$

The equivalent matrix form is

$$\begin{Bmatrix} X' \\ Y' \end{Bmatrix} = \begin{bmatrix} T^i \end{bmatrix} \begin{Bmatrix} X_i \\ Y_i \end{Bmatrix} \quad \ldots \ldots \quad (10)$$

where

$$\begin{bmatrix} T^i \end{bmatrix} = \begin{bmatrix} \operatorname{Cos}\phi_i & -\operatorname{Sin}\phi_i \\ \operatorname{Sin}\phi_i & \operatorname{Cos}\phi_i \end{bmatrix} \quad \ldots \ldots \quad (11)$$

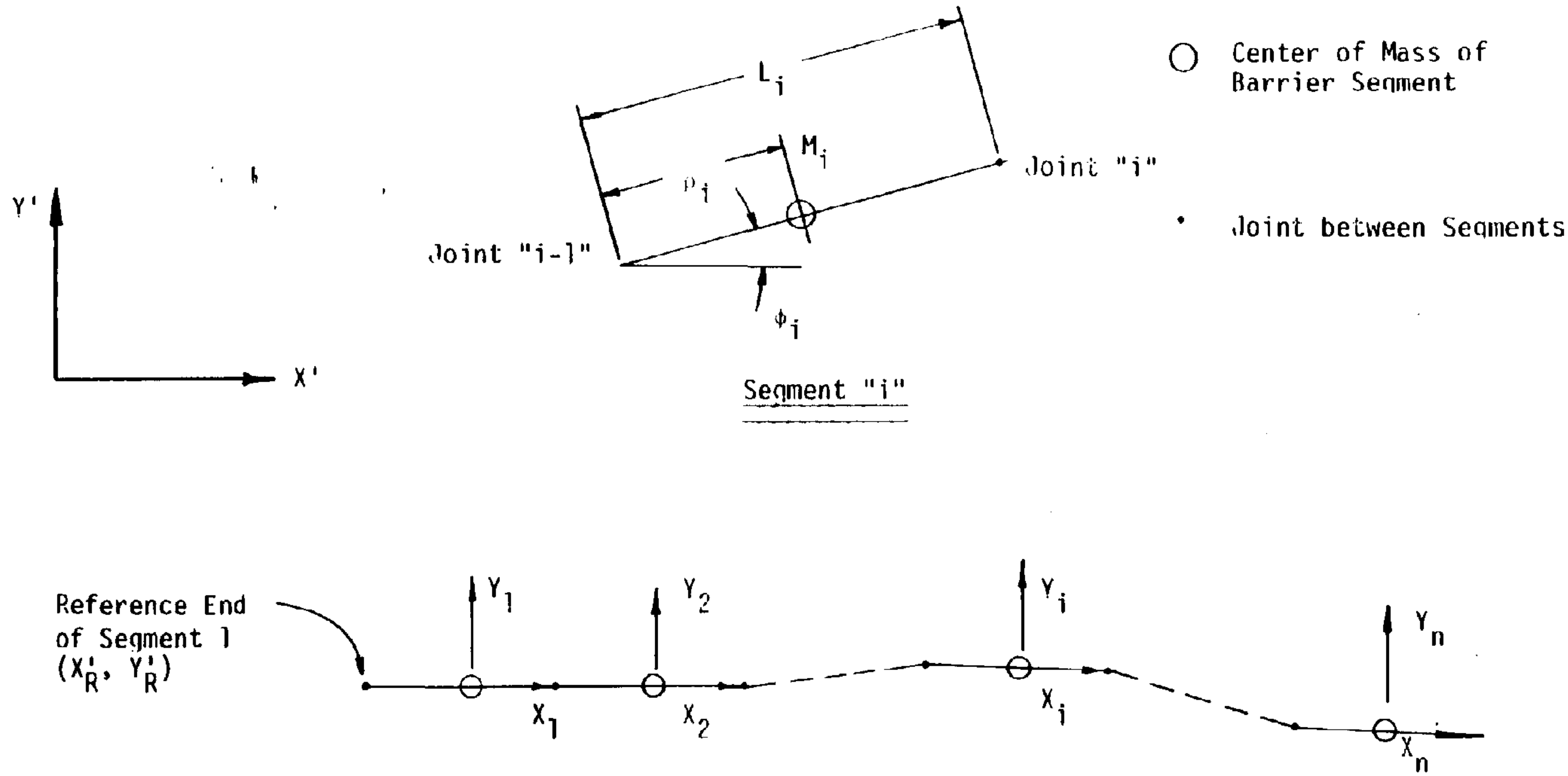

Figure 6. Idealized Model of CMB System.

It can be shown that the transformation matrix $[T]$ is an orthagonal matrix in which its inverse is identical to its transpose, and matrix multiplication of the two, $[T^i][T^i]^T = [I]$ is the identity matrix. Solving for the segment-fixed coordinates in terms of the space-fixed coordinates,

$$\begin{Bmatrix} X_i \\ Y_i \end{Bmatrix} = \begin{bmatrix} T_i \end{bmatrix}^T \begin{Bmatrix} X' \\ Y' \end{Bmatrix} \quad \ldots\ldots\ldots\ldots \quad (12)$$

The position of the center of mass of segment can be defined as

$$\begin{Bmatrix} X_1' \\ Y_1' \end{Bmatrix} = \begin{Bmatrix} X_R' \\ Y_R' \end{Bmatrix} + \begin{bmatrix} T^1 \end{bmatrix} \begin{Bmatrix} \rho_1 \\ 0 \end{Bmatrix} \quad \ldots\ldots\ldots \quad (13)$$

The position of segment 2 can be written as

$$\begin{Bmatrix} X_2' \\ Y_2' \end{Bmatrix} = \begin{Bmatrix} X_R' \\ Y_R' \end{Bmatrix} + \begin{bmatrix} T^1 \end{bmatrix} \begin{Bmatrix} L_1 \\ 0 \end{Bmatrix} + \begin{bmatrix} T^2 \end{bmatrix} \begin{Bmatrix} \rho_2 \\ 0 \end{Bmatrix} \quad \ldots\ldots\ldots \quad (14)$$

This can be generalized for any segment "i" (except for i=1) as

$$\begin{matrix} X_i' \\ Y_i' \end{matrix} = \begin{Bmatrix} X_R' \\ Y_R' \end{Bmatrix} + \sum_{j=1}^{i-1} \begin{bmatrix} T^j \end{bmatrix} \begin{Bmatrix} L_j \\ 0 \end{Bmatrix} + \begin{bmatrix} T^i \end{bmatrix} \begin{Bmatrix} \rho_i \\ 0 \end{Bmatrix} \quad \ldots\ldots \quad (15)$$

or in an expanded form

$$X_i' = X_R' + \sum_{j=1}^{i-1} T_{11}^j L_j + T_{11}^i \rho_i \quad \ldots\ldots\ldots\ldots \quad (16)$$

$$Y_i' = Y_R' + \sum_{j=1}^{i-1} T_{21}^j L_j + T_{21}^i \rho_i \quad \ldots\ldots\ldots\ldots \quad (17)$$

where $T^{i}_{11} = \text{Cos}\phi_i$ and $T^{i}_{21} = \text{Sin}\phi_i$

<u>Segment Center of Mass Velocity</u>

To get the global velocities of each center of mass, the time derivative of each term must be taken. For the first segment this gives

$$\dot{X}'_1 = \dot{X}'_{12} + \frac{\partial T'_{11}}{\partial \phi_1} \dot{\phi}_1 \rho_1 \quad \dots\dots\dots\dots\dots\dots \quad (18)$$

$$\dot{Y}'_1 = \dot{Y}'_{12} + \frac{\partial T'_{21}}{\partial \phi} \dot{\phi}_1 \rho_1 \quad \dots\dots\dots\dots\dots\dots \quad (19)$$

The velocity of the i-th segment of the remaining "n-1" segments is given by :

$$\dot{X}'_i = \dot{X}'_R + \sum_{j=1}^{i-1} \frac{\partial T^{j}_{11}}{\partial \phi_j} \dot{\phi}_j L_j + \frac{\partial T^{i}_{11}}{\partial \phi_i} \dot{\phi}_i \rho_i \quad \dots\dots\dots\dots \quad (20)$$

$$\dot{Y}'_i = \dot{Y}'_R + \sum_{j=1}^{i-1} \frac{\partial T^{i}_{21}}{\partial \phi_j} \dot{\phi}_j L_j + \frac{\partial T^{i}_{21}}{\partial \phi_i} \dot{\phi}_i \rho_i \quad \dots\dots\dots\dots \quad (21)$$

and the squared terms are

$$\left[\dot{X}'_i\right]^2 = \left[\dot{X}'_R + \sum_{j=1}^{i-1} \frac{\partial T^{j}_{11}}{\partial \phi_j} \dot{\phi}_j L_j + \frac{\partial T^{i}_{11}}{\partial \phi_i} \dot{\phi}_i \rho_i\right]^2 \quad \dots\dots\dots \quad (22)$$

$$\left[\dot{Y}'_i\right]^2 = \left[\dot{Y}'_R + \sum_{j=1}^{i-1} \frac{\partial T^{j}_{21}}{\partial \phi_j} \dot{\phi}_j L_j + \frac{\partial T^{i}_{21}}{\partial \phi_i} \dot{\phi}_i \rho_i\right]^2 \quad \dots\dots\dots \quad (23)$$

Segment Angular Velocities

The angular velocity of segment "i" (ω_i) is expressed as the time derivative of that segment's rotational displacement (ϕ_i). Therefore

$$\omega_i = \dot{\phi}_i \qquad (24)$$

and

$$(\omega_i)^2 = (\dot{\phi}_i)^2 \qquad (25)$$

LaGrange's Equation

The motion of this system of discrete masses can be described by LaGrange's equation. It is given as

$$\frac{\partial U}{\partial \dot{q}_k} - \frac{\partial U}{\partial q_k} + \frac{\partial V}{\partial q_k} = Q_k \qquad (26)$$

where t = time, U = kinetic energy of the system, V = potential energy of the system; q_k = generalized coordinate, $\dot{q}_k$ = generalized velocity, Q_k = generalized forces acting on the system not derivable from potential functions, and k = 1, 1 . . . n+2, for the generalized problem.

The generalized force on the right-hand side can be defined as

$$Q_k = Q_{e_k} + Q_{f_k} \qquad (27)$$

in which Q_{e_k} = generalized force from externally applied loads (vehicle loads), and Q_{f_k} = generalized force due to the Coulomb damping friction force at barrier-roadway interface.

In this problem, the potential energy of the system, V, is derived from the spring forces (actually end moments) due to relative rotations between two segments. The potential energy due to position is assumed to be zero. For convenience let

$$F_{s_k} = - \frac{\partial V}{\partial q_k} \quad \ldots\ldots\ldots\ldots\ldots \quad (28)$$

where F_{s_k} = generalized force due to strain energy.

By substituting Eqs. 27 and 28 into Eq. 26 and rearranging gives:

$$\frac{\partial U}{\partial \dot{q}_k} - \frac{\partial U}{\partial q_k} = F_{s_k} + Q_{e_k} + Q_{f_k} \quad \ldots\ldots\ldots\ldots \quad (29)$$

If there are "n" segments, there will be a set of "n+2" second order, coupled nonlinear differential equations. For convenience, the above equation can be written in matrix form as follows:

$$[D]\left\{\ddot{q}\right\} = \left\{E\right\} + \left\{F_s\right\} + \left\{Q_e\right\} + \left\{Q_f\right\} \quad \ldots\ldots\ldots \quad (30)$$

Matrix [D] contains all of the coefficients of the generalized accelerations and $\left\{E\right\}$ is a column vector containing the negative of all remaining terms from the left-hand side of Eq. 29.

Contributions of Kinetic Energy to Equations of Motion

The kinetic energy of a system of "n" particles is given by:

$$U = \frac{1}{2} \sum_{i=1}^{n} M_i \left[(\dot{X}_i')^2 + (\dot{Y}_i')^2 \right] + \frac{1}{2} \sum_{i=1}^{n} I_i \, \omega_i^2 \quad \ldots\ldots \quad (31)$$

where M_i = mass of segment i; I_i = mass moment of inertia of segment i about the Z_i axis; $(X_i')^2$ = square of i-th segment translational velocity in X' direction; $(Y_i')^2$ = square of i-th segment translational velocity n Y' direction; and ω_i^2 = square of i-th segment rotational velocity.

Equations 22 and 23 define $(\dot{X}_i)^2$ and $(\dot{Y}_i')^2$ and Eq. 25 gives the value of $(\omega_i)^2$. These expressions can be substituted into Eq. 26 to give the general formula for the total kinetic energy of the system. The result is

$$U = \frac{1}{2} \sum_{i=1}^{n} M_i \left\{ \left[\dot{X}_r' + \sum_{j=1}^{i-1} \frac{\partial T_{11}^j}{\partial \phi_j} \dot{\phi}_j L_j + \frac{\partial T_{11}^i}{\partial \phi_i} \dot{\phi}_i \rho_i \right]^2 + \left[\dot{Y}_r' + \sum_{j=1}^{i-1} \frac{\partial T_{21}^i}{\partial \phi_j} \dot{\phi}_j L_j + \frac{\partial T_{21}^i}{\partial \phi_i} \dot{\phi}_i \rho_i \right]^2 \right\}$$

$$+ \frac{1}{2} \sum_{i=1}^{n} I_i \, (\dot{\phi}_i)^2 \quad \ldots\ldots\ldots\ldots \quad (32)$$

By taking the derivative of this equation first with respect to each of the generalized velocities and then with respect to time, a set of "n+2" equations with functions of the generalized displacements, velocities, and accelerations will be generated. After separating the terms that include a generalized acceleration and factoring out the coefficients, a set of equations to calculate the [D] matrix will remain. The results of this expansion is summarized in EQUATIONS OF MOTION.

Next, the derivative of the kinetic energy expression with respect to the generalized displacements is taken. These terms are then added to the remaining terms from the previous step. After reversing each of their algebraic signs, there are the "n+2" equations that make up the

$\{E\}$ vector. The complete set of equations is given in EQUATIONS OF MOTION.

Contributions of Potential Energy to Equations of Motion

Each joint of this model is designed to have five regions of spring response. The first region is a slack region in which there is no moment developed due to spring deformation. There is no energy associated with this deflection. In the second range, the moment generated is proportional to the relative rotation minus some value of maximum slack rotation. This stored energy is completely recoverable by the spring. A plastic region of deformation is next, where there is little or no increase in joint moment due to additional deformation of the spring. Only a small amount of this energy can be returned to the system in elastic rebound of the spring. The fourth characteristic zone is one of lock-up, where a large increase in joint moment occurs with a very small increase in differential rotation. None of this energy can be regained. The final region is one of spring failure, in which the moment capacity falls to and remains at zero. Once this occurs all stored energy is lost. The relationship of each of these characteristic regions is shown in Figure 7.

At each joint the differential rotation will be the difference in angular rotation between segment "i" and segment "i+1".

$$\Delta\phi_i = \phi_{i+1} - \phi_i \quad \ldots\ldots\ldots\ldots\ldots\ldots \quad (33)$$

The potential energy of any one spring is defined as

$$V_i = \int_0^{\Delta\phi} Mu(\Delta\phi)d(\Delta\phi) \quad \ldots\ldots\ldots\ldots\ldots \quad (34)$$

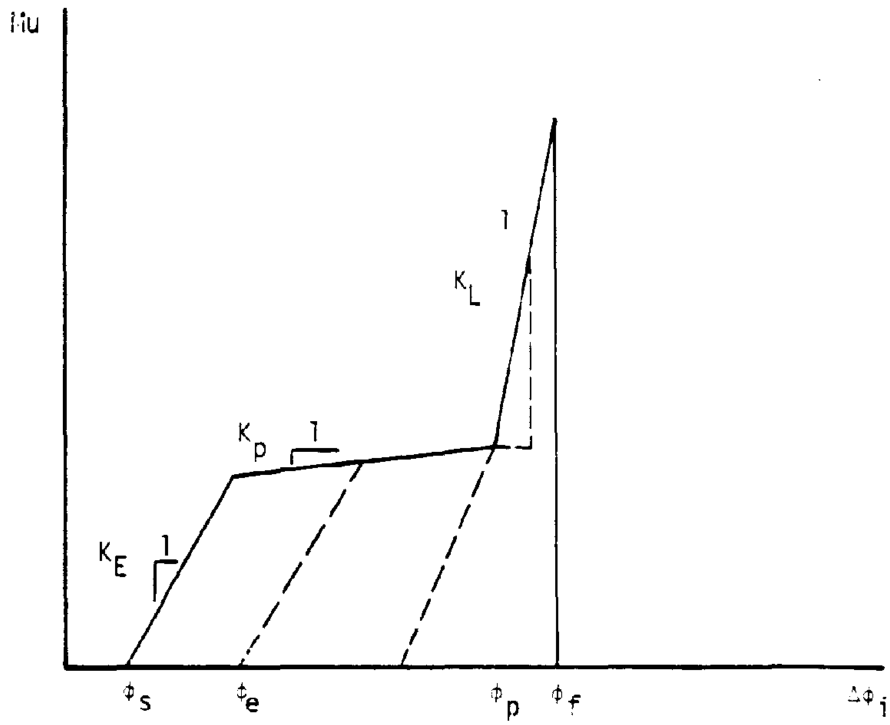

NOTE: Dashed lines show unloading direction for plastic and lockup ranges.

Figure 7. Joint Spring Moment-Differential Rotation Relationship.

which can be expanded using the relationship of Eq. 33.

$$V_i = \int_0^{\phi_{1+i}} Mu(\Delta i)\, d(\phi_{i+1}) - \int_0^{\phi_i} Mu(\Delta\phi_i)\, d\phi_i \quad . \; . \; . \; . \; . \; . \quad (35)$$

If the individual contributions are summed over the "n-1" possible springs, the total potential energy can be expressed as:

$$V = \sum_{i=1}^{n-1} \left[\int_0^{\phi_{i+1}} Mu(\Delta\phi_i)\, d(\phi_{i+1}) - \int_0^{\phi_i} Mu(\Delta\phi_i)\, d\phi_i \right] \quad . \; . \; . \; . \quad (36)$$

The contribution of this potential energy to the equations of motion is found by taking the derivative with respect to each of the generalized coordinates. However, the potential energy is independent of the X_r' and Y_r' coordinates, so the necessary derivatives must only be taken with respect to each rotation, ϕ_i. When this is done, the $\{F_s\}$ vector will be the negative of these terms, where F_{s_k} is the resultant from differentiating with respect to q_k or ϕ_{k-2}. The equations for the $\{F_s\}$ vector are contained in EQUATIONS OF MOTION.

Generalized Forces due to External Loads

The external load in this model consists of an impact force in the global Y' direction that is input with a given magnitude, location, and time of application. A second force in the global X' direction is defined as an input fractional amount of the original force. The first force is defined as $F_{Y'}$ where

$$F_{Y'} = F_{Y'}(X_F', t) \quad . \; . \; . \; . \; . \; . \; . \; . \; . \; . \; . \; . \quad (37)$$

and the second force is $F_{X'}$, where

$$F_{X'} = (K)F_{Y'}(X_{F'}, t) \quad \ldots\ldots\ldots\ldots \quad (38)$$

Before these forces can be included in the equations of motion, their contribution to each of the generalized coordinates must be determined. The principle of virtual work will be used.

<u>Location of Force</u>

To find the work of these forces, the segment on which the load is applied must be determined, and its rotation must be established. This is shown in Figure 8. This is found when a segment's end point satisfies the relation

$$X'_{iR} \leq X'_F > X'_{iT} \quad \ldots\ldots\ldots\ldots \quad (39)$$

where i is the number of the segment the force acts on. The initial end of segment i is at

$$V'_{iR} = X'_R + T^1_{11}L_1 + T^2_{11}L_2 + \ldots T^{i-1}_{11}\, L_{i-1} \quad \ldots\ldots\ldots \quad (40)$$

and the final end is at

$$X'_{iT} = X'_{iR} + T^i_{11}\, L_i \quad \ldots\ldots\ldots\ldots\ldots\ldots \quad (41)$$

<u>Virtual Work of External Loads</u>

The virtual work of the external loads is given by

$$\delta W = F_{X'}\, \delta_{XAi}' + F_{Y'}\, \delta_{YAi}' \quad \ldots\ldots\ldots\ldots\ldots \quad (42)$$

Expressed in terms of generalized coordinates and forces, this virtual work is

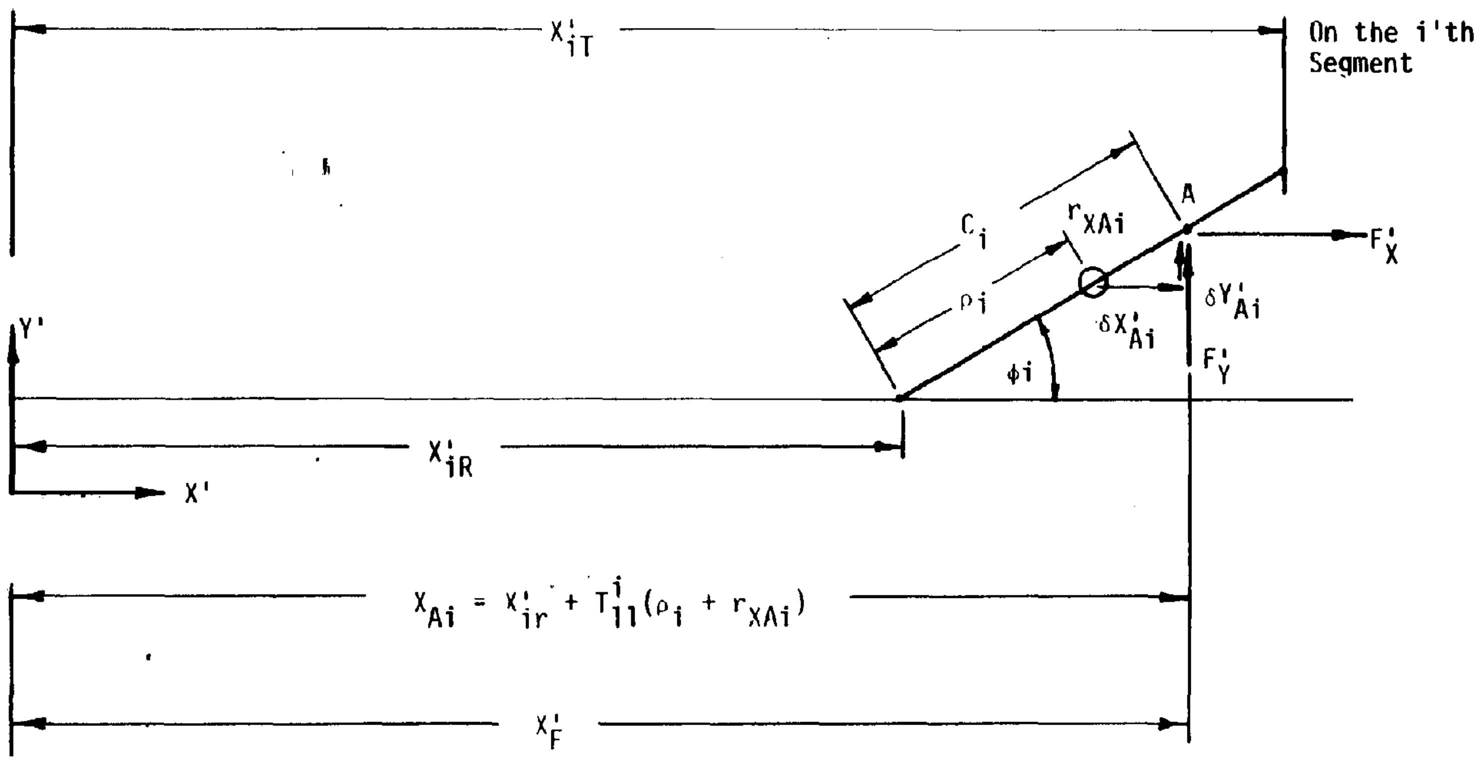

Figure 8. Location of Vehicle Impact Force Along Barrier.

$$\delta W = \sum_{K=1}^{n+2} (Q_{ek}\ \delta q_k) \quad (43)$$

where n+2 = number of degrees of freedom (n = number of barrier segments).

To transform Equation 42 into an expression with generalized coordinates, use the relation

$$X'_{Ai} = X'_{iR} + T^i_{11} (\rho_i + r_{XAi}) \quad (44)$$

where X'_{iR} was defined above and

$$r_{XAi} = \frac{X'_F - X'_{iR}}{\mathrm{Cos}\ \phi_i} - \rho_i \quad (45)$$

The impact location in the Y' direction is given by

$$Y'_{Ai} = Y'_{iR} + T^i_{21} (\rho_i + r_{XAi}) \quad (46)$$

where

$$Y'_{iR} = Y'_R + T^1_{21} L_1 + T^2_{21} L_2 + \ldots + T^{i-1}_{21} L_{i-1} \quad (47)$$

Thus, the point of application of force is

$$X'_{Ai} = X'_{iR} + T^i_{11} \left(\frac{X'_F - X'_{iR}}{\mathrm{Cos}\ \phi_i}\right) \quad (48)$$

But $T^i_{11} = \mathrm{Cos}\phi_i$, so that

$$X'_{Ai} = X'_F \quad (49)$$

In the same manner,

$$Y'_{Ai} = Y'_{iR} + T^i_{21} \frac{X'_F - X'_{iR}}{\mathrm{Cos}\ \phi_i} \quad (50)$$

and since $T^{i}_{21} = \text{Sin}\phi_i$

$$Y'_{Ai} = Y'_{iR} + \tan\phi_i \; (X'_F - X'_{iR}) \quad \ldots\ldots\ldots\ldots\ldots \quad (51)$$

With expressions for X'_{Ai} and Y'_{Ai} defined, the first differential is given as

$$\delta X'_{Ai} = \sum_{k=1}^{n+2} \frac{\partial X'_{Ai}}{\partial q_k} \delta q_k \quad \ldots\ldots\ldots\ldots\ldots \quad (52)$$

and

$$\delta Y'_{Ai} = \sum_{k=1}^{n+2} \frac{\partial Y'_{Ai}}{\partial q_k} \delta q_k \quad \ldots\ldots\ldots\ldots\ldots \quad (53)$$

These expressions can be substituted into Equation 42 to get

$$\delta W = F'_X \sum_{k=1}^{n+2} \frac{\partial X_{Ai}}{\partial q_k} \delta q_k + F'_Y \sum_{k=1}^{n+2} \frac{\partial Y_{Ai}}{\partial q_k} \delta q_k \quad \ldots\ldots \quad (54)$$

Rearranging terms gives

$$\delta W = \sum_{k=1}^{n+2} \left[F_{X'} \frac{\partial X'_{Ai}}{\partial qk} + F_{Y'} \frac{\partial Y'_{Ai}}{\partial q_k} \right] \delta q_k$$

If this is compared to Equation 43 the generalized force is found to be

$$Q_{ek} = F_{X'} \frac{\partial X'_{Ai}}{\partial q_k} + F_{Y'} \frac{\partial Y'_{Ai}}{\partial q_k} \quad \ldots\ldots\ldots\ldots\ldots \quad (55)$$

Equation 55 with k = 1, 2, . . . n+2 defines the term in row k for the column vector $\{Q_e\}$ in Equation 30. The expanded form for each row of $\{Q_e\}$ is given in EQUATIONS OF MOTION.

Generalized Forces due to Friction at the Roadway-Barrier Interface

The friction force developed at the road-barrier interface can be broken up into two components. The first part is due to translation of the barrier segment, and the second part is due to rotation of that segment. The generalized forces for translation will be found first, and then those for rotation.

Translation Friction Force

The velocity of the i-th segment in the fixed X-axis and Y-axis directions was found previously in Equations 20 and 21. Since both expressions for the center of mass location are functions of the generalized coordinates, it can be shown that

$$\dot{X}_i' = \sum_{k=1}^{n+2} \frac{\partial X_i'}{\partial q_k} \frac{\partial q_k}{\partial q_t} = \sum_{k=1}^{n+2} \frac{\partial X_i'}{\partial q_k} \dot{q}_k \quad \ldots \quad (56)$$

and in a like manner

$$\dot{Y}_i' = \sum_{k=1}^{n+2} \frac{\partial Y_i'}{\partial q_k} \dot{q}_k \quad \ldots \quad (57)$$

Define the net translational velocity to be

$$\dot{R}_i = \left[(\dot{X}_i')^2 + (\dot{Y}_i')^2 \right]^{1/2} \quad \ldots \quad (58)$$

and the maximum resultant friction force on segment i as

$$R_{F_i} = (W_i)(\mu_i) \qquad \text{(59)}$$

where W_i = weight of segment i and μ_i = coefficient of friction between roadway and barrier.

Now, expressions to find the component of force that oppose the barrier's translational motion in each fixed axis direction are found to be

$$F_{fx'i} = -\left(\frac{\dot{X}_i'}{\dot{R}_i}\right) R_{F_i} \qquad \text{(60)}$$

and

$$F_{fy'i} = -\left(\frac{\dot{Y}_i'}{\dot{R}_i}\right) R_{F_i} \qquad \text{(61)}$$

To help avoid the numerical instabilities that occur when $\dot{X}_i'$ or $\dot{Y}_i'$ change sign, an adjustment in the frictional forces will be made. For values of segment velocity less than a very small value, $\dot{\varepsilon}_T$, the force will be reduced according to the equation.

$$R_{F_i} = C_t R_{F_i} \qquad \text{(62)}$$

The relationship of reduction constant to translational velocity is given by

$$C_t = \begin{cases} \text{Sin } \frac{\pi}{2} \frac{\dot{R}_i}{\dot{\varepsilon}_T} & \text{For } \dot{R}_i < \dot{\varepsilon}_T \qquad \text{(63)} \\ 1.0 & \text{For } \dot{R}_i \geq \dot{\varepsilon}_T \qquad \text{(64)} \end{cases}$$

Figure 9 shows the C_t - $\dot{R}_i$ curve for making this adjustment.

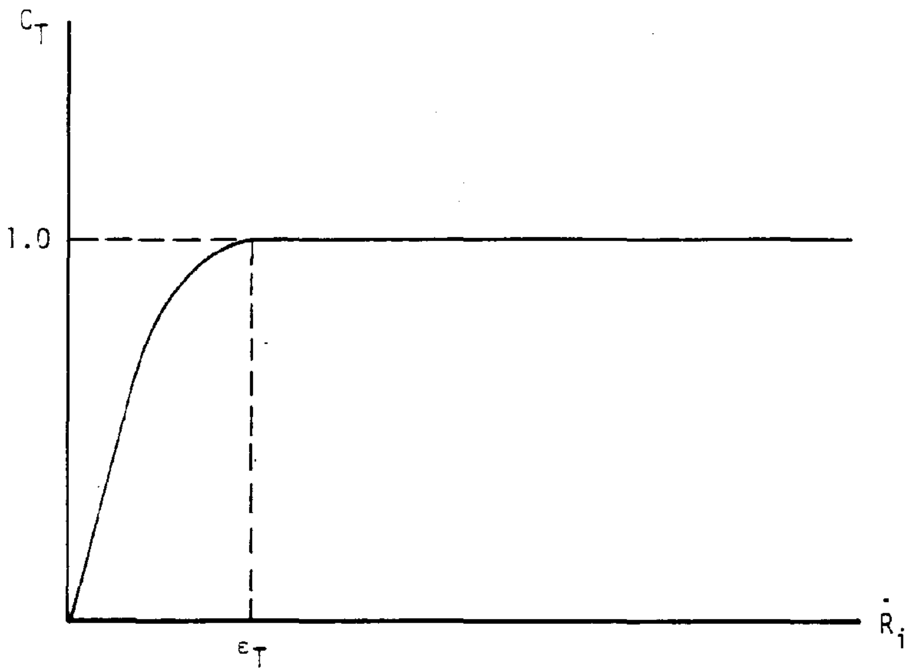

For $\dot{R}_i < \dot{\varepsilon}_T$

$$C_T = \mathrm{Sin}\left(\frac{\pi}{2}\ \frac{\dot{R}_i}{\dot{\varepsilon}_T}\right)$$

Figure 9. Adjustment Coefficient for Translational Friction Force.

Rotational Friction Force

The contribution of the rotational friction component can be found by examining the distribution of friction forces as shown in Figure 10. The moment due to the friction force can be calculated as

$$M_{f_i} = - \frac{\dot{\phi}_i}{|\dot{\phi}_i|} \frac{W_i \mu_i L_i}{4} \quad \ldots \ldots \ldots \ldots \ldots \ldots \quad (65)$$

Again, to compensate for possible numerical instability when the rotational velocity becomes very small or changes sign, an adjustment factor of

$$C_r = \mathrm{Sin}\left(\frac{\pi}{2} \frac{\dot{\phi}_i}{\dot{\varepsilon}_R}\right) \qquad \text{For } \dot{\phi}_i \leq \dot{\varepsilon}_R \quad \ldots \ldots \quad (66)$$

will be applied to the frictional moment as given here

$$M_{f_i} = C_r M_{f_i} \quad \ldots \ldots \ldots \ldots \ldots \ldots \quad (67)$$

Virtual Work of Friction Forces

The virtual work done by the translation friction force is given by

$$\delta W_{F_X} \equiv \sum_{i=1}^{n} (F_{fX'i}\, \delta X_i' + F_{fY'i}\, \delta Y_i') \quad \ldots \ldots \ldots \ldots \quad (68)$$

In a like manner the virtual work done by the generalized friction forces can be given as

$$\delta W_f = \sum_{k=1}^{n+2} (Q_{ftk})\ \delta q_k \quad \ldots \ldots \ldots \ldots \ldots \ldots \quad (69)$$

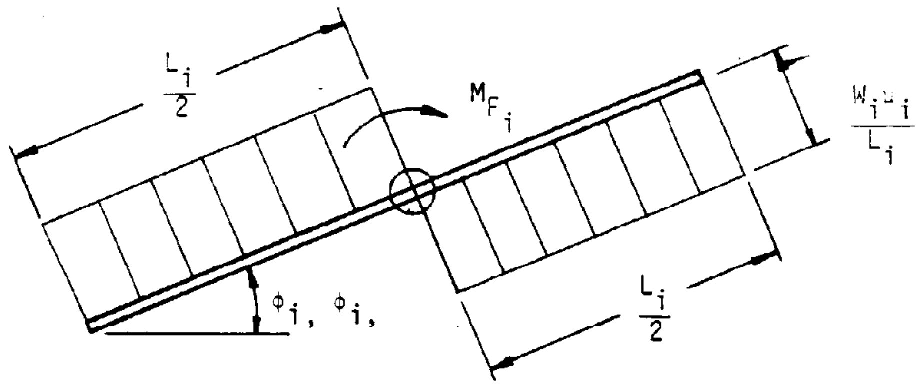

Figure 10. Distribution of Friction Force due to Rotation of Segment i.

The expressions for X_i' and Y_i' are given in Equations 22 and 23, hence

$$X_i' = \sum_{i=1}^{n+2} \frac{\partial X_i'}{\partial q_k} \delta q_k \quad \ldots\ldots\ldots\ldots\ldots\ldots (70)$$

$$Y_i' = \sum_{i=1}^{n+2} \frac{\partial Y_i'}{\partial q_k} \delta q_k \quad \ldots\ldots\ldots\ldots\ldots\ldots (71)$$

By substituting these two expressions into Equation 68,

$$\delta W_{ft} = \sum_{i=1}^{n} \sum_{k=1}^{n} \left[F_{fxi} \frac{\partial X_i'}{\partial q_k} + F_{fy'i} \frac{\partial Y_i'}{\partial q_k} \right] \delta q_k \quad \ldots\ldots\ldots (72)$$

If Equations 69 and 72 are compared it can be shown that the generalized friction force due to translational movement is

$$Q_{ftk} = \sum_{i=1}^{n} \left[F_{fx_i'} \frac{\partial X_i'}{\partial q_k} + F_{fy_i} \frac{\partial Y_i'}{\partial q_k} \right] \quad \ldots\ldots\ldots\ldots (73)$$

In the same way, the generalized rotational friction force can be found. The virtual work of the rotational forces is

$$\delta W_{fr} = \sum_{i=1}^{n} M_{Fi} \, \delta\phi_i \quad \ldots\ldots\ldots\ldots\ldots\ldots (74)$$

and the virtual work of the generalized rotational friction force is

$$\delta W_f = \sum_{k+1}^{n+2} Q_{frk} \, \delta q_k \quad \ldots\ldots\ldots\ldots\ldots\ldots (75)$$

Since each of the segment rotational angles ϕ_i correspond to the generalized coordinate q_{i+2}, the generalized force due to rotational friction is

$$Q_{frk} = M_{f(k-2)} \quad \ldots\ldots\ldots\ldots\ldots\ldots \quad (76)$$

where $M_{f(k-2)}$ is defined in Equation 65 or 67. The total generalized friction force is given by

$$Q_{fk} = Q_{ftk} + Q_{frk} \quad \ldots\ldots\ldots\ldots\ldots\ldots \quad (77)$$

The expansion of this expression is given in EQUATIONS OF MOTION.

Solution of Equations

The Runge-Kutta Method

The matrix equations of motion for the barrier system as given in Fquation 11 are of the form in which the second derivative, $\ddot{q}_k$, $(k=1, \ldots n)$, can be expressed as a function of the first derivative, q_k, the dependent variable, $\dot{q}_k$, and the independent variable, t(time). Therefore the equations were solved using the Runge-Kutta method for ordinary differential equations (1).

The right-hand side of Equation 11 can be redefined as

$$\{R\} = \{E\} + \{F_s\} + \{Q_e\} + \{Q_f\} \quad \ldots\ldots\ldots\ldots \quad (78)$$

Using the inverse of the [D] matrix to find an expression for the generalized accelerations

$$\{\ddot{q}\} = [D]^{-1} \{R\} \quad \ldots\ldots\ldots\ldots\ldots\ldots \quad (79)$$

The $[D]^{-1}$ matrix is a function of displacements only, but the $\{R\}$ column vector is dependent on both displacements and velocities. This will be noted as

$$[D]^{-1} = [D\ (\{q\})]^{-1} \quad \ldots\ldots\ldots\ldots \quad (80)$$

and

$$\{R\} = \{R(\{q\},\{\dot{q}\})\} \quad \ldots\ldots\ldots\ldots \quad (81)$$

so that

$$\{\ddot{q}\} = [D(\{q\})]^{-1} \{R(\{q\},\{\dot{q}\})\} \quad \ldots\ldots\ldots\ldots \quad (82)$$

Solution of Equation 82 was done with a stepwise increment of time, Δt, using the equations given below.

$$\{AY_1\} = \Delta t \cdot \{\dot{q}\} \quad \ldots\ldots\ldots\ldots \quad (83)$$

$$\{AZ_1\} = \Delta t \cdot [D(\{q\})]^{-1} \{R(\{q\},\{\dot{q}\})\} \quad \ldots\ldots\ldots\ldots \quad (84)$$

$$\{AY_2\} = \Delta t \cdot \{\dot{q}\} + \frac{1}{2} \Delta t \{AZ_1\} \quad \ldots\ldots\ldots\ldots \quad (85)$$

$$\{AZ_2\} = \Delta t \cdot [D(\{q\} + \frac{1}{2}\{AY_1\})]^{-1} \{R(\{q\} + \frac{1}{2}\{AY_1\},\{\dot{q}\} + \frac{1}{2}\{AZ_1\})\} \quad \ldots\ldots\ldots\ldots \quad (86)$$

$$\{AY_3\} = \Delta t \cdot \{\dot{q}\} + \frac{1}{2} \Delta t \cdot \{AZ_2\} \quad \ldots\ldots\ldots\ldots \quad (87)$$

$$\{AZ_3\} = \Delta t \cdot [D(\{q\} + \frac{1}{2}\{AY_2\})]^{-1} \{R(\{q\} + \frac{1}{2}\{AY_2\},\{\dot{q}\} + \frac{1}{2}\{AZ_2\})\} \quad \ldots\ldots\ldots\ldots \quad (88)$$

$$\{AY_4\} = \Delta t \cdot \{\dot{q}\} + t \cdot \{AZ_3\} \quad \ldots\ldots\ldots\ldots \quad (89)$$

$$\left\{AZ_4\right\} = t \cdot \left[D(\{q\} + \left\{AY_3\right\})\right]^{-1}\left\{R(\{q\} + \left\{AY_3\right\}, \{\dot{q}\} + \left\{AZ_3\right\})\right\} . \quad (90)$$

$$\left\{AY\right\} = \frac{1}{6} \cdot \left\{\left\{AY_1\right\} + 2\left\{AY_2\right\} + 2\left\{AY_3\right\} + \left\{AY_4\right\}\right\} \quad \ldots\ldots\ldots \quad (91)$$

$$\left\{AZ\right\} = \frac{1}{6} \cdot \left\{\left\{AZ_1\right\} + 2\left\{AZ_2\right\} + 2\left\{AY_3\right\} + \left\{AY_4\right\}\right\} \ldots\ldots\ldots \quad (92)$$

The new values of time, displacement, and velocity at time t_i are

$$t_i = t_{i-1} + \Delta t \quad \ldots\ldots\ldots \quad (93)$$

$$\{q\}_i = \{q\}_{i-1} + \left\{AY\right\} \quad \ldots\ldots\ldots \quad (94)$$

$$\{\dot{q}\}_i = \{\dot{q}\}_{i-1} + \left\{AZ\right\} \quad \ldots\ldots\ldots \quad (95)$$

This solution is continued using previous values of $\{q\}$ and $\{\dot{q}\}$ to solve for those at the next time step.

The Computer Program

The computer program was written in FORTRAN IV on the Amdahl 470 V/6. A LISTING OF THE COMPUTER PROGRAM is given and the input documentation is given in DESCRIPTION OF INPUT TO THE COMPUTER PROGRAM.

The Subroutines

MAIN controls the logic flow of the program. Subroutines DATAIN, INITL, LOCATE, ECHO, STEPS, RKSOLN, ACCEL, ENDFRC, and OUTPUT are called from this routine.

Subroutine DATAIN reads all of the required data for the program. Subroutine INITL initializes the values of the barrier geometry and velocity, and converts all input into a ft-lb-sec-rad system of units. Subroutine ECHO prints out the input data read in DATAIN.

Subroutine RKSOLN performs the Runge-Kutta integration and calculates the new global coordinates and velocities at each time step. It calls subroutine STEPS. Subroutine STEPS generates the equations of motion and solves for the generalized accelerations. It calls subroutines LOCATE, TRNVEL, FORCE, DMTRX, EMTRX, FSMTRX, QEMTRX, QFMTRX, ADD, and GAUSS.

Subroutine LOCATE calculates the global coordinates of each barrier segment end point.

Subroutine TRNVEL calculates the translational velocity components for each segment center of mass. Subroutine FORCE locates the impact force and determines its magnitude using linear interpolation of the input data.

Subroutine DMTRX generates the $[D]$ matrix from barrier segment properties and geometry at each time step. Subroutine EMTRX calculates the elements in each row of the $\{E\}$ column vector. Subroutine FSMTRX determines the contributions of potential energy in the joint springs to $\{F_s\}$.

Subroutine QEMTRX finds the generalized force in $\{Q_e\}$ due to the impact force on the barrier segment. Subroutine QFMTRX calculates the friction force contributions to the generalized forces in $\{Q_f\}$.

Subroutine ADD sums the $\{E\}$, $\{F_s\}$, $\{Q_e\}$, and $\{Q_f\}$ column vectors into $\{R\}$. Subroutine GAUSS solves for the generalized accelerations for a given $[D]$ and $\{R\}$ using Gaussian elimination for simultaneous equations.

Subroutine ACCEL calculates the segment center of mass accelerations using the generalized velocities and accelerations. Subroutine ENDFRC determines the member end forces on each segment due to imposed loads and accelerations. Subroutine OUTPUT prints out barrier geometry, accelerations, and end forces at each required time step.

Output

The user can request output at any time interval desired with the proper variable input. At each time step the following information is printed:

1. The global coordinates of the end points of each barrier segment;
2. The angular rotation of each barrier segment in the fixed coordinate system;
3. The components of each center of mass acceleration in the fixed coordinate system;
4. The global angular acceleration of each barrier segment;
5. The forces and moments at the ends of each barrier segment in its segment fixed coordinate system.

VALIDATION OF BARRIER MODEL

Initial Checkout

Once the equations of motion for the system had been derived, a three-step procedure was used to validate and check the coded program. These steps were a general check of matrix assembly and solution scheme logic, comparison with known solutions of theoretical problems, and simulation of previous crash tests.

After debugging was completed, the first phase of verification began. The program's results for each of the assembled matrices was checked against long-hand calculations using the equations in EQUATIONS OF MOTION. At the same time the Gauss solution scheme for linear equations and the Runge-Kutta integration technique were verified with independent tests. Finally, the matrix assembly, time integration, and elimination routines were linked into a single program and checked for stability after one time step.

Idealized Structure Modeling

Once the program was running correctly on a single time increment, the second set of checks was performed. Two idealized structures systems were modeled and run to examine exactness with theoretical solutions. The first was a single member pinned at one end and subjected to a constant force, as shown in Figure 11. By setting M_1, μ_1, and I_{0_1} very large in comparison to M_2, μ_2, and I_{0_2} and using no spring at the joint, this model showed a good relationship with the theoretical solution. Table 1 shows the values used for each of the variables and the results of each analysis.

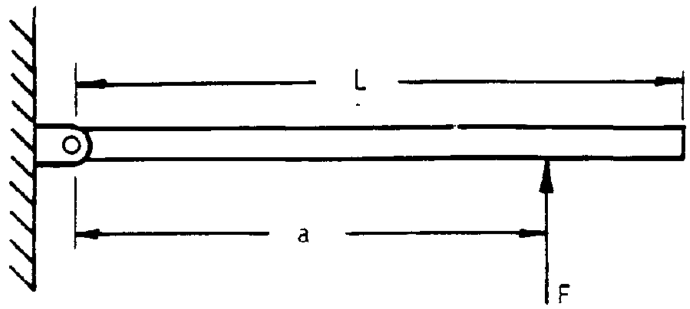

a) Idealized Structure

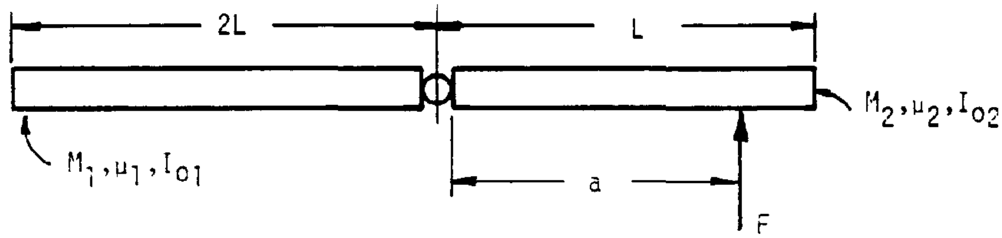

b) Modeled Structure

Figure 11. Idealized and Modeled Structures for First Theoretical Study.

Table 1. Input and Results from First Idealized Simulation.

Input	Idealized Structure	Modeled Structure
M_1 (lb-sec^2/ft)	Fixed,	6217.6
μ_1	not	1.0
I_{01} (ft-lb-sec^2)	required	82901.
M_2 (lb-sec^2/ft)	248.45	248.45
μ_2	--	0.0
I_{02} (ft-lb-sec^2)	8281.7	8281.7
Results		
Acceleration (rad/sec^2)	.906 (Constant)	.906 (Average)
Angular Displacement at Time=0.10 sec	0.260°	0.258°

Δt=0.001 sec

$\dot{\varepsilon}_t$=0.10 ft/sec

$\dot{\varepsilon}_R$=0.05 rad/sec

In the second idealized case, an elastic spring was added to the same structure with altered mass and moment of inertia values and the element was given an initial rotation. By using the stiffness and mass moment of inertia to find the natural frequency, the time for the segment to return to its initial position can be calculated. As in the first test, the program showed very good results in comparison to the idealized solution. These results are listed in Table 2.

At this point it should be noted that the three adjustable parameters were established during this phase of the research. The time increment for stability in the first test was 0.001 secs. This worked in the second analysis, and was maintained throughout the remainder of the computer runs. The translational adjustment for friction was set at 0.1 ft and the rotational adjustment was 0.05 rad. These values were also used in all subsequent simulations.

Crash Test Simulation

In the final step of the validation, six previous crash tests on concrete median barriers were selected (2,3,4,5). Each of these tests used a barrier that could be modeled with the proper selection of parameters to represent the system. On-going research (3) has established the joint properties in terms of rotations and moment capacities. Table 3 summarizes the necessary values to define the barrier and joint properties. In all cases, the barrier segments were initially straight.

The force input was the most difficult variable to establish. Tests CMB-2, CMB-24, NY-1, and NY-2, were standard structural adequacy tests (6). Force versus time data for a structural adequacy test were experimentally determined by Bronstad (7).

Table 2. Input and Results from Second Idealized Simulation.

Input	Idealized Structure	Modeled Structure
M_1 (lb-sec^2/ft)	Fixed,	6217.6
μ_1	not	1.0
I_{01} (ft-lb-sec^2)	required	82901.
M_2 (lb-sec^2/ft)	10.89	10.89
μ_2	--	0.0
I_{02} (ft-lb-sec^2)	362.8	362.8
k_e (k-ft/deg)	100.	100.
Results		
Rotation at end of one natural period	5°	4.9°

$\Delta t = 0.001$ sec

$\dot{\varepsilon}_t = 0.10$ ft/sec

$\dot{\varepsilon}_R = 0.05$ rad/sec

Table 3. Barrier Simulation Input.

Test	Barrier Properties			Joint Properties					
	No./Segment Length (ft)	Wt/Ft (lb/ft)	Friction	ϕ_s (deg)	ϕ_e (deg)	ϕ_p (deg)	ϕ_f (deg)	K_E (K/deg)	K_p (K/deg)
CAL-291	12/12.5	400	0.5	3.	5.	15.	15.	4.5	0.
CAL-294	6/20.	400	0.5	3.	5.	15.	15.	6.0	0.
NY-1	6/20.	400	0.5	10.	12.	22.	22.	48.0	0.
NY-2	6/20.	400	0.5	0.	2.	12.	12.	48.0	0.
CMB-24	5/20.	500	0.5	1.	3.	13.	13.	3.0	0.
CMB-2	3/30.	500	1.0	0.	5.	15.	15.	25.0	0.

This input is recorded in the table in DESCRIPTION OF INPUT TO THE COMPUTER PROGRAM. A rough estimate was made from vehicle accelerometer and film data for use in the other two tests, CAL-291 and CAL-294. Table 4 gives this input. With the proper barrier and joint properties, system geometry and external forces calculated, the various tests were simulated with varying success. The results and problems are summarized below.

Table 5 and Figure 12 show the values of absolute maximum lateral deflection for the actual crash test and those predicted by computer simulation. With the exception of tests NY-1 and NY-2, the comparison was very good. There were several factors in the NY tests that could not be exactly determined, and they likely contributed to this difference. The number of barrier segments and location of the vehicle impact point were unknown. Six segments were assumed to eliminate system end point movement. An impact at the center of the third segment was assumed for these two tests, since this seemed to be the most severe point. Further, the type of surface the barriers were erected on was unknown. If a grout bed or hot asphalt mix was used as a leveling course, the value of friction at the roadway would have to be much larger. It should be noted here that a friction coefficient of 1.0 was used on CMB-2 because it was built on a hot mix asphalt bed. Finally, vehicle impact conditions for the NY tests (as well as the other tests) varied from the conditions used in the Bronstad test (7).

Table 4. Impact Force Input for CAL-291 and CAL-294 Tests.

CAL-291

Time (sec)	Force (lb)	Position (ft)
0.0	0.0	41.0
0.01	18950.	41.95
0.06	18950.	46.68
0.065	24300.	47.15
0.10	0.0	50.46
0.15	24300.	55.19
0.20	0.0	59.92

CAL-294

Time (sec)	Force (lb)	Position (ft)
0.0	0.0	70.8
0.01	18800.	71.7
0.10	18800.	80.1
0.11	0.0	82.0
0.27	0.0	98.0
0.29	35250.	100.1
0.34	35250.	105.2
0.36	0.0	107.3

Table 5. Simulation Results of Previous CMB Crash Tests.

Test	Observed Maximum Deflection (ft)	Predicted Maximum Deflection (ft)
CAL-291	0.52	0.65
CAL-294	0.46	0.61
NY-1	1.33	3.63
NY-2	0.92	2.09
CMB-24	3.42	3.49
CMB-2	1.10	1.47

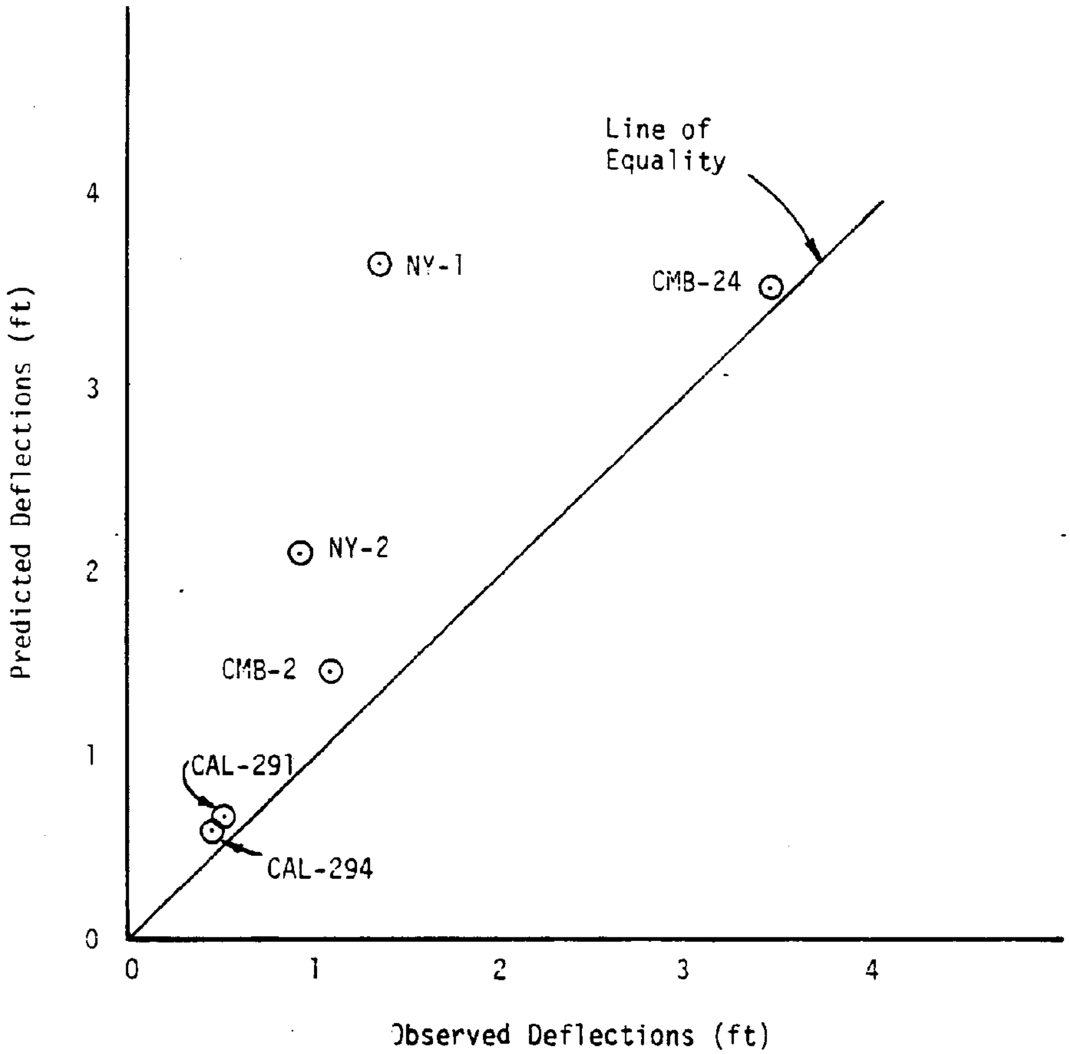

Figure 12. Predicted versus Observed Deflections for Six Crash Test Simulations.

PARAMETRIC STUDY OF BARRIER RESPONSE

Since the precast concrete median barrier has so many design configurations, the various effects of barrier length, joint moment capacity, joint rotational slack, and roadway friction on lateral deflection of the barrier due to vehicle impact were all studied. Each parameter was varied independently to give some insight into each of their effects. The results of this study will be used later in the design phase of this report.

Before the parameter study began three barrier lengths were identified as the most desirable, 12 ft, 20 ft, and 30 ft, since they have been used in previous designs. This was not a restrictive assumption, but was made initially to establish a starting point. Other lengths were also considered later.

The force vs. time input for the structural adequacy test of longitudinal barriers (a 4500 lb vehicle traveling at 60 mph with a 25° encroachment angle) was used in the parameter study. In all parameter runs, the impact was located approximately at the third point of the system. The input for this impact is given in the table in the DESCRIPTION OF INPUT TO THE COMPUTER PROGRAM.

Analysis for Length of Need and Impact Location

With the necessary forcing function established, two important questions had to be resolved. How many segments are necessary to eliminate significant end point movement, and, is an impact at the joint or the center of the barrier more critical? Significant end point movement was arbitrarily defined as greater than 2 in. of displacement at each end of the barrier in either direction. This is important because the simulation should approximate a situation where the barrier is very long, without using so many segments that the computations take an excessive amount of computer time. These questions were analyzed for each of the three segment lengths. All of the tests were done with no joint moment capacity and roadway friction, $\mu = 0.7$.

The results of this initial evaluation are summarized here. The 30 ft length required only four segments, and the 20 ft length needed six segments, but 15 segments were necessary for the 12 ft length. (More are really needed, but the program was limited to 15 segments by its array space.) It is interesting to note that this corresponds to a system length of 120 ft for the 20 ft and 30 ft segments, but 180 ft is required for the 12 ft segment. At the same time, center impacts were determined to be more critical for the 12 ft and 20 ft length, but a joint impact on the 30 ft length was more severe.

Later in the parameter study, 15 ft and 25 ft barrier lengths were added to the study. For that reason, this same evaluation was performed on those segments, and the results are presented here. The 15 ft length required 12 segments, and the 25 ft length needed five segments. Center impacts were more severe than those at the joint for the 15 ft segment, but the 25 ft segment was relatively insensitive to the impact location. The results of all these tests are tabulated in Table 6.

Effects of Joint Moment Capacity and Segment Length on Lateral Displacements

Once the initial study was finished, the second parameter set was analyzed. In this phase, various segment lengths were combined with

Table 6. Length of Need and Critical Impact Point Study Results.

Length	No.	Hit	Max. Defl.	End Point Displacement X_1	Y_1	X_2	Y_2
12	8	JT	34"	2.3"	-0.1"	-4.8"	0.0"
12	10	JT	33"	2.0"	0.2"	-4.0"	0.0"
12	12	JT	31"	1.8"	1.2"	-3.2"	0.0"
12	12	CTR	39"	3.7"	0.2"	-3.2"	0.0"
12	15	CTR	35"	2.3"	0.7"	-2.9"	0.0"
20	5	CTR	34"	1.3"	0.0"	4.3"	2.8"
20	6	CTR	32"	2.5"	0.0"	0.2"	-0.1"
20	6	JT	24"	1.0"	0.2"	1.2"	0.2"
30	3	CTR	18"	0.1"	-1.0"	1.7"	-13.3"
30	4	CTR	14"	0.2"	-1.2"	-0.4"	1.7"
30	4	JT	17"	0.5"	2.0"	0.4"	-0.6"
15	8	CTR	43"	4.7"	-0.5"	-3.7"	0.0"
15	8	JT	26"	1.3"	-0.2"	-2.2"	0.0"
15	10	CTR	39"	3.6"	0.1"	-3.7"	0.0"
15	12	CTR	35"	2.9"	0.5"	-2.9"	0.0"
25	5	CTR	22"	0.1"	0.2"	-1.8"	2.4"
25	5	JT	21"	0.2"	-0.2"	-1.2"	-1.7"

joint moment capacities ranging from 0 k-ft to 100 k-ft. The slack in the spring was constant at 3 deg and the elastic limit was 5 deg. There were no lock-up or failure limits established. The roadway friction coefficient was constant at μ = 0.7. The results are given in Table 7 and presented graphically in Figures 13 and 14. Although 12 ft, 20 ft, and 30 ft segments were the only lengths initially considered, the complex relationship of segment length and moment capacity required additional tests using 15 ft and 25 ft lengths.

Several key discoveries are revealed in Figures 13 and 14. First, it is apparent that the addition of moment capacity to the joints of 25 ft and 30 ft lengths is not very efficient. This becomes obvious if the effects of a 1 ft displacement to one joint in each barrier system is considered. The differential rotations of 12 ft, 15 ft, 20 ft, 25 ft, and 30 ft segments are, respectively, 9.5 deg, 7.6 deg, 5.7 deg, 4.6 deg, and 3.8 deg. Since the longer segments do not rotate as far as the short segments, the shorter lengths experience the joint moments sooner, and absorb more energy in plastic deformation of the spring. Next, although the 12 ft, 15 ft, and 20 ft lengths all have identical displacements at zero moment, the 12 ft length shows the optimal use of moment capacity, and the 20 ft length has the poorest response to joint spring capacity. The 15 ft length falls in between the two. Stated simply, long segments have no advantage because of a large joint moment capacity, short segments can efficiently use moderate moment capacities, and intermediate lengths require significant joint strength to minimize lateral deflections.

Table 7. Connection Moment-Segment Length-Deflection Study.

$\phi_s = 3^o$ $\phi_e = 5^o$ $\phi_p = 40^o$

Barrier Length (ft)	Connection Moment (k-ft)	Maximum Displacement (in.)	Maximum Displacement (ft)
12-15 Barriers	0	35.01	2.92
	25	25.21	2.10
	30	23.92	1.99
	50	19.80	1.65
	75	19.76	1.65
	100	21.67	1.81
15-12 Barriers	0	35.31	2.94
	25	29.06	2.42
	30	27.93	2.33
	50	22.73	1.89
	75	19.98	1.67
	100	18.76	1.56
20-6 Barriers	0	33.80	2.82
	25	28.01	2.33
	30	26.94	2.25
	50	26.70	2.23
	75	21.87	1.82
	100	19.07	1.59
25-5 Barriers	0	22.32	1.86
	25	21.37	1.78
	30	21.17	1.76
	50	19.89	1.66
	75	18.82	1.57
	100	18.34	1.53
30-4 Barriers	0	17.74	1.48
	25	16.87	1.41
	30	16.80	1.40
	50	16.55	1.38
	75	16.25	1.35
	100	15.98	1.33

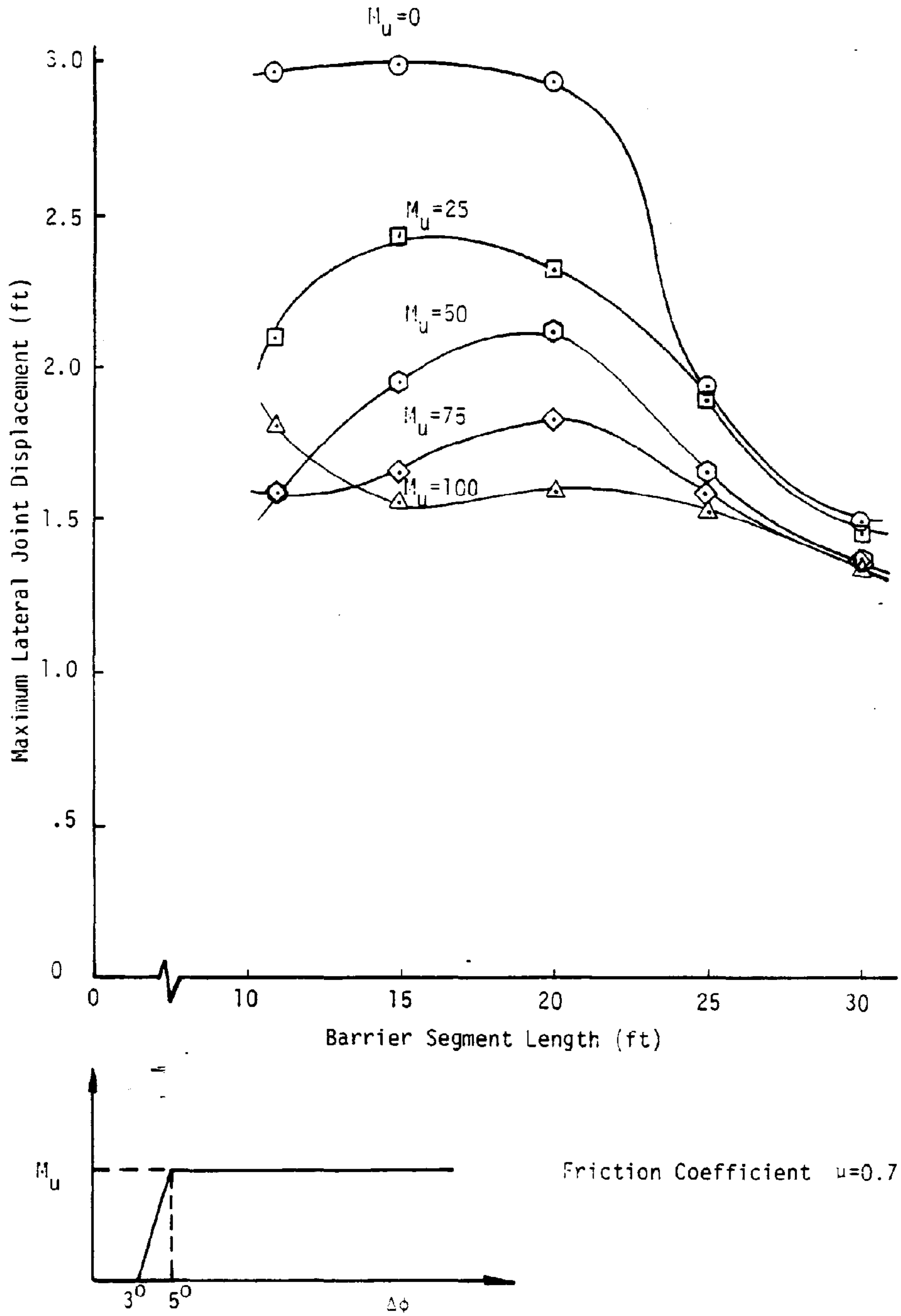

Friction Coefficient u=0.7

Figure 13. Lateral Joint Displacement Versus Segment Length, Variable Connection Moment.

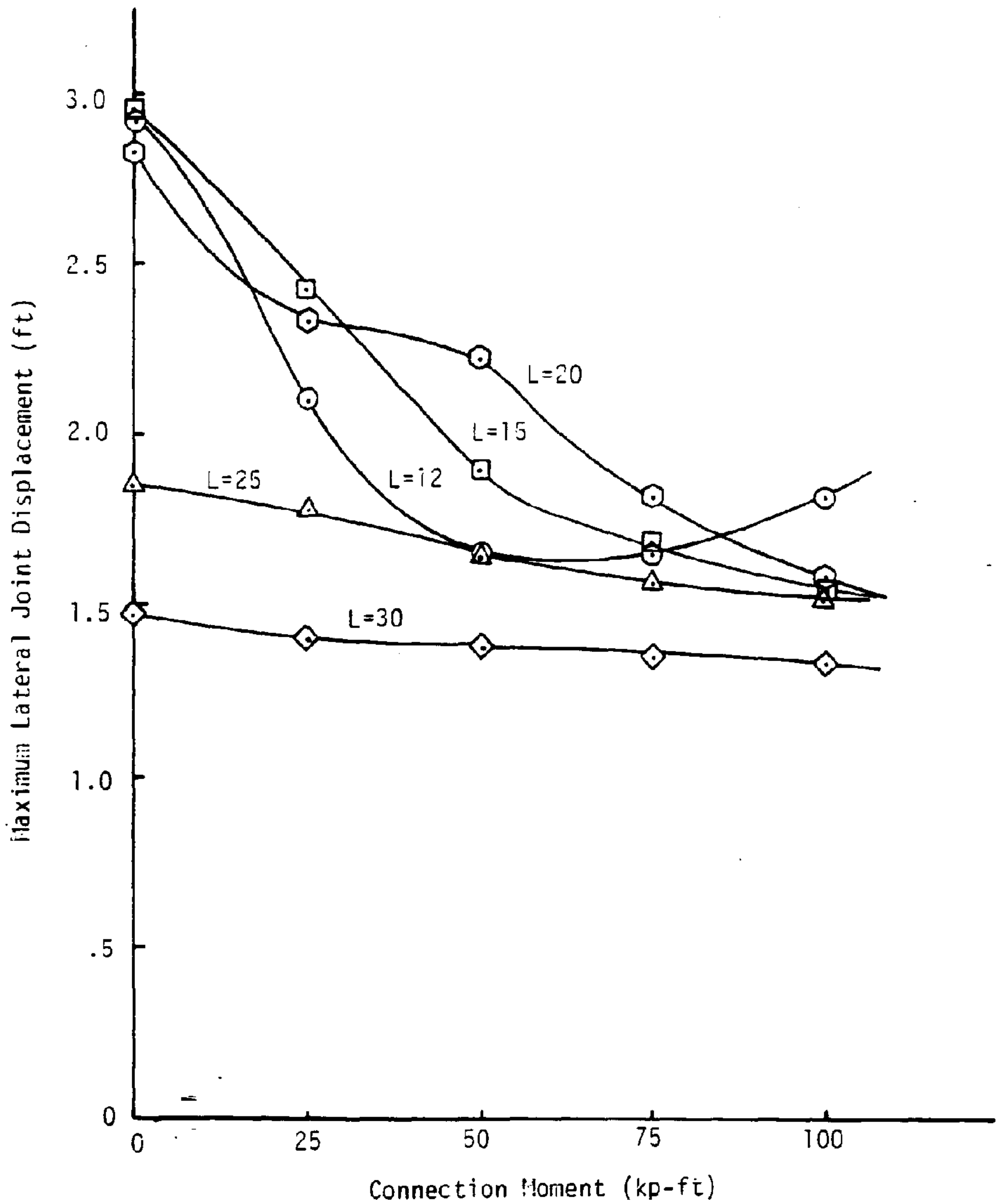

Figure 14. Lateral Joint Displacement Versus Connection Moment, Variable Segment Length.

Effects of Joint Connection Slack on Lateral Displacements

The relationship of joint connection slack to barrier displacement was investigated next. In this series of simulations, connection slack was varied from 1 deg to 8 deg for all five barrier lengths. The ultimate moment was held constant at 100 k-ft and the elastic limit, ϕ_e, was always 2 deg larger than the slack rotational limit, ϕ_s. This was done to keep the elastic spring constant, k_E, the same for all tests. As in previous studies, the friction coefficient was μ = 0.7. The results are summarized in Table 8 and are plotted in Figure 15.

The curves in Figure 15 show a general increase in deflection as the connection slack grows. However, examination of the individual curves shows some correlation with the results of the previous work on moment capacity. The 30 ft length shows the least increase in deflection of the five, and the 25 ft length follows the general upward trend with no irregularities. This is primarily due to the fact that these segment lengths generate their resisting forces with friction and not joint moments. It can be noted that while there is little difference between the two lengths for slack less than 3 deg, the displacement in the 25 ft length begins to grow faster at a slack larger than 3 deg. The 12 ft, 15 ft, and 20 ft segment lengths also show the general trend of increasing lateral deflections with increasing amounts of joint slack. The 20 ft length shows the most rapid increase in displacement at a slack of 3 deg or greater when compared to all other lengths and joint slack values. A slack up to 5 deg has very little affect on the 15 ft length, but lateral displacements grow very quickly once slack increases

Table 8. Connection Slack-Segment Length-Deflection Study Results.

$$Mu = 100 \text{ k-ft} \quad \phi_e = \phi_s + 2^0$$

LENGTH (ft)	SLACK (deg)	LATERAL DISPLACEMENT (ft)
12	1	1.61
	2	1.60
	3	1.60
	5	1.78
	8	2.20
15	1	1.45
	2	1.50
	3	1.56
	5	1.65
	8	1.99
20	1	1.37
	2	1.53
	3	1.59
	5	1.92
	8	2.34
25	1	1.13
	2	1.34
	3	1.53
	5	1.75
	8	1.86
30	1	1.06
	2	1.22
	3	1.33
	5	1.43
	8	1.43

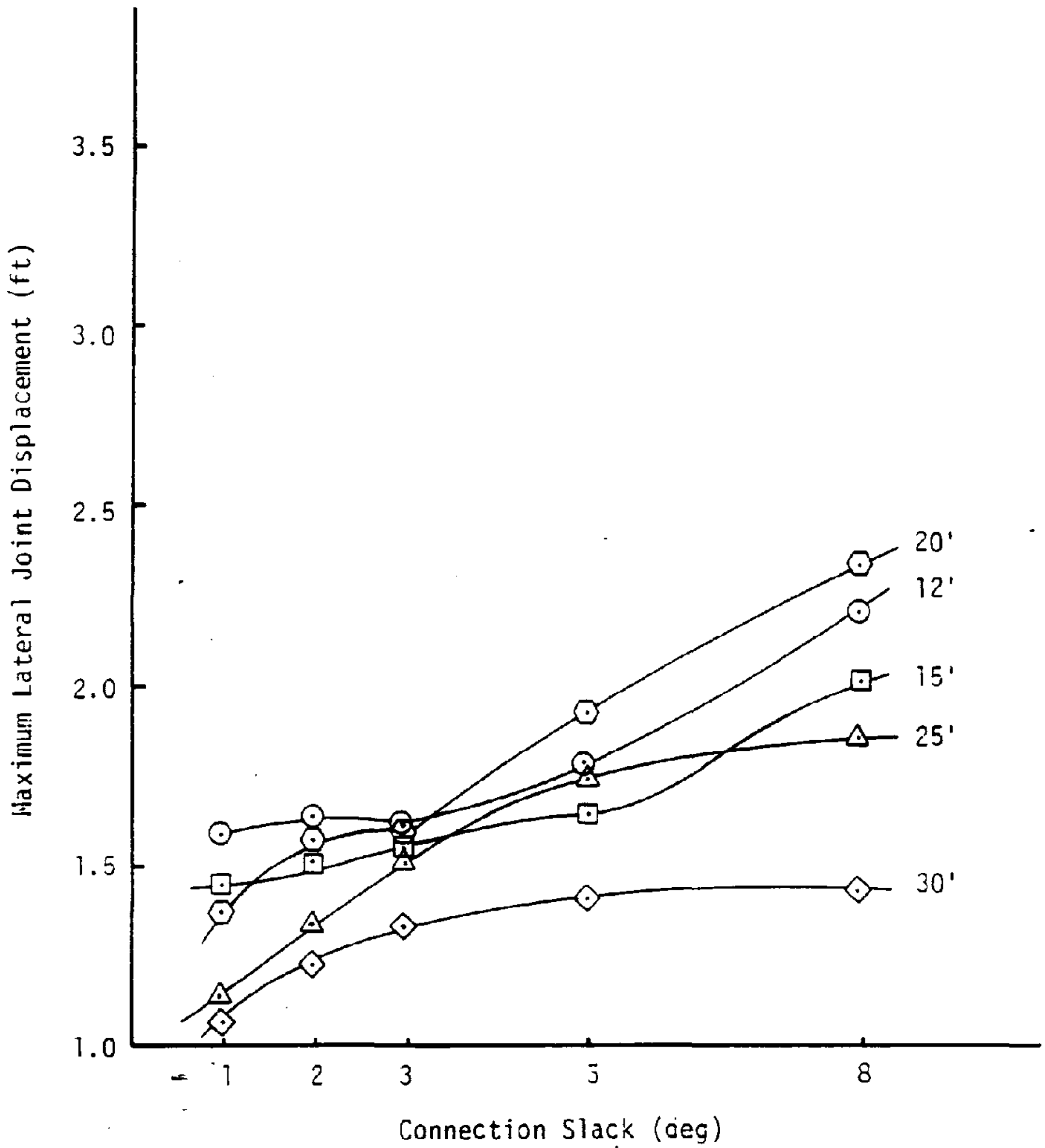

M_u=100 k-ft

$\phi_e = \phi_s + 2^0$

μ=0.7

Figure 15. Lateral Joint Displacement Versus Connection Slack, Variable Segment Length.

beyond 5 deg. The same type of response is seen in the 12 ft segment lengths. The maximum deflection of the 12 ft length is larger than that for the 15 ft length at all values of connection slack studied. However, for connection slack greater than 3 deg, the 12 ft length showed smaller deflections than for a corresponding amount of slack on a 20 ft segment. Once again, the 20 ft length shows the largest deflections at most values of joint slack.

Effects of Friction on Lateral Displacements

The final parameter to be analyzed was the effects of the friction coefficient on barrier displacement. This study was limited to lengths of 12 ft, 15 ft, and 20 ft for two reasons. First, lengths in excess of 20 ft were not considered portable enough to warrant further study. Also, the shorter lengths had previously shown the greatest response to joint moment and slack variation and were considered the most likely to show the same response. These three lengths were then singled out for continued study. A joint with moment capacity of 150 k-ft, a slack rotation of 1 deg, and an elastic limit at 3 deg was used in all tests. The friction coefficient was varied from 0.4 to 0.6. The results are given in Table 9 and displayed in Figure 16.

None of these results can be considered surprising. As the friction value decreased for each segment length, the lateral displacement increased slightly. Since the resisting friction force is proportional to the coefficient, this simply indicates that the short segment lengths are not affected very much by changes in the friction force.

Table 9. Friction Variation Study Results.

$\phi_s = 1^o \quad \phi_e = 3^o \quad M_u = 150$ k-ft

LENGTH (ft)	FRICTION COEFFICIENT (μ)	LATERAL DEFLECTION (ft)
12	0.4	1.68
	0.5	1.61
	0.6	1.50
15	0.4	1.68
	0.5	1.60
	0.6	1.52
20	0.4	1.35
	0.5	1.26
	0.6	1.20

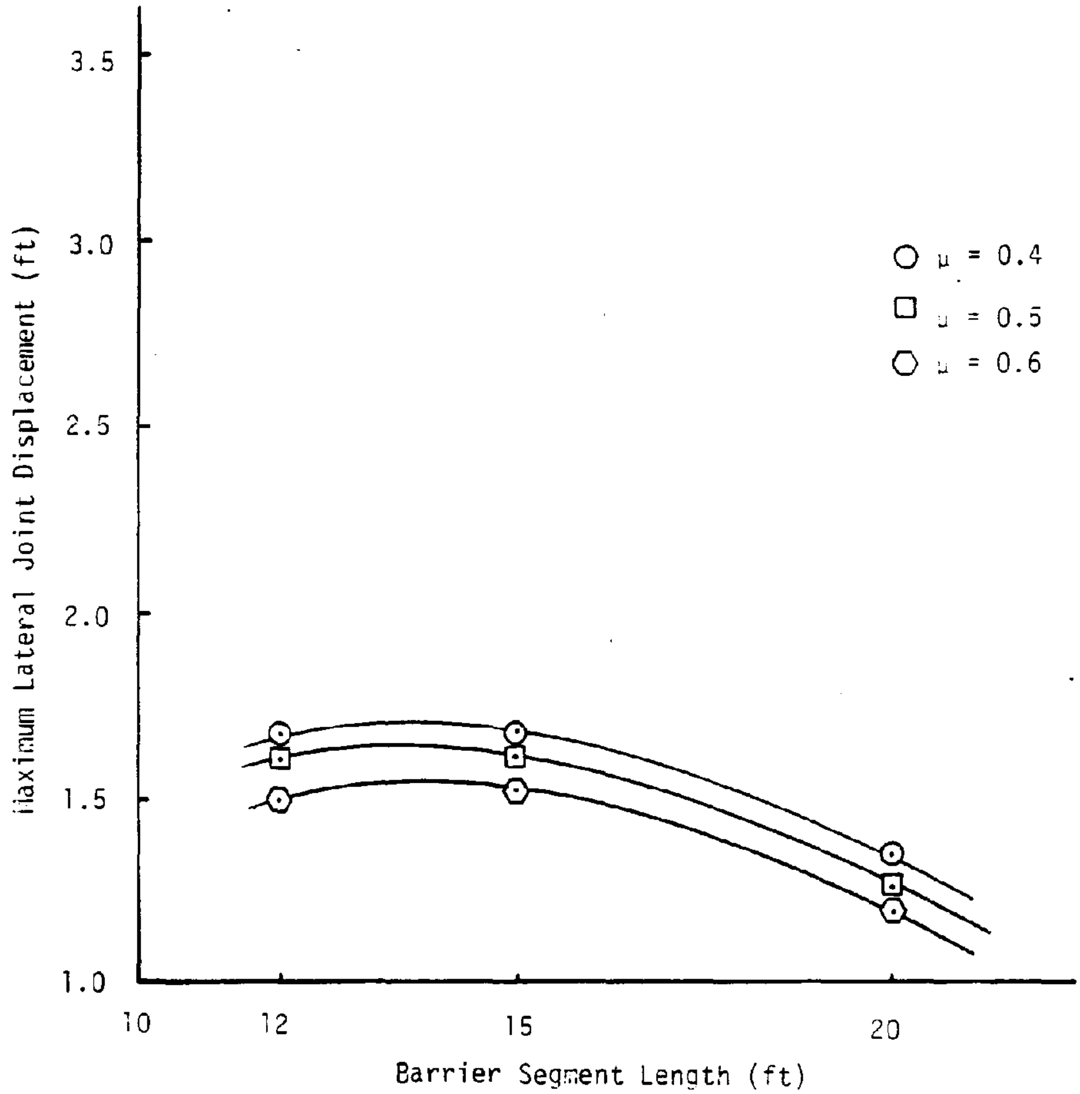

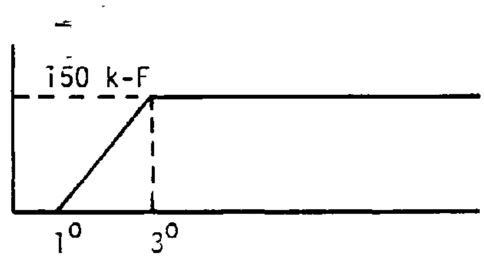

Figure 16. Lateral Joint Displacement Versus Segment Length, Variable Friction.

Analysis with Large Joint Moment Capacity and Moderate Friction

Before this part of the research was finished, there was additional interest in the effects of a high moment capacity joint with a moderate amount of friction. Three moment capacities, 50 k-ft, 100 k-ft, and 150 k-ft were selected for study. A joint with 1 deg of slack and 3 deg of elastic rotation was used, along with a friction coefficient of 0.5. Once again only 12 ft, 15 ft, and 20 ft segment lengths were used in the analysis. The displacements are given in Table 10 and are also plotted in Figures 17 and 18.

These two figures summarize the important factors to be used in the design stage. First, at 100 k-ft of moment capacity, all barriers experience approximately the same movement. At lesser joint capacities the 12 ft length shows the smallest deflection, and at 150 k-ft, the 20 ft length begins to look best. Finally, the range of 100 to 150 k-ft for joint moment capacities appears to be the maximum the 12 ft and 15 ft segments can utilize. The 20 ft length still shows a decreasing trend at 150 k-ft and may be able to use more available moment at the joint.

Table 10. Additional Results of Joint Moment-Segment Length-Deflection Study.

$\phi_s = 1^o \quad \phi_e = 3^0 \quad \mu = 0.5$

LENGTH (ft)	CONNECTION MOMENT (k-ft)	LATERAL DISPLACEMENT (ft)
12	50	1.85
	100	1.68
	150	1.61
15	50	2.11
	100	1.54
	150	1.60
20	50	2.32
	100	1.56
	150	1.26

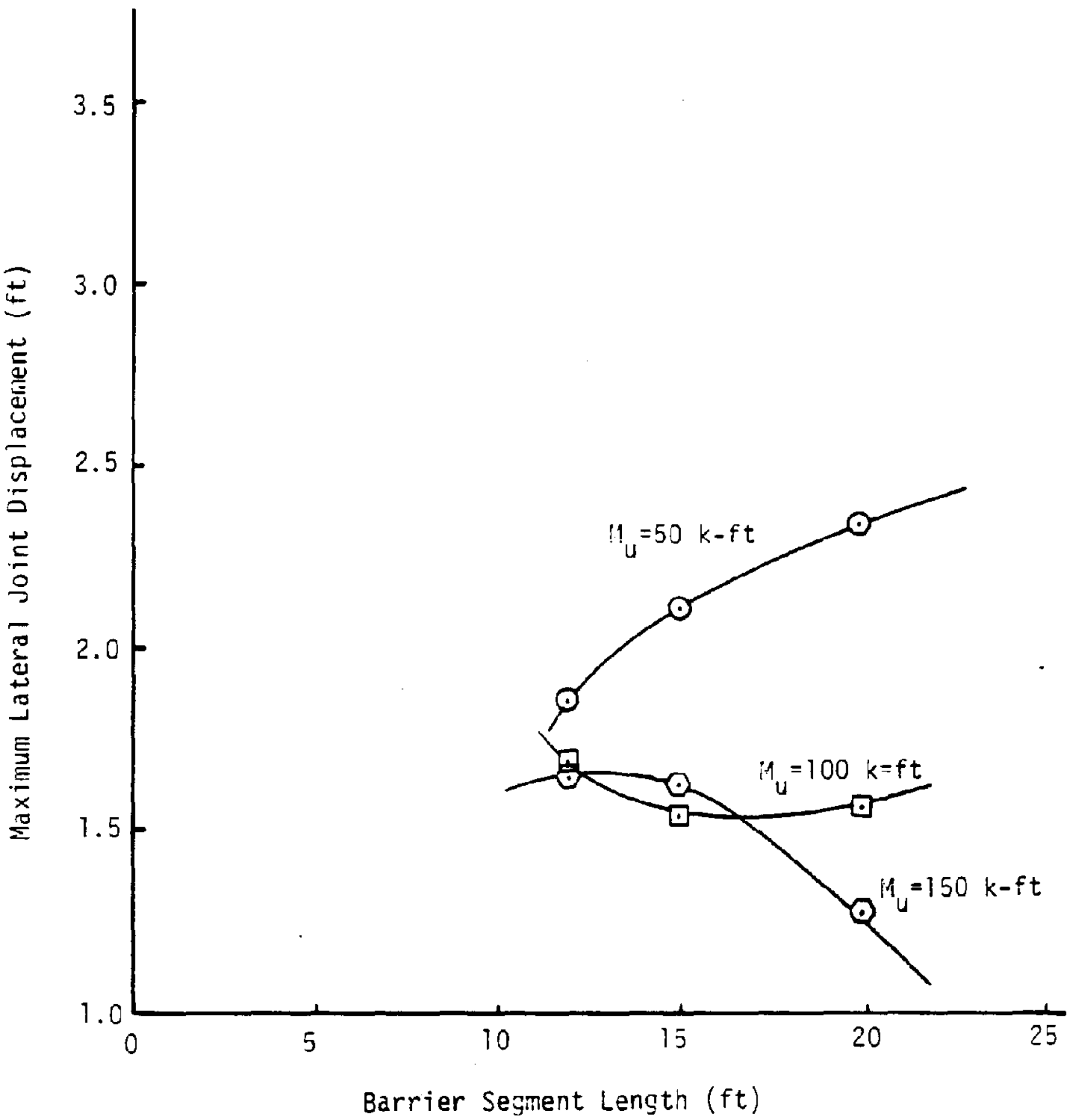

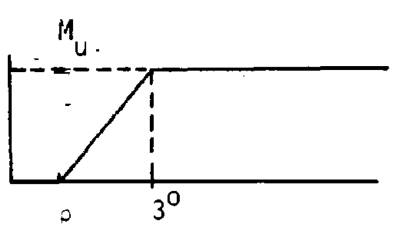

Friction Coefficient μ=0.5

Figure 17. Lateral Joint Displacement Versus Segment Length, Variable Connection Moment and Moderate Friction.

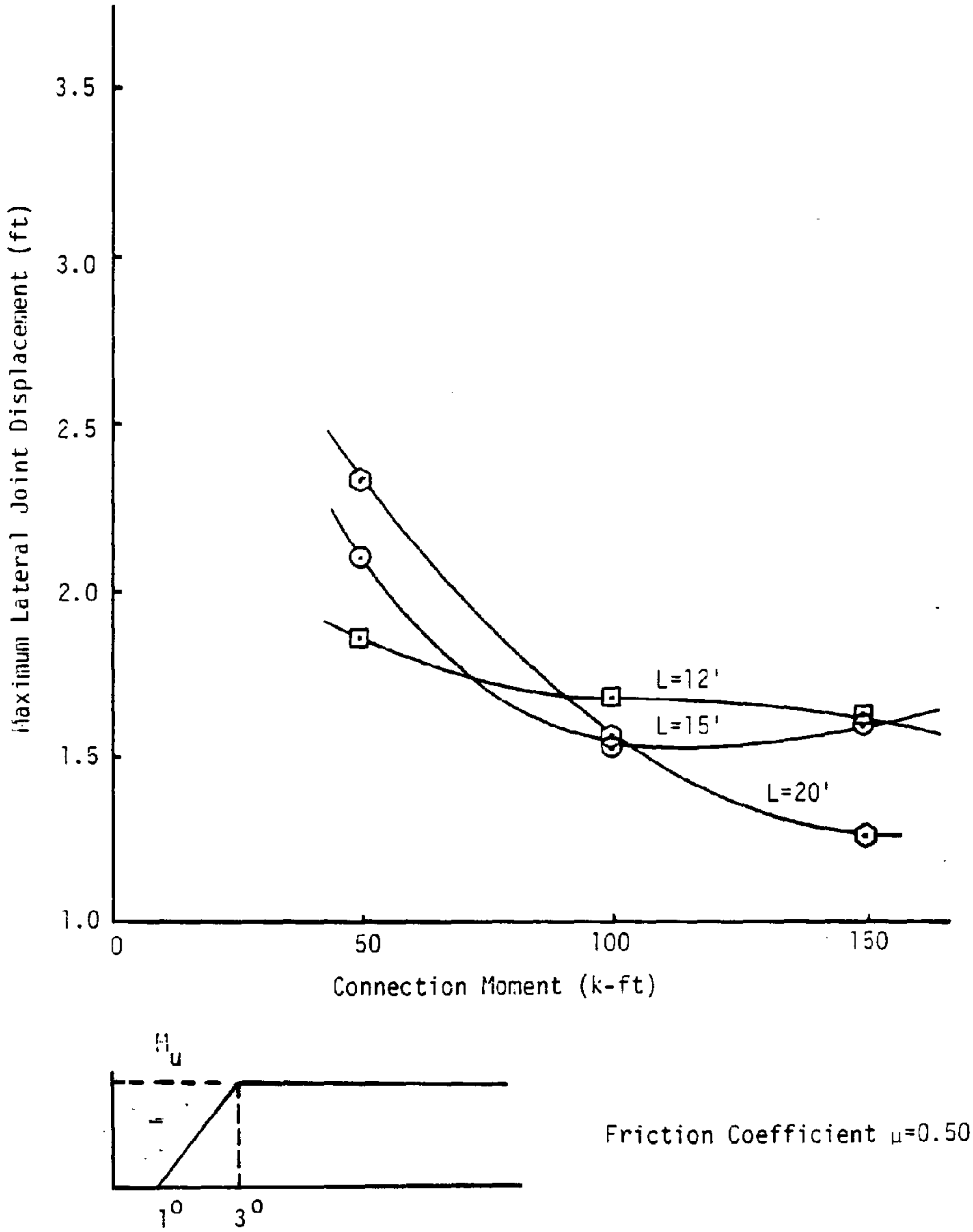

Figure 18. Lateral Joint Displacement Versus Connection Moment, Variable Length and Moderate Friction.

EQUATIONS OF MOTION

$$[D]\{\ddot{q}\} = \{E\} + \{F_s\} + \{Q_e\} + \{Q_f\} \quad \ldots\ldots\ldots \quad (96)$$

The above matrix equation defines a set of "n+2" nonlinear, second-order, simultaneous differential equations that describe the motion of the individual barrier segments.

Matrices $[D]$ and $\{E\}$ result directly from operations with the kinetic energy terms; $[D]$ may be thought of as a psuedo-mass matrix and $\{E\}$ as an inertial force matrix.

Column vector $\{F_s\}$ contains generalized forces due to potential energy in the rotational joint springs.

Column vector $\{Q_f\}$ contains generalized forces produced by friction between the barrier and the roadway.

Column vector $\{Q_e\}$ contains generalized forces resulting from external forces (impact loads).

Following are the expressions to calculate the $[D]$ matrix:
For the diagonal terms,

$$D_{1,1} = \sum_{i=1}^{n} M_i \quad \ldots\ldots\ldots \quad (97)$$

$$D_{2,2} = \sum_{i=1}^{n} Mi \quad \ldots\ldots\ldots \quad (98)$$

$$D_{i,i} = \rho_i^2 M_i + L_i \sum_{j=i+1}^{n} M_j \qquad \text{For } i = 1,2, \ldots . \text{ n-1} \quad . \quad (99)$$

$$D_{i+2,\ i+2} = \rho_n^2 M_n \qquad \text{For } i = n \quad \ldots\ldots\ldots \quad (100)$$

For the remaining row one terms,

$$D_{1,2} = 0 \quad \dots \dots \quad (101)$$

$$D_{1,i} = \rho_i M_i \text{Sin}\phi_i - L_i \text{Sin}\phi_i \sum_{j=i+1}^{n} M_j \qquad \text{For } i - 1,2, \dots n-1 \quad \dots (102)$$

$$D_{1,i+2} = -\rho_n M_n \text{Sin}\phi_n \qquad \text{For } i = n \quad \dots \dots (103)$$

For row two terms,

$$D_{2,i+2} = \rho_i M_i \text{Cos}\phi_i + L_i \text{Cos}\phi_i \sum_{j=i+1}^{n} M_j \qquad \text{For } i = 1,2, \dots n-1 \quad \dots (104)$$

$$D_{2,i+2} = \rho_n M_n \text{Cos}\phi_n \qquad \text{For } i = n \quad \dots \dots (105)$$

For row 3 to row n+1

$$D_{i+2,j+2} = L_i \text{Cos}(\phi_u - \phi_j)(\rho_j M_j + L_j \sum_{k=j+1}^{n} M_k) \qquad \text{For } i = 1,2, \dots n-1, \quad j = 1,2, \dots n-1 \quad \dots (106)$$

For n+2 column,

$$D_{i+2,n+2} = L_i \rho_{n+2} M_{n+2} \text{Cos}(\phi_i - \phi_{n+2}) \qquad \text{For } i = 1,2, \dots n \quad \dots (107)$$

[D] is a symmetric matrix, so it is only necessary to calculate half of the matrix, and then set

$$D_{ji} = D_{ij} \qquad \text{For } j = 2,3, \dots n-12, \quad i = 1, \dots j-1 \quad \dots (108)$$

Following are the elements for column vector $\{E\}$:

For row one

$$E_1 = \sum_{i=1}^{n} \dot{\phi}_i^2 \text{ Cos}\phi_i \ \rho_i M_i + L_i (\sum_{j=i+1}^{n} M_i) \quad \dots \dots (109)$$

For row two term,

$$E_2 = \sum_{i=1}^{n} \phi_i^2 \text{ Cos}\phi_i \ \rho_i M_i + L_i \sum_{j=i+1}^{n} M_j) \quad \dots \dots (110)$$

Remaining terms, rows 3 through n+2,

$$E_{i+2} = \sum_{j=1}^{i-1} L_j \phi_j^2 \, \text{Sin} (\phi_j - \phi_i) \quad (\rho_i M_i + L_i \sum_{k=i+1}^{n} M_k)$$

$$+ L_i \sum_{j=i+1}^{n} M_j \rho_j \phi_j^2 \, \text{Sin}(\phi_j - \phi_i)$$

$$+ L_i \sum_{j=i+1}^{n} L_j \phi_j^2 \, \text{Sin}(\phi_j - \phi_i \sum_{k=j+1}^{n} M_k \quad \ldots\ldots\ldots\ldots\ldots (111)$$

Note that the first term is not included in the E_3 calculation, the second term is not included in the E_{n+2} calculation, and the third term is not a part of the E_{n+1} or E_{n+2} calculation.

Following are the elements for column vector $\{F_s\}$:

$F_{s_1} = 0$ . . . . (112)

$F_{s_2} = 0$ . . . . (113)

$F_{s_{i+2}} = -M_{u_i}$ For i = 1 . . . . (114)

$F_{s_{i+2}} = M_{u_{i-1}} - M_{u_i}$ For i = 2,3, ... n-1 . . . . (115)

$F_{s_{i+2}} = M_{u_{i-1}}$ For i = n . . . . (116)

where M_{u_i} is the moment in spring "i". This value is dependent on the particular response range the spring has been deformed to and the spring's previous loading history. This relationship or spring moment to displacement is shown in Figure 7 of the main body of this appendix.

Following are the elements of the $\{Q_e\}$ column vector:

For a force located on segment j

$Q_{e1} = -Fy' \tan_j$ . . . . (117)

$Q_{e2} = Fy'$ . . . . (118)

$$Q_{e_{i+2}} = Fy' L_i (\cos\phi_i + \sin\phi_i \tan\phi_j) \qquad \text{For } i = 1,2, \ldots j-1 \quad \ldots (119)$$

$$Q_{e_j} = Fy' \sec^2\phi_j (X_F' - X_{ir}') \quad \ldots (120)$$

$$Q_{e_{i+2}} = 0 \qquad \text{For } i > j \quad \ldots (121)$$

Following are the elements for the $\{Q_f\}$ column vector:

$$Qf_1 = -\sum_{i=1}^{n} C_{ti} \frac{\dot{X}_i'}{\dot{R}_i} W_i \mu_i \quad \ldots (122)$$

$$Qf_2 = \sum_{i=1}^{n} C_{ti} \frac{\dot{Y}_i'}{\dot{R}_i} W_i \mu_i \quad \ldots (123)$$

$$Qf_{i+2} = C_{ti} \frac{\rho_i W_i \mu_i}{\dot{R}_i} \dot{X}_i' \sin\phi_1 + \dot{Y}_i' \cos\phi_i$$

$$+ L_i \sum_{j=i+1}^{n} C_{tj} \frac{W_j \mu_j}{\dot{R}_j} X_j' \cos\phi_i + \dot{Y}_j' \sin\phi_i$$

$$- Cr_i \frac{\dot{\phi}_i}{\dot{\phi} i} \frac{W_i \mu_i L_i}{4} \qquad \text{For } i = 1,2, \ldots n \quad \ldots (124)$$

LISTING OF THE COMPUTER PROGRAM

```
      REAL PHI(15), PHID(15), PHIO(15)
      REAL RHS(17)
      REAL KE, KP, XL, M, L, IO
      CHARACTER*80 HEAD1, HEAD2
      COMMON /TITLE/ HEAD1, HEAD2
      COMMON /MEMBER/ M(15), P(15), L(15), IO(15), U(15), W(15)
      COMMON /SPRING/ PHIS,PHIE,PHIP,PHIF,KE,KP,KL,EMOM,PMOM
     +                .PHIZ(14).KEY(14).OPHI(14)
      COMMON /ENDPT/ XI(15), YI(15), XT(15), YT(15)
      COMMON /CGPROP/ XD(15), YD(15), XDD(15), YDD(15)
      COMMON /MATRIX/ D(17,18), E(17), FS(17), QE(17), QF(17)
      COMMON /CONST/ N,NP1,NP2,NM1,NPROT,MARK,INDEX,DT,ET,ER,PI
      COMMON /IMPACT/ TMPT(50), XPT(50), FPT(50), NPTS, IPT, XF, IMPACT
     +                 , CF, FX, FY
      COMMON /ALPHAS/  AYD(17), AZD(17), QDD(17)
      COMMON /MAXDIS/ DEFL, NOPT, TIMEMX
      EQUIVALENCE (E(1),RHS(1))
      PI = 4.0*ATAN(1.0)
    1 CALL DATAIN (XRO,YRO,PHIO)
      IF (N.EQ.0) GO TO 100
      NP2 = N + 2
      NP1 = N + 1
      NM1 = N - 1
      IPT = 1
      CALL INITL (PHI,PHIO,PHID,XR,XRO,XRD,YR,YRO,YRD,TIME)
      CALL LOCATE (XR,YR,PHI,TIME)
      CALL ECHO (PHIO)
      AYD(1) = XR
      AYD(2) = YR
      AZD(1) = XRD
      AZD(2) = YRD
      DO 5 K = 1,N
      KP2 = K + 2
      AYD(KP2) = PHI(K)
      AZD(KP2) = PHID(K)
    5 CONTINUE
      CALL STEPS (TIME)
      NOT = 0
      NTIME = TMPT(NPTS)/DT + 0.001
      DO 75 NSTEP = 1, NTIME
      CALL RKSOLN (XR,YR,PHI,XRD,YRD,PHID,TIME)
      IF (MARK.GT.0) GO TO 100
      IF (INDEX.EQ.1) GO TO 100
      NOT = NOT + 1
      TIME = TIME + DT
      IF (NOT - NPROT) 75,60,60
   60 NOT = 0
      CALL LOCATE (XR,YR,PHI,TIME)
      CALL ACCEL (PHI,PHID,QDD)
      CALL ENDFRC (PHI)
      CALL OUTPUT (TIME,PHI)
75    CONTINUE
      DEFL = DEFL*12.0
      WRITE (6,630) DEFL, NOPT, TIMEMX
      GO TO 1
100   WRITE (6,699)
      STOP
630 FORMAT ('1',T15,'MAXIMUM DEFLECTION = ',F8.2,' INCHES' // T15,
   + 'AT END POINT NUMBER ',I5 // T15,'AT TIME = ',F7.3,' SECONDS')
699 FORMAT ('-',15X,'** PROGRAM=CMBTEST,NORMAL END **')
      END
```

```
      SUBROUTINE DATAIN (XRO,YRO,PHIO)
      COMMON /TITLE/ HEAD1, HEAD2
      COMMON /CONST/ N,NP1,NP2,NM1,NPROT,MARK,INDEX,DT,ET,ER,PI
      COMMON /MEMBER/ M(15), P(15), L(15), IO(15), U(15), W(15)
      COMMON /SPRING/ PHIS,PHIE,PHIP,PHIF,KE,KP,KL,EMOM,PMOM
     +                 ,PHIZ(14),KEY(14),DPHI(14)
      COMMON /IMPACT/ TMPT(50), XPT(50), FPT(50), NPTS, IPT, XF, [NUMAA
     +                 , CF, FX, FY
      CHARACTER*80 HEAD1, HEAD2
      REAL  PHIO(15)
      REAL KE, KP, KL, M, L, IO
C    *   FIRST CARD, DESRIPTIVE INFORMATION
      READ (5,500,END=99) HEAD1
C    *   SECOND CARD, ADDITIONALINFORMATION
      READ (5,500) HEAD2
C    *   THIRD CARD, PROGRAM CONSTANTS
      READ (5,520) N, NPROT, DT, ET, ER
      IF (N.EQ.0) GO TO 100
C    *   FOURTH CARD SERIES, READ IN THE BARRIER SEGMENT PROPERTIES
      READ (5,540) (M(I),L(I),P(I),IO(I),U(I),I=1,N)
C    *   FIFTH CARD SET, JOINT SPRING PARAMETERS
      READ (5,540) PHIS, PHIE, PHIP, PHIF
      READ (5,540) KE, KP, KL
C    *   SIXTH CARD SET, INITIAL POSITON OF BARRIER
      READ (5,540) XRO, YRO
      READ (5,540) (PHIO(I),I=1,N)
C    *   SEVENTH CARD SET, IMPACT FORCE ON BARRIER
      READ (5,560) NPTS, PTIMP,  CF
      READ (5,580) (TMPT(I),XPT(I),FPT(I),I=1,NPTS)
      RETURN
   99 WRITE (6,699)
      N = 0
      RETURN
  100 WRITE (6,690)
      RETURN
  500 FORMAT (A80)
  520 FORMAT (2I5,3F10.5)
  540 FORMAT (9F10.4)
  560 FORMAT (I5,5X,2F10.2)
  580 FORMAT (6F10.2)
  690 FORMAT ('1',15X,'** ERROR **' / 18X,'NUMBER OF ELEMENTS = 0')
  699 FORMAT ('1',15X,'** ERROR **' / 19X,'NO DATA FOUND')
      END


      SUBROUTINE INITL (PHI,PHIO,PHID,XR,XRO,XRD,YR,YRO,YRD,TIME)
      COMMON /MEMBER/ M(15), P(15), L(15), IO(15), U(15), W(15)
      COMMON /CONST/ N,NP1,NP2,NM1,NPROT,MARK,INDEX,DT,ET,ER,PI
      COMMON /SPRING/ PHIS,PHIE,PHIP,PHIF,KE,KP,KL,EMOM,PMOM
     +                 ,PHIZ(14),KEY(14),DPHI(14)
      COMMON /MEMFRC/ Q1(15), Q2(15), Q3(15), Q4(15), Q5(15), Q6(15)
      COMMON /MAXDIS/ DEFL, NOPT, TIMEMX
      REAL PHI(15), PHIO(15), PHID(15)
      REAL KE, KP, KL, M
      XF = 0.0
      TIME = 0.0
      DEFL = 0.0
C    *   INITAILIZE THE BARRIER POSITION AND CONVERT PHI TO RADIANS
      XR = XRO
      YR =YRO
      DO 20 I = 1,N
      PHI(I) =  PHIO(I)/180.0*PI
   20 CONTINUE
C    *   SET THE INITIAL VELOCITIES TO ZERO
      XRD = 0.0
      YRD = 0.0
      DO 30 I = 1,N
      PHID(I) = 0.0
   30 CONTINUE
C    *   CALCULATE THE BARRIER WEIGHTS FROM THE MASS VALUES
      DO 40 I = 1,N
```

```
      W(I) = 32.2*M(I)
   40 CONTINUE
C    *    INTIALIZE JOINT SPRING PROPERTIES
      EMOM = KE*(PHIS-PHIS)
      PMOM = KP*(PHIP-PHIE)
      DO 50 I = 1,NM1
      IP1 = I + 1
      DPHI(I) = PHI(I) - PHI(IP1)
      PHIZ(I) = 0.0
      KEY(I) = 0
   50 CONTINUE
C    *    SET MEMBER END FORCES OF BARRIER ONE TO ZERO
      Q1(1) = 0.0
      Q2(1) = 0.0
      Q3(1) = 0.0
      Q6(N) = 0.0
      RETURN
      END

      SUBROUTINE ECHO (PHI0)
      COMMON /TITLE/ HEAD1, HEAD2
      COMMON /MEMBER/ M(15), P(15), L(15), IO(15), U(15), W(15)
      COMMON /CONST/ N,NP1,NP2,NM1,NPROT,MARK,INDEX,DT,ET,ER,PI
      COMMON /ENDPT/ XI(15), YI(15), XT(15), YT(15)
      COMMON /SPRING/ PHIS,PHIE,PHIP,PHIF,KE,KP,KL,EMOM,PMOM
     +                ,PHIZ(14),KEY(14),DPHI(14)
      COMMON /IMPACT/ TMPT(30), XPT(30), FPT(30), NPTS, IPT, XF, IMPAC
     +                , CF, FX, FY
      CHARACTER*80 HEAD1, HEAD2
      REAL    PHI0(15)
      REAL KE, KP, KL, M, L, IO
      WRITE (6,600) HEAD1, HEAD2
      WRITE (6,610) (I,M(I),L(I),IO(I),U(I), I=1,N)
      WRITE (6,620)
      WRITE (6,630) (I,PHI0(I),XI(I),YI(I),XT(I),YT(I), I=1,N)
      WRITE (6,640) ET, ER
      WRITE (6,650)
      WRITE (6,660) (TMPT(J),XPT(J),FPT(J), J=1,NPTS)
      WRITE (6,670) PHIS, PHIE, PHIP, PHIF, KE, KP, KL
C    *    CONVERT THE STIFFNESS' TO FT-LB/RADIAN
      KE = KE*180./PI
      KP = KP*180./PI
      KL = KL*180./PI
C    *    ADJUST THE ANGLE CHECK VALUES TO RADIANS
      PHIS = PHIS*PI/180.
      PHIE = PHIE*PI/180.
      PHIP = PHIP*PI/180.
      RETURN
  600 FORMAT ('1',5X,A80 // 5X,A80 //
     +       / 10X,'ELEMENT PROPERTIES FOR SEGMENTAL CONCRETE MEDIAN'
     + ,' BARRIER SYSTEM' // T20,'ELEMENT',T54,'MOMENT OF',T66,'BARRIER'
     +/ T22,'NO.',T32,'MASS',T42,'LENGTH',T55,'INERTIA',T66,'FRICTION'/)
  610 FORMAT (' ',20X,I2,5X,F9.3,5X,F6.2,5X,F9.3,5X,F5.3)
  620 FORMAT ('-'///30X,'INITIAL POSITION FOR SEGMENTAL BARRIER SYSTEM',
     + // T20,'ELEMENT',T44,'INITIAL END',T68,'TERMINAL END' / T22,'NO.'
     + ,T31,'PHI',T43,'X''',T55,'Y''',T67,'X''',T79,'Y'''/)
  630 FORMAT (' ',20X,I2,5X,F6.2,5X,F7.2,5X,F7.2,5X,F7.2,5X,F7.2)
  640 FORMAT ('1',T10,50('*') / T10,'TRANSLATIONAL ADJUSTMENT FOR FRICTI
     +ON =',F10.4 // T10,'ROTATIONAL ADJUSTMENT FOR FRICTION =',3X,
     + F10.4 / T10,50('*') )
  650 FORMAT ('-',T13,'TIME-DISPLACEMENT-FORCE INPUT' / T13,'TIME',T23,
     + 'POSTION',T37,'FORCE' / T13,'(SEC)',T25,'(FT)',T37,'(LBS)' / T12,
     + 31('*') /)
  660 FORMAT (' ',10X,F5.4,3X,F6.2,5X,F9.2)
  670 FORMAT ('-',T18,'JOINT MOMENT PROPERTIES' / T12,35('*') // T15,
     + 'JOINT ROTATION IS:' / T20,'SLACK UP TO',F8.2 / T20,'ELASTIC UP T
     +O',F6.2 / T20,'PLASTIC UP TO',F6.2 / T20,'FAILURE AT',3X,F6.2
     + //    T15,'ELASTIC STIFFNESS = ',
     + F10.1 / T15,'PLASTIC STIFFNESS = ',F10.1 / T15,
     + 'LOCK-UP STIFFNESS = ',F10.1 / T12,35('*') )
      END
```

```
      SUBROUTINE RKSOLN (XR,YR,PHI,XRD,YRD,PHID,TIME)
      COMMON /ALPHAS/  AYD(17), AZD(17), QDD(17)
      COMMON /CONST/ N,NP1,NP2,NM1,NPRDT,MARK,INDEX,DT,ET,ER,PI
      REAL PHI(15), PHID(15)
      REAL AY(17), AYY(17), AZ(17), AZZ(17)
      AY(1) = DT*XRD
      AY(2) = DT*YRD
      DO 10 K = 3,NP2
      KM2 = K - 2
      AY(K) = DT*PHID(KM2)
   10 CONTINUE
      DO 20 K = 1,NP2
      AZ(K) = DT*QDD(K)
   20 CONTINUE
      DO 30 K = 1,NP2
      AYY(K) = AY(K)/6.0
      AZZ(K) = AZ(K)/6.0
   30 CONTINUE
      DO 80 J = 2,4
      FRAC = 0.5
      IF (J.EQ.4) FRAC = 1.0
      AYD(1) = XR + FRAC*AY(1)
      AYD(2) = YR + FRAC*AY(2)
      AZD(1) = XRD + FRAC*AZ(1)
      AZD(2) = YRD + FRAC*AZ(2)
      DO 40 K = 3,NP2
      KM2 = K - 2
      AYD(K) = PHI(KM2) + FRAC*AY(K)
      AZD(K) = PHID(KM2) + FRAC*AZ(K)
   40 CONTINUE
      TMINC = TIME + DT*FRAC
      CALL STEPS (TMINC)
      IF (MARK.GT.0) GO TO 100
      IF (INDEX.EQ.1) GO TO 100
      DO 60 I = 1,NP2
      AY(I) = DT*AZD(I)
      AZ(I) = DT*QDD(I)
      AYY(I) =  AYY(I) + AY(I)/(6.0*FRAC)
      AZZ(I) = AZZ(I) + AZ(I)/(6.0*FRAC)
   60 CONTINUE
   80 CONTINUE
      XR = XR + AYY(1)
      YR = YR + AYY(2)
      XRD = XRD + AZZ(1)
      YRD = YRD + AZZ(2)
      DO 90 K = 3,NP2
      KM2 = K - 2
      PHI(KM2) = PHI(KM2) + AYY(K)
      PHID(KM2) = PHID(KM2) + AZZ(K)
   90 CONTINUE
  100 RETURN
      END
```

```
      SUBROUTINE STEPS (TIME)
      COMMON /ALPHAS/  AYD(17), AZD(17), QDD(17)
      COMMON /CONST/ N,NP1,NP2,NM1,NPROT,MARK,INDEX,DT,ET,ER,PI
      REAL XD(15), YD(15), PHI(15), PHID(15), RHS(17)
      EQUIVALENCE (AYD(1),XR), (AYD(2),YR), (AZD(1),XRD), (AZD(2),YRD)
      EQUIVALENCE (AYD(3),PHI(1)), (AZD(3),PHID(1))
C     EQUIVALENCE (RHS,QDD)
      COMMON /MATRIX/ D(17,18), RHS
      CALL LOCATE (XR,YR,PHI,TIME)
      CALL TRNVEL (XRD,YRD,PHID,PHI)
      CALL FORCE (TIME)
      CALL DMTRX (PHI)
      CALL EMTRX (PHI,PHID,XRD,YRD)
      CALL FSMTRX (PHI)
      CALL DEMTRX (PHI)
      IF (MARK.GT.0) GO TO 100
      CALL DFMTRX (PHI,PHID)
      CALL ADD
      CALL GAUSS (QDD)
  100 RETURN
      END


      SUBROUTINE LOCATE (XR,YR,PHI,TIME)
      COMMON /CONST/ N,NP1,NP2,NM1,NPROT,MARK,INDEX,DT,ET,ER,PI
      COMMON /MEMBER/ M(15), P(15), L(15), IO(15), J(15), W(15)
      COMMON /MAXDIS/ DEFL, NDPT, TIMEMX
      COMMON /ENDPT/ XI(15), YI(15), XT(15), YT(15)
      REAL PHI(15), L
C    *   CALCULATE X-COORDINATES OF SEGMENT ENDPOINTS
      XI(1) = XR
      DO 20 J = 1,NM1
      JP1 = J + 1
      XI(JP1) = XI(J) + COS(PHI(J))*L(J)
      XT(J) = XI(JP1)
   20 CONTINUE
      XT(N) = XI(N) + COS(PHI(N))*L(N)
C    *   CALCULATE Y-COORDINATES OF SEGMENT ENDPOINTS
      YI(1) = YR
      DO 40 J = 1,NM1
      JP1 = J + 1
      YI(JP1) = YI(J) + L(J)*SIN(PHI(J))
      YT(J) = YI(JP1)
   40 CONTINUE
      YT(N) = YI(N) + SIN(PHI(N))*L(N)
C    *   CHECK FOR MAXIMUM ENDPOINT DISPLACEMENT
      DO 60 I = 1,N
      IF (ABS(YI(I))-DEFL) 60,55,55
   55 DEFL = ABS(YI(I))
      NDPT = I
      TIMEMX = TIME
   60 CONTINUE
      IF (ABS(YT(N))-DEFL) 70,65,65
   65 DEFL = ABS(YT(N))
      NDPT = N + 1
      TIMEMX = TIME
   70 CONTINUE
      RETURN
      END
```

```
      SUBROUTINE TRNVEL (XRO,YRO,PHID,PHI)
      COMMON /MEMBER/ M(15), P(15), L(15), IO(15), J(15), W(15)
      COMMON /CONST/ N,NP1,NP2,NM1,NPROT,MARK,INDEX,DT,ET,ER,PI
      COMMON /CGPROP/ XD(15), YD(15), XDD(15), YDD(15)
      REAL PHI (15), PHID(15), L
C    *   FIND CENTER OF MASS TRANSLATIONAL VELOCITY IN GLOBAL X-DIRECTION
      DO 50 I = 1,N
      XD(I) = XRO - P(I)*SIN(PHI(I))*PHID(I)
      IF (I.EQ.1) GO TO 50
      SUM = 0.0
      IM1 = I - 1
      DO 40 K = 1,IM1
      SUM = SUM + L(K)*SIN(PHI(K))*PHID(K)
   40 CONTINUE
      XD(I) = XD(I) - SUM
   50 CONTINUE
C    *   FIND CENTER OF MASS TRANSLATIONAL VELOCITY IN GLOBAL Y-DIRECTION
      DO 100 I = 1,N
      YD(I) = YRO + P(I)*COS(PHI(I))*PHID(I)
      IF (I.EQ.1) GO TO 100
      SUM = 0.0
      IM1 = I - 1
      DO 90 K = 1,IM1
      SUM = SUM + L(K)*COS(PHI(K))*PHID(K)
   90 CONTINUE
      YD(I) = YD(I) + SUM
  100 CONTINUE
      RETURN
      END
```

```
      SUBROUTINE FORCE (TIME)
      COMMON /IMPACT/ TMPT(50), XPT(50), FPT(50), NPTS, IPT, XF, IMPBAR
     +                , CF, FX, FY
C    *   FIND RANGE OF TIME TO INTERPOLATE BETWEEN
      IPTP1 = IPT + 1
      IF (TIME.GE.TMPT(IPT) .AND. TIME.LT.TMPT(IPTP1)) GO TO 30
      DO 20 N = IPT,NPTS
      I = N
      IF ((TMPT(N).LE.TIME) .AND. (TMPT(NP1).GT.TIME)) GO TO 25
   20 CONTINUE
      MARK = 20
      GO TO 100
   25 IPT = I
      IPTP1 = IPT + 1
C    *   FIND CORRESPONDING FORCE AND LOCATION FOR CURRENT VALUE OF TIME
   30 XF = XPT(IPT) + (XPT(IPTP1)-XPT(IPT))/(TMPT(IPTP1)-TMPT(IPT))*
     + (TIME-TMPT(IPT))
      FY = FPT(IPT) + (FPT(IPTP1)-FPT(IPT))/(TMPT(IPTP1)-TMPT(IPT))*
     + (TIME-TMPT(IPT))
      FX = CF*FY
  100 RETURN
      END
```

```
      SUBROUTINE DMTRX (PHI)
      COMMON /MEMBER/ M(15), P(15), L(15), IO(15), U(15), W(15)
      COMMON /MATRIX/ D(17,18), E(17), FS(17), GE(17), GF(17)
      COMMON /CONST/ N,NP1,NP2,NM1,NPROT,MARK,INDEX,DT,ET,ER,PI
      REAL PHI(15)
      REAL M, L, IO
C   *   CALCULATE DIAGONAL TERMS
      SUM = 0.0
      DO 1 I = 1,N
      SUM = SUM + M(I)
    1 CONTINUE
      D(1,1) = SUM
      D(2,2) = SUM
      DO 10 I = 3,NP2
      IM1 = I - 1
      IM2 = I - 2
      D(I,I) = P(IM2)**2 *M(IM2) + IO(IM2)
      IF ( IM2.GE.N) GO TO 10
      SUM = 0.0
      DO 5 J = IM1,N
      SUM = SUM + M(J)
    5 CONTINUE
      D(I,I) = D(I,I) + SUM*L(IM2)**2
   10 CONTINUE
C   *   CALCULATE ROW ONE TERMS
      D(1,2) = 0.0
      DO 20 J = 3,NP2
      JM1 = J - 1
      JM2 = J - 2
      D(1,J) = -P(JM2)*M(JM2)
      IF (JM2.GE.N) GO TO 20
      SUM = 0.0
      DO 15 JJ = JM1,N
      SUM = SUM + M(JJ)
   15 CONTINUE
      D(1,J) =  D(1,J) - SUM*L(JM2)
   20 D(1,J) = D(1,J)*SIN(PHI(JM2))
C   *   CALCULATE ROW TWO TERMS
      DO 30 J = 3,NP2
      JM1 = J - 1
      JM2 = J - 2
      D(2,J) = P(JM2)*M(JM2)
      IF (JM2.GE.N) GO TO 30
      SUM = 0.0
      DO 25 JJ = JM1,N
      SUM = SUM + M(JJ)
   25 CONTINUE
      D(2,J) =  D(2,J) + SUM*L(JM2)
   30 D(2,J) = D(2,J)*COS(PHI(JM2))
C   *   CALCULATE REMAINING D MATRIX ELEMENTS
      DO 50 I = 3,NP1
      IP1 = I + 1
      IM2 = I - 2
      DO 50 J = IP1,NP2
      JM1 = J - 1
      JM2 = J - 2
      D(I,J) = L(IM2)*P(JM2)*M(JM2)
      IF (JM1.GT.N) GO TO 50
      SUM = 0.0
      DO 45 JJ = JM1,N
      SUM = SUM + M(JJ)
   45 CONTINUE
      D(I,J) =  D(I,J) + SUM*L(IM2)*L(JM2)
   50 D(I,J) = D(I,J)*COS(PHI(JM2)-PHI(IM2))
      DO 60 I = 2,NP2
      IM1 = I - 1
      DO 60 J = 1,IM1
      D(I,J) = D(J,I)
   60 CONTINUE
      RETURN
      END
```

```
      SUBROUTINE EMTRX (PHI,PHID,XRO,YRO)
      COMMON /MEMBER/ M(15), P(15), L(15), IO(15), J(15), W(15)
      COMMON /MATRIX/ D(17,13), E(17), FS(17), DE(17), DF(17)
      COMMON /CONST/ N,NP1,NP2,NM1,NPROT,MARK,INDEX,DT,ET,ER,PI
      REAL  PHI(15), PHID(15)
      REAL LI, L, M
C    *   CALCULATE ROW ONE TERM
      E(1) = 0.0
      DO 20 K = 1,N
      KP1 = K + 1
      SUM = 0.0
      IF (K.EQ.N) GO TO 15
      DO 10 I = KP1,N
      SUM = SUM + M(I)
   10 CONTINUE
   15 E(1) = E(1) + (L(K)*SUM + P(K)*M(K))*PHID(K)**2*COS(PHI(K))
   20 CONTINUE
C    *   CALCULATE ROW TWO TERM
      E(2) = 0.0
      DO 70 K = 1,N
      KP1 = K + 1
      SUM = 0.0
      IF (K.EQ.N) GO TO 65
      DO 50 I = KP1,N
      SUM = SUM + M(I)
   50 CONTINUE
   65 E(2) = E(2) + (L(K)*SUM + P(K)*M(K))*PHID(K)**2*SIN(PHI(K))
   70 CONTINUE
C    *   CALCULATE REMAINING E MATRIX TERMS
   80 DO 200 I = 1,N
      IP1 = I + 1
      IP2 = I + 2
      E(IP2) = 0.0
      PMI = P(I)*M(I)
      LI = L(I)
      IF (I.EQ.1) GO TO 135
      IM1 = I - 1
      SUM = 0.0
      IF (I.EQ.N) GO TO 125
      DO 120 K = IP1,N
      SUM = SUM + M(K)
  120 CONTINUE
  125 DO 130 J = 1,IM1
      E(IP2) = E(IP2) + PHID(J)**2*L(J)*
     + SIN(PHI(J)-PHI(I))*(PMI + LI*SUM)
  130 CONTINUE
      IF (I.EQ.N) GO TO 200
  135 SUM = 0.0
      DO 140 K = IP1,N
      SUM = SUM + M(K)*P(K)*PHID(K)**2
     + *SIN(PHI(K) -  PHI(I))
  140 CONTINUE
      E(IP2) = E(IP2) + L(I)*SUM
      SUM = 0.0
      IF (IP1.GE.NM1) GO TO 200
      DO 160 J = IP1,NM1
      SUM = SUM + L(J)*PHID(J)**2*SIN(PHI(J)-PHI(I))
      JP1 = J + 1
      PROD = 0.0
      DO 150 K = JP1,N
      PROD = PROD + SUM*M(K)
  150 CONTINUE
      E(IP2) = E(IP2) + LI*PROD
  160 CONTINUE
  200 CONTINUE
      RETURN
      END
```

```
      SUBROUTINE FSMTRX (PHI)
      COMMON /MATRIX/ D(17,18), E(17), FS(17), QE(17), QF(17)
      COMMON /CONST/ N,NP1,NP2,NM1,NPROT,MARK,INDEX,DT,ET,ER,PI
      COMMON /SPRING/ PHIS,PHIE,PHIP,PHIF,KE,KP,KL,EMOM,PMOM
     *               ,PHIZ(14),KEY(14),DPHI(14)
      COMMON /MEMFRC/ Q1(15), Q2(15), Q3(15), Q4(15), Q5(15), Q6(15)
      REAL PHI(15), KE, KP, KL
      DO 10 I = 1,3
      FS(I) = 0.0
   10 CONTINUE
      DO 100 I = 1,NM1
      IP1 = I + 1
      IP2 = I + 2
      IP3 = I + 3
      PHIL = DPHI(I)
C   *   CALCULATE DIFFERENTIAL SPRING ROTATION
      DPHI(I) = PHI(I) - PHI(IP1)
      IF (KEY(I).EQ.3) GO TO  75
C   *   CHECK FOR JOINT SPRING FAILURE
      IF (ABS(DPHI(I))-PHIF)  20,15,15
   15 KEY(I) = 3
      GO TO  75
   20 IF (DPHI(I).NE.0.0) GO TO  25
      SGN = 1.0
      GO TO  30
   25 SGN = ABS(DPHI(I))/DPHI(I)
   30 ADPHI = ABS(DPHI(I))
C   *   CHECK FOR DECREASING SPRING ROTATION
      IF (ADPHI.GT.ABS(PHIL)) GO TO  60
      IF (KEY(I)-1)  35, 65, 35
   35 KEY(I) = 1
C   *   FIND RANGE OF SPRING ROTATION, AND ADJUST IF NECESSARY
      IF (ADPHI-PHIE)  74, 74, 40
   40 IF (ADPHI.GT.PHIP) GO TO  50
   45 PHIU = (KP*(ABS(PHIL-PHIZ(I))-PHIE)+EMOM)/KE
      GO TO  55
   50 PHIU = (PMOM + EMOM)/KE
   55 PHIZ(I) =  PHIL - SGN*(PHIU + PHIS)
      GO TO  65
   60 IF  (KEY(I).EQ.1) KEY(I)=2
   65 DDPHI = DPHI(I) - PHIZ(I)
      ADPHI = ABS(DDPHI)
      IF (DDPHI.NE.0.0) GO TO  70
      SGN = 1.0
      GO TO  71
   70 SGN = ADPHI/DDPHI
C   *   FIND RANGE OF ADJUSTED SPRING DEFORMATION
   71 IF (ADPHI-PHIF)  72, 72, 15
   72 IF (ADPHI-PHIP)  73, 73, 90
   73 IF (ADPHI-PHIE)  74, 74, 85
   74 IF (ADPHI-PHIS)  75, 75, 80
C   *   FIND FORCE (MOMENT) DUE TO DEFORMED SPRING
   75 FORCE = 0.0
      GO TO  95
   80 FORCE = KE*SGN*(ADPHI-PHIS)
      GO TO  95
   85 FORCE = SGN*(EMOM + KP*(ADPHI-PHIE))
      GO TO  95
   90 FORCE = SGN*(EMOM + PMOM + KL*(ADPHI-PHIP))
C   *   ARRANGE SPRING FORCE INTO GENERALIZED FORCE MATRIX
   95 FS(IP2) =  FS(IP2) - FORCE
      FS(IP3) =  FORCE
      Q6(I) = FORCE
  100 CONTINUE
      RETURN
      END
```

```
      SUBROUTINE QEMTRX (PHI)
      COMMON /MEMBER/ M(15), P(15), L(15), IO(15), U(15), W(15)
      COMMON /ENDPT/ XI(15), YI(15), XT(15), YT(15)
      COMMON /MATRIX/ D(17,18), E(17), FS(17), QE(17), QF(17)
      COMMON /CONST/ N,NP1,NP2,NM1,NPROT,MARK,INDEX,DT,ET,ER,PI
      COMMON /IMPACT/ TMPT(50), XPT(50), FPT(50), NPTS, IPT, XF, I
     +                , CF, FX, FY
      REAL PHI(15), L
      MARK = 0
C    *   FIND BARRIER SEGMENT IMPACT FORCE IS APPLIED TO
      DO 20 J = 1,N
      IF (XI(J).GT.XF) GO TO 20
      I = J
      IF (XT(J).GT.XF) GO TO 25
   20 CONTINUE
      WRITE (6,600) XF
      MARK = 10
      GO TO 100
   25 TANPHI = TAN(PHI(I))
C    *   CALCULATE EACH ROW OF THE QE MATRIX
      QE(1) = -FY*TANPHI
      QE(2) = FY
      IF (I.EQ.1) GO TO 55
      IM1 = I - 1
      DO 50 J = 1,IM1
      JP2 = J + 2
      QE(JP2) = FY*L(J)*(COS(PHI(J)) + TANPHI*SIN(PHI(J)))
   50 CONTINUE
   55 IP2 = I + 2
      QE(IP2) = FY*(XF-XI(I))/(COS(PHI(I))**2)
      IP3 = I + 3
      DO 70 J = IP3,NP2
      QE(J) = 0.0
   70 CONTINUE
  100 RETURN
  600 FORMAT ('-',10X,'NO POINT OF APPLICATION FOR THE EXTERNAL LOAD' /
     + 15X, 'COULD BE FOUND FOR XF = ',F10.3)
      END
```

```
      SUBROUTINE QFMTRX (PHI,PHID)
      COMMON /MEMBER/ M(15), P(15), L(15), IO(15), U(15), W(15)
      COMMON /MATRIX/ D(17,18), E(17), FS(17), QE(17), QF(17)
      COMMON /FRCTN/ FFX(15), FFY(15)
      COMMON /CGPROP/ XD(15), YD(15), XDD(15), YDD(15)
      COMMON /CONST/ N,NP1,NP2,NM1,NPROT,MARK,INDEX,DT,ET,ER,PI
      REAL  QFT(17), QFR(17), RD(15), PHI(15), PHID(15)
      REAL M, L, IO
C   *   FIND RESULTANT TRANSLATIONAL VELOCITY FOR EACH BARRIER SEGMENT
      DO 40 I = 1,N
      RD(I) = (XD(I)**2 + YD(I)**2)**0.5
      IF (RD(I).NE.0.0) GO TO 10
      FFX(I) = 0.0
      FFY(I) = 0.0
      GO TO 40
C   *   DETERMINE FRICTION FORCES IN X- AND Y- DIRECTIONS
   10 FFX(I) = -W(I)*U(I)/RD(I)*XD(I)
      IF (RD(I).GE.ET) GO TO 30
      FFX(I) = FFX(I)*ABS(SIN(PI*RD(I)/(2.*ET)))
   30 FFY(I) = -W(I)*U(I)/RD(I)*YD(I)
      IF (RD(I).GE.ET) GO TO 40
      FFY(I) = FFY(I)*ABS(SIN(PI*RD(I)/(2.*ET)))
   40 CONTINUE
C   *   CALCULATE THE GENERALIZED FORCES DUE TO TRANSLATIONAL FRICTION FORCES
      SUM1 = 0.0
      SUM2 = 0.0
      DO 50 I = 1,N
      SUM1 = SUM1 + FFX(I)
      SUM2 = SUM2 + FFY(I)
   50 CONTINUE
      QF(1) = SUM1
      QF(2) = SUM2
      DO 80 K = 1,N
      KP1 = K + 1
      KP2 = K + 2
      QFT(KP2) = -P(K)*(FFX(K)*SIN(PHI(K)) - FFY(K)*COS(PHI(K)))
      IF (K.EQ.N) GO TO 80
      SUM1 = 0.0
      SUM2 = 0.0
      DO 60 I = KP1,N
      SUM1 = SUM1 + FFX(I)
      SUM2 = SUM2 + FFY(I)
   60 CONTINUE
      QFT(KP2) = QFT(KP2) - L(K)*(SUM1*SIN(PHI(K)) - SUM2*COS(PHI(K)))
   80 CONTINUE
C   *   EVALUATE FRICTION MOMENT DUE TO ROTATION OF SEGMENT
      DO 90 K = 1,N
      KP2 = K + 2
      QFR(KP2) = -PHID(K)*W(K)*U(K)*L(K)/4.
      IF (PHID(K).EQ.0.0) GO TO 90
      QFR(KP2) = QFR(KP2)/ABS(PHID(K))
      IF (ABS(PHID(K)).GE.ER) GO TO 90
      QFR(KP2) = QFR(KP2)*ABS(SIN(PI*PHID(K)/(2.*ER)))
   90 CONTINUE
C   *   SUM TRANSLATIONAL AND ROTATIONAL GENERALIZED FORCES
      DO 100 K = 3,NP2
      QF(K) = QFT(K) + QFR(K)
  100 CONTINUE
      RETURN
      END

      SUBROUTINE ADD
      COMMON /MATRIX/ D(17,18), E(17), FS(17), QE(17), QF(17)
      COMMON /CONST/ N,NP1,NP2,NM1,NPROT,MARK,INDEX,DT,ET,ER,PI
      REAL RHS(17)
      EQUIVALENCE (RHS(1),E(1))
      DO 20 I = 1,NP2
      RHS(I) = E(I) + FS(I) + QE(I) + QF(I)
   20 CONTINUE
      RETURN
      END
```

```
      SUBROUTINE GAUSS (X)
      COMMON /MATRIX/ A(17,18), C(17)
      COMMON /CONST/ NM2,NM1,N,NM3,NPROT,MARK,INDEX,DT,ET,EP,PI
      DIMENSION X(17)
      DO  5 I = 1,N
      A(I,NP1) = C(I)
    5 CONTINUE
      DO 30 K = 1,NM1
      KP1 = K + 1
      IF (A(K,K).NE.0.0) GO TO 40
   15 IF (A(KP1,K).NE.0.0) GO TO 20
      IF (KP1.EQ.N) GO TO 125
      KP1 = KP1 + 1
      GO TO 15
   20 DO 30 J = K,NP1
      STOREA = A(K,J)
      A(K,J) = A(KP1,J)
      A(KP1,J) = STOREA
   30 CONTINUE
   40 B = A(K,K)
      DO 50 J = K,NP1
      A(K,J) = A(K,J)/B
   50 CONTINUE
      DO 80 I = KP1,N
      B = A(I,K)
      DO 80 J = K,NP1
      A(I,J) = A(I,J) - B*A(K,J)
   80 CONTINUE
      X(N) = A(N,NP1)/A(N,N)
      DO 110 L = 1,NM1
      K = N - L
      X(K) = A(K,NP1)
      KP1 = K + 1
      DO 110 J = KP1,N
      X(K) = X(K) - A(K,J)*X(J)
  110 CONTINUE
      INDEX = 2
      RETURN
  125 INDEX = 1
      WRITE (6,600)
  600 FORMAT ('-',10X,'*** THE ACCELERATIONS COULD NOT BE SOLVED FOR ',
     + '***' / 11X,'***    DUE TO A SINGULARITY IN THE D MATRIX      ***')
      RETURN
      END

      SUBROUTINE ACCEL (PHI,PHID,QDD)
      COMMON /MEMBER/ M(15), P(15), L(15), IO(15), J(15), W(15)
      COMMON /CGPROP/ XD(15), YD(15), XDD(15), YDD(15)
      COMMON /CONST/ M,NP1,NP2,NM1,NPROT,MARK,INDEX,DT,ET,EP,PI
      REAL PHI(15), PHID(15), QDD(17)
      REAL L
      DO 50 I = 1,N
      IP2 = I + 2
      XDD(I) = QDD(1) - P(I)*(SIN(PHI(I))*QDD(IP2) + COS(PHI(I))*
     + PHID(I)**2)
      YDD(I) = QDD(2) + P(I)*(COS(PHI(I))*QDD(IP2) - SIN(PHI(I))*
     + PHID(I)**2)
      IF (I.EQ.1) GO TO 50
      IM1 = I - 1
      DO 45 J = 1,IM1
      JP2 = J + 2
      XDD(I) = XDD(I) - L(J)*(SIN(PHI(J))*QDD(JP2) + COS(PHI(J))*
     + PHID(J)**2)
      YDD(I) = YDD(I) + L(J)*(COS(PHI(J))*QDD(JP2) - SIN(PHI(J))*
     + PHID(J)**2)
   45 CONTINUE
   50 CONTINUE
      RETURN
      END
```

```
      SUBROUTINE ENDFRC (PHI)
      COMMON /MEMBER/ M(15), P(15), L(15), IO(15), U(15), W(15)
      COMMON /SPRING/ PHIS,PHIE,PHIP,PHIF,KE,KP,KL,EMOM,PMOM
     +               ,PHIZ(14),KEY(14),DPHI(14)
      COMMON /IMPACT/ TMPT(50), XPT(50), FPT(50), NPTS, IPT, KF, IMPBAR
     +               , CF, FX, FY
      COMMON /FRCTN/ FFX(15), FFY(15)
      COMMON /MEMFRC/ Q1(15), Q2(15), Q3(15), Q4(15), Q5(15), Q6(15)
      COMMON /CGPROP/ XD(15), YD(15), XDD(15), YDD(15)
      COMMON /CONST/ N,NP1,NP2,NM1,NPROT,MARK,INDEX,DT,ET,EP,PI
      REAL PHI(15)
      REAL  KE, KP, KL, M
      DO 110 I = 1,N
      IM1 = I - 1
      IF (IM1) 40,40,30
   30 Q1(I) = -Q4(IM1)*COS(DPHI(IM1)) + Q5(IM1)*SIN(DPHI(IM1))
      Q2(I) = -Q4(IM1)*SIN(DPHI(IM1)) - Q5(IM1)*COS(DPHI(IM1))
   40 Q5(I) = M(I)*YDD(I) - FFY(I) - Q2(I)
      Q4(I) = M(I)*XDD(I) - FFX(I) - Q1(I)
      IF (I-IMPBAR) 60,50,60
   50 Q4(I) = Q4(I) - FY*SIN(PHI(I))
      Q5(I) = Q5(I) - FY*COS(PHI(I))
   60 CONTINUE
      IF (IM1) 110,110,70
   70 Q3(I) = -Q6(IM1)
  110 CONTINUE
      RETURN
      END

      SUBROUTINE OUTPUT (TIME,PHI)
      COMMON /TITLE/ HEAD1, HEAD2
      COMMON /ENDPT/ XI(15), YI(15), XT(15), YT(15)
      COMMON /ALPHAS/ AYD(17), AZD(17), QDD(17)
      COMMON /MEMFRC/ Q1(15), Q2(15), Q3(15), Q4(15), Q5(15), Q6(15)
      COMMON /CGPROP/ XD(15), YD(15), XDD(15), YDD(15)
      COMMON /CONST/ N,NP1,NP2,NM1,NPROT,MARK,INDEX,DT,ET,EP,PI
      CHARACTER*80 HEAD1, HEAD2
      REAL PHI(15), PHIDD(15)
      EQUIVALENCE (QDD(3), PHIDD(1))
      WRITE (6,600) TIME, HEAD1, HEAD2
      WRITE (6,610)
      DO 20 J = 1,N
      WRITE (6,620) J, XI(J), YI(J), XT(J), YT(J), PHI(J), XDD(J),
     + YDD(J), PHIDD(J)
   20 CONTINUE
      WRITE (6,650)
      DO 60 J = 1,N
      WRITE (6,660) J, Q1(J), Q2(J), Q3(J), Q4(J), Q5(J), Q6(J)
   60 CONTINUE
      RETURN
  600 FORMAT ('1',10X,'***  TIME =',F10.4,'  ***',5X,A80 // 42X,A80)
  610 FORMAT ('0',T40,'END POINT LOCATION',T104,'CENTER OF MASS' / T14,
     + 'MEMBER',T32,'INITIAL END',T56,'TERMINAL END',T105,'ACCELERATION'
     + / T15,'NO.',T31,'X''',T43,'Y''',T55,'X''',T67,'Y''',T79,'PHI',
     + T94,'XDD',T109,'YDD',T123,'PHIDD' /)
  620 FORMAT (' ',13X,I2,10X,4(F7.2,5X),F7.4,3X,3(5X,E10.3) )
  650 FORMAT ('-',T56,'MEMBER END FORCES' / T9,'MEMBER',T37,'INITIAL END
     + ',T86,'TERMINAL END' / T11,'NO.',T24,'AXIAL',T39,'SHEAR',T54,
     + 'MOMENT',T74,'AXIAL',T89,'SHEAR',T104,'MOMENT' /)
  660 FORMAT (' ',9X,I2,3X,2(3(5X,E10.3),5X))
```

DESCRIPTION OF INPUT TO THE COMPUTER PROGRAM

First Card, Format (A80)

Col. No.	Program Variable	Description
1-80	HEAD1	Alphanumeric information for identification, printed on each output page

Second Card, Format (A80)

Col. No.	Program Variable	Description
1-80	HEAD2	Additional information continued from card one

Third Card, Format (2I5,3F10.2)

Col. No.	Program Variable	Description
1-5	N	Number of barrier segments*
6-10	NPRDT	Output print interval
11-20	DT	Time integration interval
21-30	ET	Translational velocity check
31-40	ER	Rotational velocity check

*Must be 15 or less.

Fourth Card Series, Format (5F10.2)

Properties of Barrier Segments

Col. No.	Program Variable	Description
1-10	M(I)	Mass of segment I (lb sec^2/ft)
11-20	L(I)	Length of segment I (ft)
21-30	P(I)	Distance from reference end to center of mass for segment I (ft)
31-40	IO(I)	Mass moment of inertia about center of segment I (ft-lb-sec^2)
41-50	U(I)	Friction coefficient for segment I

There are N cards in this series.

Fifth Card Set, Format (4F10.2)

Joint Spring Parameters

Card 1 Col. No.	Program Variable	Description
1-10	PHIS	Limit of slack rotation in joint spring (deg)
11-20	PHIE	Limit of elastic rotation in joint spring (deg)
21-30	PHIP	Limit of plastic rotation in joint spring (deg)
31-40	PHIF	Rotation in joint spring at failure (deg)

Card 2 Col. No.	Program Variable	Description
1-10	KE	Elastic spring stiffness (ft-lb/deg)
11-20	KP	Plastic spring stiffness (ft-lb/deg)
21-30	KL	Lock-up spring stiffness (ft-lb/deg)

Sixth Card Set, Format (8F10.2)

Initial Position of Barrier

Card 1 Col. No.	Program Variable	Description
1-10	XRO	Global X-position of initial end of system (ft)
11-20	YRO	Global Y-position of initial end of system (ft)

Card 2 Col. No.	Program Variable	Description
1-10	PHIO(1)	Initial rotation of segment 1 (deg)
11-20	PHIO(2)	Initial rotation of segment 2 (deg)
.	.	
.	.	
.	.	
71-80	PHIO(8)	Initial rotation of segment 8 (deg)

input each of the N initial rotations; use additional cards as necessary.

Coordinate orientation and sign convention shown here:

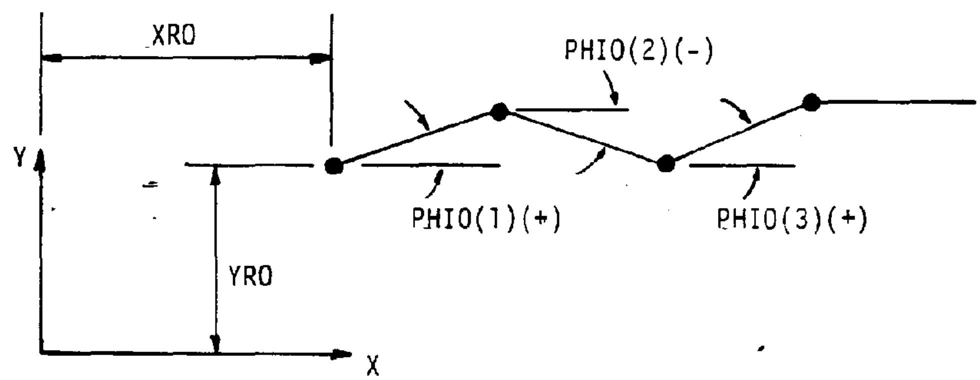

Seventh Card Set

Impact Force on Barrier

Format (I5,5X,2F10.2)

Card 1 Col. No.	Program Variable	Description
1-5	NPTS	Number of points in force input
5-10		Blank
11-20	PTIMP	Distance from reference end of barrier to XPT(1) = 0.0 (ft)
21-30	CF	Coefficient relating longitudinal to lateral force components

Format (6F10.2)

Card 2 Col. No.	Program Variable	Description
1-10	TMPT(1)	Time at value of FPT(1) (sec)
11-20	XPT(1)	X-coordinate of location of FPT(1) (ft)
21-30	FPT(1)	Force perpendicular to barrier segment (lb)
31-40	TMPT(2)	Continue for second set of points
41-50	XPT(2)	
51-60	FPT(2)	

This same format is followed for the remaining sets of TMPT(I), XPT(I), FPT(I), punching two sets per card.

Suggested values for the impact force, time of application, and location on the barrier are given in the following table for two standardized crash tests. This input was used throughout the parameter evaluation of this research, and gives favorable comparisons with actual crash test results. (See results of test 2 for additional details.)

Standardized Force Input

4500 lb Vehicle, 60 mph, 15° Encroachment

TIME (sec)	FORCE (lb)	DISTANCE FROM IMPACT (ft)
0.0	0.0	0.0
0.03	21100.	2.45
0.05	30800.	4.03
0.06	33600.	4.80
0.07	35200.	5.56
0.08	35600.	6.30
0.09	35000.	7.03
0.10	33400.	7.74
0.13	25100.	9.83
0.17	11400.	12.55
0.20	4500.	14.58
0.21	2800.	15.26
0.22	1500.	15.97
0.23	600.	16.62
0.24	0.0	17.30

4500 lb Vehicle, 60 mph, 25° Encroachment

TIME (sec)	FORCE (lb)	DISTANCE FROM IMPACT (ft)
0.0	0.0	0.0
0.01	0.0	0.35
0.02	5560.	1.70
0.05	60400.	4.21
0.06	72800.	5.02
0.07	72800.	5.83
0.08	77600.	6.62
0.09	70200.	7.41
0.13	18000.	10.47
0.14	8390.	11.22
0.15	3170.	11.97
0.16	1510.	12.72
0.17	2600.	13.46
0.19	8400.	14.96
0.20	10800.	15.71
0.21	11800.	16.46
0.23	8730.	17.97
0.25	1490.	18.72
0.26	0.0	19.47

BARRIERS IN CONSTRUCTION ZONES

APPENDIX D

Strength of Portable Median Barrier Connections

Prepared for
Contract DOT-FH-11-9458
Office of Research

Federal Highway Administration

U. S. Department of Transportation

by

W. Lynn Beason
Assistant Research Engineer

Texas A&M Research Foundation

Texas Transportation Institute

The Texas A&M University System

April 1985

PORTABLE CONCRETE MEDIAN BARRIER CONNECTIONS

In the past few years modified versions of concrete median barriers (CMB) have become popular as portable construction zone barriers. Such a portable construction zone barrier is constructed by interconnecting several CMB sections as shown in Figure 19. When CMB sections are used in this fashion there is usually no positive connection of the barrier to the ground. The barrier segments are connected with specially fabricated connections. Several different types of portable CMB connections have been designed by different groups. The strength and utility of the various types of connections are highly variable. The degree to which continuity between the CMB segments is maintained, and hence the ability of the portable barrier to prevent enchroachment into the work zone is controlled to a large degree by the strength of the connection. The purpose of the research reported herein is to present the calculated strengths of different types of portable CMB connections in use today.

Fifteen different portable CMB connections were examined in the research report herein. Details of the different barrier connections were obtained by contacting various agencies and designers involved in the design, construction, or use of the portable CMB's. For various reasons, it was not possible to assemble a complete set of details concerning the material strengths associated with each of the different connections. Therefore, in many cases it was necessary to assume material strengths to calculate connection strengths. Table 11 presents a uniform set of material strength assumptions which were used in this study in lieu of more precise information. Using the barrier geometries, elementary principals of mechanics, and assumed or actual material properties, the tensile, shear, bending, and torsional strengths of each of the different portable CMB connections were calculated.

The remainder of this appendix is devoted to a detailed presentation of the connection strength calculations for each of the different CMB connections considered. Results of these calculations are summarized in Table 12. It would certainly be possible to perform more rigorous analyses to determine the strengths of the connections than those reported herein. However, the quality of the calculated strengths would not be improved because of the uncertainties in the material properties and construction tolerances. Therefore, it is the opinion of the writers that more complicated analyses are unwarranted.

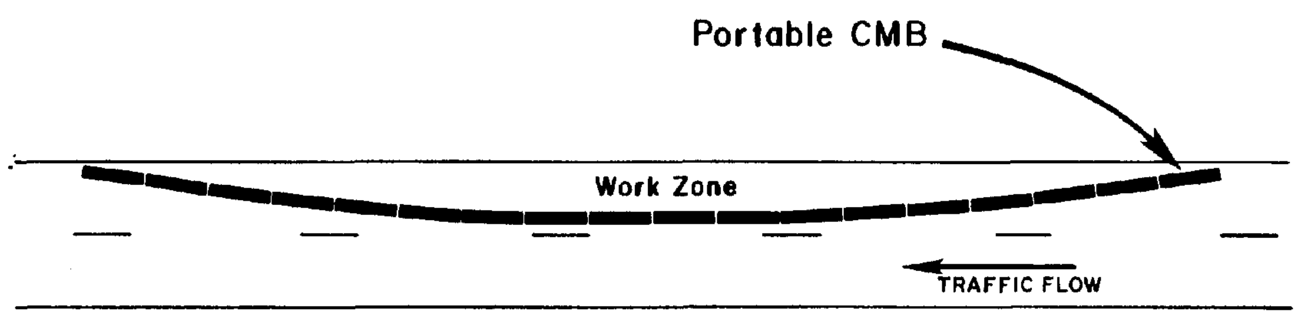

Figure 19. Portable Construction Zone Barrier.

Table 11. Assumed Material Strengths.

Material	Ultimate Compressive Strength (ksi)	Yield Strength in Tension (ksi)	Yield Strength in Shear (ksi)
Concrete	$f'_c = 3.0$	---	$\tau_{ult} = 0.3$
Rebar Bolts, and welds	---	$\sigma_y = 36$	$\tau_y = 20.8$
Structural Steel	---	$\sigma_y = 36$	$\tau_y = 20.8$
Wire Rope and Cable	---	$\sigma_{ult} = 91.7$[2]	$\tau_{ult} = 52.9$[2]
Structural Steel Tube	---	$\sigma_y = 46$	$\tau_y = 26.6$

1 all shear strengths except for concrete are based on energy of distorion theory, i.e. $\tau_y = \sigma_y / \sqrt{3}$

2 strengths based on gross cross-sectional area

Table 12. Calculated Connection Strengths.

Connection	Tensile Capacity (k)	Shear Capacity (k)	Moment Capacity (ft-k)	Torsion Capacity (ft-k)	Designation Appendix E
Welsback Interlock (NJ)	208	156	139	94	C10
I-Lock (NY)	92	208	61	87	C7
Pin and Rebar (CA)	85	85	57	60	C6
Corregation and Cable (CA)	41	23	27	19	**
Lapped Joint and Bolt (TX)	27	47	22	24	C5
Pin and Eye Bolt (MN)	20	12	13	9	C6*
Pin and Wire Rope (ID)	61	61	41	41	C6*
Pin and Rebar (GA)	46	46	31	31	C6*
Dowel (TX)	0	60	0	37	C2
Tongue and Groove (OR)	0	27	0	9	C1***
Tongue and Groove (VA)	0	32	0	7	C1
Hook and Rebar (CO)	7	5	5	0	**
Channel Splice	96	67	80	21	C9
T-Lock (Base)	46	588	97	375	C8
T-Lock (Top)	16	193	11	56	C4
Grid-Slot (TX)	0	60	0	30	C3

* These connections are similar to C6 but have a lower structural capacity. The model for C6 used in the cost section (Appendix E) was the California Pin and Rebar.

** Not considered in the cost section

*** Different end connection geometry than the Virginia Tongue and Groove.

WELSBACH INTERLOCK (New Jersey)

The New Jersey Welsbach Interlock connection is shown in Figure 2. This connection consists of two specially fabricated steel interlocks which are cast into one end of the barrier section and two grooves which are cast into the other end of the barrier section. The connection is accomplished by lifting the end of the barrier section with the interlocks and inserting the steel interlocks into the grooves on the opposite end of another barrier as shown in Figure 20.

TENSION CAPACITY

The tension capacity, F_T, of this connection is controlled by the tensile strengths of the steel interlocks loaded as shown in Figure 21.

SHEAR CAPACITY OF FILET WELDS

If it is assumed that the yield strength of the weld in shear is 34.6 ksi and that the weld has a 1/4 in. throat, the tensile strength of the connection is given as follows:

F_T = 4(.707)(.25 in.)(5 in.)(34.6 ksi),

F_T = 122.3 k.

If the throat of the weld is assumed to be 1/2 in., the strength of the connection is given as follows:

F_T = 2(122.3 k),

F_T = 244.6 k

TENSILE CAPACITY AT POINT A

If it is assumed that the yield strength of the steel interlock in tension is 36 ksi, the strength of the connection is given as follows:

F_T = 2(5 in.)(.75 in.)(36 ksi),

F_T = 270 k.

SHEAR CAPACITY AT POINT B

If it is assumed that the yield strength of the steel interlock in shear is 20.8 ksi, the tensile strength of the connection is given as follows:

F_T = 4(5 in.)(.50 in.)(20.8 ksi),

F_T = 208 k.

Assuming that the weld is sized so that it is not the weakest point, the calculated tensile capacity of the connection is determined to be 208 k.

SHEAR CAPACITY

The shear capacity, V, of this connection is controlled by the shear strength of the steel interlock loaded as shown in Figure 22. If it is assumed that the yield strength of the steel interlock in shear is 20.8 ksi, the shear strength of the connection is given as follows:

$V = 2(5 \text{ in.})(.75 \text{ in.})(20.8 \text{ ksi})$,

$V = 156$ k.

The shear strength of this connection is thus calculated to be 156 k.

BENDING CAPACITY

The bending capacity, M, of this connection is controlled by the couple that develops between the tensile force in the steel interlock and the barrier faces in contact as shown in Figure 23. If it is assumed that the tensile force in the interlock is 208 k, as previously calculated, and that the moment arm, d, shown in Figure 23 is 8 in., the bending strength of the connection is given as follows:

$M = (208 \text{ k})(8 \text{ in.})$,

$M = 1664$ in.-k or 139 ft-k.

The bending strength of the connection is thus calculated to be 139 ft-k.

TORSION CAPACITY

The torsion capacity, T, of this connection is controlled by the couple which develops between the shear forces in the interlocks as shown in Figure 24. The moment arm, d, in Figure 24 is taken to be 14.5 in. If it is assumed that the interlock forces are equal to half of the shear capacity of the connection (calculated to be 156 k), the torsional strength of this connection is given as follows:

$T = (14.5 \text{ in.})(156 \text{ k} / 2)$,

$T = 1131$ in.-k or 94.3 ft-k.

The torsion capacity of the connection is thus calculated to be 94 ft-k.

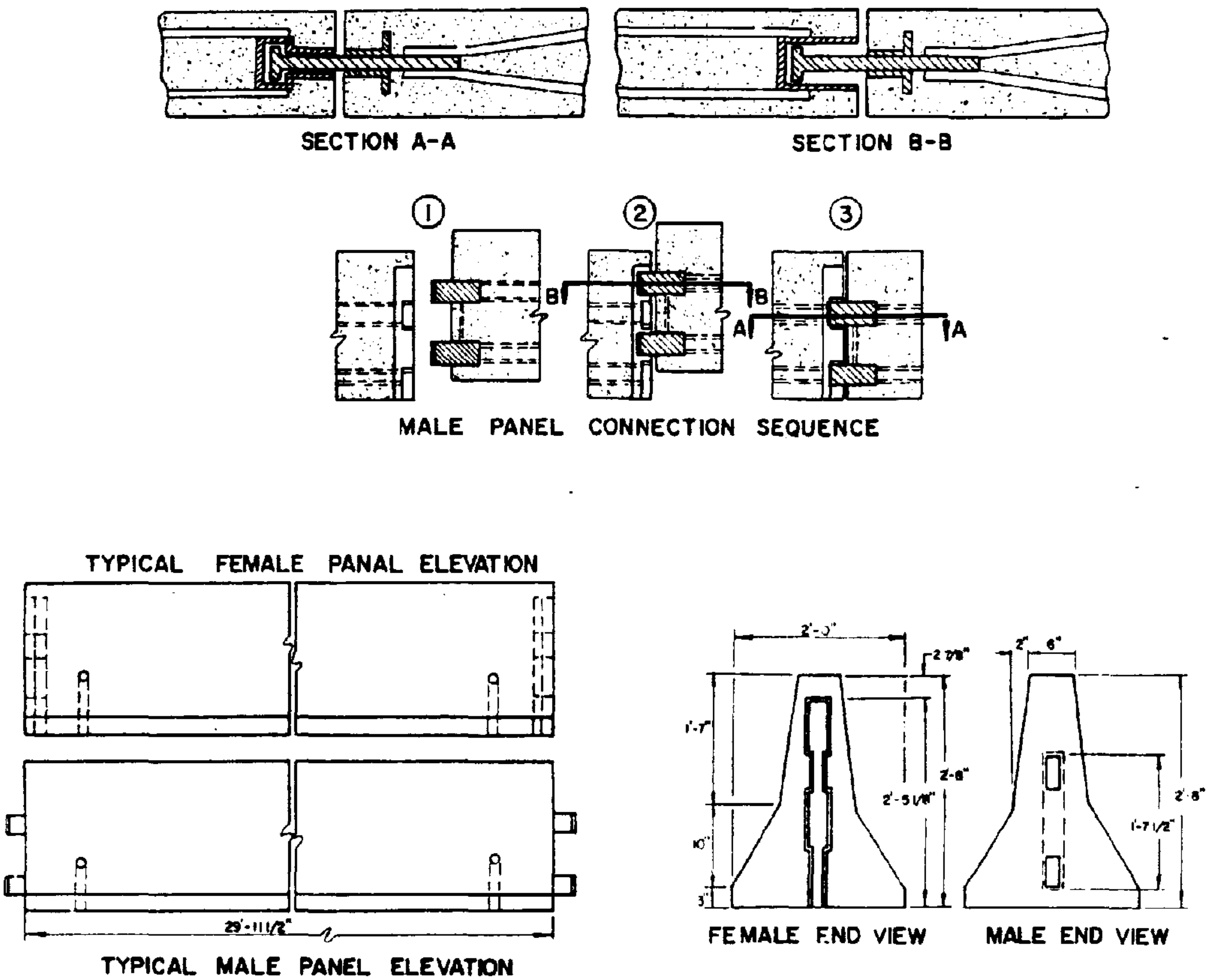

Figure 20. Welsbach Interlock (New Jersey).

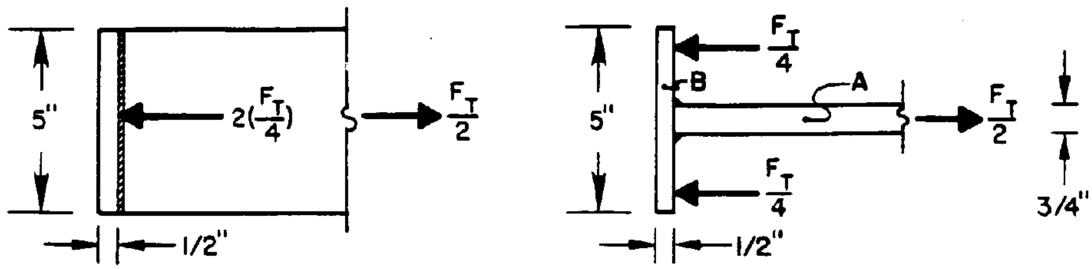

(a) Side View of Interlock (b) Top View of Interlock

Figure 21. Forces on Interlock Due to Tension in Connection.

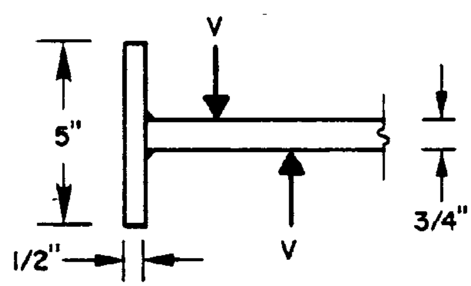

Figure 22. Forces on Interlock Due to Shear in Connection.

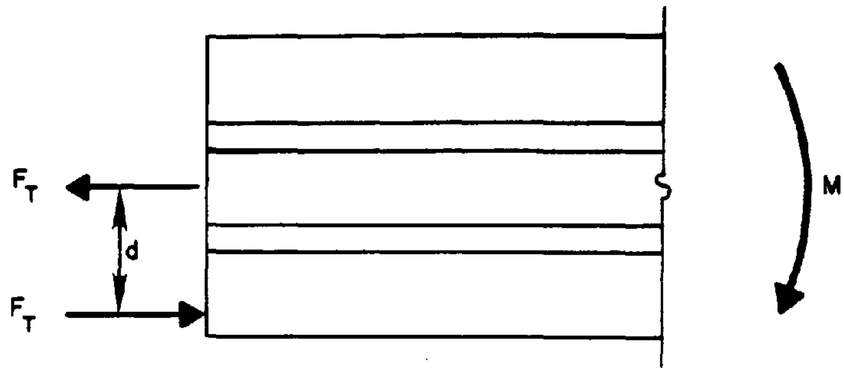

Figure 23. Forces on Barrier Face When Connection is in Bending.

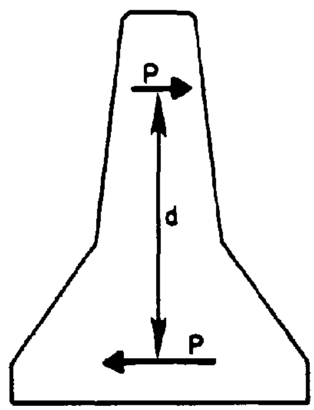

Figure 24. Forces on Barrier When Connection is in Torsion.

I-LOCK (New York)

The New York I-Lock connection is shown in Figure 25. The connection between barrier sections is accomplished by inserting a specially fabricated steel key into slotted steel tubes which are cast in the barrier ends.

TENSILE CAPACITY

The tensile capacity, F_T, of this connection is controlled by the strength of the I-lock loaded as shown in Figure 26, or the capacity of the structural tube loaded as shown in Figure 27. The strength of the I-lock will be checked first.

SHEAR CAPACITY OF FILET WELDS

If the yield strength of the weld shown in Figure 26 is assumed to be 34.6 ksi, the tensile strength of the connection is given as follows:

F_T = 2(20 in.)(.707)(5/16 in.)(34.6 ksi),

F_T = 305.8 k.

SHEAR STRENGTH AT POINT B

If the yield strength of the I-lock at point B in shear is assumed to be 20.8 ksi (ref. Fig. 26), the tensile strength of the connection is given as follows:

F_T = 2(1/2 in.)(20 in.)(20.8 ksi),

F_T = 416 k.

TENSILE STRENGTH AT POINT A

If the yield strength of the I-lock in tension is assumed to be 36 ksi (ref. Fig. 26), the tensile strength of the connection is given as follows:

F_T = 1/2 in.(20. in.)(36 ksi),

F_T = 360 ksi.

FLEXURAL STRENGTH OF STRUCTURAL TUBE AT POINT A

If the yield strength of the structural tube is assumed to be 46 ksi, the maximum plastic moment, M_{pl}, at point A on the tube (ref. Fig. 27) is given as follows:

M_{pl} = 46 ksi(1/4 in.)(20 in.)(1/4 in.),

M_{pl} = 57.5 in.-k.

The tensile capacity of the connection is then calculated as follows:

F_T = 2(57.5 in.-k)/(1.25 in.),

F_T = 92 k.

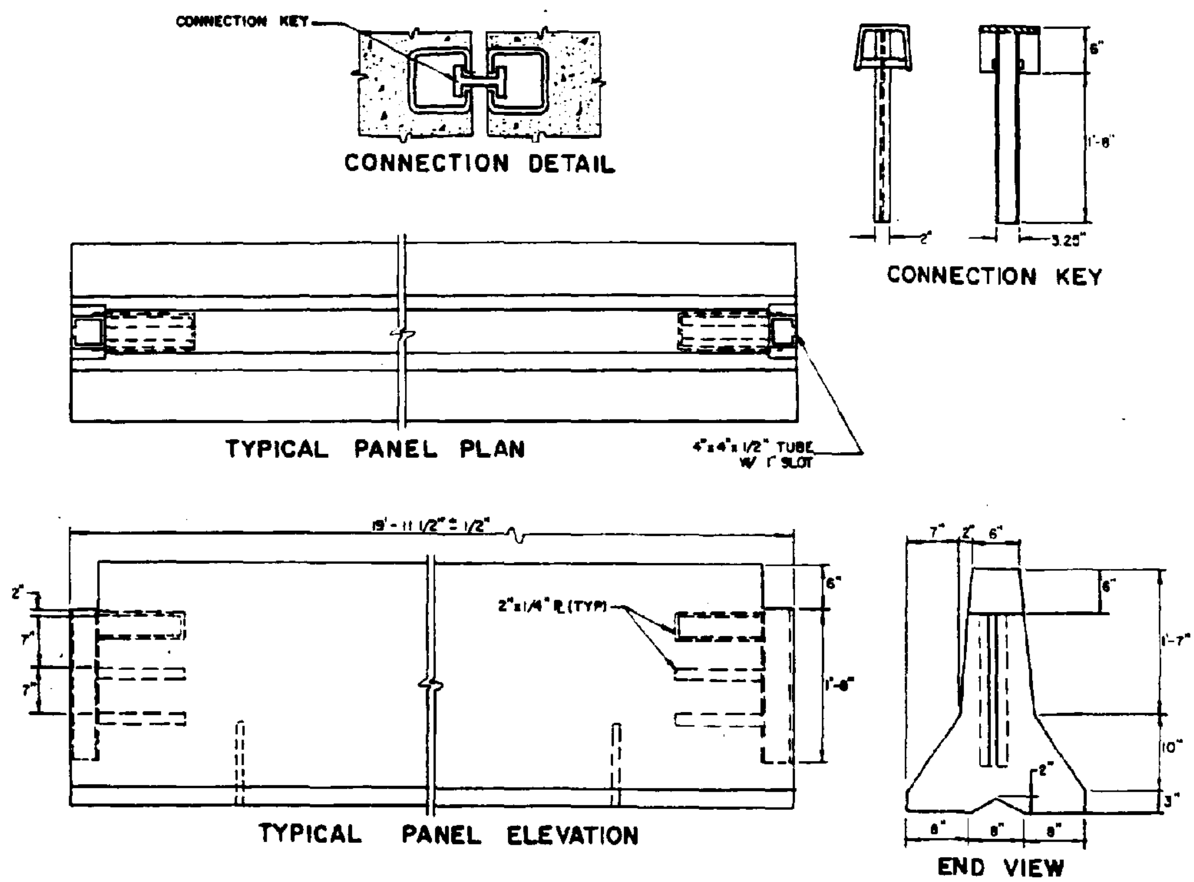

Figure 25. I-Lock (New York).

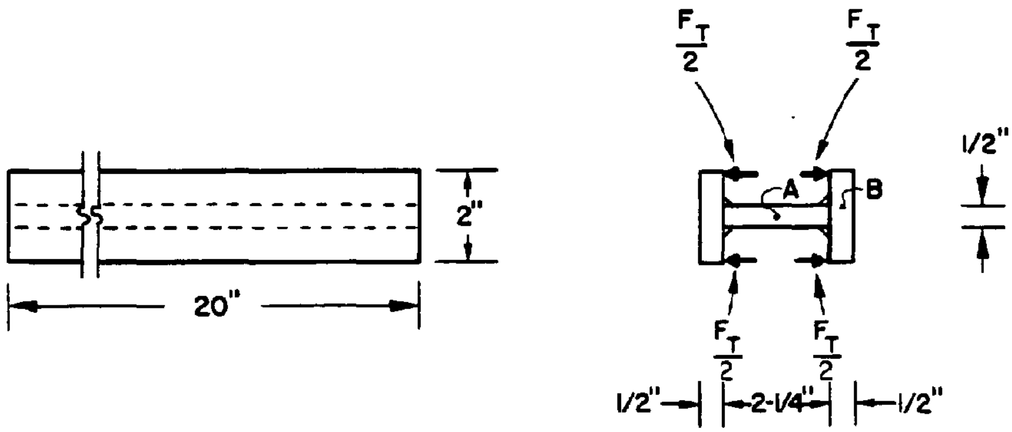

(a) Side View of I-Lock (b) I-Lock Cross-Section

Figure 26. Forces in I-Lock Due to Tension in Connection.

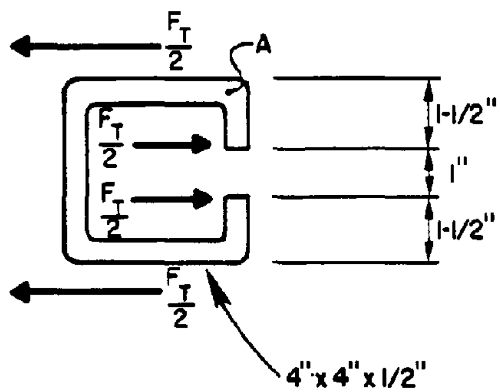

Figure 27. Forces on Structural Tube When Connection is in Tension.

SHEAR CAPACITY OF STRUCTURAL TUBE BELOW POINT A

If it is assumed that the yield strength of the tube in shear just below point A is 26.6 ksi (ref. Fig. 27), the tensile strength of the connection is given as follows:

F_T = 2(20 in.)(1/2 in.)(26.6 ksi),

F_T = 532 k.

The tensile capacity of this connection is thus calculated to be 92 k.

SHEAR CAPACITY

The shear strength, V, of this connection is controlled by the shear strength of the I-lock loaded as shown in Figure 28. If the yield strength of the I-lock in shear is assumed to be 20.8 ksi, the shear strength of the connection is given as follows:

V = 1/2 in.(20 in.)(20.8 ksi),

V = 208 k.

The shear capacity of connection is thus calculated to be 208 k.

BENDING CAPACITY

The bending capacity, M, of this connection is controlled by the couple that develops between the tensile force in the I-lock and the compressive force in the concrete barrier face as shown in Figure 23. If it is assumed that the moment arm, d, shown in Figure 23 is equal to 8 in., the bending capacity of this connection is given as follows:

M = 92 k(8 in.),

M = 736 in.-k or 61.3 ft-k.

The bending capacity of this connection is thus calculated to be 61 ft-k.

TORSION CAPACITY

The torsion capacity, T, of this connection is the result of shearing stresses in the web of the I-lock as shown in Figure 29. If it is assumed that the yield strength of the I-lock in shear is equal to 20.8 ksi, the torsion capacity of the connection is given as follows:

T = 10 in.(1/2 in.)(20.8 ksi)(10 in.),

T = 1040 in.-k or 86.7 ft-k.

The torsion capacity of this connection is thus calculated to be 87 ft-k.

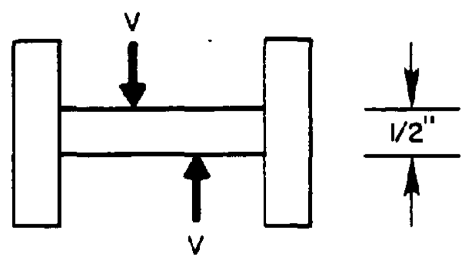

Figure 28. Forces on I-Lock Cross-Section When Connection is in Shear.

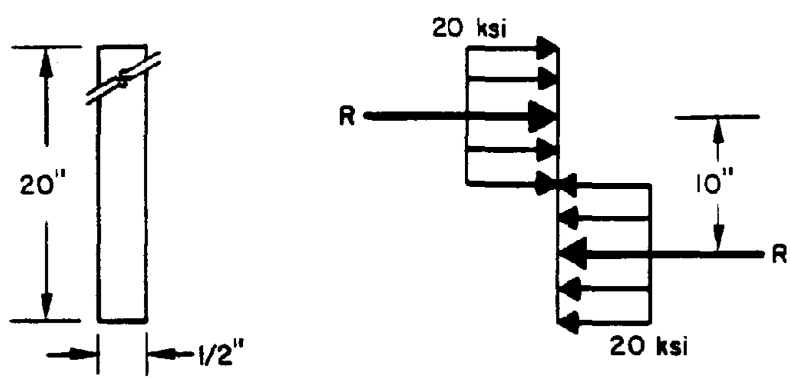

(a) I-Lock Web

(b) Assumed Shearing Stress Distribution

Figure 29. Shear Stress Distribution in I-Lock Web When Connection is in Torsion.

PIN AND REBAR (California)

The California pin and rebar connection is shown in Figure 30. Steel loops are cast in the ends of the barrier face so that loops in opposing ends of the barrier align as shown. The connection is accomplished by inserting a bolt through the loops and installing a nut and washer on the bolt end.

TENSION CAPACITY

The tension capacity, F_T, of this connection is controlled by the strength of the steel loops loaded as shown in Figure 31 or the strength of the bolt loaded as shown in Figure 32. The strength of the steel loops will be addressed first.

TENSILE CAPACITY OF STEEL LOOPS

If it is assumed that the yield strength of the steel loops in tension is 60 ksi (ref. Fig. 31), the tensile strength of the connection is calculated as follows:

$F_T = 2(2)(\pi)(3/8 \text{ in.})^2(60 \text{ ksi}),$

$F_T = 106 \text{ k}.$

SHEAR STRENGTH OF BOLT

If the shear strength of the bolt is assumed to be 34.7 ksi (ref Fig. 32), the tensile capacity of the connection is given as follows:

$F_T = 2(\pi)(5/8 \text{ in.})^2(34.7 \text{ ksi}),$

$F_T = 85.2 \text{ k}.$

BENDING STRENGTH OF BOLT

The bending strength of the bolt in this connection is not at issue because the nut on the bottom of the bolt prevents failure of the bolt in this mode.

The tensile capacity of this connection is thus calculated to be 85 k.

SHEAR CAPACITY

The shear capacity, V, of this connection is controlled by the same mechanism as the tension capacity. Therefore, the shear capacity is calculated to be 85 k.

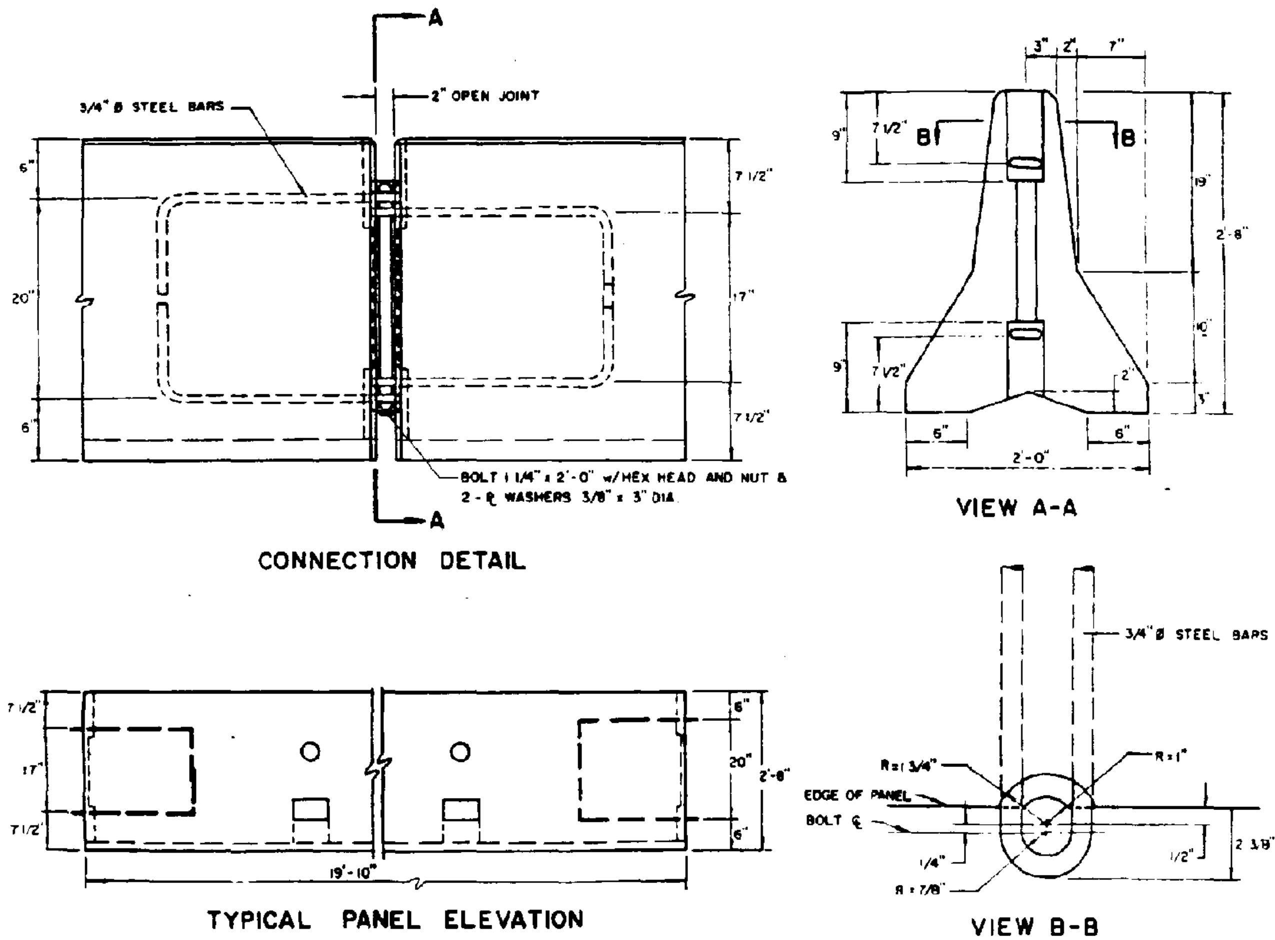

Figure 30. Pin and Rebar (California).

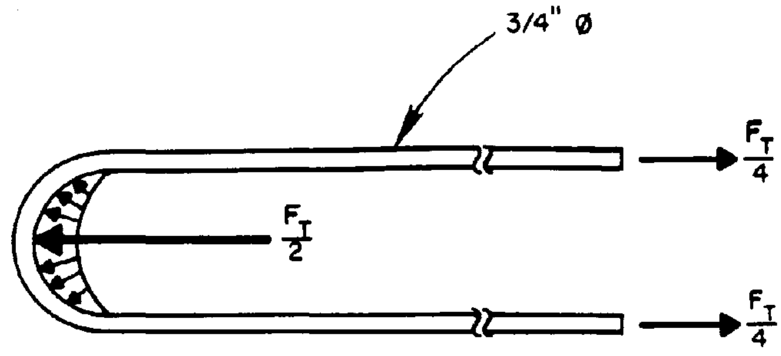

Figure 31. Forces in Steel Loops Due to Tension in Connection.

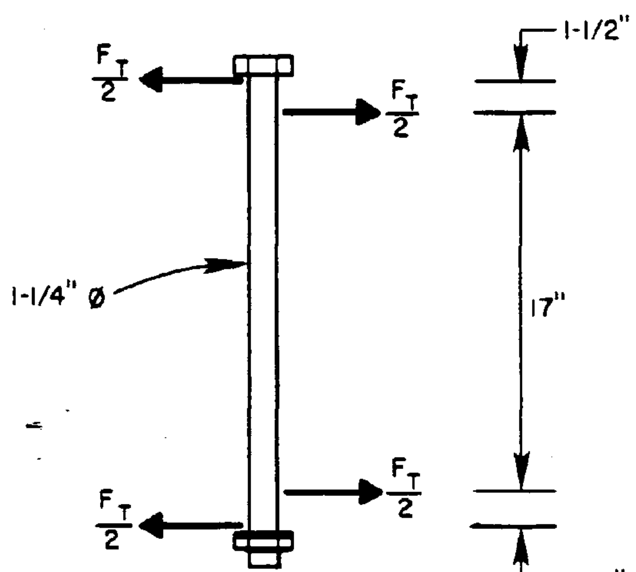

Figure 32. Forces on Bolt Due to Tension in Connection.

BENDING CAPACITY

The bending capacity, M, of this connection is the result of the couple which developes between the tensile force in the steel loops and the compressive force in the extreme fibers of the barrier end as shown in Figure 23. If it is assumed that the moment arm, d, in Figure 23 is 8 in., the bending strength of the connection is given as follows:

M = 85.2 k(8 in.),

M = 681.6 in.-k or 56.8 ft-k.

The bending capacity of the connection is thus calculated to be 57 ft-k.

TORSION CAPACITY

The torsion capacity, T, of this connection is the result of the couple which develops between the forces on the steel loops as shown in Figure 24. The moment arm, d, for this connection is 17 in. If it is assumed that this force is limited by the shear strength of the pin, the torsion capacity of the connection is given as follows:

T = (85.2 k/2)(17 in.),

T = 724.2 in.-k or 60.4 ft-k.

The torsion capacity of this connection is thus calculated to be 60 ft-k.

CORREGATION AND CABLE (California)

The California corregation and cable connection is shown in Figure 33. The connection is accomplished by post tensioning the corregated barrier ends together as shown in Figure 33.

TENSION CAPACITY

The tension capacity, F_T, of this connection is controlled by the tensile strength of the wire rope loaded as shown in Figure 34. If it is assumed that the ultimate tensile strength of the wire rope is 91.7 (on the gross cross-section), the tensile strength of the connection is given as follows:

$F_T = \pi(3/8 \text{ in.})^2(91.7 \text{ ksi}),$

$F_T = 40.5 \text{ k}.$

The tensile capacity of the connection is thus calculated to be 41 k.

SHEAR CAPACITY

When this connection is subjected to shear, the tendency will be for the connection to open as shown in Figure 35. This results in a tensile force in the wire rope and a normal force between the barrier sections. Therefore, the shear capacity, V, of the connection is limited by one of two factors, the magnitude of the friction between the concrete barriers as shown in Figure 36, or the shear strength of the cable as shown in Figure 37.

FRICTION BETWEEN BARRIERS.

The maximum tensile force that the wire rope can develop was calculated above to be 40.5 k. If it is assumed that the coefficent of friction between the barrier sections is 0.70, the shear strength of the barrier is given as follows:

$V = (.7)\ (40.5 \text{ k}),$

$V = 28.4 \text{ k}.$

SHEAR STRENGTH OF CABLE

If it is assumed that the ultimate shear strength of the cable is 52.9 ksi on the gross area (ref. Fig. 37), the shear strength of the connection can be calculated as follows:

$V = \pi(3/8 \text{ in.})^2(52.9 \text{ ksi}),$

$V = 23.4 \text{ k}.$

The shear strength of the connection is thus calculated to be 23 k.

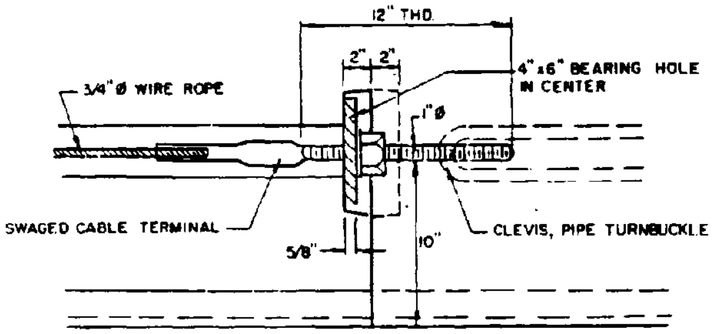

CABLE TIE DETAIL

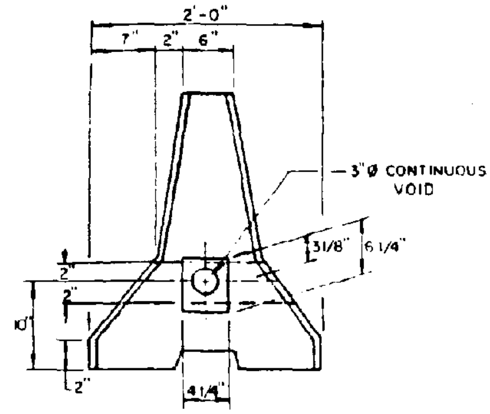

END VIEW

TYPICAL PANEL ELEVATION

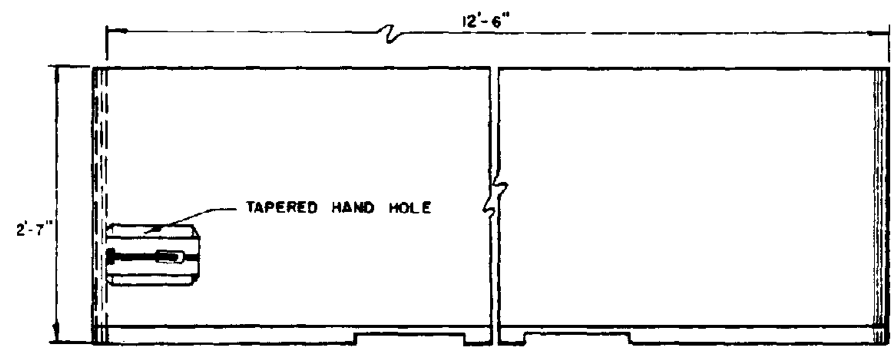

Figure 33. Corrugation and Cable (California).

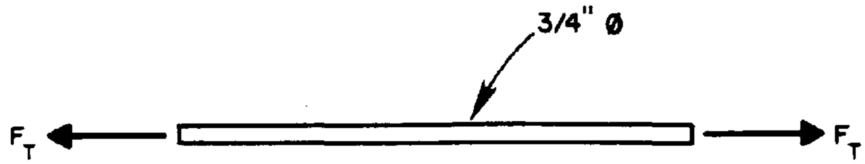

Figure 34. Forces on Wire Rope When Connection is in Tension.

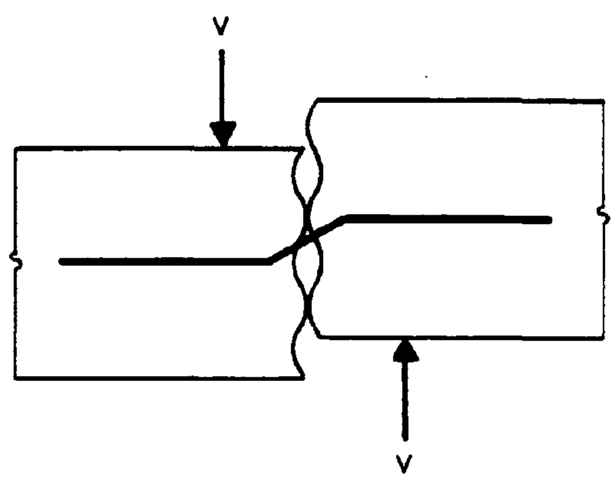

Figure 35. Connection in Shear.

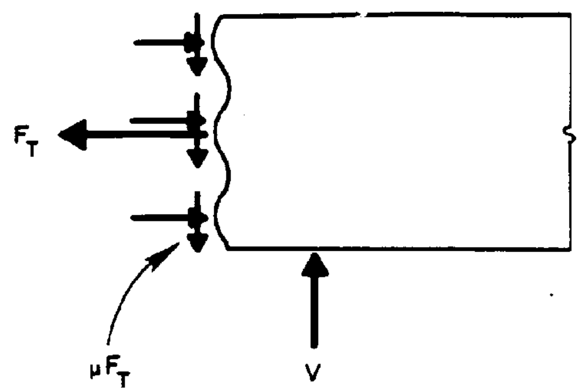

Figure 36. Friction on Barrier Face When Connection is in Shear.

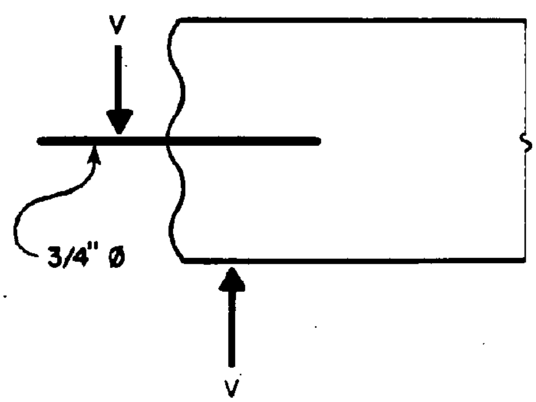

Figure 37. Forces on Cable When Connection is in Shear.

BENDING CAPACITY

The bending capacity, M, of this connection is the result of the couple which forms between the wire rope and the extreme fibers of the barrier segments as shown in Figure 23. The magnitude of the tensile force in the wire rope was previously calculated to be 40.5 k. If it is assumed that the moment arm, d, in Figure 23 is equal to 8 in., the bending capacity of the connection can be calculated as follows:

M = (40.5 k)(8 in.),

M = 324.0 in.-k or 27.0 ft-k.

Therefore, the bending capacity of this connection is calculated to be 27 ft-k.

TORSION CAPACITY

The torsion capacity, T, of this connection barrier is the result of the frictional shear forces on the barrier face as shown in Figure 38. The resultant shear force on the barrier face will be 28.4 k as previously calculated. If it is assumed that the moment arm associated with this resultant force is 8 in., the torsion capacity of the section is given as follows:

T = (28.4 k)(8 in.),

T = 227.2 in.-k or 18.9 ft-k.

The torsion capacity of this connection is thus calculated to be 19 ft-k.

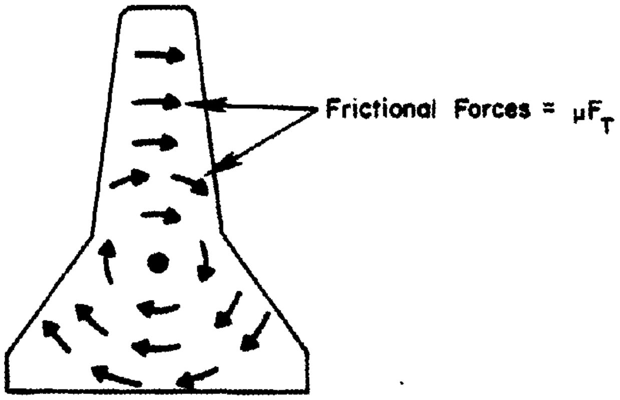

Figure 38. Frictional Forces on Barrier Face When Connection is in Torsion.

LAPPED JOINT AND BOLT (Texas)

The Texas lapped joint and bolt connection is shown in Figure 39. The ends of each barrier segment are specially fabricated so that they overlap in a vertical plane. The connection is accomplished by inserting and tightening a single 1 in. diameter steel bolt.

TENSILE CAPACITY

The tensile capacity, F_T, of this joint is controlled by the shear strength of the connecting bolt as shown in Figure 40. If the yield strength of the bolt in shear is assumed to be 34.6 ksi (ref. Fig. 40), the tensile strength of the connection is given as follows:

$$F_T = \pi(1/2 \text{ in.})^2(34.6 \text{ ksi}),$$

$$F_T = 27.2 \text{ k.}$$

The tensile capacity of the joint is thus calculated to be 27 k.

SHEAR CAPACITY

The shear capacity, V, of this connection is controlled by either the tensile strength of the connecting bolt as shown in Figure 41 or the shearing strength of the failure plane as indicated in Figure 42.

TENSILE STRENGTH OF BOLT

If the yield strength of the bolt in tension is assumed to be 60 ksi, the shear strength of the connection is given as follows:

$$V = \pi(1/2 \text{ in.})^2(60 \text{ ksi}),$$

$$V = 47.1 \text{ k.}$$

SHEAR STRENGTH ACROSS FAILURE PLANE

If failure of the barrier connection occurs along the failure plane indicated in Figure 42, a total of four bars of unknown diameter (assumed to be 3/8 in.), one steel plate with a 4 in. x 1/2 in. cross-section, and the concrete itself must fail in shear (ref. Fig. 39). If it is assumed that the yield strength of the steel bars in shear is 34.6 ksi, the yield strength of the steel plate in shear is 20.8 ksi, and the ultimate shear strength of the concrete is 110 psi, the shear strength of the connection is given as follows:

$$V = 4(\pi)(3/16 \text{ in.})^2(34.6 \text{ ksi})+(4 \text{ in.})(1/2 \text{ in.})(36 \text{ ksi})$$
$$+(200 \text{ sq. in.})(.110 \text{ ksi}),$$

$$V = 109.3 \text{ k.}$$

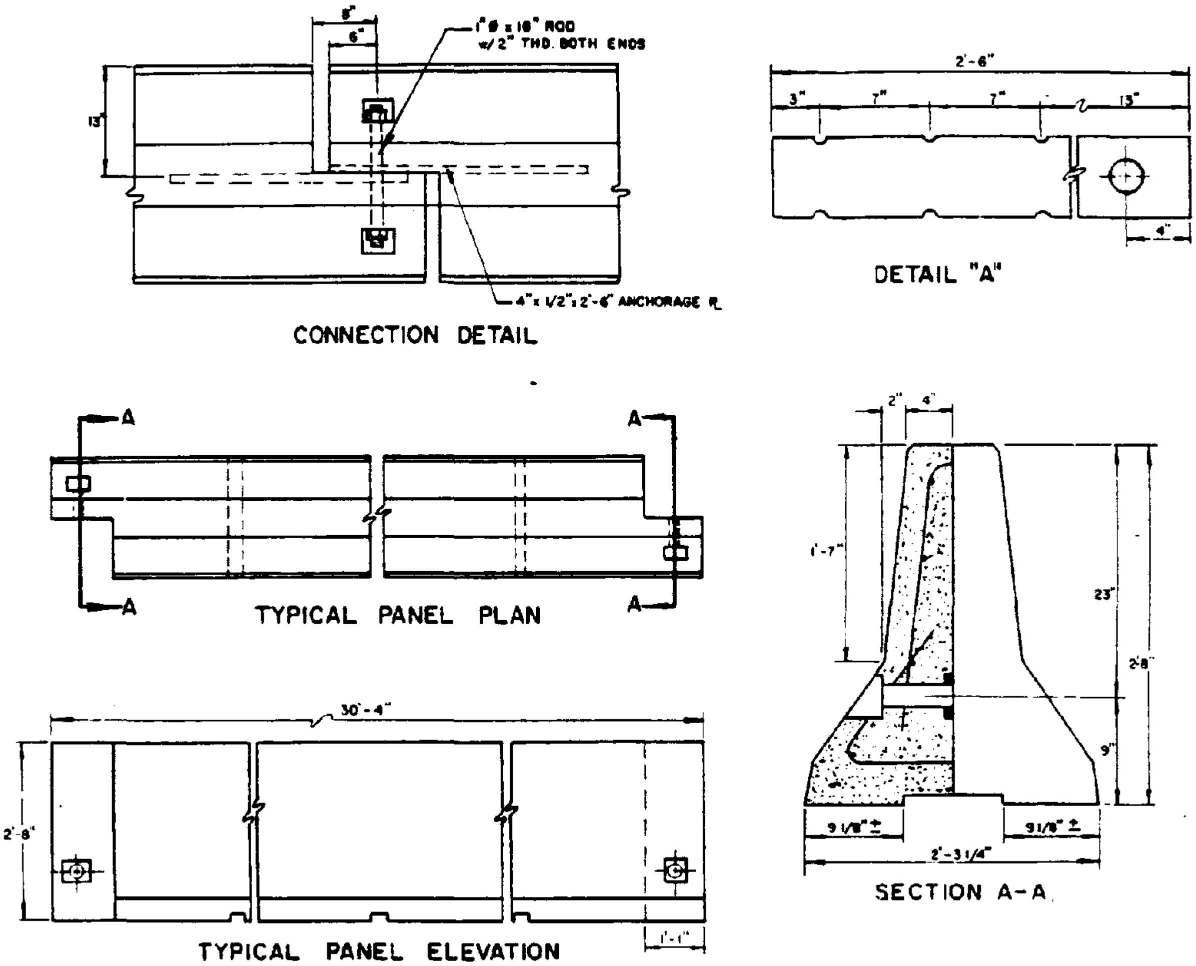

Figure 39. Lapped Joint and Bolt (Texas).

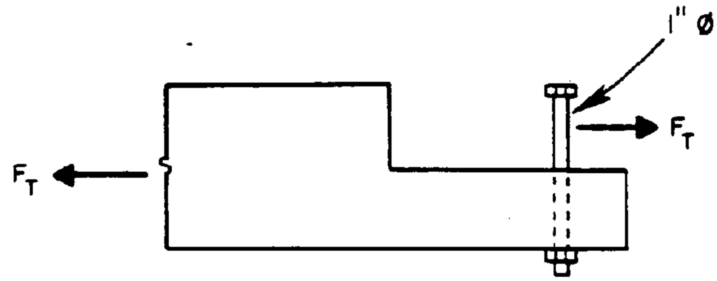

Figure 40. Shear Force in Bolt When Connection is in Tension.

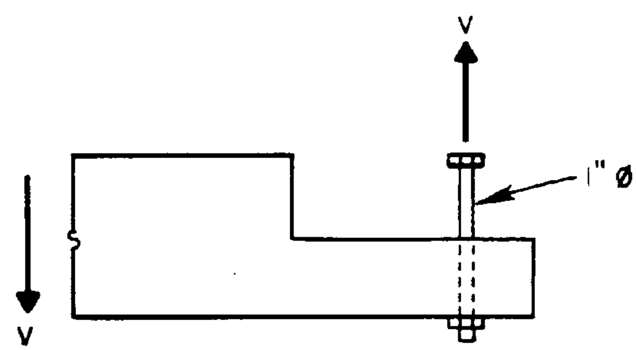

Figure 41. Tensile Force in Bolt When Connection is in Shear.

The shear strength of this connection is thus calculated to be 47 k.

BENDING CAPACITY

The bending capacity, M, of this connection is developed as a result of the couple which develops between the tensile force in the connecting bolt and the compressive force between the concrete barrier ends as shown in Figure 43. If the tensile strength of the bolt is taken to be 47.1 k as calculated earlier and the ultimate compressive strength of the concrete is taken as 0.85 (3000 ksi), the width, w, of the compressive zone shown in Figure 43 is given as follows:

$w = 47.1/[(30 \text{ in.})(.85)(3 \text{ ksi})]$

$w = .62 \text{ in.}$

The value of moment arm, d, is then be calculated as follows:

$d = 6 \text{ in.} - .62 \text{ in.}/2,$

$d = 5.7 \text{ in.}$

The moment capacity of the connection is then given as follows:

$M = 47.1 \text{ k}(5.7 \text{ in.}),$

$M = 268.5 \text{ in.-k or } 22.4 \text{ ft-k.}$

The bending capacity of this connection is thus calculated to be 22 ft-k.

TORSION CAPACITY

The torsion capacity, T, of this section is controlled by the couple which develops between the tensile force in the bolt and the compressive force on the barrier as shown in Figure 44. If it is assumed that the moment arm, d, is equal to 6 in., the torsion capacity of the connection is calculated as follows:

$T = 47.1 \text{ k}(6 \text{ in.}),$

$T = 282.6 \text{ in.-k or } 23.6 \text{ ft-k.}$

The torsion capacity of the connection is thus calculated to be 24 ft-k.

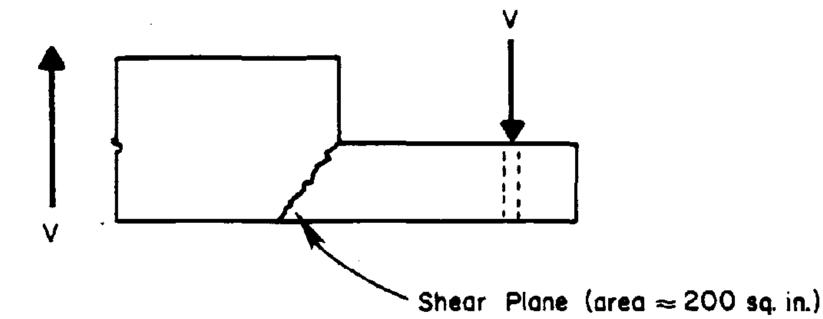

Figure 42. Shear Plane in Concrete When Connection is in Shear.

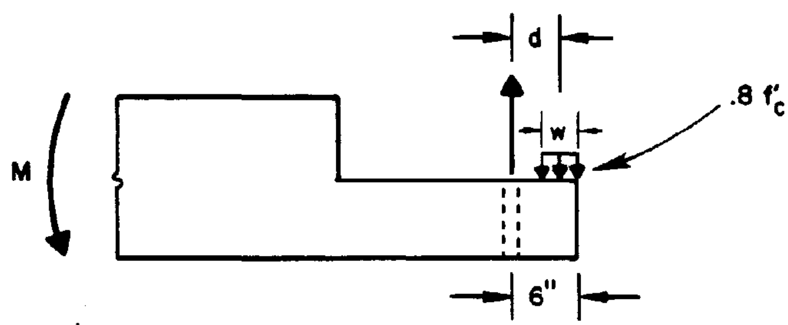

Figure 43. Forces on Barrier Face When Connection is in Bending.

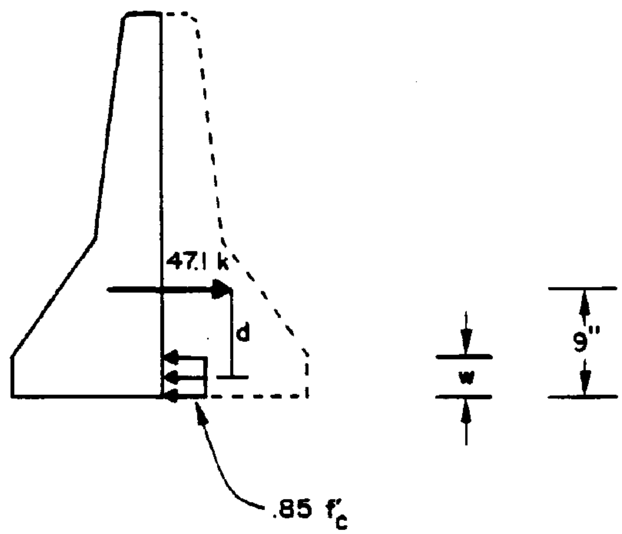

Figure 44. Forces on Barrier When Connection is in Torsion.

PIN AND EYE BOLT (Minnesota)

The Minnesota pin and eye bolt connection is shown in Figure 45. Eye bolts are cast into the ends of the barrier segments so that the bolts in opposing ends of the barrier align as shown. The connection is completed by inserting a connection pin through the eye bolts.

TENSION CAPACITY

The tensile capacity, F_T, of this connection is controlled by the strengths of the eye bolts or the strength of the pin. If moments are summed about point A in Figure 46 the following relationship between the forces in the eye bolts results:

$$P_I = 1.25\ P_O$$

Therefore

$$F_T = 2.25\ P_O$$

or

$$F_T = 1.80\ P_I$$

STRENGTH OF THE EYE BOLTS

It is assumed that the strength of the eye bolt is controlled by the tensile strength of the shank as shown in Figure 47. If it is assumed that the yield strength of the eye bolt shank in tension is 36 ksi, the tensile strength of the connection is given as follows:

$$F_T = 1.8(3/8\text{ in.})^2(\pi)(.70)(36\text{ ksi}),$$

$$F_T = 20.0\text{ k}.$$

SHEAR STRENGTH OF THE PIN

The maximum shear in the pin occurs just above point A (ref. Fig. 46). If it is assumed that the yield strength of the pin in shear is 34.6 ksi, the tensile strength of the connection is given as follows:

$$F_T = 2.25\ (34.6\text{ ksi})(\pi)(5/8\text{ in.})^2,$$

$$F_T = 95.5\text{ k}.$$

FLEXURAL STRENGTH OF THE PIN

The maximum moment in the pin occurs 2 in. above point A as shown in Figure 46. If it is assumed that the yield strength of the pin in tension is 60 ksi, the plastic moment capacity of the pin is given as follows:

$$M_{pl} = 4/3(5/8\text{ in.})^3(60\text{ ksi}),$$

$$M_{pl} = 19.5\text{ in.-k}.$$

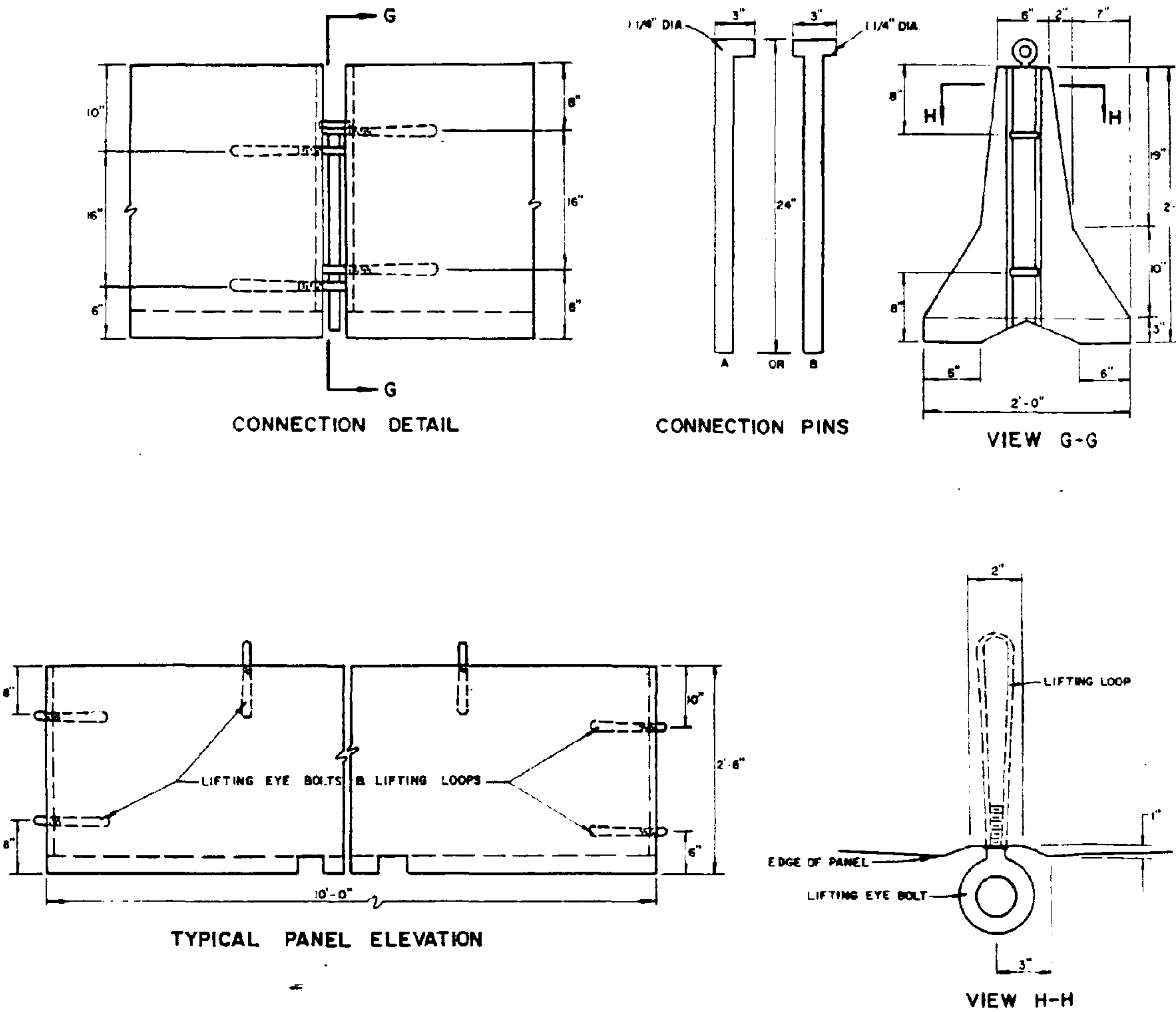

Figure 45. Pin and Eye Bolt (Minnesota).

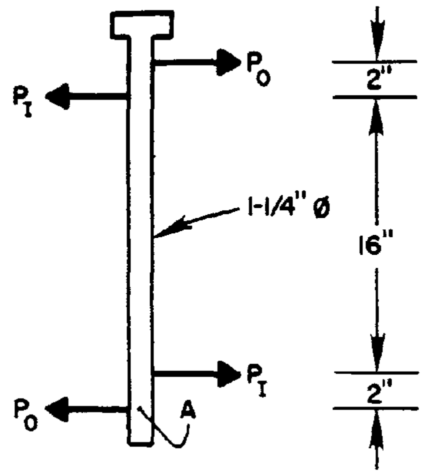

$$\Sigma M_A = 0$$

$$2\,P_I - 18\,P_I + 20\,P_O = 0$$

$$P_I = 1.25\,P_O$$

Figure 46. Forces on Pin When Connection is in Tension.

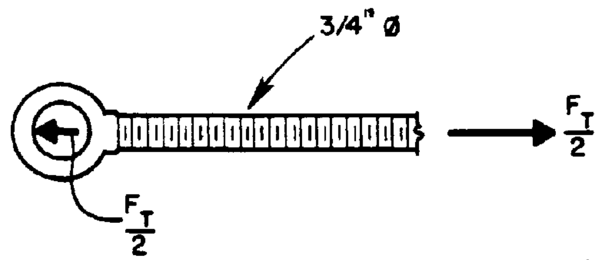

Figure 47. Forces on Eye Bolt When Connection is in Tension.

The tensile strength of the connection can then be calculated as follows:

$F_T = 2.25\ (19.5\ \text{in.-k}/2\ \text{in.}),$

$F_T = 21.9\ \text{k}.$

The tensile strength of the connection is thus calculated to be 20 k.

SHEAR CAPACITY

The shear strength, V, of this connection is controlled by either the strengths of the eye bolts loaded as shown in Figure 48, or the strength of the pin loaded essentially the same as shown in Figure 46.

SHEAR STRENGTH OF THE EYE BOLT

If the yield strength of the eye bolt in shear is assumed to be 20.8 ksi, the shear strength of the connection is given as follows:

$V = 1.8(20.8\ \text{ksi})(\pi)(3/8\ \text{in.})^2(.70),$

$V = 11.6\ \text{k}.$

STRENGTH OF PIN

The shear and bending strengths of the pin are the same as calculated above in the tensile capacity section.

The shear strength of the connection is thus calculated to be 12.0 k.

BENDING CAPACITY

The bending capacity, M, of this connection is controlled by the couple which develops between the tensile force in the eye bolt and the compression between the concrete barriers in contact as shown in Figure 23. If it is assumed that the moment arm, d, shown in Figure 23 is 8 in., the moment capacity of the connection is calculated as follows:

$M = 20.0\ \text{k}(8\ \text{in.}),$

$M = 160.0\ \text{in.-k or } 13.3\ \text{ft-k}.$

The bending capacity of the connection is thus calculated to be 13 ft-k.

TORSION CAPACITY

The torsion capacity of this connection is the result of the couple which develops between the forces acting on the pin as shown in Figure 49. The following equilibrium equation can be developed by summing moments about point A in Figure 49.

$P_O = P_I$

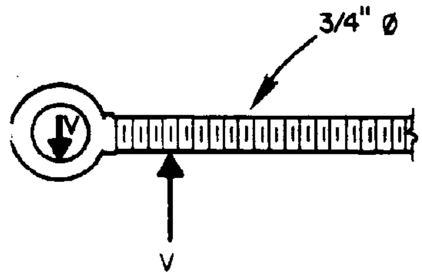

Figure 48. Forces Acting on Eye Bolt When Connection is in Shear.

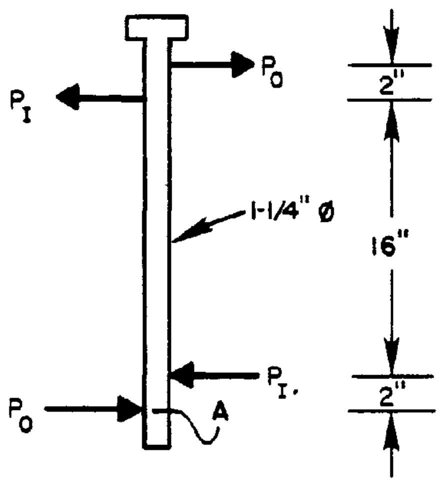

$$\Sigma M_A = 0$$

$$2\,P_I + 18\,P_I - 20\,P_O = 0$$

$$P_I = P_O$$

Figure 49. Forces Acting on Pin When Connection is in Torsion.

The forces are limited by either the strength of the eye bolt or the strength of the pin.

SHEAR STRENGTH OF EYE BOLT

If it is assumed that the yield strength of the eye bolts in shear is 20.8 ksi, the torsional capacity of the connection is given as follows:

$T = 20.8\ \text{ksi}(\pi)(3/8\ \text{in})^2(.70)(16\ \text{in.}),$

$T = 102.9\ \text{in.-k or } 8.6\ \text{ft-k}.$

SHEAR STRENGTH OF PIN

If the yield strength of the pin in shear is assumed to be 34.6 ksi, the torsional capacity of the connection is given as follows:

$T = \pi(5/8\ \text{in.})^2(34.6\ \text{ksi})16\ \text{in.}),$

$T = 679.4\ \text{in.-k or } 56.6\ \text{ft-k}.$

FLEXURAL STRENGTH OF PIN

If the yield strength of the pin in tension is assumed to be 60 ksi, the plastic moment capacity is 19.5 in.-k as calculated earlier. The torsional capacity of the connection is calculated as follows:

$T = (19.5\ \text{in.-k}/2\text{in.})(16\ \text{in.}),$

$T = 156.0\ \text{in.-k or } 13.0\ \text{ft-k}.$

The torsion capacity of the connection is thus calculated to be 9 ft-k.

PIN AND WIRE ROPE (Idaho)

The Idaho pin and wire rope connection is shown in Figure 50. Wire rope loops are cast into the ends of the barrier segments so that the loops in opposing ends of the barrier overlap as shown. The connection is completed by inserting a threaded steel pin through the loops and installing a nut and washer on the bottom end of the steel pin.

TENSION CAPACITY

The tensile capacity, F_T, of this connection is controlled by the strength of the pin and wire rope loaded as shown in Figure 51. If moments are summed about point A of the pin as shown in Figure 51, the following equilibrium equation results:

$$P_I = 1.25\ P_O$$

Therefore

$$F_T = 2.25\ P_O$$

or

$$F_T = 1.80\ P_I$$

TENSILE STRENGTH OF WIRE ROPE

The wire rope loops are loaded in tension as shown in Figure 52. If it is assumed that the tensile strength of the wire rope is 91.7 ksi (on the gross cross-section), the tensile strength of the connection is given as follows:

$$F_T = 1.8(2)(91.7\text{ ksi})(\pi)(1/4\text{ in.})^2$$

$$F_T = 64.8\text{ k.}$$

SHEAR CAPACITY OF PIN

If it is assumed that the yield strength of the pin in shear is 34.6 ksi, the tensile strength of the connection is given as follows:

$$F_T = (2.25)(34.6\text{ ksi})(\pi)(1/2\text{ in.})^2$$

$$F_T = 61.1\text{ k.}$$

BENDING CAPACITY OF PIN

The bending strength of the pin is not a controlling factor for this connection because the pin is equipped with a nut and washer.

The tensile capacity of this connection is thus calculated to be 61 k.

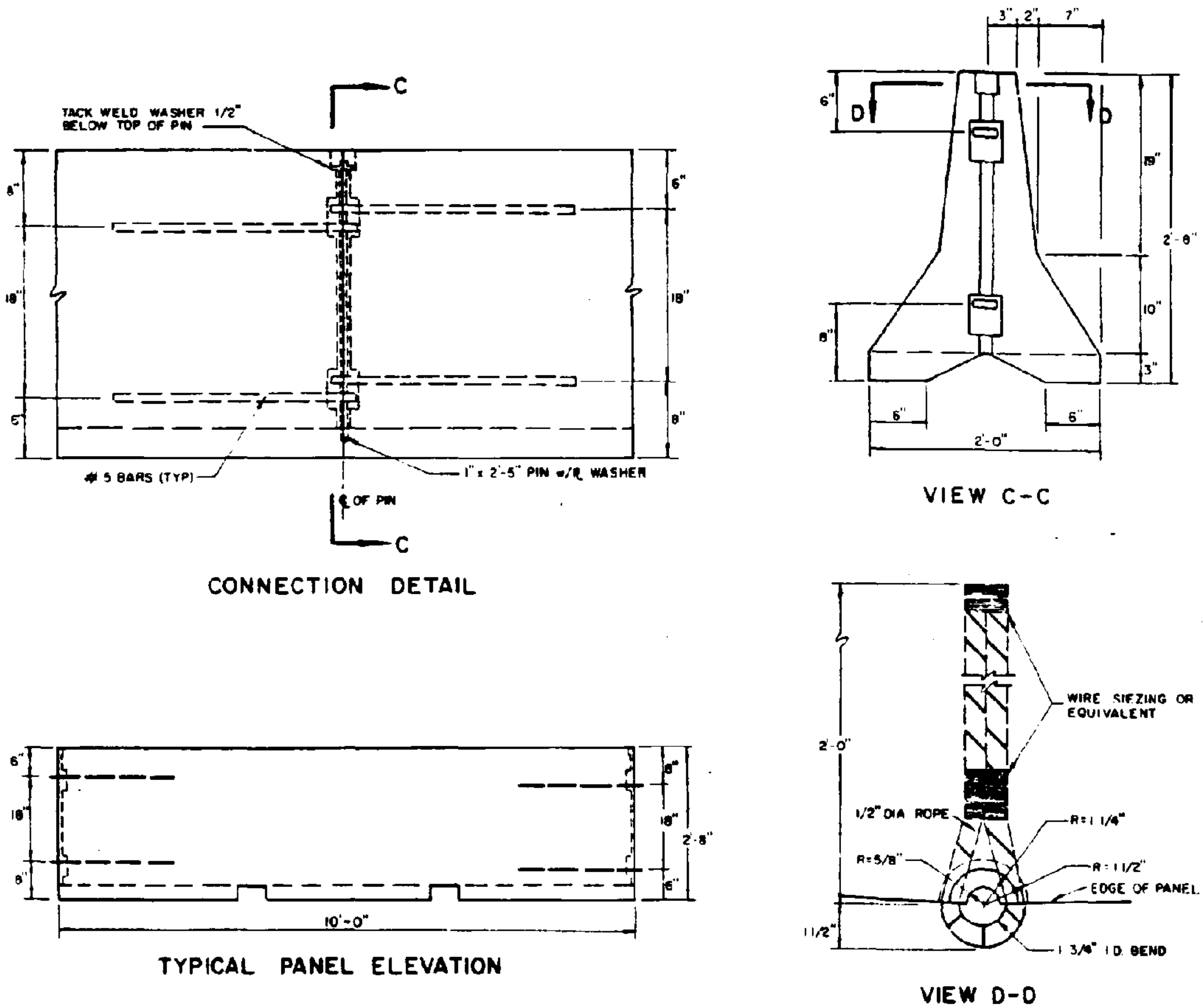

Figure 50. Pin and Wire Rope (Idaho).

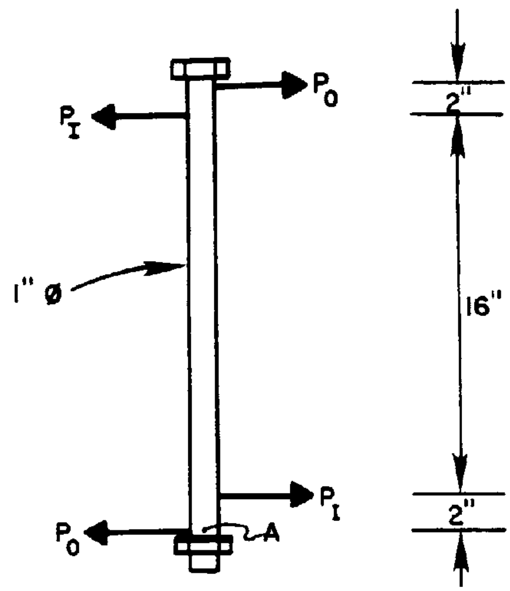

$$\Sigma M_A = 0$$

$$2P_I - 18P_I + 20P_O = 0$$

$$P_I = 1.25\ P_O$$

Figure 51. Forces on Pin When Connection is Tension.

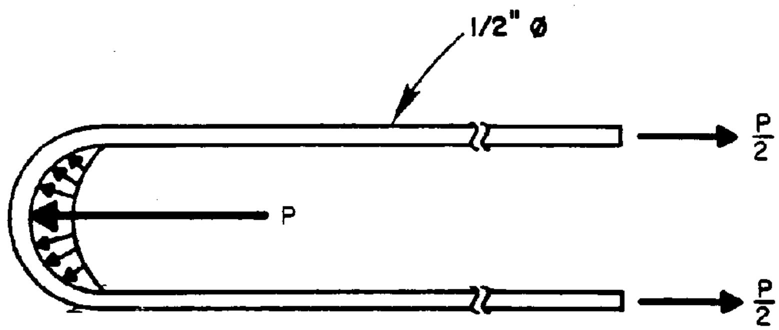

Figure 52. Forces on Loops When Connection is Tension.

SHEAR CAPACITY

The shear capacity, V, of this connection is controlled by the same mechanism as the tension capacity. Therefore, the shear capacity of the connection is 61 k.

BENDING CAPACITY

The bending capacity, M, of this connection is controlled by the couple which develops between the tensile force developed by the pin connection and the compression between the concrete barrier sections as shown in Figure 23. If the moment arm, d, shown in Figure 23 is assumed to be 8 in. then the bending capacity of the connection is calculated as follows:

$M = (61.1\ k)(8\ in.),$

$M = 488.8\ in.\text{-}k$ or $40.7\ ft\text{-}k.$

The bending capacity of this connection is thus calculated to be 41 ft-k.

TORSION CAPACITY

The torsion capacity, T, is the result of the couple which develops between the forces acting on the pin as shown in Figure 53. The following equilibrium relationship can be developed by summing moments about point A.

$P_O = P_I$

The forces are limited by either the strength of the loops or the strength of the pin.

TENSILE STRENGTH OF LOOPS

If the tensile strength of the loops is assumed to be 91.7 ksi (on the gross cross-section), the torsional capacity of the connection is given as follows:

$T = 91.7\ ksi(1/2\ in.)^2(\pi)(18\ in.),$

$T = 1296.4\ in.\text{-}k$ or $108.0\ ft\text{-}k.$

SHEAR STRENGTH OF PIN

If the yield strength of the pin in shear is assumed to be 34.6 ksi, the torsional capacity of the connection is given as follows:

$T = \pi(1/2\ in.)^2(34.6\ ksi)(18\ in.),$

$T = 489.1\ in.\text{-}k$ or $40.8\ ft\text{-}k.$

The torsion capacity of this connection is thus calculated to be 41 ft-k.

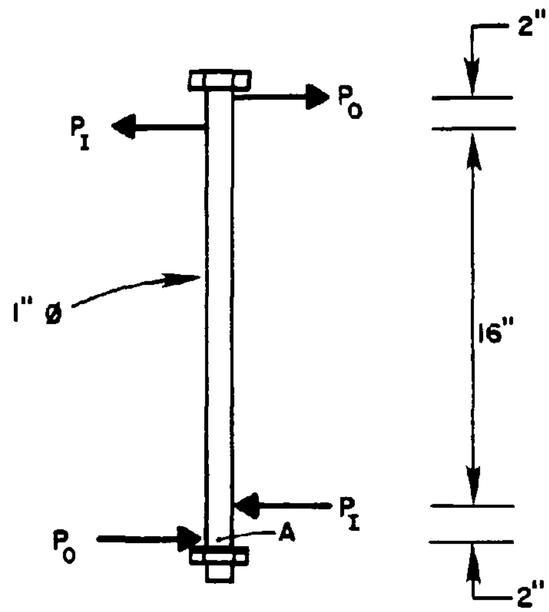

$$\Sigma M_A = 0$$

$$2 P_I + 18 P_I - 20 P_O = 0$$

$$P_O = P_I$$

Figure 53. Forces Acting on Pin When Connection is in Torsion.

PIN AND REBAR (Georgia)

The Georgia pin and rebar connection is shown in Figure 54. Steel loops are cast in the ends of the concrete median barrier so that the loops in the opposing ends overlap as shown. The connection is completed by inserting a 7/8 in. diameter pin which is held in place with a nut and washer as shown in Figure 54.

TENSION CAPACITY

The tension capacity, F_T, of this connection is controlled by the strength of the loops loaded as shown in Figure 56, or the strength of the pin loaded as shown in Figure 55. If moments are summed about point A in Figure 55 the following relationship between the forces on the pin results:

$$P_I = 1.22\ P_O$$

therefore

$$F_T = 2.22\ P_O$$

or

$$F_T = 1.82\ P_I$$

The first set of calculations is concerned with the strength of the steel loops.

TENSILE STRENGTH OF LOOPS

Figure 56 presents the tensile loads acting on a typical steel loop. If it is assumed that the yield strength of the loop in shear is 60 ksi, the tensile strength of the connection is given as follows:

$$F_T = 2(1.82)(\pi)(3/8\text{ in.})^2(60\text{ ksi}),$$

$$F_T = 96.5\text{ k.}$$

SHEAR CAPACITY OF PIN

If the yield strength of the pin in shear is assumed to be 34.7 ksi, the tensile capacity of the connection is given as follows:

$$F_T = 2.22\ (\pi)(7/16\text{ in.})^2(34.7\text{ ksi}),$$

$$F_{FT} = 46.3\text{ k.}$$

BENDING STRENGTH OF PIN

The bending strength of the pin is not a controlling mechansism for this connection because the pin is securely fastened in place with a nut.

The tensile capacity of this connection is thus calculated to be 46 k.

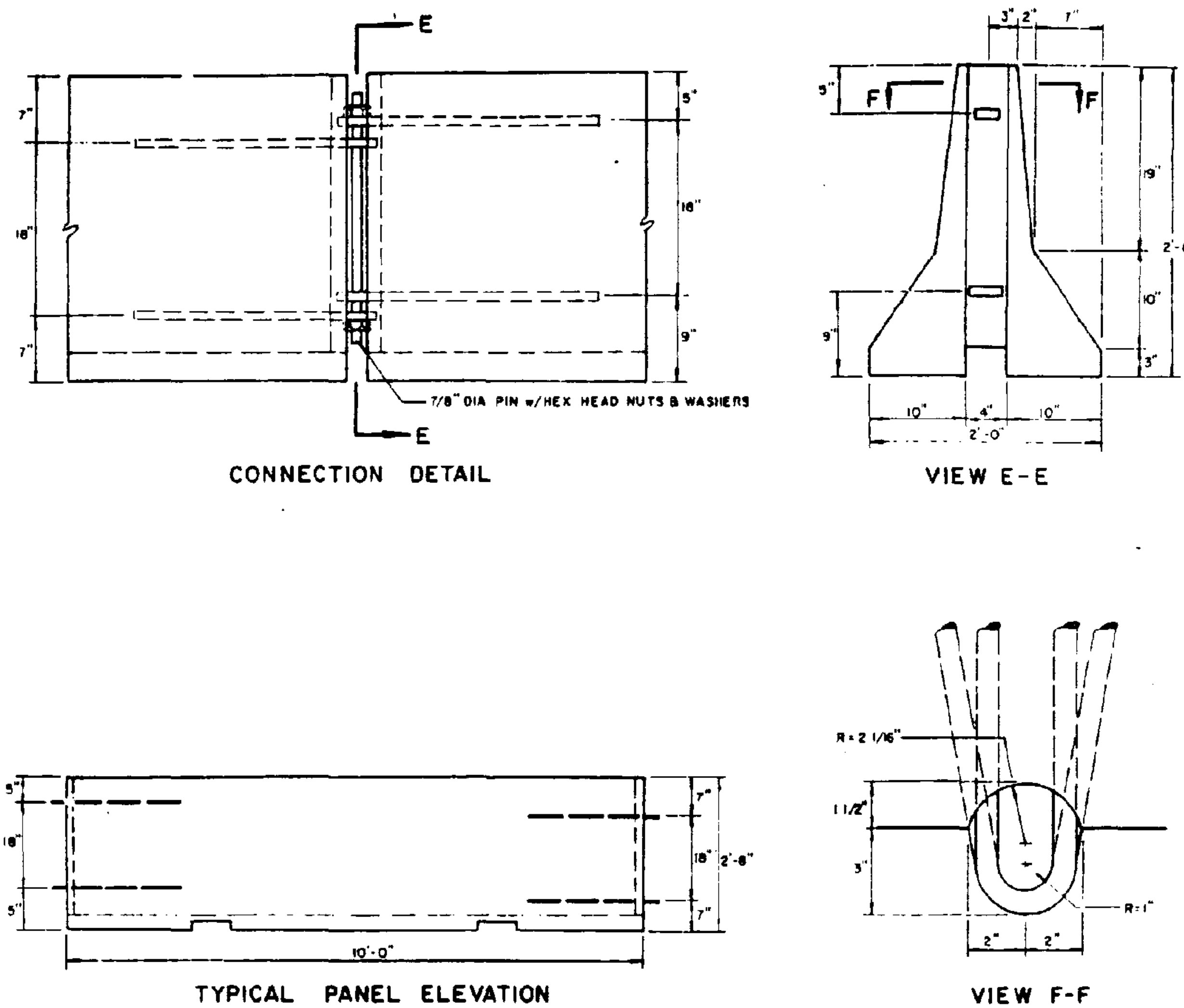

Figure 54. Pin and Rebar (Georgia).

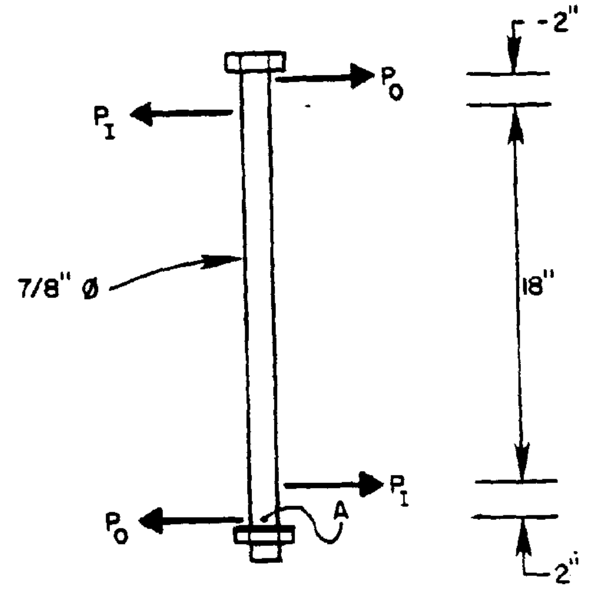

$$\Sigma M_A = 0$$

$$2 P_I - 20 P_I + 22 P_O = 0$$

$$P_I = 1.22\ P_O$$

Figure 55. Forces Acting on Pin When Connection is in Tension.

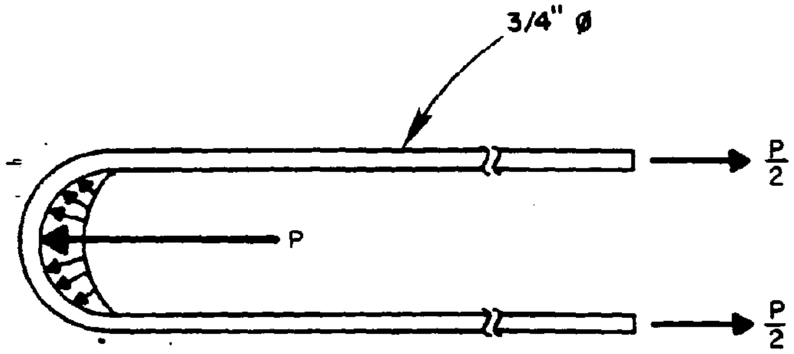

Figure 56. Forces Acting on Steel Loop When Connection is in Tension.

SHEAR CAPACITY

The shear capacity, V, of the connection is controlled by the same mechanism as the tension capacity. Therefore the shear capacity of the connection is 46 k.

BENDING CAPACITY

The bending capacity, M, of this connection is developed as a result of the couple between the tensile force in the hooks and the compressive force in the extreme fibers of the concrete barriers in contact as shown in Figure 23. If the magnitude of the tensile force is taken to be 41.3 k as calculated above and the moment arm, d, in Figure 23 is assumed to be 8 in., the bending capacity of the connection is given as follows:

$M = 46.3$ k (8 in.),

$M = 370.4$ in.-k or 30.9 k-ft.

The bending capacity of this connection is thus calculated to be 31 ft-k.

TORSION CAPACITY

The torsion capacity, T, of this connection is the result of the couple which develops between the forces between the pin and the loops as shown in Figure 57. If moments are summed about point A in Figure 57, the following relationship between the forces results:

$P_O = P_I$

The magnitudes of the forces between the pin and the hooks is controlled by either the strength of the hooks or the strength of the pin.

TENSILE STRENGTH OF HOOKS

Figure 57 presents the tensile forces acting on a steel loop. If it is assumed that the yield strength of the loop in tension is 60 ksi, the torsion capacity of the section is given as follows:

$T = 2\ (\pi)(7/16\ \text{in.})^2(60\ \text{ksi})(18\ \text{in.})$,

$T = 1298.9$ in.-k or 108.2 ft-k.

SHEAR STRENGTH OF PIN

If the yield strength of the pin in shear is assumed to be 34.7 ksi, the torsion capacity of the connection is given as follows:

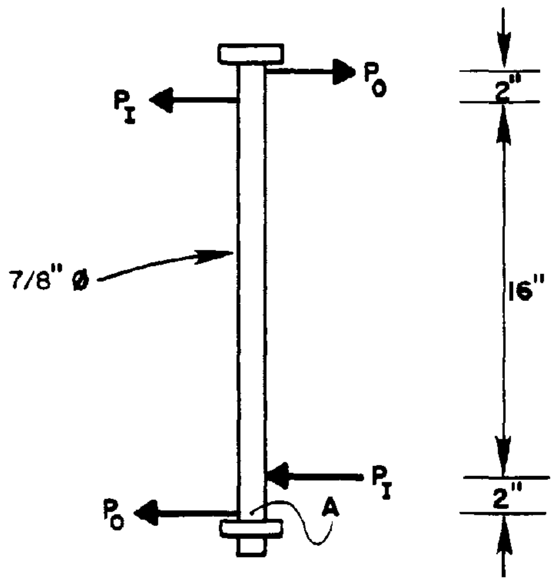

$$\Sigma M_A = 0$$

$$2 P_I + 18 P_I - 20 P_O = 0$$

$$P_I = P_O$$

Figure 57. Forces on Pin When Connection is in Torsion.

$T = \pi(7/16 \text{ in.})^2(34.7 \text{ ksi})(18 \text{ in.}),$

$T = 375.6 \text{ in.-k}$ or $31.3 \text{ ft-k}.$

The torsion capacity of the connection is thus calculated to be 31 ft-k.

DOWEL (Texas)

The Texas Dowel connection is shown in Figure 58. Three steel dowels are cast into one end of the barrier section and three grooves are cast into the other end of the barrier section. The connection is made by inserting the dowels on one end of a barrier section into the grooves on the end of another barrier section. When this connection is used in a permanent installation grout is pumped into the grooves and into the interface area between the barrier sections; however, grout is not used in a temporary installation.

TENSILE CAPACITY

The tensile capacity, F_T, of this connection is zero because grout is not used in a temporary installation.

SHEAR CAPACITY

The shear capacity, V, of this connection is controlled by the shear strength of the dowels as shown in Figure 59, or the bending strength of the dowels as shown in Figure 60.

SHEAR STRENGTH OF DOWELS

If it is assumed that the yield strength of the steel dowels in shear is 34.6 ksi, the shear strength of the connection is given as follows:

$V = 3(\pi)(1/2\ \text{in.})^2(34.6\ \text{ksi}),$

$V = 81.5\ \text{k}.$

BENDING STRENGTH OF DOWELS

If it is assumed that the yield strength of the steel dowels in tension is 60 ksi, the plastic moment capacity of the dowel is calculated as follows:

$M_{pl} = 4/3(1/2\ \text{in.})^3(60\ \text{ksi}),$

$M_{pl} = 10.0\ \text{in.-k}.$

If it is assumed that the moment arm, d, shown in Figure 60 is equal to 1 in., the shear strength of the connection is calculated as follows:

$V = 3(2)(10\ \text{in.-k}/1\ \text{in.}),$

$V = 60.0\ \text{k}.$

The shear capacity of this section is thus calculated to be 60 k.

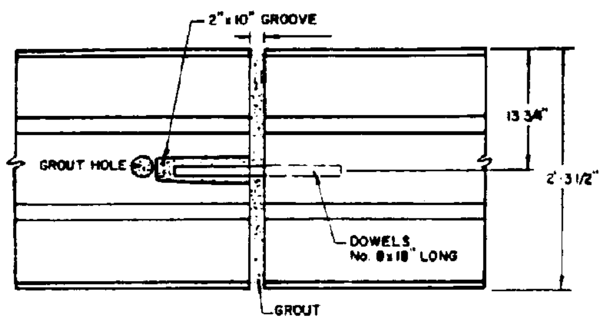

CONNECTION DETAIL

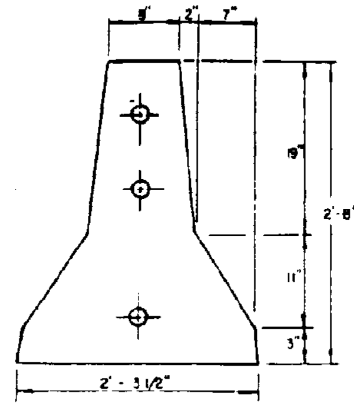

END VIEW

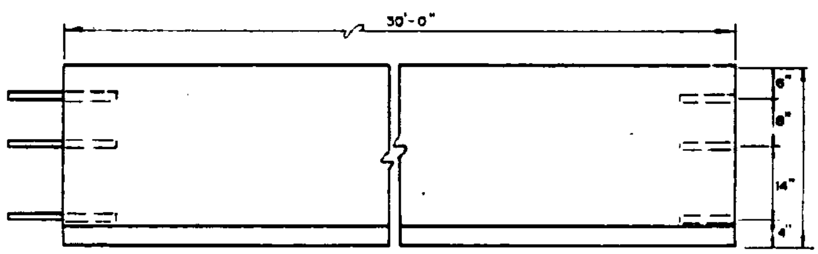

TYPICAL PANEL ELEVATION

Figure 58. Dowel (Texas).

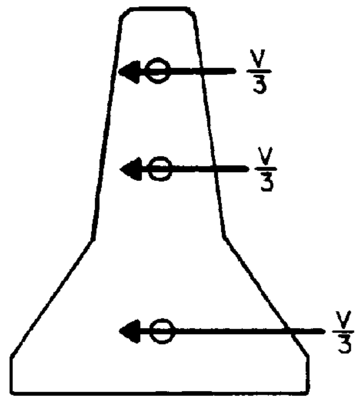

Figure 59. Shear Forces on Dowel When Connection is in Shear.

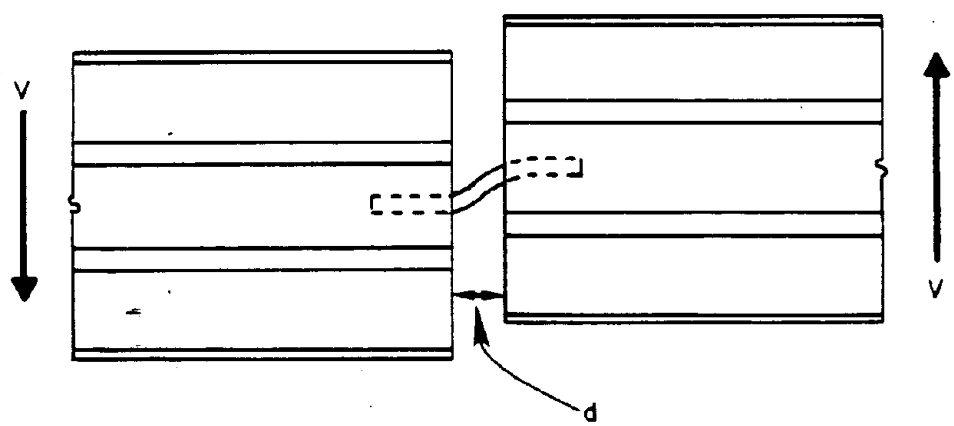

Figure 60. Dowels in Bending When Connection is in Shear.

BENDING CAPACITY

The bending capacity, M, of this connection is zero because grout is not used in temporary connections.

TORSION CAPACITY

It is assumed that the torsion capacity, T, of this connection is the result of the couple which develops between the two outer dowels as shown in Figure 61. It was seen earlier that the maximum shear force in the dowel, is limited by the bending strength of the dowels. Assuming that the plastic moment capacity of a dowel is 10.0 in.-k as calculated earlier, the torsion capacity of the connection is given as follows:

$T = 2(10 \text{ in.-k}/1 \text{ in.})(22 \text{ in.})$,

$T = 440.0 \text{ in.-k}$ or 36.7 ft-k.

The torsion capacity of the section is thus calculated to be 37 ft-k.

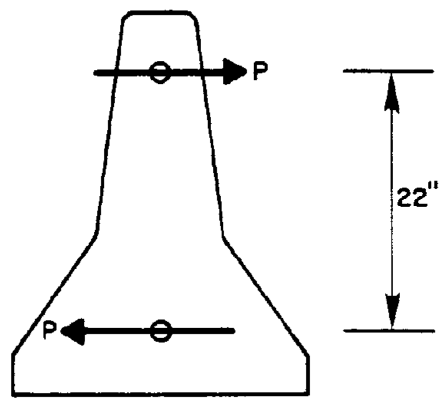

Figure 61. Forces on Dowels When Connection is in Torsion.

TONGUE AND GROOVE (Oregon)

The Oregon tongue and groove connection is shown in Figure 62. Two protrusions are cast on the face of one end of the barrier and two grooves are cast on the other end of the barrier. The connection is accomplished by inserting the protrusions on one end of the barrier into the groove on the other end of the barrier.

TENSILE CAPACITY

The tensile capacity, F_T, of this connection is zero because there is no positive attachment between barrier sections.

SHEAR CAPACITY

The shear capacity, V, of this connection is controlled by the force required to shear the concrete protrusions from the end of a barrier as shown in Figure 63. The total area of the concrete which must be sheared is 88.8 sq. in. If the ultimate shear strength of the concrete is assumed to be 0.30 ksi., the shear strength of the connection is given as follows:

$V = (88.8 \text{ sq. in.})(0.30 \text{ ksi}),$

$V = 26.6 \text{ k}.$

The shear strength of this connection is thus calculated to be 27 k.

BENDING CAPACITY

The bending capacity, M, of this connection is zero because the connection has no tension capacity.

TORSION CAPACITY

To calculate the torsion capacity, T, of the connection it is assumed that the ultimate shearing strength of the concrete is 0.30 ksi and that the shearing stress distribution in the concrete protrusions is as shown in Figure 64. The torsion capacity of the connection is thus calculated as follows:

$T = (5.95 \text{ k})(10.6 \text{ in.}) + (.75 \text{ k})(3.8 \text{ in.}) + (5.20 \text{ k})(7.9 \text{ in.}),$

$T = 107 \text{ in.-k} \text{ or } 8.9 \text{ ft-k}.$

The torsion capacity of the connection is thus calculated to be 9 ft-k.

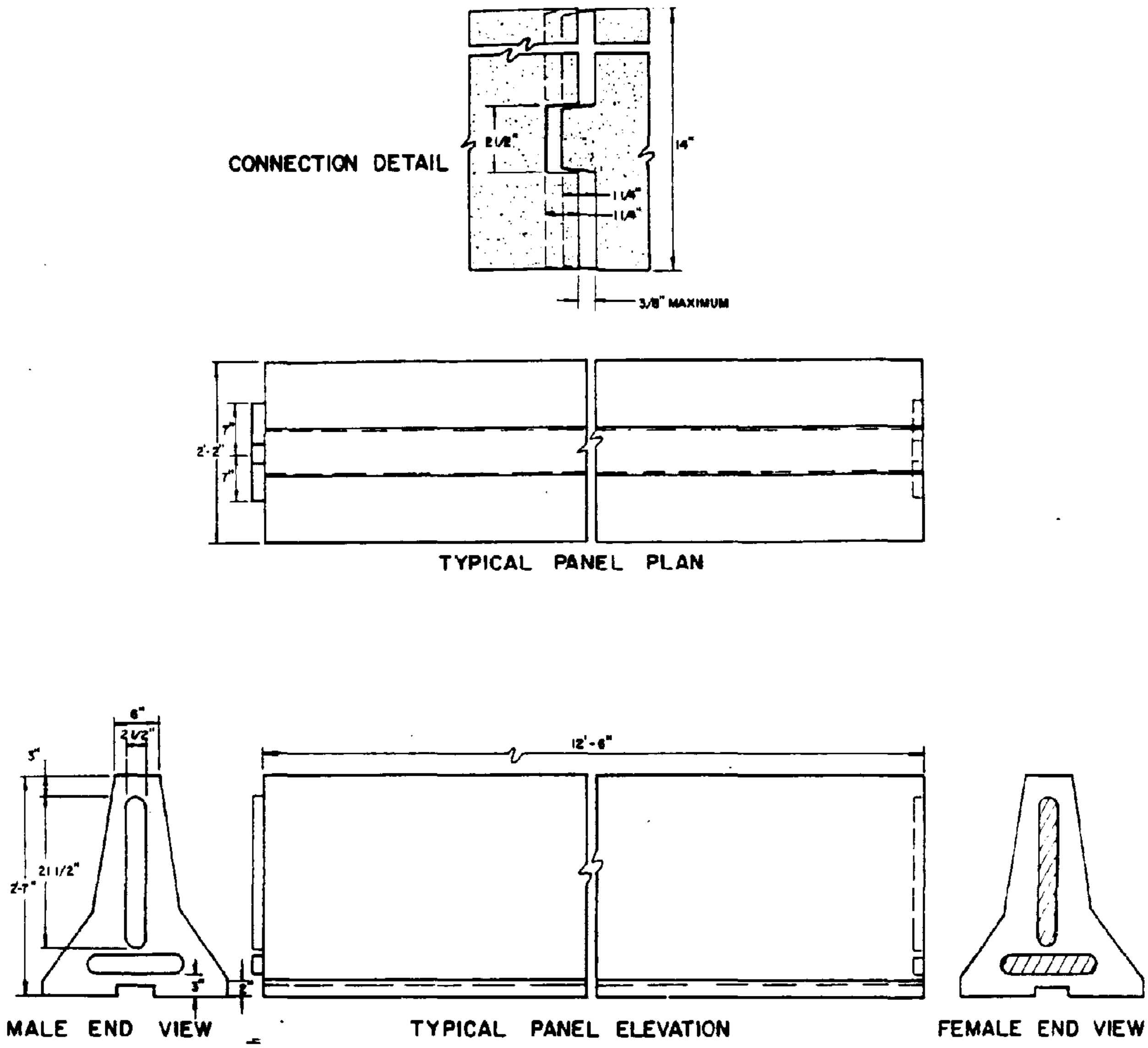

Figure 62. Tongue and Groove (Oregon).

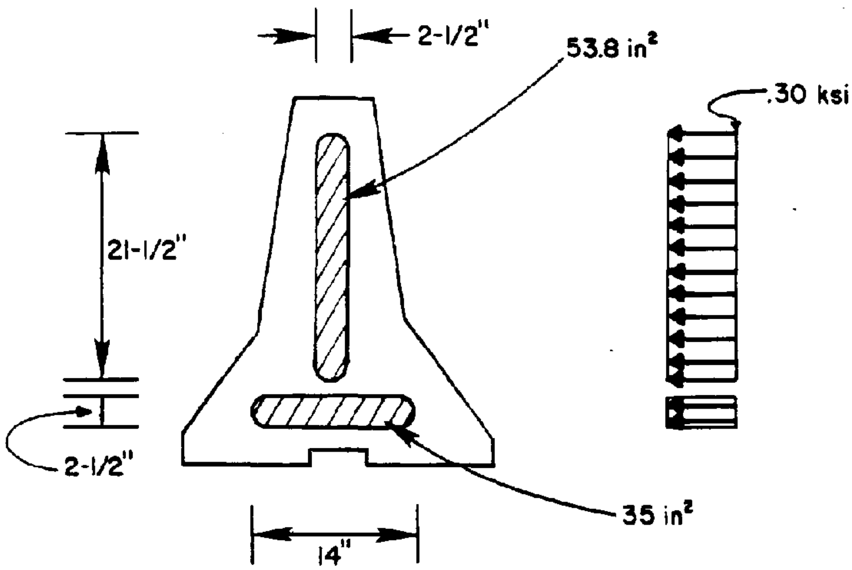

(a) Barrier Cross-Section

(b) Assumed Shearing Stress Distribution

Figure 63. Shearing Stress Distribution in Barrier Tongue When Connection is in Shear.

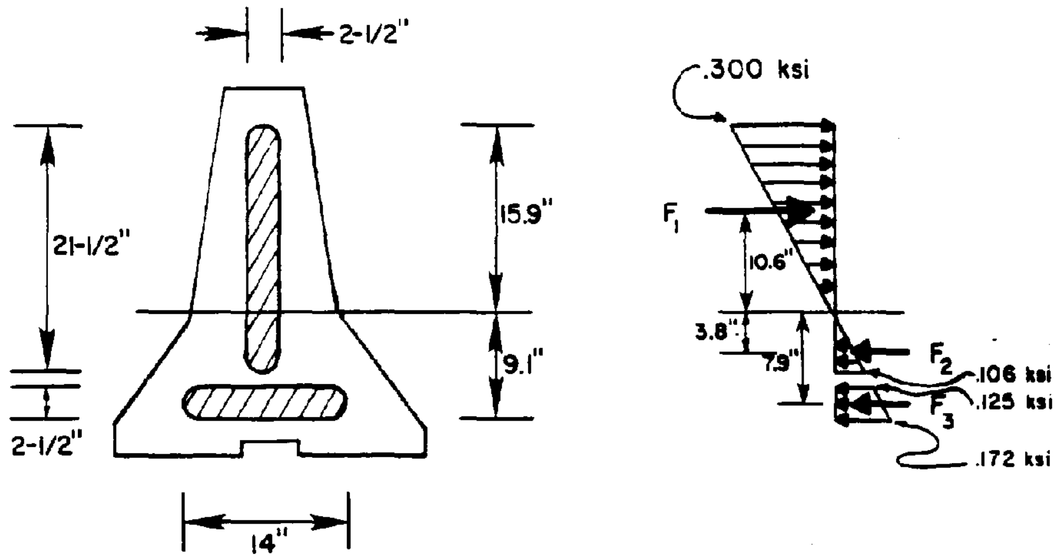

(a) Barrier Cross-Section

(b) Assumed Shearing Stress Distribution

$F_1 = 5.95$ k , $F_2 = 0.75$ k , $F_3 = 5.20$ k

Figure 64. Shearing Stress Distribution in Tongue When Connection is in Torsion.

TONGUE AND GROOVE (Virginia)

The Virginia tongue and groove connection is shown in Figure 65. A single vertical protrusion is cast into one end of the barrier section and a groove is cast into the other end. The connection is accomplished by inserting the protrusion on one end of a barrier section into the groove on the other end of another barrier.

TENSION CAPACITY

The tension capacity, F_T, of this connection is zero because there is no positive attachment.

SHEAR CAPACITY

The shear capacity, V, of this connection is controlled by the force required to shear the concrete protrusion from the end of the barrier section as shown in Figure 66. The area of the protrusion that must be sheared is 107.6 sq. in. If the ultimate shear strength of the concrete is assumed to be 0.30 ksi, the shear strength of the connection is calculated as follows:

$V = (107.6 \text{ sq in.})(0.30 \text{ ksi})$,

$V = 32.3 \text{ k}$.

The shear capacity of the connection is thus calculated to be 32 k.

BENDING CAPACITY

The bending capacity, M, of this section is zero because the tension capacity of the connection is zero.

TORSION CAPACITY

To calculate the torsion capacity, T, of this connection it is assumed that the ultimate shear strength of the concrete is 0.30 ksi and that the shearing stress distribution shown in Figure 67 acts in the concrete protrusion. The torsion capacity of the section is then given as follows:

$T = (6.4 \text{ k})(13.6 \text{ in.})$,

$T = 87.0 \text{ in.-k}$ or 7.3 ft-k.

The torsion capacity of this connection is thus calculated to be 7 ft-k.

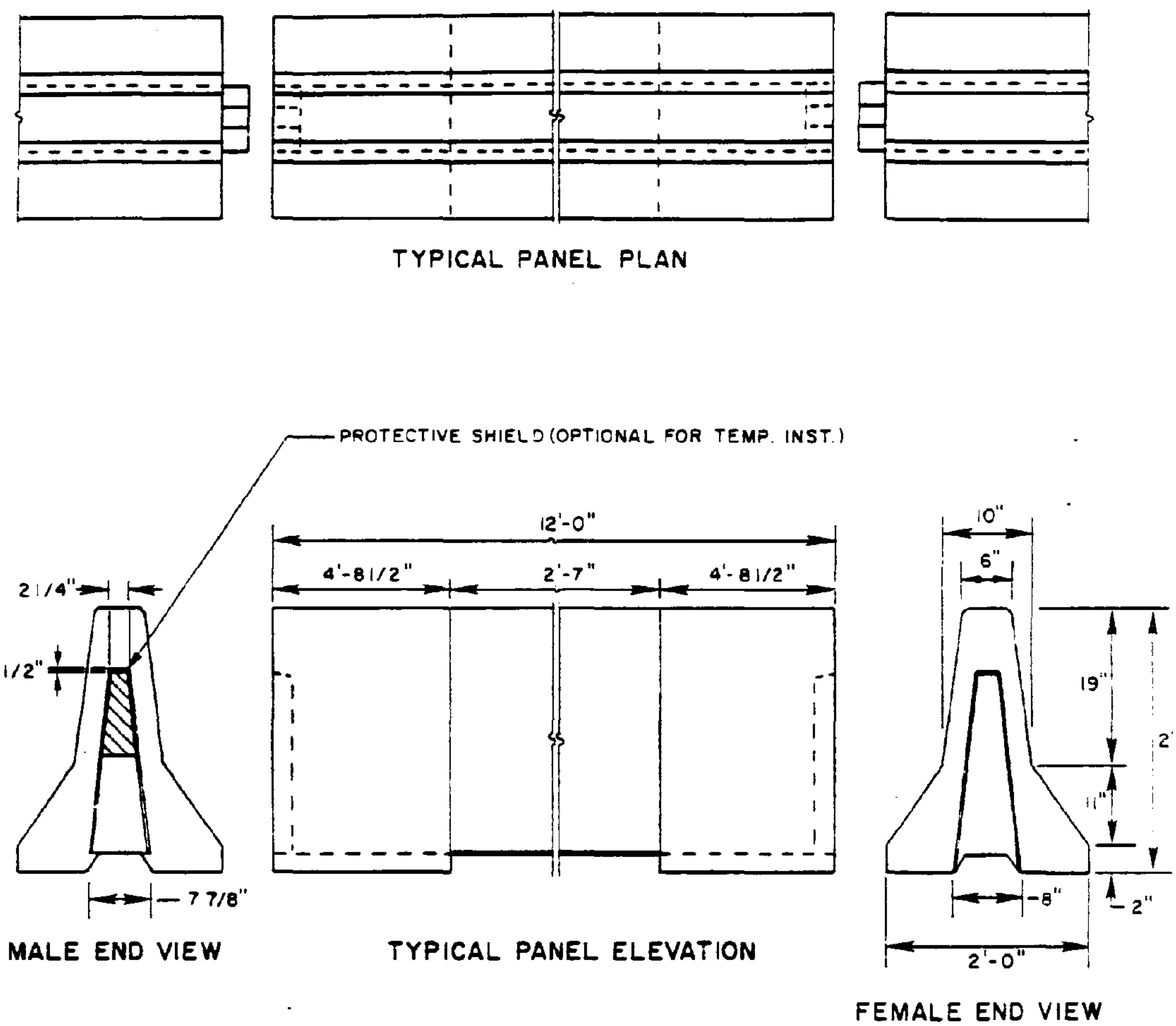

Figure 65. Tongue and Groove (Virginia).

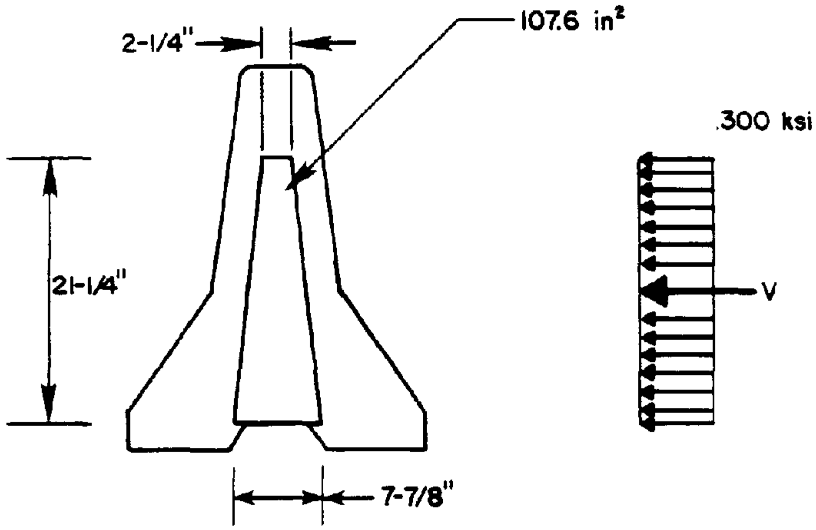

(a) Barrier Cross-Section

(b) Assumed Shearing Stress Distribution

Figure 66. Shearing Stress Distribution in Tongue When Connection is in Shear.

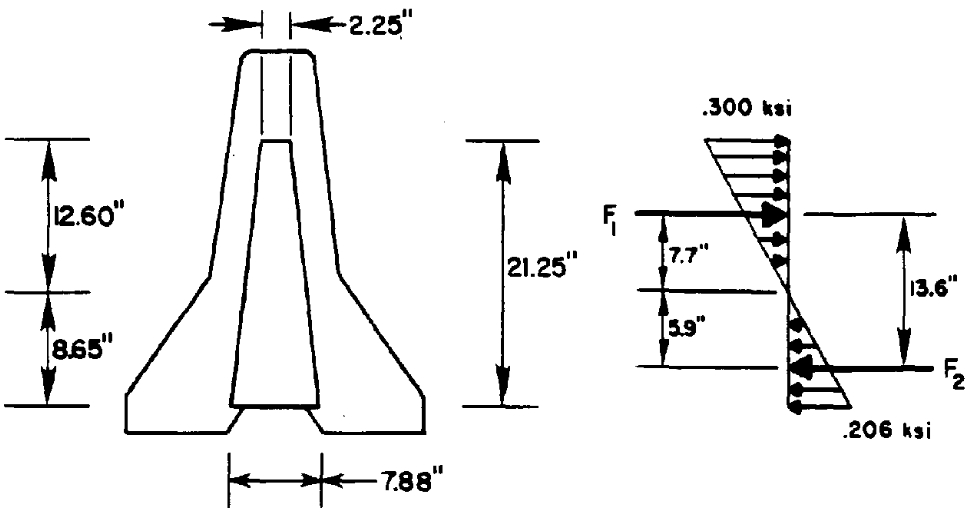

(a) Barrier Cross-Section

(b) Assumed Shearing Stress Distribution

$F_1 = 6.4$ k , $F_2 = 6.4$ k

Figure 67. Shearing Stress Distribution in Tongue When Connection is in Shear.

TOP HOOK AND REBAR (Colorado)

The Colorado top hook and rebar connection is shown in Figure 68. Steel loops are cast into both ends of the barrier section. The barrier connection is accomplished by installing the steel hook as shown in Figure 68.

TENSION CAPACITY

The tensile capacity, F_T, of this connection is controlled by the strength of the steel hook (Ref. Fig. 69) or the strength of the steel loops (Ref. Fig. 70).

TENSILE STRENGTH OF HOOK

If the yield strength of the hook in tension is assumed to be 60 ksi, the tensile strength of the connection at point A (Ref. Fig. 69) is given as follows:

$T = \pi(7/16 \text{ in.})^2(60 \text{ ksi}),$

$T = 36.1 \text{ k}.$

FLEXURAL STRENGTH OF HOOK

If the yield strength of the hook in tension is assumed to be 60 ksi, the plastic moment capacity of the hook at point B, as shown in Figure 69, is given as follows:

$M_{pl} = (4/3)(7/16 \text{ in.})^3(60 \text{ ksi}),$

$M_{pl} = 6.7 \text{ in.-k}.$

The tensile capacity of the hook is then given as follows:

$F_T = 6.70 \text{ in.-k}/(15/16 \text{ in.}),$

$F_T = 7.1 \text{ k}.$

SHEAR STRENGTH OF HOOK

If the yield strength of the hook in shear is assumed to be 34.6 ksi, the tensile strength of the connection is given as follows:

$F_T = 34.6 \text{ ksi } (\pi)(7/16 \text{ in.})^2,$

$F_T = 20.8 \text{ k}.$

TENSILE STRENGTH OF LOOP

If the yield strength of the loop in tension is assumed to be 60 ksi, the tensile strength of the loop loaded as shown in Figure 70 is given as follows:

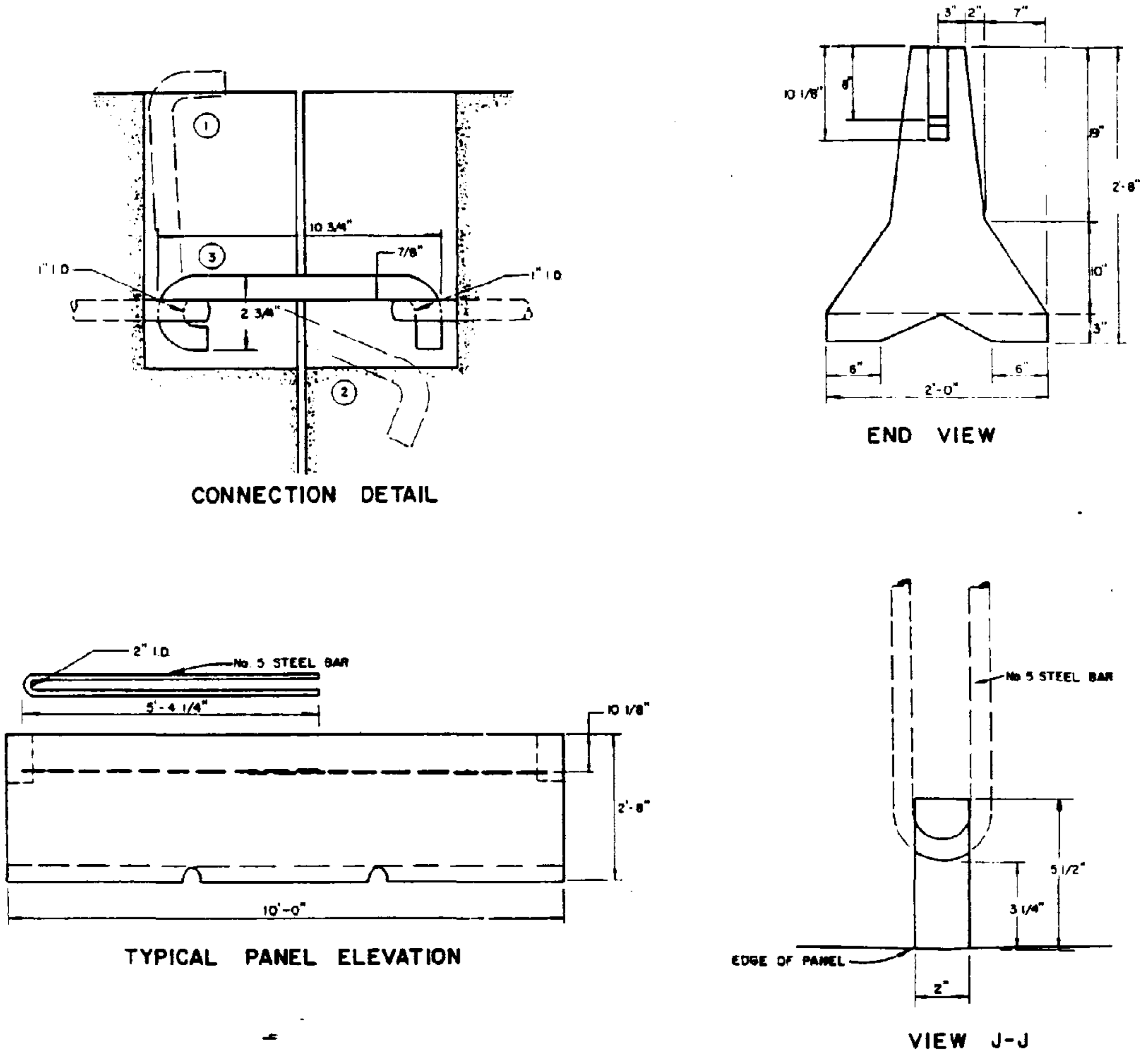

Figure 68. Top Hook and Rebar (Colorado).

$F_T = 2(\pi)(5/16 \text{ in.})^2(60 \text{ ksi})$,

$F_T = 36.8$ k.

The tensile capacity of the connection is thus calculated to be 7 K.

SHEAR CAPACITY

The shear capacity, V, of this connection is controlled by the shear strength of the hook loaded as shown in Figure 71, or the frictional resistance between the barrier sections in contact as shown in Figure 72.

SHEAR STRENGTH OF HOOK

The shear strength of the hook was previously calculated to be 20.8 k.

FRICTIONAL RESISTANCE BETWEEN BARRIERS

The maximum normal force between the barriers was previously determined to be 7.2 k. If the coefficient of friction between the concrete barriers is assumed to be 0.7 (Ref. Fig. 73), the shear strength of the connection is thus calculated to be 5. k.

$V = .7\ (7.2)$,

$V = 5.0$ k.

The shear capacity of the connection is thus calculated to be 5 k.

BENDING CAPACITY

The bending capacity, M, of this connection is controlled by the couple which develops between the tensile force in the hook and the compressive force between the concrete barriers in contact as shown in Figure 23. If the moment arm, d, shown in Figure 23 is assumed to be 8 in., the bending strength of the connection is given as follows:

$M = (7.2 \text{ k})(8 \text{ in.})$,

$M = 57.6$ in.-k or 4.8 ft-k.

The bending capacity of this connection is thus calculated to be 5 ft-k.

TORSION CAPACITY

The torsion capacity is controlled by the torque required to twist the hook loaded as shown in Figure 74. If it is assumed that the yield strength of the hook in shear is 34.6 ksi, the torsion capacity of the connection is given as follows:

$T = (2/3)(34.6 \text{ ksi})(7/16 \text{ in.})^3$,

$T = 1.9$ in.-k or .16 ft-k.

The torsion capacity of the connection is thus calculated to be effectively zero.

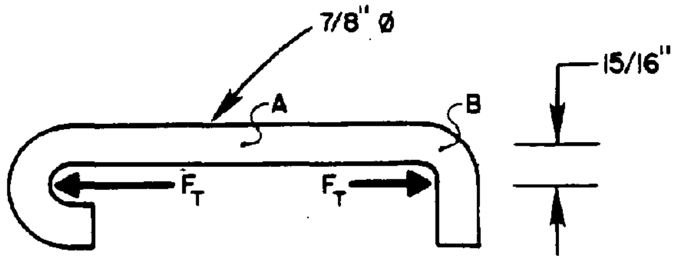

Figure 69. Forces on Top Hook When Connection is in Tension.

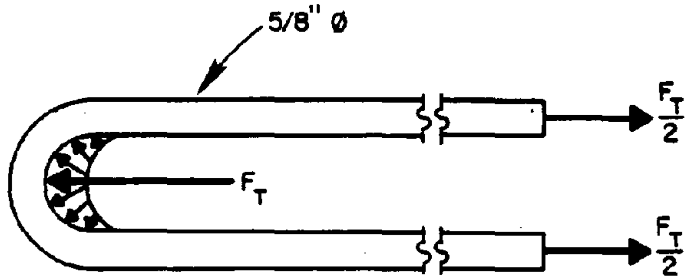

Figure 70. Forces on Loop When Connection is in Tension.

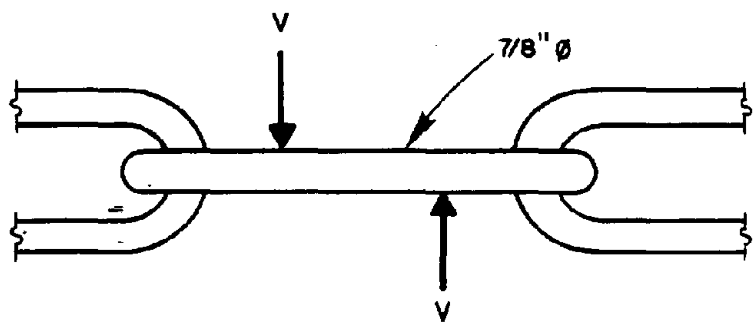

Figure 71. Forces on Top Hook When Connection is in Shear.

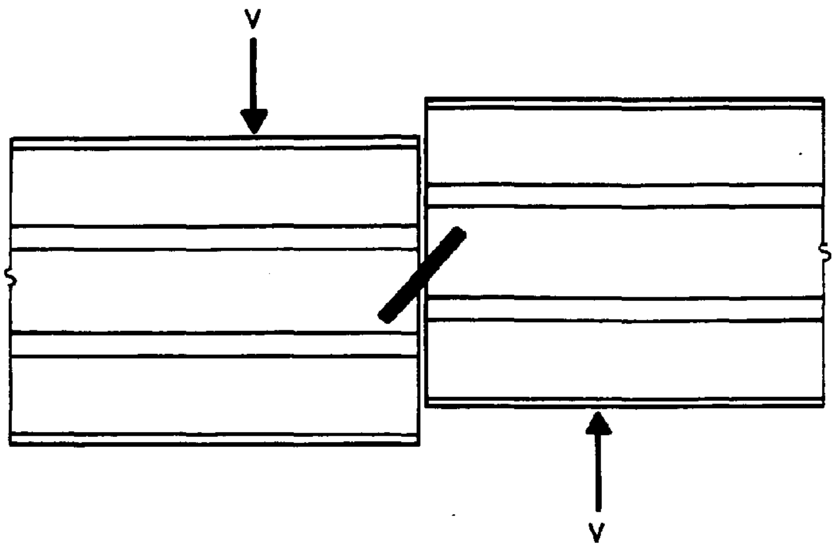

Figure 72. Barrier Faces in Contact When Connection is in Shear.

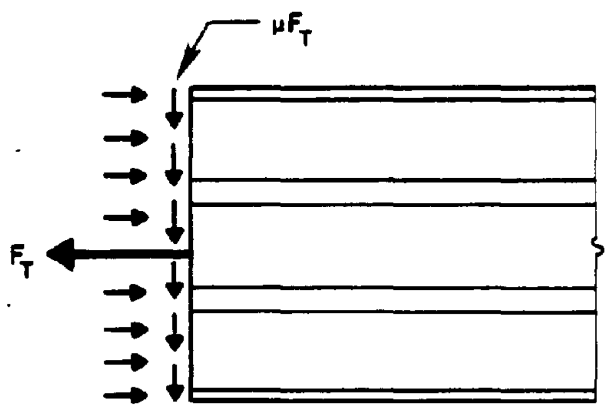

Figure 73. Friction Forces on Barrier Face When Connection is in Shear.

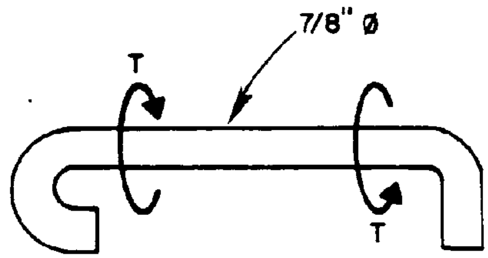

Figure 74. Forces on Top Hook When Connection is in Torsion.

CHANNEL SPLICE

The TTI channel splice connection is shown in Figure 75. The barrier sections are fabricated with two bolt holes through the thickness of the barrier. The barrier connection is accomplished by connecting the barrier ends together using channel splice plates which are bolted to the barrier ends with bolts which go through the full width of the barrier section as shown.

TENSILE CAPACITY

The tensile capacity, F_T, of this connection is controlled by either the strength of the channel splice plates, or the strength of the bolts loaded as shown in Figure 76.

TENSILE STRENGTH OF SPLICE

If it is assumed that the yield strength of the splice in tension is 36 ksi, the tensile capacity of the connection is given as follows (Ref. Fig. 76):

F_T = 2[2.64 sq in.-(7/4 in.)(.325 in.](36ksi),

F_T = 149.1 k.

SHEAR STRENGTH OF BOLTS

If it is assumed that the yield strength of the bolts in shear is 34.6 ksi, the tensile strength of the connection is given as follows:

$F_T = 4(.70)(\pi)(9/16 \text{ in.})^2(34.6 \text{ ksi})$,

F_T = 96.3 k.

The tensile strength of the connection is thus calculated to be 96 k.

SHEAR CAPACITY

The shear capacity, V, of the connection is controlled by either the shear strength of the channel splice plate as shown in Figure 77, or the frictional resistance between the barrier ends in contact as shown in Figure 78.

SHEAR STRENGTH OF SPLICE

If the yield strength of the channel splice plate in shear is assumed to be 20.8 ksi, (Ref. Fig. 77) the shear strength of the connection is given as follows:

V = 2(2.64 sq. in.)(20.8 ksi),

V = 109.8 k.

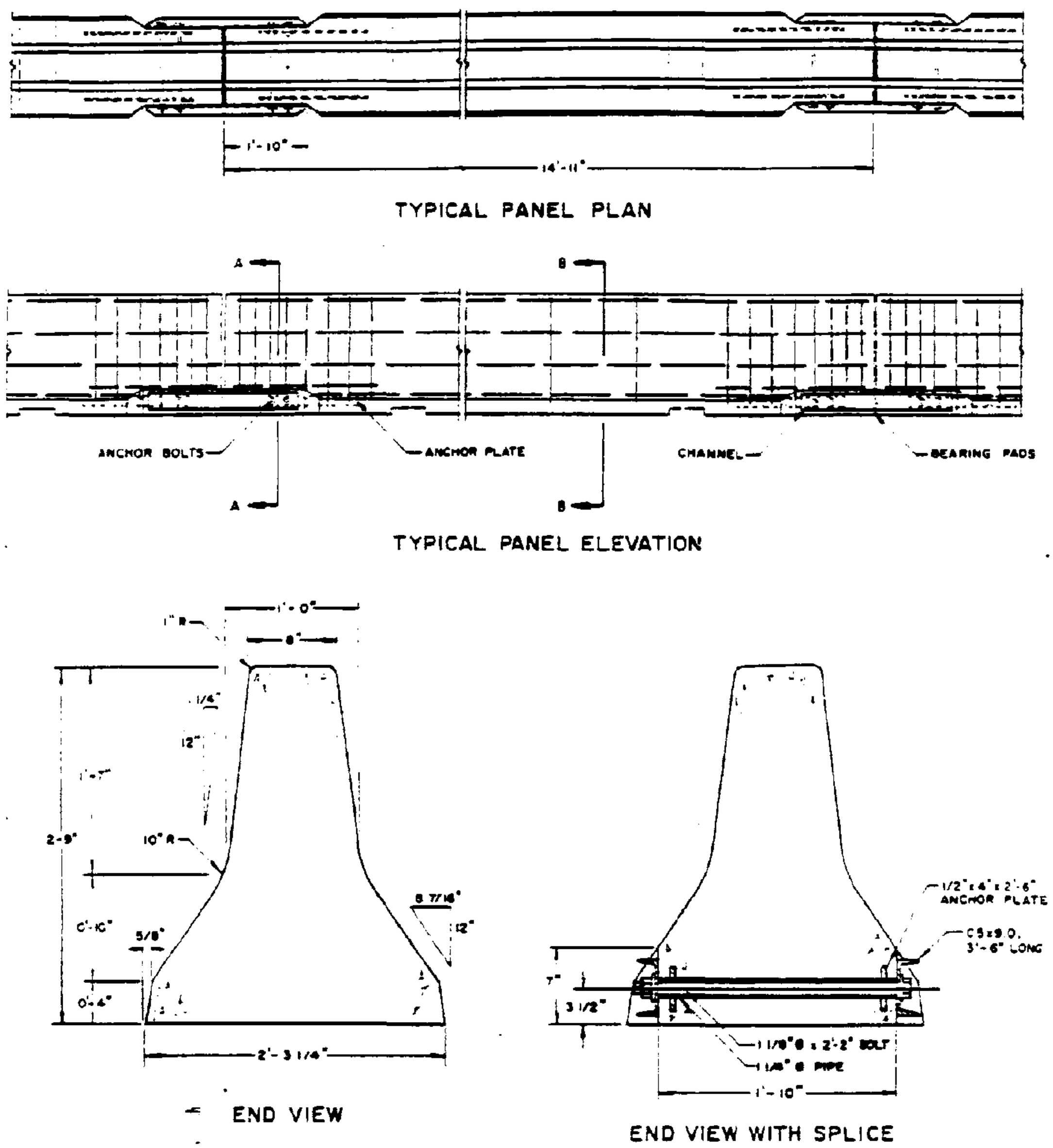

Figure 75. Channel Splice.

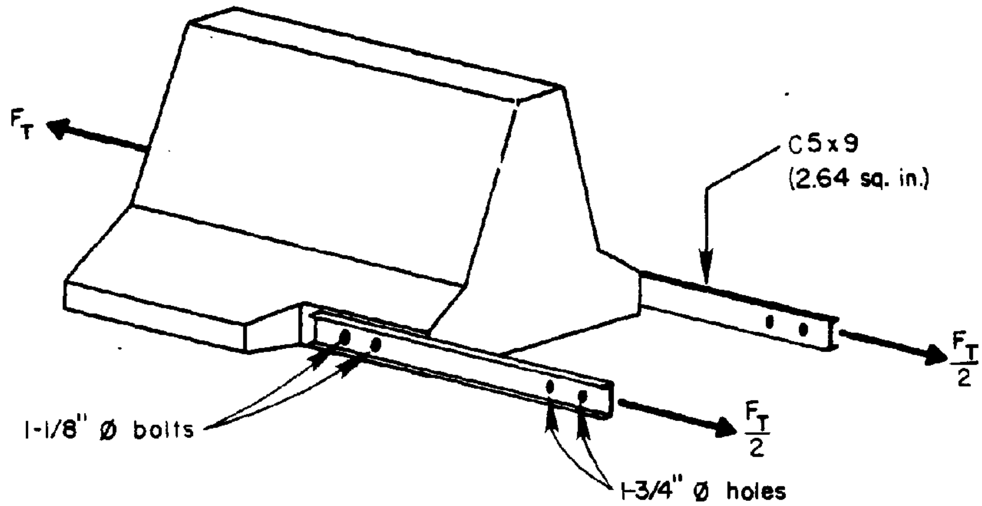

Figure 76. Forces on Bolts and Channels When Connection is in Tension.

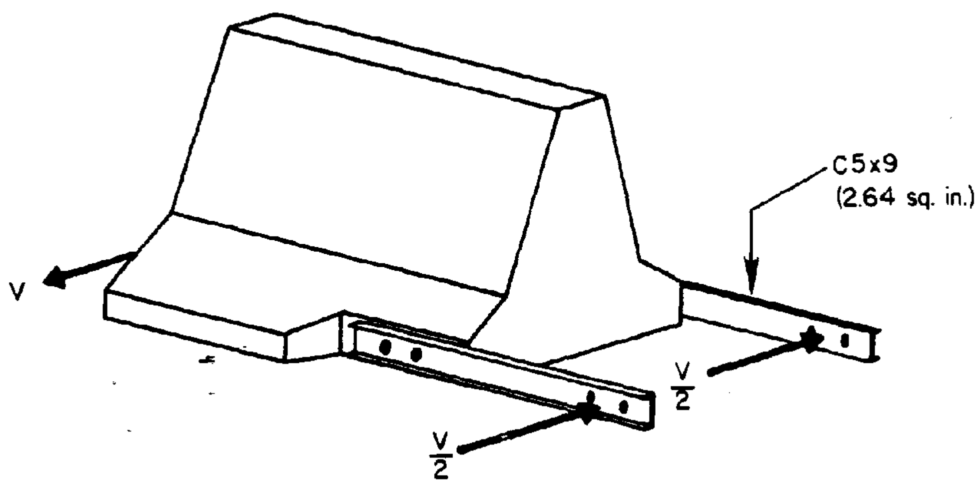

Figure 77. Forces on Channel When Connection is in Shear.

FRICTIONAL RESISTANCE BETWEEN BARRIERS

The maximum normal force between the barriers was calculated earlier to be 96.3 k. If the coefficient of friction between the barriers is assumed to be 0.7, the shear strength of the connection is given as follows (Ref. Fig. 79):

$V = .7(96.3\ k),$

$V = 67.4\ k.$

The shear capacity of the connection is thus calculated to be 67 k.

BENDING CAPACITY

The bending capacity of this connection is controlled by the couple which develops between the splice plate in tension and the compressive force between the barriers in contact as shown in Figure 80. The maximum force in each channel was calculated to be 96.3/2 k. If the moment arm, d, shown in Figure 80 is assumed to be 20 in., the bending capacity of the connection is given as follows:

$M = (96.3/2\ k)(20\ in.),$

$M = 963.0\ in.\text{-}k$ or $80.3\ ft\text{-}k.$

The bending capacity of the connection is thus calculated to be 80 ft-k.

TORSION CAPACITY

The torsion capacity of this connection is controlled by the couple which develops in the channel splice plates as shown in Figure 81. The force in the splice plates is limited by either the shear or bending capacity of the splice plates loaded as shown in Figure 82.

SHEAR STRENGTH OF SPLICE PLATES

If the yield strength of the splice plates in shear is assumed to be 20.4 ksi, the torsion capacity of the connection is given as follows:

$T = (2.64\ sq.\ in.)(20.4\ ksi)(22\ in.),$

$T = 1184.8\ in.\text{-}k$ or $98.7\ ft\text{-}k.$

BENDING STRENGTH OF SPLICE PLATES

If the yield strength of the splice plates in tension is assumed to be 36 ksi, the plastic moment capacity of the section is given as follows:

$$M_{pl} = 2[(2.18\ in.)(.325\ in.)(36\ ksi)(2.18\ in./2) + (1.56\ in.)(.32\ in.)(2.34\ in.)(36\ ksi)],$$

$$M_{pl} = 139.7\ in.\text{-}k.$$

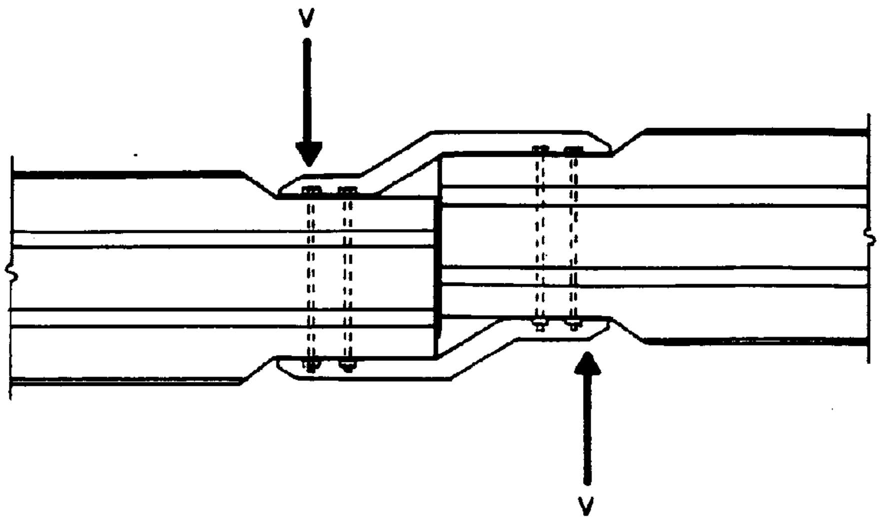

Figure 78. Connection in Shear.

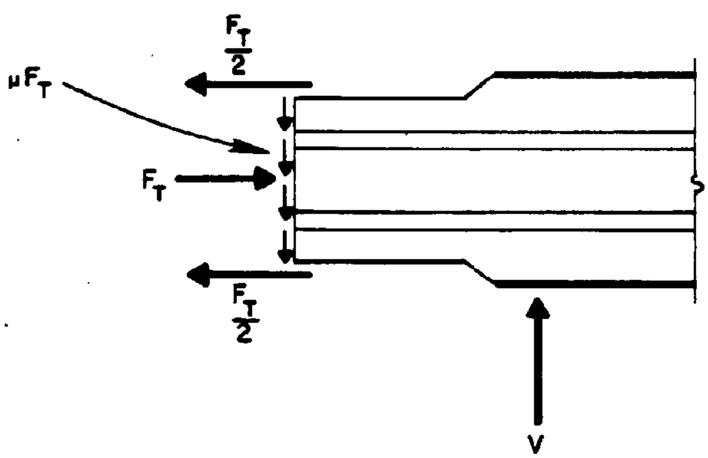

Figure 79. Frictional Forces on Barrier Face When Connection is in Shear.

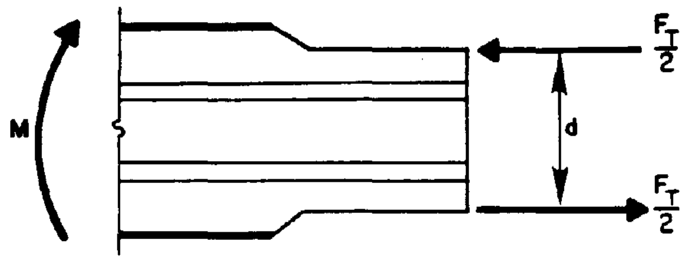

Figure 80. Forces on Barrier Face When Connection is in Bending.

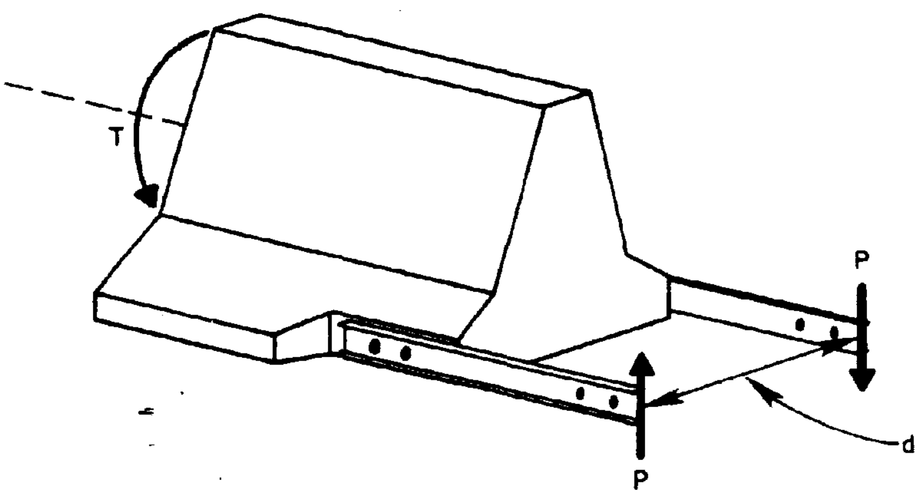

Figure 81. Forces on Channels When Connection is in Torsion.

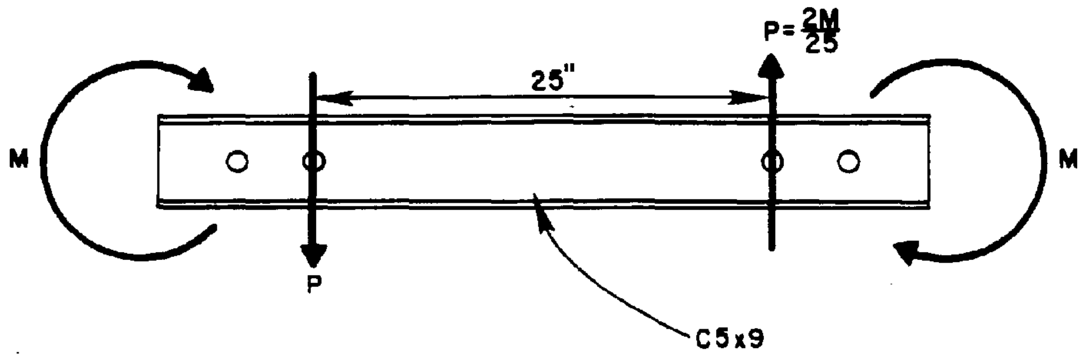

(a) Forces on Channel

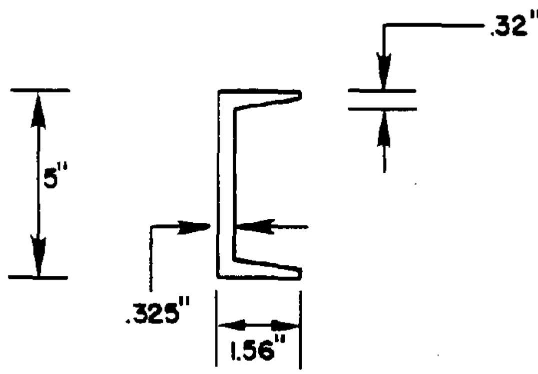

(b) Cross-Section of Channel

Figure 82. Forces on Channel When Connection is in Torsion.

The torsion capacity of the section is then given as follows:

T = (2/25 in.)(139.7 in.-k)(22 in.),

T = 245.9 in.-k or 20.5 ft-k.

The torsion capacity of this connection is thus calculated to be 21 ft-k.

T-LOCK (BASE)

The TTI T-Lock connection is shown in Figure 83. Vertical holes are cast into the bottom ends of the barrier section as shown. The holes are aligned so that they mate with the vertical members of the steel T-Lock. The connection is accomplished by placing the steel T-Lock in position and lifting the barrier sections onto the T-Lock as shown in Figure 83.

TENSILE CAPACITY

The tensile capacity, F_T, of this connection is controlled by the strength of the steel T-Lock loaded as shown in Figure 84. This strength is limited by either the tensile strength of the horizontal structural tube or the shearing strength of the vertical end pipes.

TENSILE STRENGTH OF STRUCTURAL TUBE

If it is assumed that the yield strength of the structural tube in tension is 46 ksi, the tensile capacity of the connection is given as follows:

F_T = (8.36 sq. in.)(46 ksi),

F_T = 384.6 k.

SHEAR STRENGTH OF VERTICAL PIPE

If it is assumed that the yield strength of the pipe tube in shear is 20.8 ksi, the tensile capacity of the connection is given as follows:

F_T = (2.23 sq. in.)(20.8 ksi),

F_T = 46.4 k.

The tensile capacity of the connection is thus calculated to be 46 k.

SHEAR CAPACITY

The shear capacity, V, of this connection is controlled by the strength of the steel T-Lock loaded as shown in Figure 85. If the yield strength of the structural tube in shear is assumed to be 26.6 ksi, the shear strength of the connection is given as follows:

V = [8.36 sq. in. + 13.75 sq. in.](26.6 ksi),

V = 588.1 k.

The shear strength of this connection is thus calculated to be 588 k.

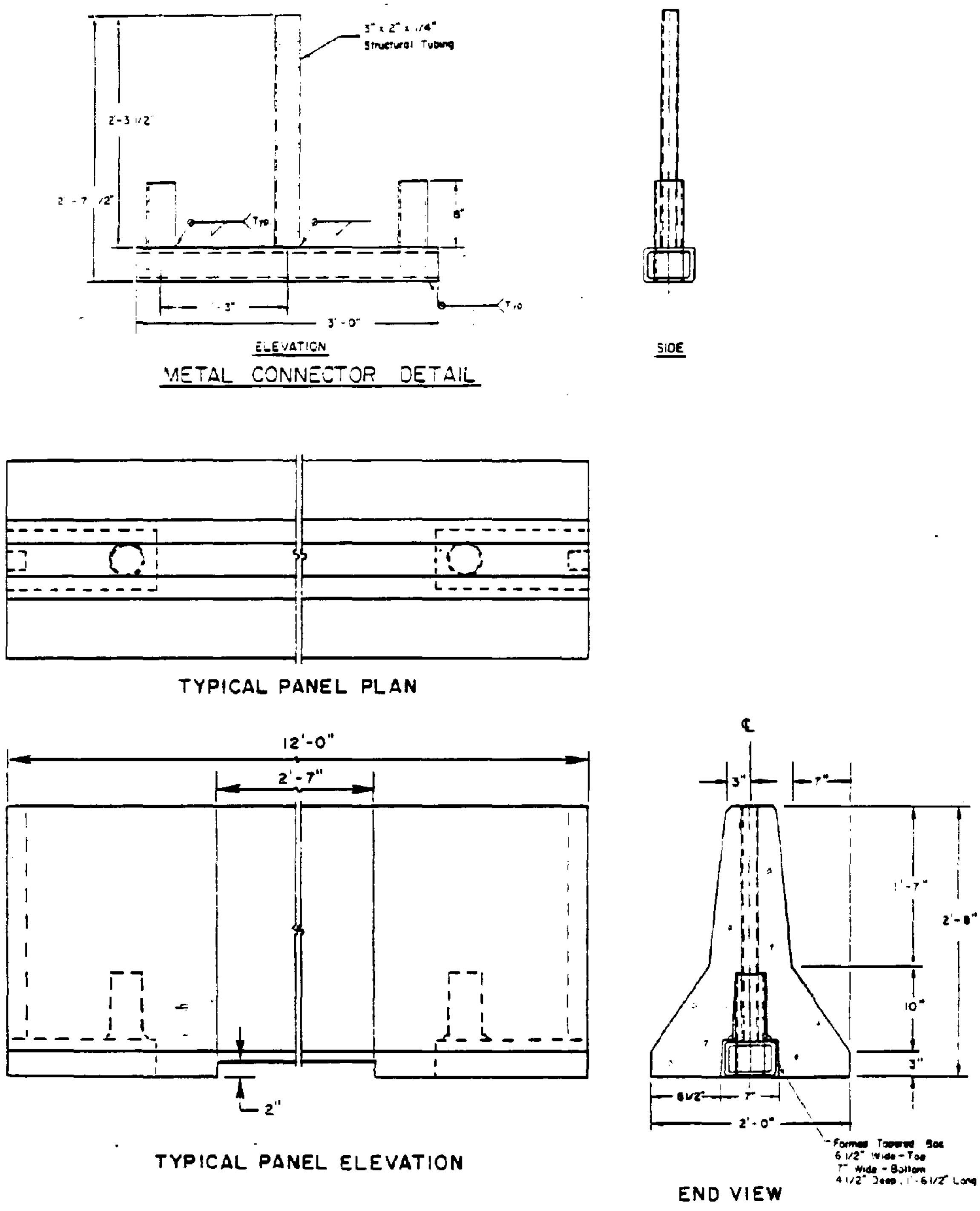

Figure 83. T-Lock (Base).

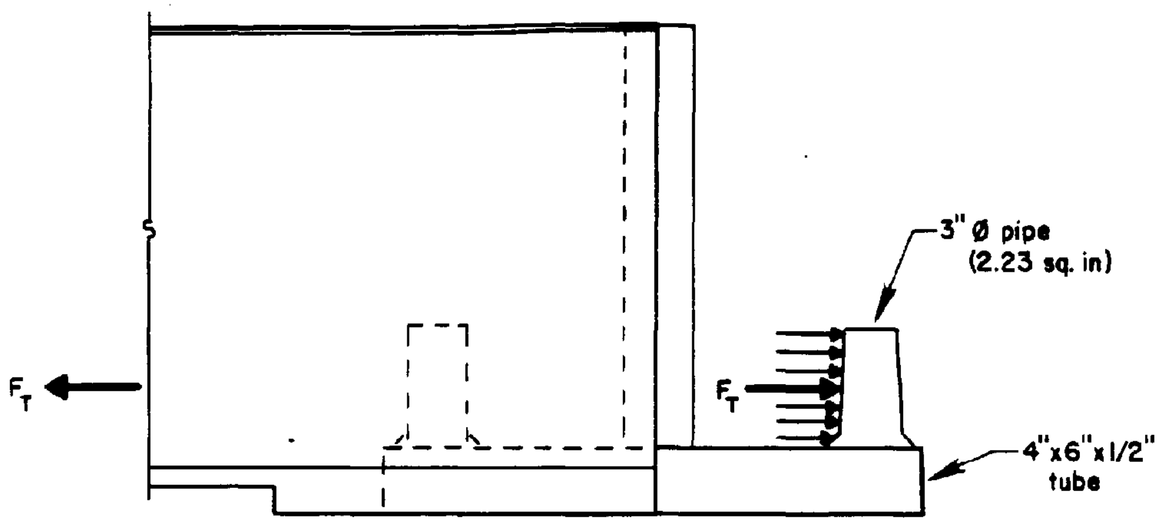

Figure 84. Forces on T-Lock When Connection is in Tension.

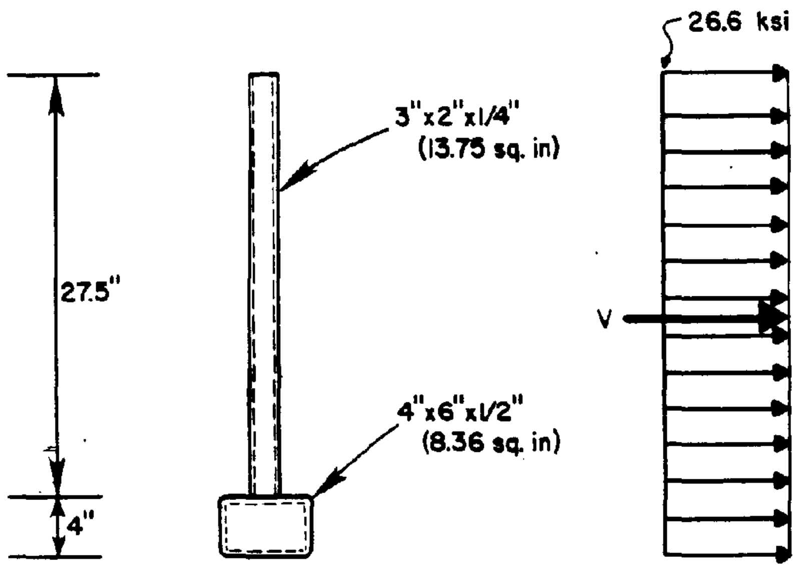

(a) Cross-Section of T-Lock in Shear

(b) Assumed Shearing Stress Distribution

Figure 85. Shearing Forces on T-Lock When Connection is in Shear.

BENDING CAPACITY

The bending capacity, M, of this connection is the result of the combined actions of the couple which develops between the tensile force in the T-Lock and the compressive force between the barrier ends in contact (Ref. Fig. 23), and the bending strength of the structural tube. The combined bending capacities are closely approximated by simply summing the two effects. If it is assumed that the yield strength of the structural tube is 46 ksi, the bending capacity of the connection is given as follows:

M = 2[(3 in.)(1 in.)(1.5 in.)+(3 in.)(.5 in.)(2.75 in.)](46 ksi)+(46.4 k)(8 in.),

M = 1164.7 in.-k or 97.1 ft-k.

The moment capacity of the connection is thus calculated to be 97 ft-k.

TORSION CAPACITY

The torsion capacity of the connection is controlled by the strength of the steel T-Lock with the assumed shear stress distribution shown in Figure 86. If the yield strength of the structural tube in shear is assumed to be 26.6 ksi, the torsion capacity of the connection is give as follows:

T = (294 k)(11.1 in.)+(71.7 k)(2.7 in.)+(222.3 k)(4.7 in.).

T = 4501.8 in.-k or 375.2 ft-k.

The torsion capacity of the connection is thus calculated to be 375 ft-k.

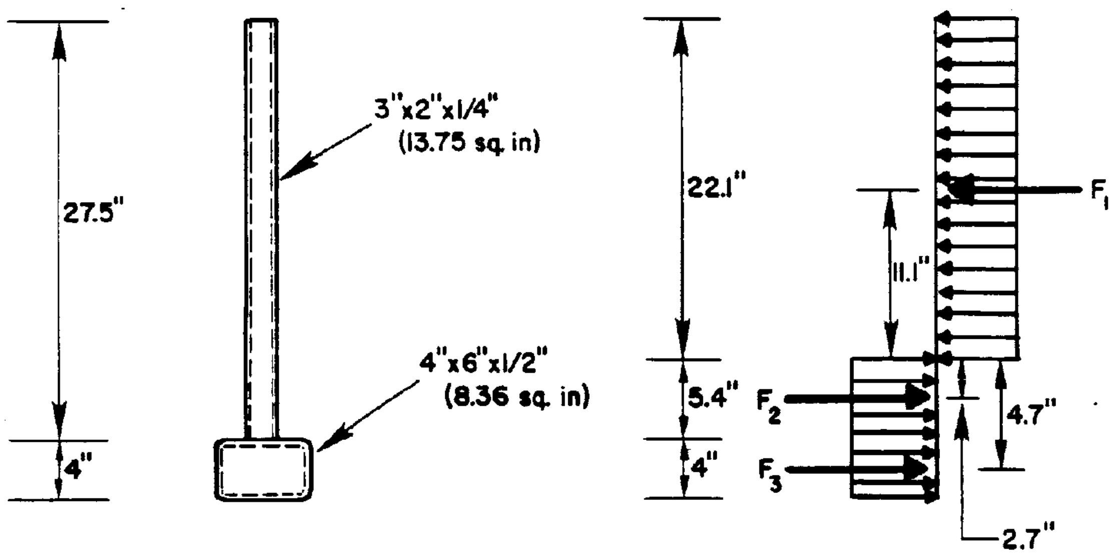

(a) Cross-Section of T-Lock in Shear

(b) Assumed Shearing Stress Distribution

$F_1 = 294.0$ k , $F_2 = 71.7$ k , $F_3 = 222.3$ k

Figure 86. Shearing Forces on T-Lock When Connection is in Tension.

T-LOCK (TOP)

The Harris county T-Lock connection is shown in Figure 87. Vertical holes are cast into the top ends of the barrier section as shown. The holes are aligned so that they mate with the vertical members of the steel T-Lock. The connection is accomplished by positioning the barrier sections end to end and then lowering the T-Lock into place from the top as shown in Figure 87.

TENSILE CAPACITY

The tensile capacity, F_T, of this connection is controlled by the strength of the steel T-Lock loaded as shown in Figure 88. This strength is limited by either the tensile strength of the horizontal steel channel, or the shearing strength of the vertical steel pins.

TENSILE STRENGTH OF CHANNEL

If it is assumed that the yield strength of the steel channel in tension is 36 ksi, the tensile capacity of the connection is give as follows:

F_T = (1.59 sq. in.)(36 ksi),

F_T = 57.2 k.

SHEARING STRENGTH OF PINS

If it is assumed that the yield strength of the steel pins in shear is 20.8 ksi, the tensile capacity of the connection is given as follows:

$F_T = \pi(.5 \text{ in.})^2(20.8 \text{ ksi})$,

F_T = 16.3 k.

The tensile strength of the connection is thus calculated to be 16. k.

SHEAR CAPACITY

The shear capacity of the connection is controlled by the strength of the steel T-Lock with the assumed shearing stress distribution shown in Figure 89. If it is assumed that the yield strength of the steel channel in shear is 20.8 ksi and that the yield strength of the structural tube in shear is 26.6 ksi, the shear strength of the connection is given as follows:

V = (1.59 sq. in.) (20.8 ksi) + (12 in.)(1/2 in.) (26.6 ksi),

V = 192.7 k.

The shear strength of this connection is thus calculated to be 193 k.

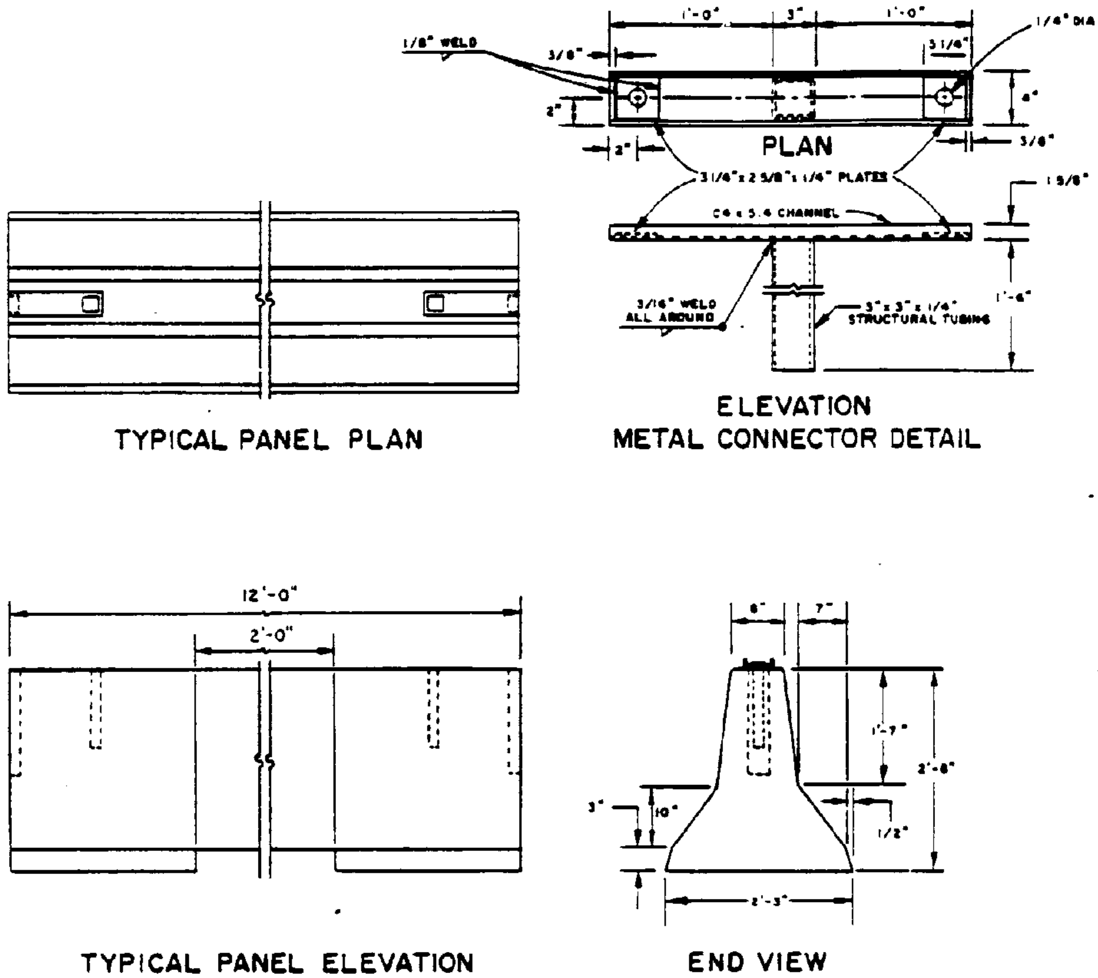

Figure 87. T-Lock (Top).

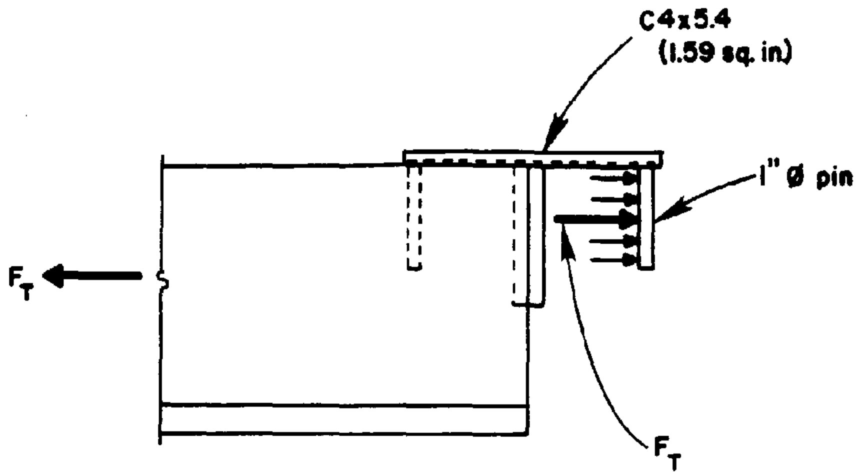

Figure 88. Forces on T-Lock When Connection is in Tension.

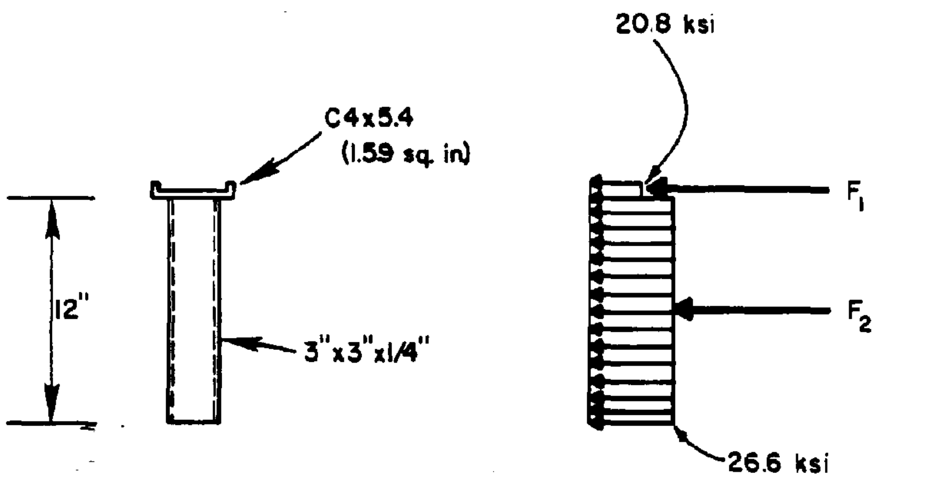

(a) Cross-Section of T-Lock in Shear

(b) Assumed Shearing Stress Distribution

F_1 = 33.1 k , F_2 = 159.6 k

Figure 89. Forces on T-Lock When Connection is in Shear.

BENDING CAPACITY

The bending capacity, M, of this connection is controlled by the couple which develops between the tensile force in the T-Lock and the compressive force between the barrier ends in contact as shown in Figure 23. If the moment arm, d, in Figure 23 is assumed to be 8 in., the moment capacity of the connection is given as follows:

M = (16.3 k) (8 in.),

M = 130.4 in.-k or 10.9 ft-k.

The bending capacity of this connection is thus calculated to be 11 ft-k.

TORSION CAPACITY

The torsion capacity, T, of this connection is controlled by the strength of the T-Lock with the assumed shear stress distribution shown in Figure 90. If the yield strengths of the channel and the structural tube are assumed to be 20.8 ksi and 26.6 ksi respectively, the torsional capacity of this connection is given as follows:

T = 96.4 k (3.6 in.) + 63.3 k(2.4 in.) + 33.1 k (5.2 in.),

T = 671.1 in.-k or 55.9 ft-k.

The torsion capacity of this connection is thus calculated to be 56 ft-k.

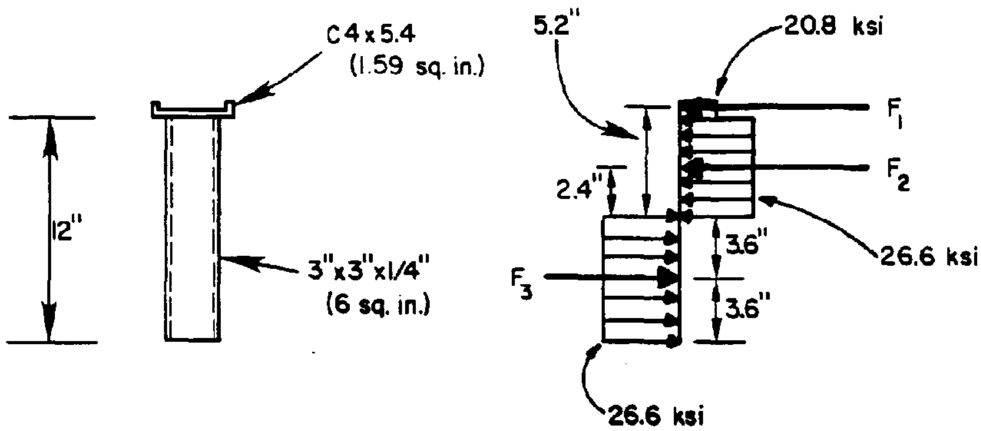

(a) Cross-Section of T-Lock in Torsion

(b) Assumed Shearing Stress Distribution

$F_1 = 33.1$ k , $F_2 = 63.3$ k , $F_3 = 96.4$ k

Figure 90. Forces on T-Lock When Connection is in Torsion.

GRID-SLOT (Texas)

The Texas grid-slot connection is shown in Figure 91. An orthogonal connection grid is fabricated by welding three horizontal steel bars welded to two vertical steel bars as shown in Figure 91. Identical vertical slots are cast into each end of the barrier segments. The connection is accomplished by aligning the ends of two barrier sections and inserting the steel grid described above into the slot. In permanent installations the grid is then grouted in place; however, in temporary installations grout is not used.

TENSILE CAPACITY

The tensile capacity, F_T, of this connection is zero because there is no positive connection between the barrier section ends.

SHEAR CAPACITY

The shear capacity, V, of this connection is controlled by either the shear strength (ref. Fig. 92) or bending strength (ref. Fig. 93) of the horizontal grid bars.

SHEAR STRENGTH OF GRID BARS

If it is assumed that the shear strength of the grid bars in shear is 34.6 ksi, the shear strength of the connection is given as follows:

$V = 3\ (\pi)(.5\ \text{in.})^2(34.6\ \text{ksi}),$

$V = 81.5\ \text{k}.$

BENDING STRENGTH OF GRID BARS

If it is assumed that the yield strength of the grid bars in tension is 60 ksi, the plastic moment capacity of the bars is calculated as follows:

$M_{pl} = 4/3\ (.5\ \text{in.})^3(60\ \text{ksi}),$

$M_{pl} = 10.0\ \text{in.-k}.$

If it is then assumed that the moment arm, d, shown in Figure 93 is assumed to be 1 in., the shear strength of the connection is given as follows:

$V = 3(2)(10\ \text{in.-k}/1\ \text{in.}),$

$V = 60\ \text{k}.$

The shear capacity of the connection is thus calculated to be 60 k.

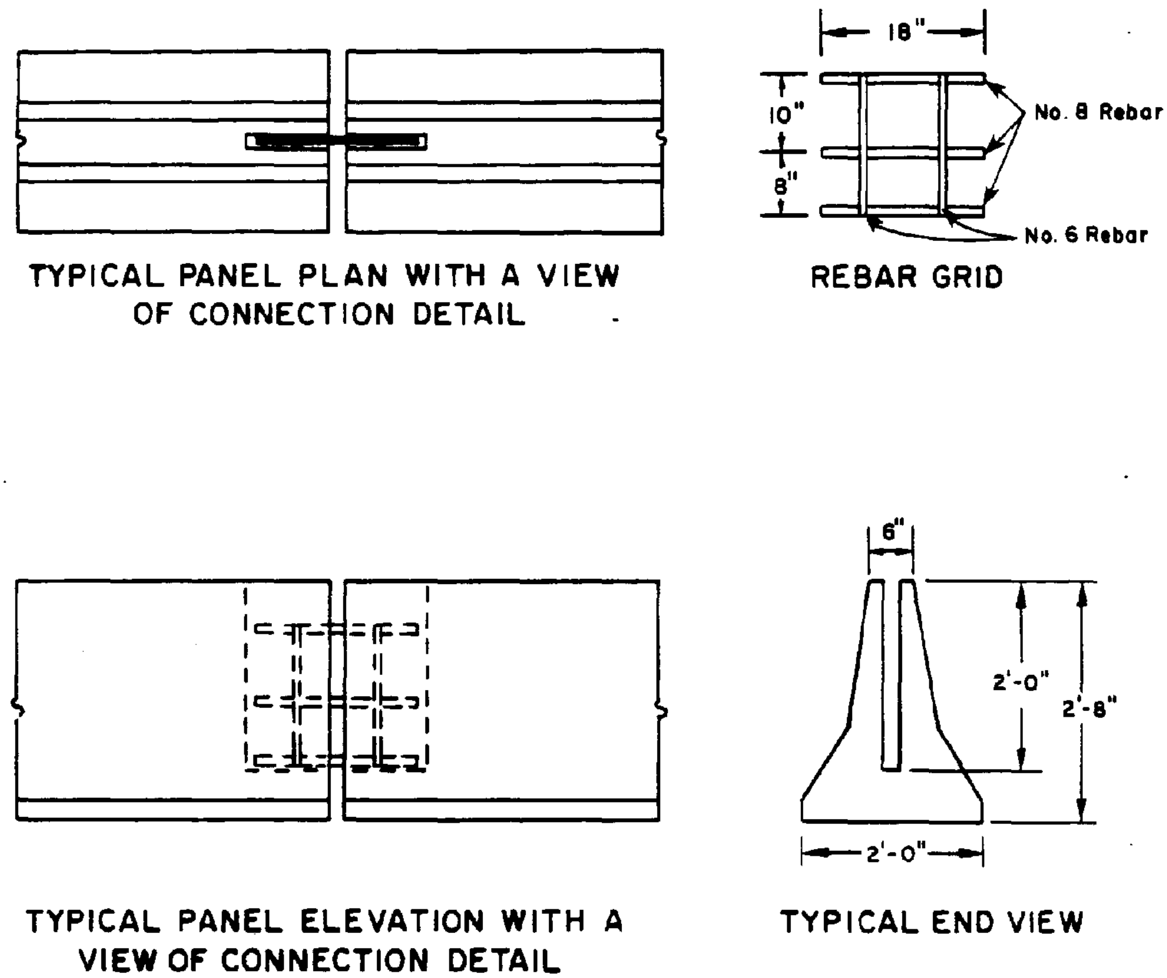

Figure 91. Grid-Slot (Texas).

BENDING CAPACITY

The bending capacity, M, of this connection is zero because grout is not used in temporary connections.

TORSION CAPACITY

It is assumed that the torsional capacity, T, of this connection is the results of the couple which develops between the two outer grid bars as shown in Figure 94. It was seen earlier that the maximum shear force in the bars is limited by the bending strength of the bars. If it is assumed that the plastic moment capacity of the grid bars is 10 in.-k as calculated earlier, the torsion capacity of the connection is given as follows:

T = 2(10 in.-k/1 in.) (18 in.),

T = 360 in.-k or 30 ft-k.

The torsion capacity of the connection is thus calculated to be 30 ft-k.

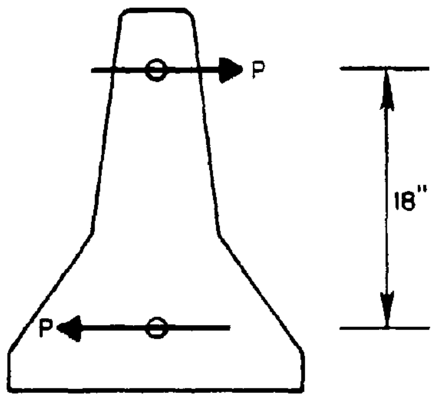

Figure 94. Forces on Outer Grid Bars When Connection is in Torsion.

BARRIERS IN CONSTRUCTION ZONES

APPENDIX E

Cost of Portable Concrete Barriers

Prepared for
Contract DOT-FH-11-9458
Office of Research

Federal Highway Administration

U. S. Department of Transportation

by

Roger J. Koppa
Research Psychologist

Texas A&M Research Foundation

Texas Transportation Institute

The Texas A&M University System

April 1985

THE COST OF PORTABLE CONCRETE BARRIERS

INTRODUCTION

In order to develop a solid basis for comparative ratings of portable concrete barrier concepts, a number of cost estimates were performed on various aspects of fabricating, installing, relocating, maintaining, and removing these barriers at construction sites. Some of this work was based on field observations carried out in the early summer of 1983, and some was based on estimates of the tasks, manpower and equipment times and costs that it might take to perform these operations. As will be described below, man-minute and equipment-time estimates for analytic cases were based on standard construction industry information such as that obtainable from the Dodge Manual (8). Other pricing guides were used as a backup, and industrial engineering standard references were used to estimate time for jobs such as joint fabrication.

Ten different portable concrete barrier (PCB) concepts were used in this analysis. They run the gamut so far as joint design is concerned, from the very simplest tongue-and-groove or mortise design to the very complex Welsbach interlocking joint. All but one of these joints (Bottom T-Lock, Concept C-8) are in use somewhere in the United States. Except for details of reinforcing steel and hardware cast into the body of the barrier itself, these ten concepts differ only in the joint design. Each design is also considered for three different lengths: 10, 20, and 30 ft. Other lengths, of course, are both feasible and occasionally found in use, but the results of the analyses presented in this chapter can readily be interpolated for any length less than 30 ft. For lengths greater than 30 ft, physical limitations of cranes and flatbed truck trailers assumed or observed in this study would greatly and nonlinearly change these cost estimates.

The ten concepts are as follows:

- C1: Tongue and Groove
- C2: Steel Dowel Joint
- C3: Grid Slot--a Gridiron inserted down a slot in the ends of abutting PCB's
- C4: Top T-Lock--a T-shaped connector is pinned on each side of a joint

C5: Lapped joint--each end of a PCB at a joint is scarfed to overlap, with a single bolt holding the joint together

C6: Pin and Re-Bar--a long bolt drops through rings embedded in the ends of each PCB to form a hinge-like joint

C7: Vertical I-Beam--the joint consists of an I-beam which is dropped through a split pipe embedded in each PCB end

C8: Bottom T-Lock--somewhat like C4, but pins become short pipe ends, and the PCB's are placed over the joint assembly

C9: Channel Splice--Channel sections are bolted across the two PCB ends to form the joint

C10: Welsbach--steel T-hooks engage matching slots in the mating end of a PCB to form an interlocking joint.

These ten joint concepts are pictured in Figures 95 through 104. Detailed technical descriptions and further views of these joints and the reinforcing structures required in their respective barrier structure are given in Appendix D.

Field research was performed in the late spring and early summer of 1983 to witness first hand actual operations by several different contractors and to conduct time and motion studies of representative PCB handling procedures. With the very kind assistance of the Texas State Department of Highways and Public Transportation, resident maintenance engineers in all the major urban districts of the Department were contacted and asked to alert TTI researchers when movement, installation, or removal of PCB's was scheduled in their district. Three field trips resulted from this. Each trip followed the same protocol.

Researchers traveled to the site and checked in with the SDHPT supervisor, and the contractor supervisor. After observing several cycles of manipulation of the PCB's, individual procedure times were taken by stopwatch. Still photographs of the joint design and representative stages in the moving, loading, and placement of PCB's, etc. were made. Then several complete cycles were videotaped. Supervisory personnel were debriefed to clear up any details. The procedure followed the format given in Figure 105, which is a reproduction of the field visit data sheet. The three sites visited were:

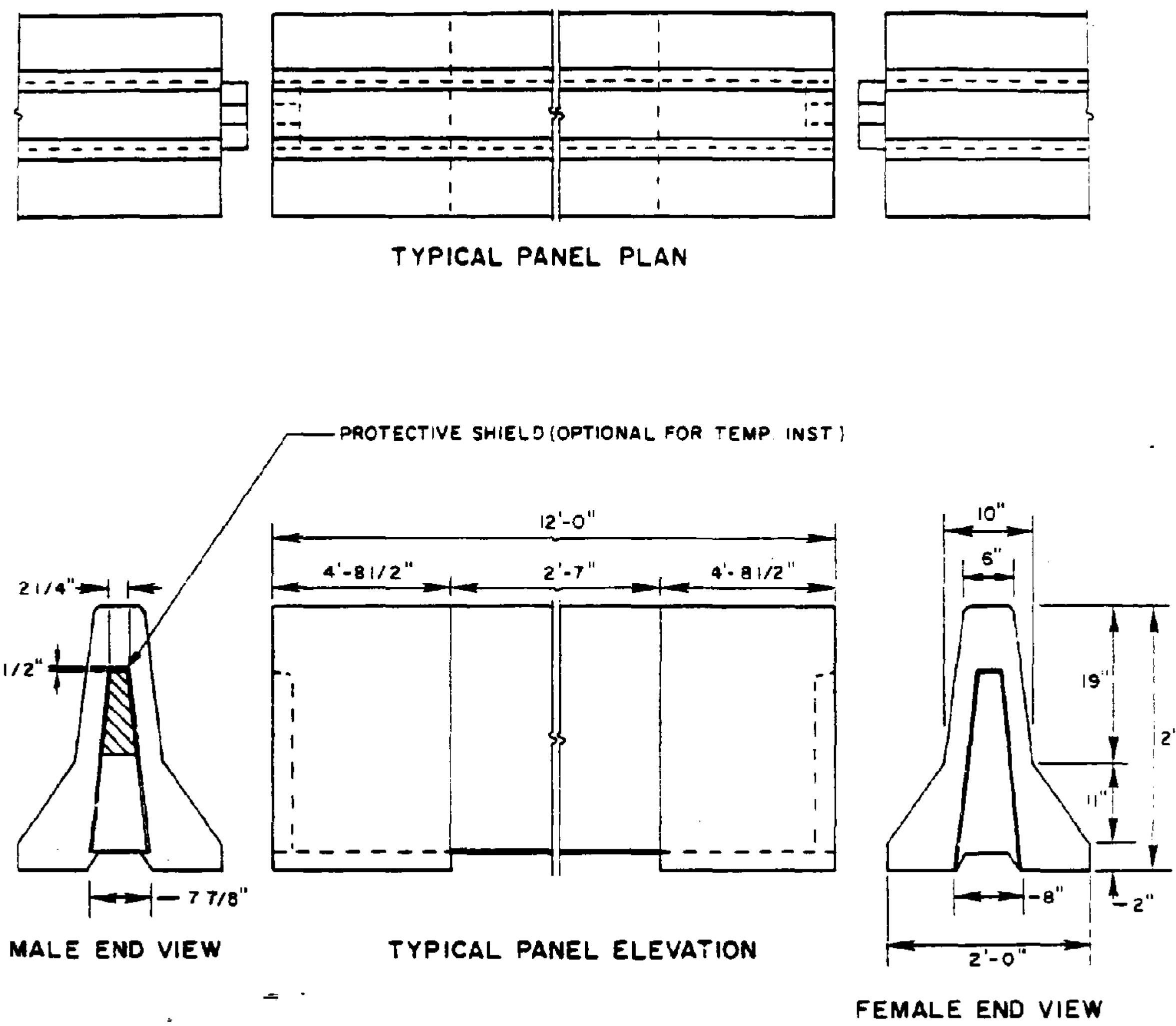

Figure 95. Joint Concept C1--Tongue and Groove.

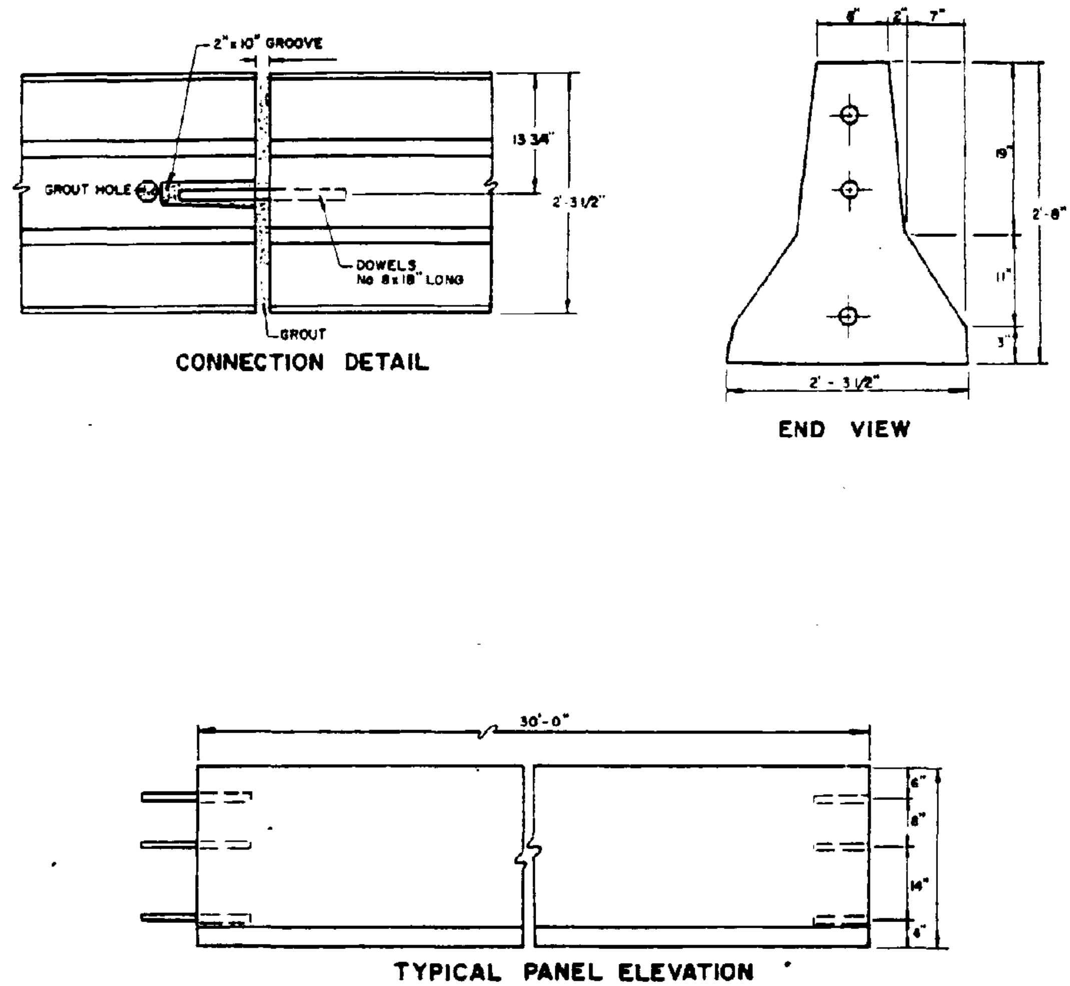

Figure 96. Joint Concept C2--Dowel.

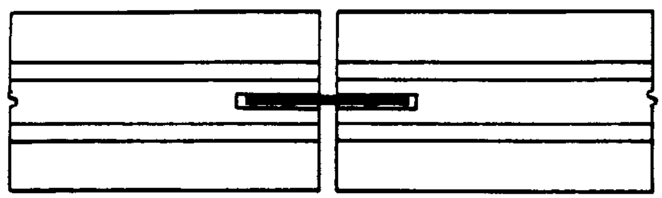

TYPICAL PANEL PLAN WITH A VIEW OF CONNECTION DETAIL

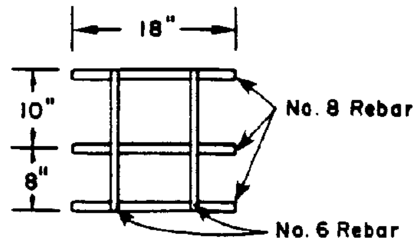

REBAR GRID

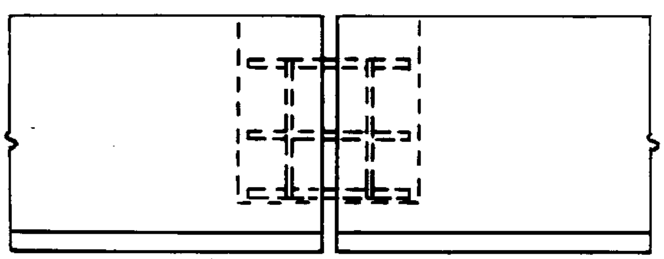

TYPICAL PANEL ELEVATION WITH A VIEW OF CONNECTION DETAIL

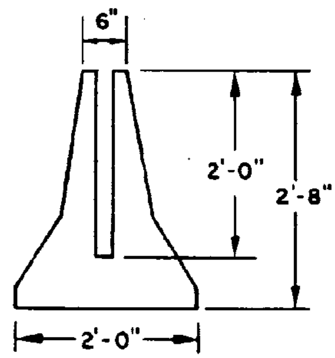

TYPICAL END VIEW

Figure 97. Joint Concept C3--Grid-Slot.

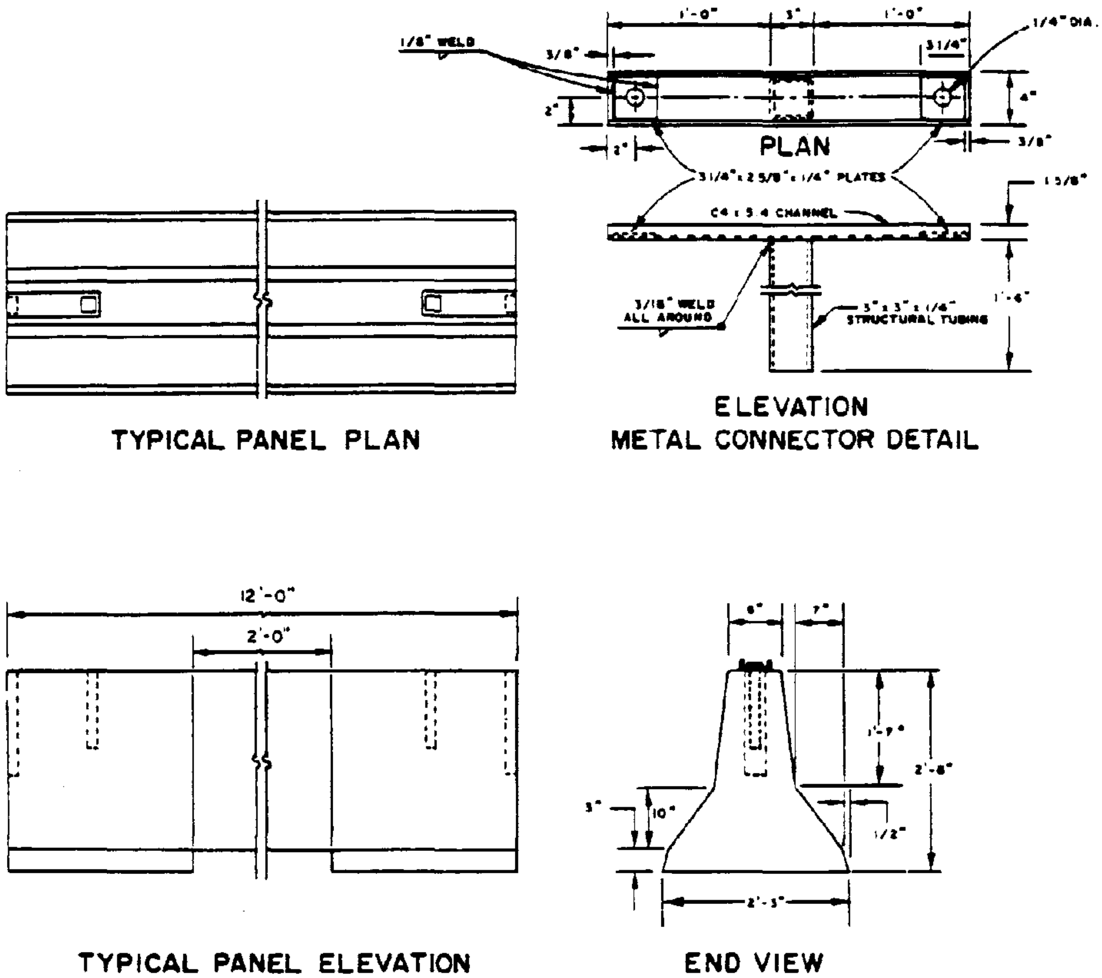

Figure 98. Joint Concept C4--T-Lock.

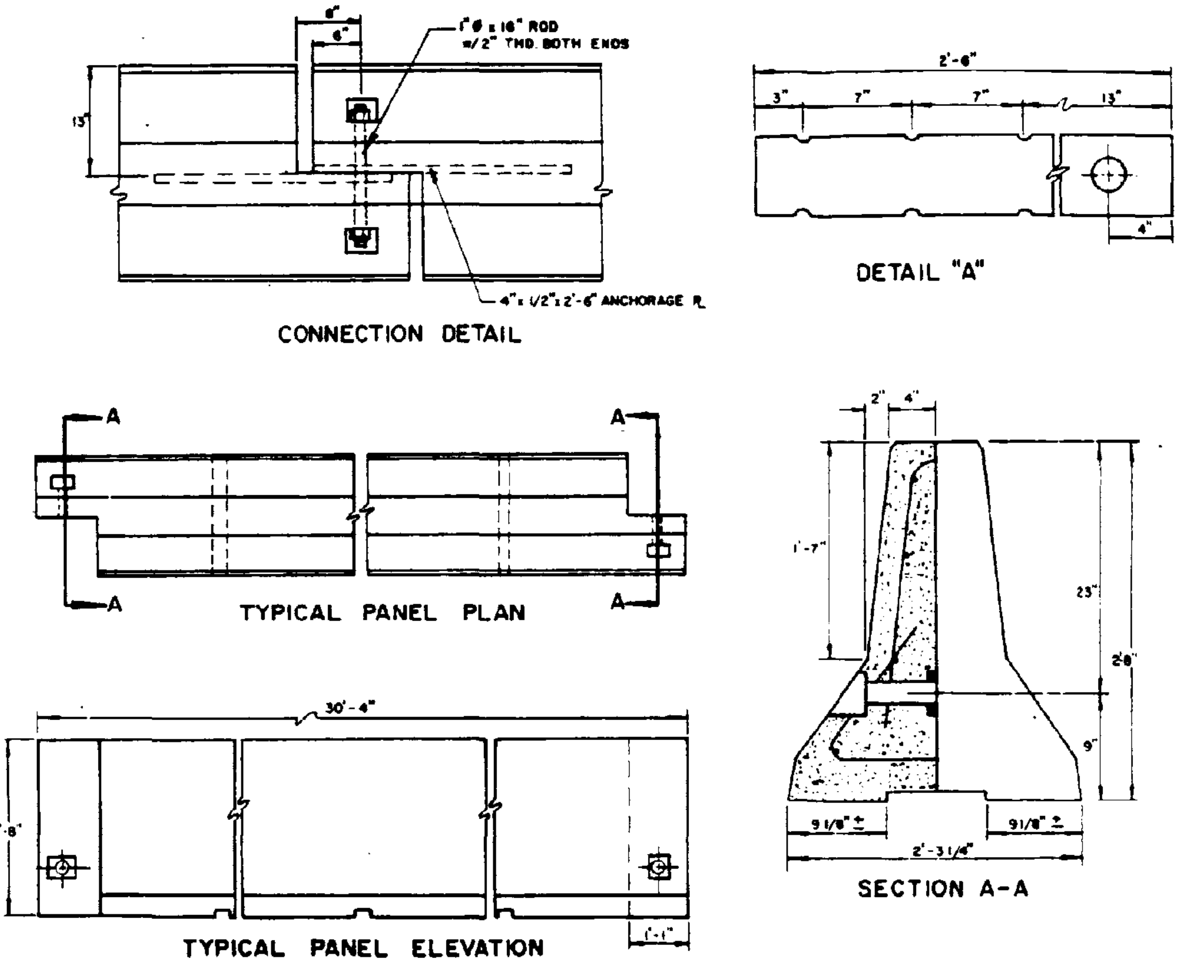

Figure 99. Joint Concept C5--Lapped Joint and Bolt.

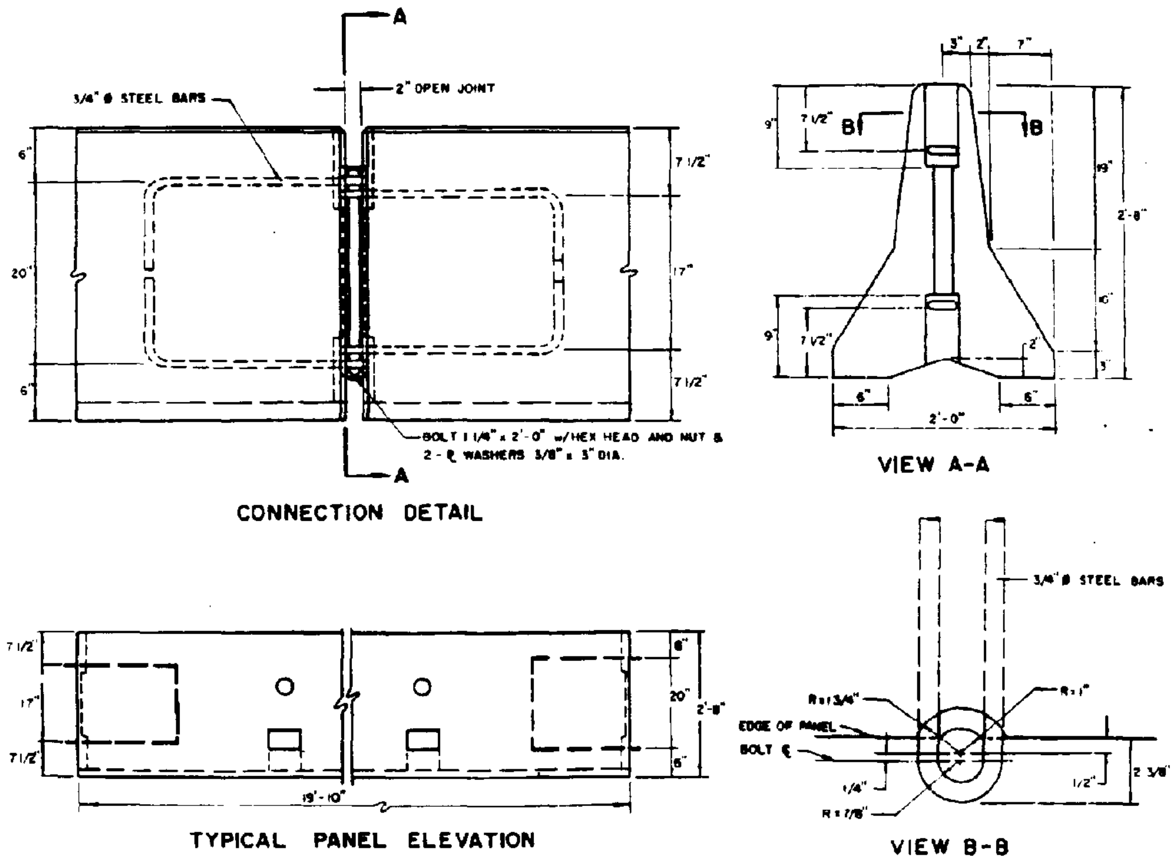

Figure 100. Joint Concept C6-Pin and Rebar.

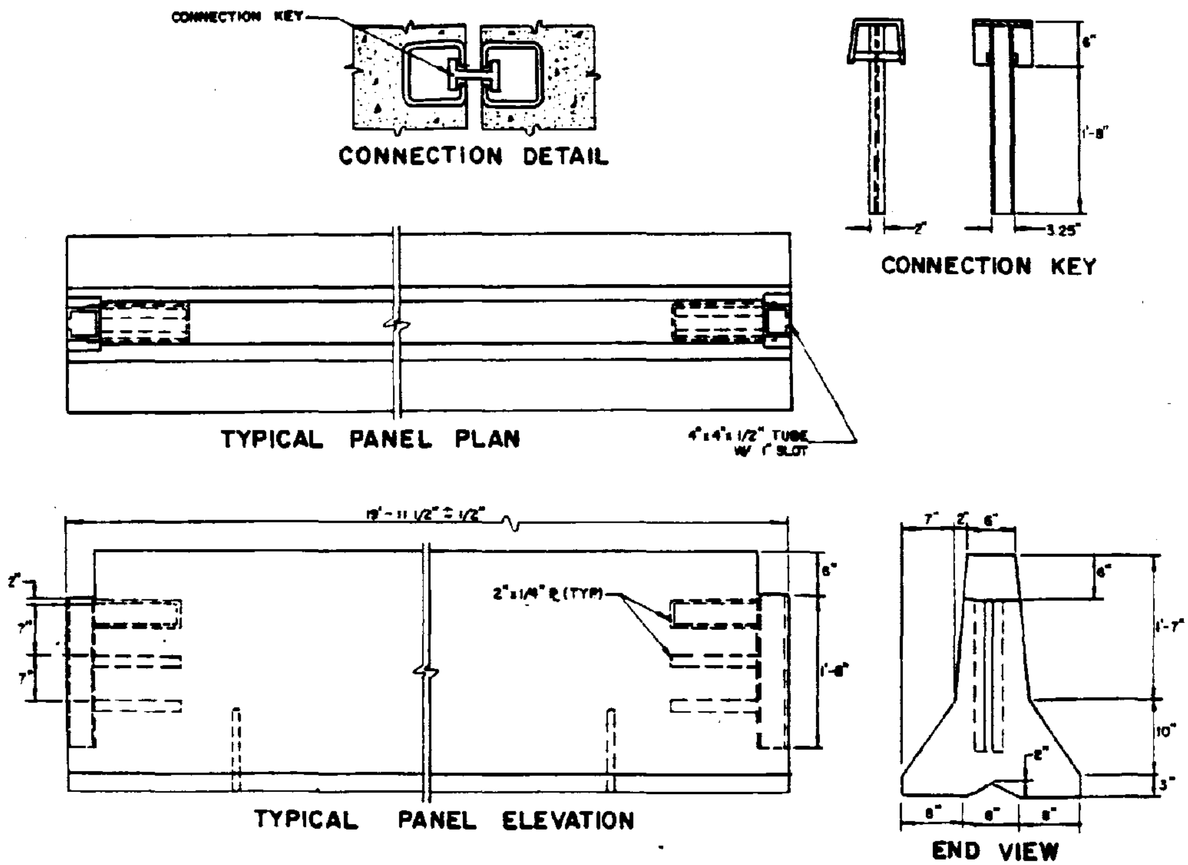

Figure 101. Joint Concept C7--I-Lock.

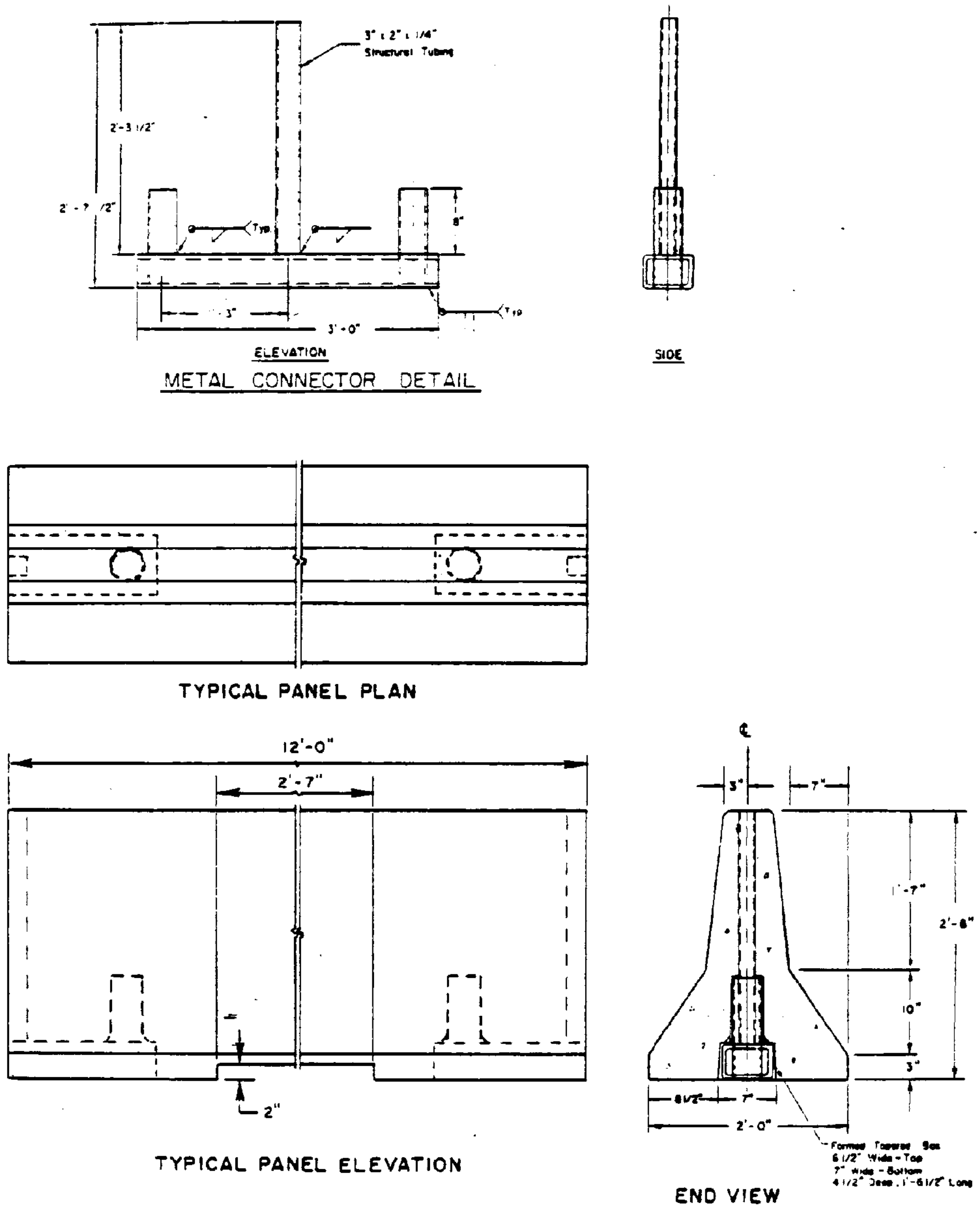

Figure 102. Joint Concept C8--T-Lock.

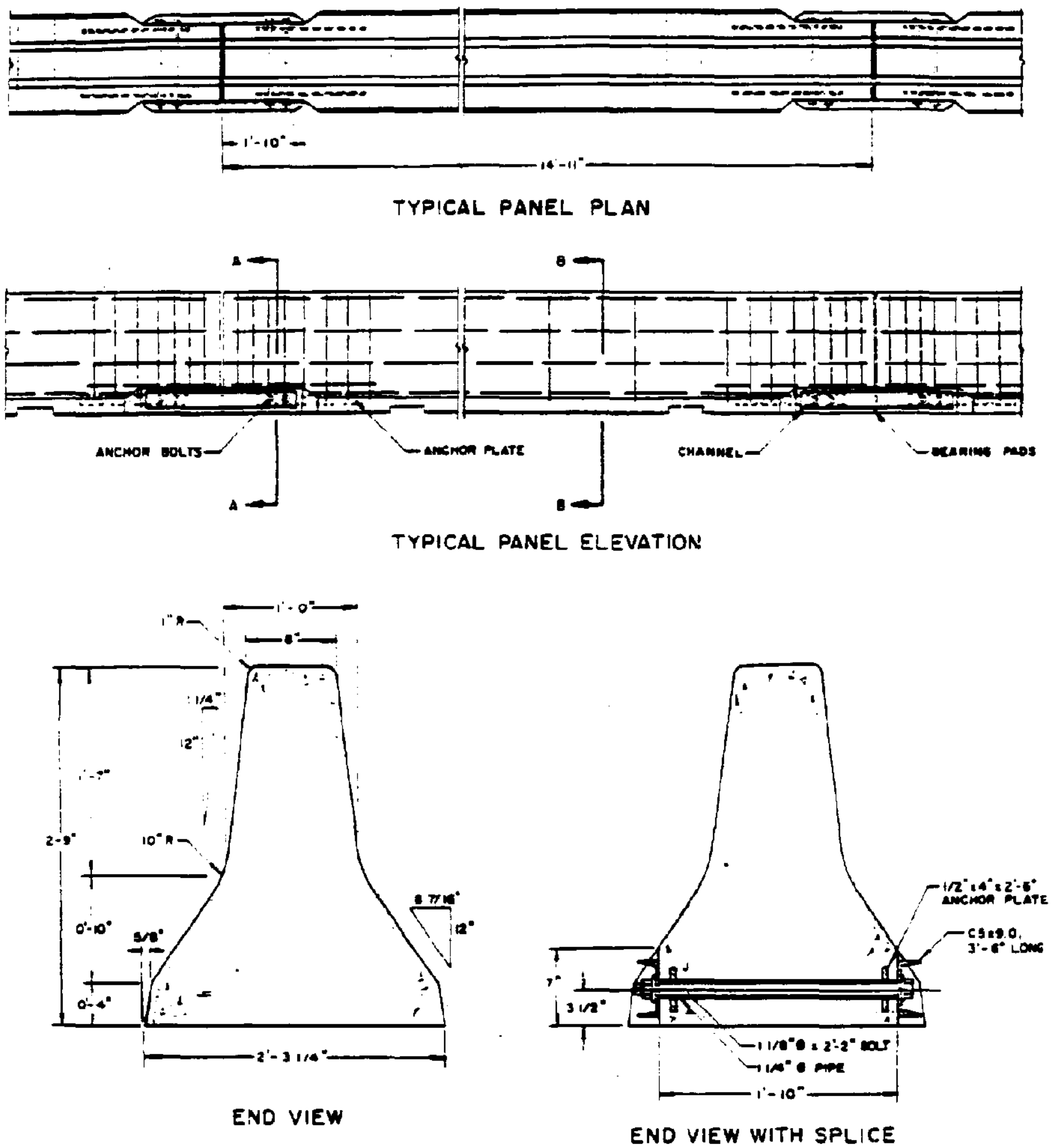

Figure 103. Joint Concept C9--Channel Splice.

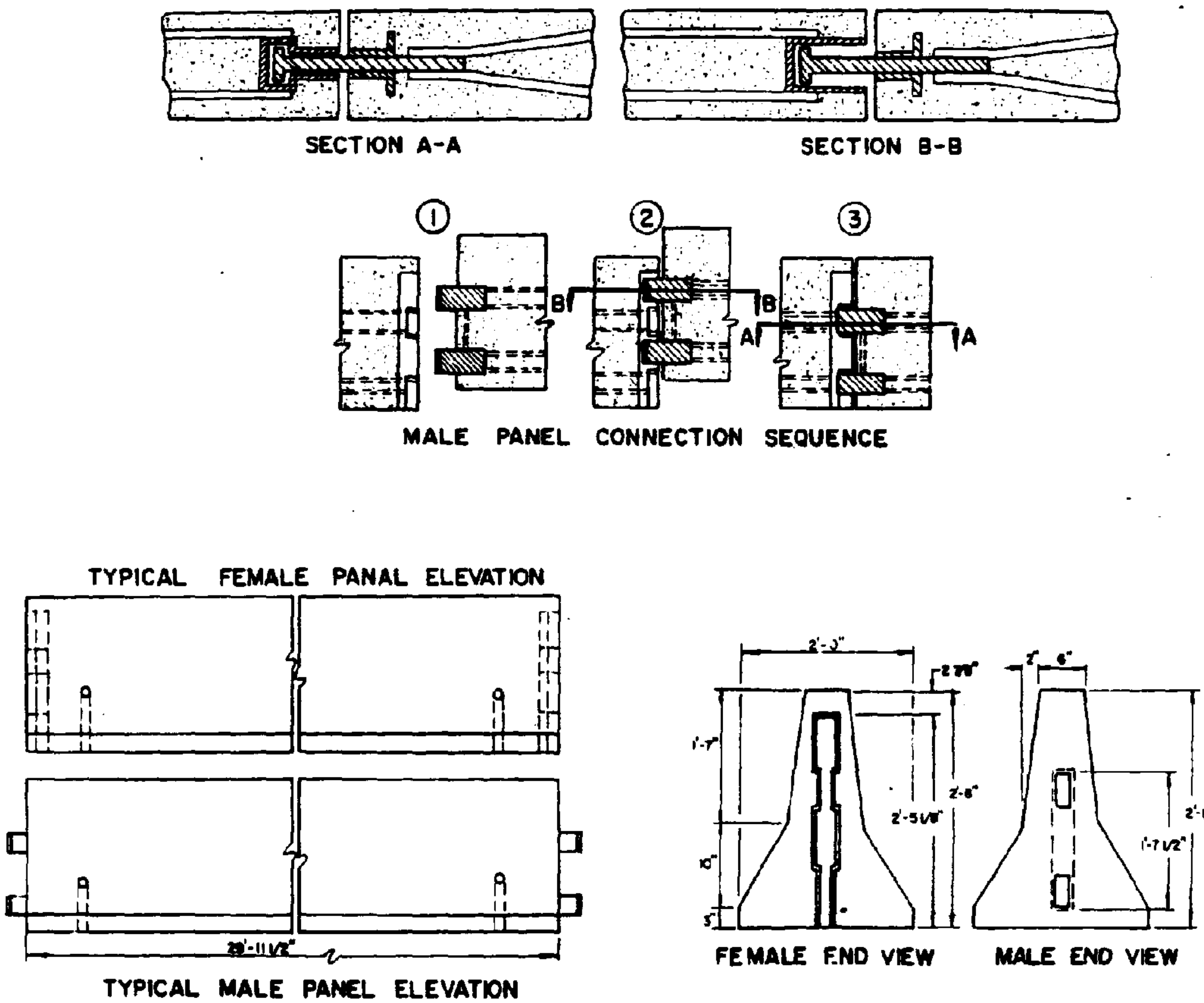

Figure 104. Joint Concept C10--Welsbach Interlock.

THE TEXAS A&M UNIVERSITY SYSTEM
TEXAS TRANSPORTATION INSTITUTE
COLLEGE STATION, TEXAS 77843

HUMAN FACTORS DIVISION

Area Code 713
Telephone 845-2736

DATA FORM

Project RF3825: "Development of Safer Barriers for Construction Sites" (DOT-FH-11-9458)

TASK 1: Barrier Rating System

1. Date ______ District ______ TTI Observer ______

   Time ______ Contact ______

   To ______ Site Supervisor ______

   Location: Highway ______ Direction ______ Specifics ______

   ______

   Film Roll# ______ Exposures ______ to ______

   Video Cartridge# ______

2. Barrier Type: ( ) PCB: ( ) 12 ( ) 15 ( ) 24 ( ) 30 ( ) Other ______

   Joint: ( ) None
   ( ) Tongue and groove
   ( ) Positive Joint
   ( ) Other design

   Sketch Joint

   ( ) Other type (specify) ______

   ______

   ______

Figure 105. Field Visit Data Sheet.

3. Operation: ( ) Barrier Placement
( ) Barrier Relocation
( ) Barrier Removal
( ) Other (Specify) ______________________

---

4. Sections: __________ Sections or __________ ft. Total during Observation Period

---

5. Crew Size: ( ) Supervisor(s) ______________________

__________ Personnel Directly Involved

__________ Personnel Traffic Control

__________ Personnel other duties

(Specify) ______________________

---

6. Equipment

( ) A. Trucks: ______ Trucks (Specify Types) ______________

( ) B. Crane: Describe ______________________

( ) C. Forklift: Describe: ______________________

( ) D. Other Heavy Equipment (Specify) ______________________

( ) E. Small Tools Used (Specify) ______________________

Figure 105. Field Visit Data Sheet. (Continued)

7. Time Estimates

Suboperation ______________________

Beginning Point ______________________

End Point ______________________ Elapsed time:

Manpower engaged __________ ______ min.

Suboperation ______________________

Beginning Point ______________________

End Point ______________________ Elapsed time:

Manpower engaged __________ ______ min.

Suboperation ______________________

Beginning Point ______________________

End Point ______________________ Elapsed time:

Manpower engaged __________ ______ min.

Suboperation ______________________

Beginning Point ______________________

End Point ______________________ Elapsed time:

Manpower engaged __________ ______ min.

Suboperation ______________________

Beginning Point ______________________

End Point ______________________ Elapsed time:

Manpower engaged __________ ______ min.

Figure 105. Field Visit Data Sheet. (Continued)

8. Total Elapsed Time for ______________________________ Sections or

______________________________ ft. Handled.

REMARKS: ____

____

____

____

____

____

____

____

____

____

____

____

____

____

Figure 105. Field Visit Data Sheet. (Continued.

(1) State Highway 288, just north of city limits of Angleton, Texas. This was a relocation job, ancillary to widening the pavement. The barriers were of the C9 type, Channel Splice.

(2) I-35 west of Dallas downtown area, relocation job to protect the median while the median barrier was being improved from a Steel W-beam to a concrete median barrier. The type joint was C5--Lapped Joint.

(3) I-10, west of Houston, PCB placement job, as part of a creation of a median dedicated lane for mass transitway. These barriers will ultimately become permanent CMB's. The joint design was C3--Grid Slot.

COSTS OF FABRICATION OF PORTABLE CONCRETE BARRIERS

Estimates for Casting Barriers

Cost estimates for casting the main structure of Portable Concrete Barriers (PCB) were derived from several sources. The Dodge Manual (8) indicates a cost per linear foot of nearly 84 dollars for the construction of precast beams for construction which are approximately the size (though not shape nor for the same purpose) of PCB. This compares with a cost to TTI for special experimental PCB's of $80 per foot. Reports from other sources in State Highway Departments suggest that in large quantities which would characterize operational purchases of PCB, the price for these barriers would be of the order of 16 to 30 dollars per ft. The 16 dollar price is for materials, casting, and labor exclusive of any special provisions for joints. For purposes of comparing different concepts, since they differ principally in the design of the joint, a figure of $16.00 per linear foot will be used throughout this chapter. This value is a reasonable approximation of cost to produce without overhead or profit to the contractor, i.e., direct costs to fabricate.

Estimates of Joint Fabrication Costs

It was necessary to make a number of assumptions in analyzing the work and materials involved in fabricating joints. The 20-city labor cost average from the Dodge Manual was used as a basis for all fabrication labor, with categories of general worker or laborer, welder, skilled metal worker/machinist. These labor costs do not include overhead or profit by the contractor, but do include fringe benefits, and a 22 percent surcharge for insurance and taxes. They are as follows:

General labor --------	\$16.54 per hour
Welder ---------------	\$20.00 per hour
Skilled machinist ----	\$21.50 per hour

Material costs were obtained by inquiry to several local suppliers of building and construction metal. Fabrication times were estimated by using the following rationale:

It was assumed that no special tooling or mandrells except for stamped metal parts would be used, but rather fabrication would involve only general shop machinery such as drill presses, lathes, brakes, bending machines, electric arc welders, etc. It was assumed that suitable modifications could be made in any PCB casting assembly to accommodate the joint system without extra cost to the major casting operation. Another assumption was that fasteners, i.e. bolts and nuts, would be purchased at commercial rates and not specially fabricated. Costs for the purchase of these items was estimated from the Dodge Manual, with cross check of prices in Engelsman (9). Cutting, welding and forming man-minute rates were estimated by reference to standard sources, such as Niebel (10) and Kent (11). These estimates should thus be considered to be very conservative, i.e. high, since a large contract to fabricate PCB would lead most fabricators to invest in some kind of special tooling and mass-production techniques to facilitate joint fabrication. Although the cost per joint might be less if mass-production techniques were used, the relative cost of fabrication of one joint vs. another should hold.

Analysis, with a good measure of engineering judgement, of the ten different PCB joints yielded Table 13. Each joint is considered as a unit. Column 1 identifies the concept, column 2 briefly lists the hardware that must be fabricated or procured to make the joint. The manufacturing operations needed to ready the joint parts for incorporation in the casting of the PCB's are listed in Column 3. These costs range from a minimum of about three dollars for C1--Tongue and Groove to a high of 87 dollars for the complex Welsbach design (C10).

Table 13. Joint Fabrication Cost Analysis

CONCEPT (1)	HARDWARE REQ'D (2)	MFG OPRNS (3)	NAT'L COST (4)	LABOR COSTS (5)	TOTAL DIRECT COST (6)	NEAREST $.50 (7)
C1-Tongue & Groove	Nose Cap over Tongue	Cut Stamp	$2.40	$ .69	$3.09	3.00
C2-Dowel	Steel Rods	Cut	$3.20	$ .33	$3.53	4.00
C3-Grid Slot	Grid of Steel Bar	Cut Weld	$5.33	$1.69	$7.02	7.00
C4-Top T-Lock	Channel Tubes Plates Pins	Cut Drill Weld	$9.00	$3.52	$12.52	13.00
C5-Lapped Joint	Bolt Re-Plates	Cut Notch Drill	$8.55	$1.72	$10.27	10.00
C6-Pin & Rebar	Rebars Bolt	Cut & Form Bars	$13.62	$7.08	$20.70	21.00
C7-Vertical I-Beam	I-Beam Tubes Re-Plates	Cut Slot Weld	$24.27	$14.82	$39.09	39.00
C8-Bottom T-Lock	Tube Base Pipe Tubes	Cut Split Weld	$34.00	$4.15	$38.15	38.00
C9-Channel Splice	Channel 4 Bolts Re-Plates	Cut Drill Clear	$50.00	$5.35	$55.35	55.00
C10-Welsbach	T-Rails L-Anchors Socket Assy. Anchors	Cut Form Bend Weld	$45.96	$41.16	$87.12	87.00

These joint fabrication costs operate on the base cost of 16 dollars per linear foot for casting PCB as shown in Table 14 for three different lengths of PCB, 10 ft, 20 ft, and 30 ft. Obviously, cost per foot decreases as the length of PCB increases. These costs run from a minimum of $16.10 for a 30 ft tongue-and-groove PCB to $24.70 for a 10 ft Welsbach jointed section.

COST ESTIMATES FOR BARRIER ASSEMBLY, DISASSEMBLY, AND RELOCATION

Bases for Cost Estimates

The primary basis for estimating the costs of moving barriers, i.e.

(1) Picking up barrier sections from a depot, transporting them to a construction site, and placing them

(2) Relocating barrier sections from one location to another within a construction site as the work progresses

(3) Picking up barrier sections and returning them to a depot,

was observation of typical operations of this type at three construction sites, was the C9--Channel Splice concept at Angleton on 288, the C5--Lapped Joint on Stemmons Freeway, Interstate 35 in Dallas, and the C3--Grid Slot on I-10 west of Houston. Tables 15 through 20 summarize the tasks, work crew and equipment observed during these site visits. Table 21 summarizes these observations in terms of man-minutes of labor required, plus adds some estimated times based on similarity to these operations.

Some contractors were much more labor-intensive than others in the operation of hoisting and placing these barriers. One such operational sequence is depicted in Figures 106 through 108. In Figure 106, two men place hoisting rods and lifting cables in place up on the flatbed trailer (note that four barriers are carried at one time). Two other workers wait below. Four men under a supervisor's direction are used to maneuver the barrier section into place (one of the workers, just before final placement, places a plywood spacer between the sections to assure proper clearance for the joint. In Figure 108, the workers are shown removing the hoisting rods after final placement of the section. A typical time for this operation was 2 minutes. Figure 109 shows the extreme simplicity of installing the Grid Slot.

Table 14. Fabrication Costs

CONCEPT	LENGTH (FT)	JOINT COST	TOTAL COST/FT.	TOTAL COST PER SECTION
C1-Tongue and Groove	10 20 30	3.00 3.00 3.00	16.30 16.15 16.10	163.00 323.00 483.00
C2-Dowell	10 20 30	4.00 4.00 4.00	16.40 16.20 16.13	164.00 324.00 484.00
C3-Grid Slot	10 20 30	7.00 7.00 7.00	16.70 16.35 16.23	167.00 327.00 487.00
C4-Top T-Lock	10 20 30	13.00 13.00 13.00	17.30 16.65 16.43	173.00 333.00 493.00
C5-Lapped Joint	10 20 30	10.00 10.00 10.00	17.00 16.50 16.33	170.00 330.00 490.00
C6-Pin and Rebar	10 20 30	21.00 21.00 21.00	18.10 17.05 16.70	181.00 341.00 501.00
C7-Vertical I-Beam	10 20 30	39.00 39.00 39.00	19.90 17.95 17.30	199.00 359.00 519.00
C8-Bottom T-Lock	10 20 30	38.00 38.00 38.00	19.80 17.90 17.27	198.00 358.00 518.00
C9-Channel Splice	10 20 30	55.00 55.00 55.00	21.50 18.75 17.83	215.00 375.00 535.00
C10-Welsbach	10 20 30	87.00 87.00 87.00	24.70 20.35 18.90	247.00 407.00 567.00

Figure 106. Method 1 (Labor Intensive)--Placing Hoisting Rods.

Figure 107. Method 1--Maneuvering Section into Place.

Figure 108. Method 1--Removing Hoisting Rods after Placement.

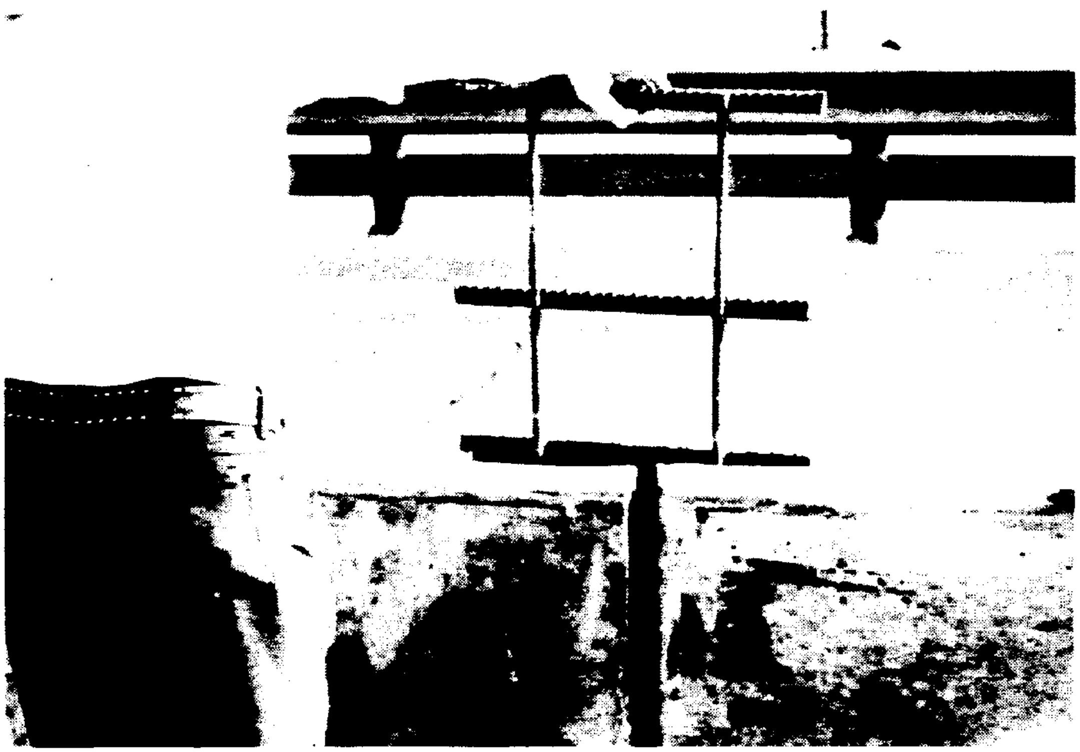

Figure 109. Installation of Grid in Slot (Concept C3).

Table 15. Activity Analysis - Relocate 25 ft C9.

RF3825: DEVELOPMENT OF SAFER BARRIERS FOR CONSTRUCTION SITES

A C T I V I T Y A N A L Y S I S

EQUIPMENT Crane - 15 Tons

BARRIER 25' PCB, C9 Channel Splice

ACTIVITY Relocate PCB for later placement

T = 1.75 min SD = .34 min. N = 5

No.	ELEMENT	BEGINNING	END	CREW					
				SUPER	CRANE	TRUCK	HNDLR	OTHER	OTHER
1	Install eye bolts (2)	Remove from last PCB	Release	1	-	-	2	-	-
2	Attach lifting cables (2)	Grasp	Release 2nd	1	1	-	2	-	-
3	Lift PCB	Tension Cables	PCB clear	1	1	-	2	-	-
4	Move PCB to one side	PCB moves	PCB on ground	1	1	-	2	-	-
5	Detach lifting cables (2)	Slack cables	Remove cable 2	1	1	-	2	-	-
6	Remove eye bolts (2)	Grasp 1	Remove 2	1	-	-	2	-	-
7	Move Crane	Props retract	Props extend	1	1	-	-	Crane Driver	-
	SUMMARY			1	1		2	1	

Table 16. Activity Analysis - Disassemble 15 ft C9.

RF3825: DEVELOPMENT OF SAFER BARRIERS FOR CONSTRUCTION SITES

ACTIVITY ANALYSIS

EQUIPMENT Impact Wrench
Socket Wrench & Cheater
APV

BARRIER 15' PCB, C9 Channel Splice

ACTIVITY Disassemble Splice

6.00 min. 2 joints

No.	ELEMENT	BEGINNING	END	CREW					
				SUPER	CRANE	TRUCK	HNDLR	OTHER	OTHER
1	Take off 8 Nuts	Wrench on 1	Wrench off 8					2	
2	Pull Bolts	Pull 1	8 out					2	
3	Take off channels 4	Lay 1st down (drop 2 over from	Lay 4 down other side					2	
	SUMMARY Note: about 25% of bolts are cross-threaded and stubborn about 1 in 40 must be cut with oxyacetylene torch.							2	

Table 17. Activity Analysis - Load 30 ft C5.

RF3825: DEVELOPMENT OF SAFER BARRIERS FOR CONSTRUCTION SITES

A C T I V I T Y A N A L Y S I S

EQUIPMENT Crane - 22 Ton
C hooks on Bar
Flatbed Trucks (3)

BARRIER PCB, C5 Lapped Joint & Bolt 30 ft.

ACTIVITY Pick up PCB, place on Flatbed
$\bar{T}$ = 0.97 min. SD = 0.15 min. N = 5

No.	ELEMENT	BEGINNING	END	CREW					
				SUPER	CRANE	TRUCK	HNDLR	OTHER	OTHER
1	Swing 'C' assembly into place	Lower assembly	'C' next to slots	1	1	-	-	-	-
2	Secure 'C's into slots	C contacts slots	'C's in place	1	1	-	2	-	-
3	Pick up PCB	Tension on Assembly	PCB clear	1	1	-	-	-	-
4	Swing PCB onto flatbed	PCB moves	PCB on bed	1	1	-	2	-	-
5	Trip 'C's from slots	Slack on Assembly	'C's clear	1	1	-	2	-	-
6	Move crane	Props retract	Props extend	1	1	-	-	-	-
7	Move flatbed	Engage clutch	Truck stops	1	-	1	-	-	-
	SUMMARY			1	1	1.5*	2		

Note: Supervisor was doubling as crane operator, but this would not be nominal procedure

*1 in position
1 at other end
1 in transit

Table 18. Activity Analysis - Bolt/unbolt C5.

RF3825: DEVELOPMENT OF SAFER BARRIERS FOR CONSTRUCTION SITES

A C T I V I T Y   A N A L Y S I S

EQUIPMENT 30" Ratchet Wrench
30" Socket Wrench

BARRIER PCB, C5 Lapped Joint & Bolt

ACTIVITY Bolt/Unbolt Joint

0.3 min.

No.	ELEMENT	BEGINNING	END	CREW					
				SUPER	CRANE	TRUCK	HNDLR	OTHER	OTHER
1	Place bolt through lap joint holes							1	
2	Place nut on bolt								1
3	Tighten nut on bolt							1	1
	OR								
1	Loosen nut on bolt							1	1
2	Remove nut								1
3	Pull out bolt							1	
	SUMMARY							!	!

Table 19. Activity Analysis - Place 30 ft C5.

RF3825: DEVELOPMENT OF SAFER BARRIERS FOR CONSTRUCTION SITES

A C T I V I T Y A N A L Y S I S

EQUIPMENT Crane - 22 Ton
C Hooks
Flatbed Trucks (3)

BARRIER PCB, C5 Lapped Joint & Bolt 30 ft.

ACTIVITY Place PCB at Construction Site

$\bar{T}$ = 1.35 min.   SD = 0.29 min.   N = 5

No.	ELEMENT	BEGINNING	END	CREW					
				SUPER	CRANE	TRUCK	HNDLR	OTHER	OTHER
1	Swing 'C' assembly into place	Lower assembly	'C' next to slots	1	1	-	-	-	-
2	Secure 'C's into slots	Get on truck	'C's in place	1	1	-	2	-	-
3	Pick up PCB	Tension on assembly	PCB clear	1	1	-	-	-	-
4	Swing PCB into position	PCB moves	PCB in line	1	1	-	2	-	-
5	Position PCB	Gauge PCB Separation	PCB on ground	1	1	-	2	-	-
6	Trip 'C's from slots	Slack on assembly	'C's clear	1	1	-	2	-	-
7	Move crane	Props retract	Props extend	1	1	-	-	-	-
8	Move flatbed	Engage clutch	Truck stops	1	-	1	-	-	-
	SUMMARY			1	1	1.5*	2		

*1 in position
1 at other end
1 in transit

Table 20. Activity Analysis - Place 30 ft C3.

RF3825: DEVELOPMENT OF SAFER BARRIERS FOR CONSTRUCTION SITES

A C T I V I T Y   A N A L Y S I S

EQUIPMENT 30 Ton Galion
4 Flatbed Trucks
(haul 4 each)

BARRIER PCB 30', C3 Drop in Grid

ACTIVITY Place PCB at Construction Site

$\bar{T}$ = 2.09 min SD = 0.50 min N = 8

No.	ELEMENT	BEGINNING	END	CREW					
				SUPER	CRANE	TRUCK	HNDLR	OTHER	OTHER
1	Place rods in PCB	Climb on Bed	2nd rod in place	1			2		
2	Attach cables (4) to rods	Grasp 1st cable	Climb down off bed	1			2		
3	Lift PCB off Flatbed	Tension cables	PCB clear	1	1				
4	Move flatbed forward	Engage clutch	Stop	1		1			
5	Move PCB into position	PCB moves	PCB in line	1	1		4		
6	Final position, gauging separation	Gauge inserted	PCB on ground	1	1	1	4		
7	Detach cables (4)	Slack cables	Unhook 4th	1	1		2		
8	Pull rods from PCB	Grasp	2nd rod out	1			2		
9	Move crane	Props retract	Props extend	1	1				
	SUMMARY			1	1	2*	4		
	Note: Joint consists of grid dropped into complex slot. Done by one of handlers in lulls.					*1 at site 1 at depot 2 in transit			

Table 21. Summary of Man-Minutes for Operations.

*Comparison of PCB Designs with Respect to Disassembly, Pickup, Placement, Reassembly

DESIGN	DISASSY	PICKUP	PLACEMENT	REASSY	TOTALS	
C3 Drop in Grid	0.10	9.00	12.54	0.10	21.74	
C5 Lapped Joint	0.60	3.88	5.40	0.60	10.48	Ratio Place to P/U = 1.40
C9 Channel Splice	6.00	8.75	12.30	6.00	33.05	
RANK ORDERS						Actual Other Costs Estimated
B&R Drop in Grid	1	2.5	2.5	1	8	
Texas Lapped Joint	2	1	1	2	6	
TTI Channel Splice	3	2.5	2.5	3	11	
TYPICAL		8.88	12.42			

*Exclusive of transportation costs.

Figure 110 depicts C-shaped hooks on a spreader beam which one contractor uses to expedite handling of the PCB's. The crew consists of only two individuals for maneuvering (and sometimes securing or releasing the hooks) with the supervisor operating the crane. Figure 111 shows the final placement operation, with a stick used as a spacer. Figure 112 shows the section finally in place. This operation takes about one minute of time with less than half the manpower.

Figure 114 depicts the C-5--Lapped Joint used in this installation. Figure 115 shows the equipment and workers necessary to assemble or disassemble a C9--Channel Splice joint, including the APU for the impact wrench.

For costing typical operations, it was assumed that most contractors would use the more labor-intensive, less specialized equipment approach for lifting and moving the sections. It was assumed that contractors would use forklift trucks for 10 ft sections, but a "cherry picker" or similar self-propelled crane (approximately 20 to 30 ton capacity) for longer sections. Contractors informed researchers that at least three flatbed trucks were used for relocating barrier sections within a construction zone (less than 2 miles) but five were used for initial placement from a depot, or for return to a depot if the depot was more than two but less than ten miles distant. These numbers were used in this analysis. It was further assumed that the crane or forklift was rented equipment, but trucks were owned by the contractor and hence only operating costs and five year straight-line depreciation were assumed, plus, of course, direct costs for operator or driver labor. These costs worked out as follows (8):

Truck, flatbed, 1/2 day	=	$64
Crane, 22 ton capacity, 1/2 day	=	$165
Forklift, 9 ton capacity, 1/2 day	=	$138

Not considering direct costs for transportation but only labor required for operations at site, the labor man-minute estimates shown in Table 22 were derived, and used as a basis for further analysis.

Transportation of barrier sections was costed at $64 per truck for a 4-hour period, and $17.33 per hour for the driver.

Figure 110. Method 2 (Mechanized) C-hooks Used to Hoist Section.

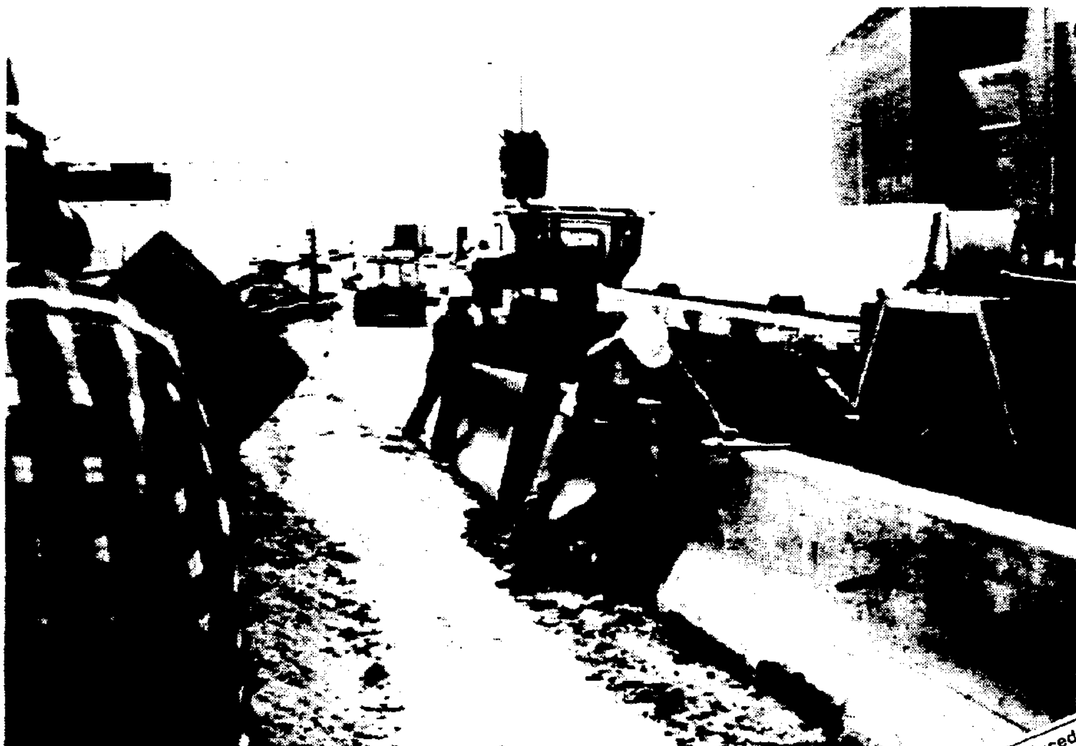

Figure 111. Method 2--Initial Maneuvering Operation.

Figure 112. Method 2--Final Placement (Note shim usage).

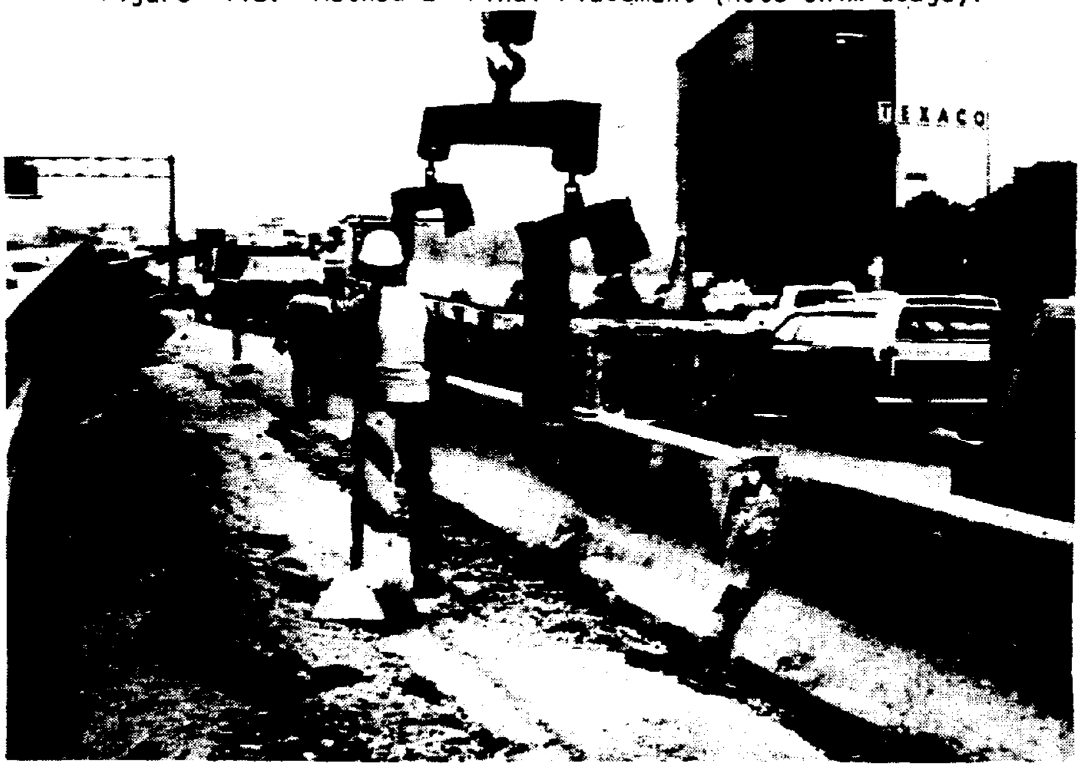

Figure 113. Method 2--End of Procedure, C-hooks Released.

Figure 114. Lapped Joint (C5) Installed.

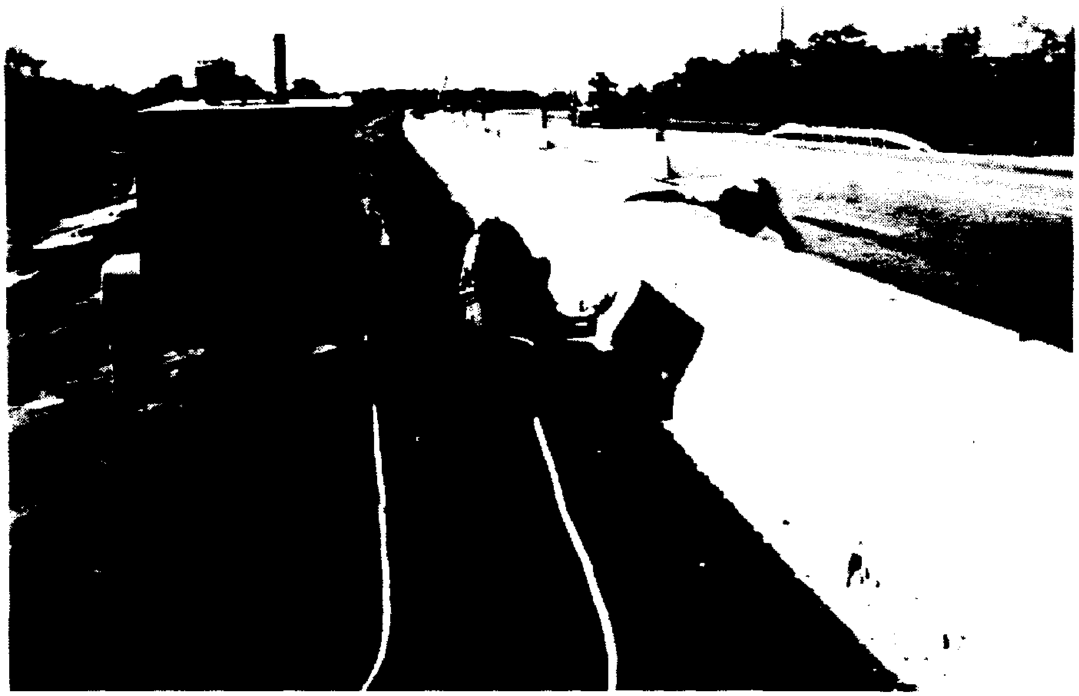

Figure 115. Workers Installing C9 Channel Splice Joints.

Table 22. Labor in Moving PCB

Unit: Man Minutes (M-M)

DESIGN	DISASSEMBLY	PICKUP*	PLACEMENT*	REASSY	NOTES
C1-Tongue & Groove	0	2.69	3.00	0	1(perhaps)
C2-Dowel	0	2.69	3.00	0	1
C3-Grid Slot	.03	2.69	3.77	.03	2
C4-Top T-Lock	.11	2.69	3.77	.11	2
C5-Lapped Joint	.17	2.69	3.00	.17	3 4
C6-Pin & Rebar	.55	2.69	3.77	.55	2
C7-Vertical I-Beam	.03	2.69	3.77	.03	2
C8-Bottom T-Lock	0	2.69	3.77	0	2
C9-Channel Splice	2.00	2.69	3.77	2.00	2,3, 4
C10-Welsback	0	2.69	3.77	0	1 & 2

NOTES:
1. Constrains replacement of individual sections.
2. Requires precise alignment and spacing (20% penalty on placement)
3. Bolts become damaged; disassembly cost can be much higher
4. Crew size 2 for disassembly/assembly

*Mean cost is average of 4 laborers @ 16.54, 1 crane opr. @ 21.50, 1 supervisor @ 21.50 = 18.20

Placement 12.42 M-M (including penalty)
Pickup 8.88 M-M

Cost Estimates for Relocating Barriers

A nominal job consisting of moving 1,000 ft of barrier was used throughout this, and the following movement analyses. Since 10 ft sections can be picked up by one man on a forklift, at a wage of $21.50 per hour, and he can place 1,000 ft of barrier in four hours, the cost of initial pickup is $21.50 x 4/100 or 86 cents per section. Costs of labor for a 30 ft section are, of course, much higher, $2.69, but since there are only 33 sections to be moved, the total cost of pickup is comparable. These cost estimates plus others are shown in Table 23. Note that transportation cost is invarient, since a 60,000 lb capacity flatbed, a standard size in the industry, can handle four 30 ft sections, four 20 ft sections, or twelve 10 ft sections.

Section placement costs are taken from Table 22 for the 30 ft section operations already described. The 10 ft sections are assumed to require a two man crew: one on a forklift at $21.50 per hour, and a worker on the ground to assist in placement and use the spacer at $16.54 per hour. These costs multiplied by a four-hour time period total $152 for 100 sections placed, or $1.52 per section.

Joint disassembly times are costed out from observational or analytic data summarized in Table 22, and then multiplied by the number of joints that must be disassembled for a 1,000 ft barrier. This same logic applies to assembly costs. Then equipment rentals are totalled in, assuming that equipment cannot be rented for less than a half-day, and indeed a 1,000 ft job would require four hours. Finally, total estimated costs for this 1,000 ft relocation within a site are presented. As a check on this entire analysis, several contractors doing work for the Texas State Department of Highways and Public Transportation were queried for the direct cost they charge for this same operation. These estimates were in the range of one dollar per foot, an excellent agreement with the results of this analysis.

The mean cost per foot for relocating 10 ft sections is $1.19, with a range of $1.11 to $1.54, whereas the mean cost for 30 ft sections is 95 cents, ranging from $.92 to $1.07. The major cost differential in this 25 per cent difference is attributable to joint disassembly and assembly operations, even thought less manpower is required for 10 ft sections. Twenty foot sections would tend to reflect a cost intermediate or more like the 30 ft sections, since handling equipment is much the same for these sections as it is for 30 foot sections.

Table 23. Job: Release 1000 ft of PCB.

Concept	Length	No. Joints	Cost/ Joint Dissas.	Total Joint Dissas. Cost	Pick Up Section Cost	Total Pickup Cost	Transp. Cost	Place Section Cost	Total Place Cost	Cost/ Joint Assy.	Total Joint Assy. Cost	Equip. (2)	Equip. Cost	Total Cost 5+7+8+ 10+12+14	Cost/ft.
C1-Tongue	10'	98	0	0	.86	86.00	400.00	1.52	152.00	0	0	Fork-Lift	475	1113	1.11
C1-Tongue	30'	31	0	0	2.69	88.77	400.00	3.00	99.00	0	0	Crane	330	917	.92
C2-Dowel	10'	98	0	0	.86	86.00	400.00	1.52	152.00	0	0	Fork	475	1113	1.11
C2-Dowel	30'	31	0	0	2.69	88.77	400.00	3.00	99.00	0	0	Crane	330	917	.92
C3-Grid	10'	98	.03	2.94	.86	86.00	400.00	1.82	182.00	.03	2.94	Fork	475	1149	1.15
C3-Grid	30'	31	.03	.93	2.69	88.77	400.00	3.77	124.41	.03	.93	Crane	330	945	.95
C4-Top "T"	10'	98	.11	10.78	.86	86.00	400.00	1.82	182.00	.11	10.78	Fork	475	1165	1.17
C4-Top "T"	30'	31	.11	3.41	2.69	88.77	400.00	3.77	124.41	.11	3.41	Crane	330	950	.95
C5-Lapped	10'	98	.17	16.66	.86	86.00	400.00	1.52	152.00	.17	16.66	Fork	475	1146	1.15
C5-Lapped	30'	31	.17	5.27	2.69	88.77	400.00	3.00	99.00	.17	5.27	Crane	330	928	.93
C6-PIN	10'	98	.55	53.90	.86	86.00	400.00	1.82	182.00	.55	53.90	Fork	475	1252	1.25
C6-PIN	30'	31	.55	17.05	2.69	88.77	400.00	3.77	124.41	.55	17.05	Crane	330	977	.98
C7-I Beam	10'	98	.03	2.94	.86	86.00	400.00	1.82	182.00	.03	2.94	Fork	475	1149	1.15
C7-I Beam	30'	31	.03	.93	2.69	88.77	400.00	3.77	124.41	.03	.93	Crane	330	945	.95
C8-Bottom "T"	10'	98	0	0	.86	86.00	400.00	1.82	182.00	0	0	Fork	475	1143	1.14
C8-Bottom "T"	30'	31	0	0	2.69	88.77	400.00	3.77	124.41	0	0	Crane	330	943	.94
C9-Channel	10'	[illegible]	2.00	196.00	.86	86.00	400.00	1.82	182.00	2.00	196.00	Fork	475	1535	1.54
C9-Channel	30'	31	2.00	62.00	2.69	88.77	400.00	3.77	124.41	2.00	62.00	Crane	330	106[illegible]	1.07
C10-Welsbach	10'	98	0	0	.86	86.00	400.00	1.82	182.00	0	0	Fork	475	1143	1.14
C10-Welsbach	30'	31	0	0	2.69	88.77	400.00	3.77	124.41	0	0	Crane	330	943	.94

SUMMARY: Mean Cost/ft, 10' Sections = $1.19 range 1.11 to 1.54

Mean Cost/ft, 30' Sections = $ .95 range .92 to 1.07

25% penalty by going with 10' vs 30' sections

Cost Estimates for Initial Installation of Barriers

Costs for bringing barriers from a depot to the construction site can be estimated by considering this operation to be a special case of relocation, with the subtraction of the disassembly operation and the addition of two extra trucks and their drivers to keep up a steady flow from the depot to the site. Thus, for 1,000 ft of barrier, for each of the ten concepts, Table 24 was generated, again at the limiting case lengths of 10 and 30 ft. These costs closely correlate with those for relocation.

Costs for removal of these barriers in those cases in which the barriers are not going to be permanently installed somewhere on the site, can also be estimated in a similar way from the relocation analysis. The total cost of relocation is debited by the cost for assembly of joints, and credited by two extra trucks to transport the sections back to the depot for storage. This analysis is shown in Table 25.

Supplementary Data from State DOT's

A complementary study in the Texas Transportation Institute (12) has obtained some preliminary work and cost estimates for operations similar to those discussed above. Researchers sent a questionnaire to cognizant construction engineers in North Carolina, Tennessee, Virginia and Florida. These results are summarized in Table 26. They are not inconsistent with the cost estimates produced analytically in this project. The joint concepts involved were (North Carolina) C6--Pin and Re-Bar, also C9--Channel Splice; (other States) Tongue and Groove (C1).

MAINTENANCE COST ESTIMATES FOR BARRIER

Assumptions and Basis of Estimates

There are many ways in which a portable concrete barrier can be impacted by passing traffic and damaged, but for the purposes of this analysis it was assumed that the supervising agency would not repair a section in situ but would allow a damaged section to remain unless it was no longer able to perform its function or redirecting an impinging motor vehicle. Hence in this analysis "maintenance" means outright replacement of one or more sections. Conversations with construction engineers suggest that this is not an unrealistic assumption.

A maintenance activity therefore consists of:

Table 24. Installation of PCB at Construction Site

CONCEPT	RELOCATE TOTAL	LESS DISASSY	PLUS 2 MORE TRUCKS	TOTAL INSTALL	COST/FT
C1-10 ft	1113	0	267	1380	1.38
C1-30 ft	917	0	267	1184	1.18
C2-10 ft	1113	0	267	1380	1.38
C2-30 ft	917	0	267	1184	1.18
C3-10 ft	1149	2.94	267	1413	1.41
C3-30 ft	945	.93	267	1209	1.21
C4-10 ft	1165	10.78	267	1421	1.42
C4-30 ft	950	3.41	267	1213	1.21
C5010 ft	1146	16.66	267	1396	1.40
C5-30 ft	928	5.27	267	1190	1.19
C6-10 ft	1252	53.90	267	1465	1.47
C6-30 ft	977	17.05	267	1227	1.23
C7-10 ft	1149	2.94	267	1413	1.41
C7-30 ft	945	.93	267	1211	1.21
C8-10 ft	1143	0	267	1410	1.41
C8-30 ft	943	0	267	1210	1.21
C9-10 ft	1535	196.00	267	1606	1.61
C9-30 ft	1067	62.00	267	1272	1.27
C10-10 ft	1143	0	267	1410	1.41
C10-30 ft	943	0	267	1210	1.21

1000 ft of barrier

Table 25. Cost Estimates for Removal

CONCEPT	RELOCATE COST	ASSEMBLY COST	TOTAL COST
C1-10 ft	1113.00	0.00	1380.00
C1-30 ft	917.00	0.00	1184.00
C2-10 ft	1113.00	0.00	1380.00
C2-30 ft	917.00	0.00	1184.00
C3-10 ft	1149.00	2.94	1413.06
C3-30 ft	945.00	0.93	1211.07
C4-10 ft	1165.00	10.78	1421.22
C4-30 ft	950.00	3.41	1213.59
C5-10 ft	1146.00	16.66	1396.34
C5-30 ft	928.00	5.27	1189.73
C6-10 ft	1252.00	53.90	1465.10
C6-30 ft	977 00	17.05	1226.95
C7-10 ft	1149.00	2.94	1413.06
C7-30 ft	945.00	0.93	1211.07
C8-10 ft	1143.00	0.00	1410.00
C8-30 ft	943.00	0.00	1210.00
C9-10 ft	1535.00	196.00	1606.00
C9-30 ft	1067.00	62.00	1272.00
C10-10 ft	1143.00	0.00	1410.00
C10-30 ft	943.00	0.00	1210.00

Table 26 : Summary of Self Reports from State DOT's

Cost Category	N. Carolina Winston-Sal	N. Carolina Old Fort	Tennessee Site 1	Tennessee Site 2	Virginia	Florida	Mean Times or Mean Costs
Relocation	6.00 m-m	0.30 m-m	5.40 m-m	-	6.00 m-m	6.00 m-m	4.74 m-m
Relocation Cost Per foot	$ 1.82	0.09	1.64	-	1.82	1.82	$ 1.44
Removal	6.00 m-m	6.60 m-m	6.00 m-m	-	6.00 m-m	6.00 m-m	6.12 m-m
Remove Cost Per Foot	$ 1.82	2.00	1.82	-	1.82	1.82	$ 1.86
Transport Per Ft/Mile	$ 0.15	1.20	1.31	0.00	0.02	0.02	$ 0.45
Fabricate Cost/ Ft	$20.00	13.30	13.80	21.00	15.00	16.50	$16.60
Install Cost/ Ft	$ 2.50	4.90	2.04	2.00	0.65	1.00	$ 2.18
Relocate Cost/ Ft	$ 2.50	9.81	2.39	7.00	0.65	1.00	$ 3.89
Remove Cost/ Ft	$ 6.60	6.39	2.41	11.50	0.85	2.25	$ 5.00

(1) special traffic control or diversion (not costed here)

(2) pickup of replacement sections from the depot

(3) transportation of sections to the construction site

(4) removal of damaged sections to a position nearby original position

(5) offload of sections and placement in original barrier

(6) pickup of damaged sections or debris

(7) transport of damaged sections to depot or other disposal

It was further assumed, as for the analyses in previous sections of this section that the depot is less than 10 miles from the site. Flatbed trailer capacities and load limits will permit four 30 ft sections to be transported, four 20 ft sections, or twelve 10 ft sections.

A "cherry-picker" crane was assumed to go with transport trucks to the depot or meet them there to load sections, although a forklift truck could also serve at the depot. After loading the needed sections, both the crane and the flatbed truck-trailers proceed to the construction site. It was further assumed that sufficient trucks would be requisitioned to accomplish the maintenance activity in one trip from the depot to the site and return. The handling crew for attaching lift cables and maneuvering the PCB's into place was assumed to ride to the depot in some fashion (perhaps the supervisor took them) but to ride back to the site after loading the sections in the truck(s).

It was finally assumed that equipment would have to be paid for in four-hour (half-day) increments.

In order to cost the effort required to replace sections, it is necessary to consider how many sections at most might need to be replaced at a site as a result of a collision. The dynamic and structural analysis presented in Appendix C or D provides an estimate of number of sections that would be damaged in absorbing varying levels of energy as a function of joint design. If the conservative assumption is made that a damaged section must be replaced, it is possible to arrive at some conclusions as to amounts of time and numbers of trucks that would be required as a maximum. Table 27 provides these estimates of number of sections damaged as a result of levels of collision energy ranging from 20.4 to 322 kip-ft (27.7 to 437 kN-m). An examination of this table reveals that no more than one truck would be required for repair of barriers hit with energy levels no greater than Level 3. These data lead directly to Table 28, which presents the cost breakdown

Table 27. Damage Estimates

Barrier Connection Type	Section Length (ft)	Representative Collisions 4500/15/45 Level A *20.4 K-ft	4500/15/60 Level 1 36.5 K-ft	4500/25/60 Level 2A 97.3 K-ft	40,000/15/60 Level 3 322 K-ft
C1 Tongue & Groove	10	1	2	4	8
	20	1	2	3	4
	30	1	2	2	3
C2 Dowell	10	1	2	4	8
	20	1	2	3	4
	30	1	2	2	3
C3 Grid Slot	10	1	2	4	8
	20	1	2	3	4
	30	1	2	2	3
C4 Top T-Lock	10	0	1	4	8
	20	0	1	2	4
	30	0	1	2	3
C5 Lapped Joint	10	1	1	4	8
	20	1	1	2	4
	30	1	1	2	3
C6 Pin and Rebar	10	0	0	2	8
	20	0	0	2	4
	30	0	0	1	3
C7 Vertical I-Beam	10	0	0	2	8
	20	0	0	2	4
	30	0	0	1	3
C8 Bottom T-Lock	10	0	0	2	8
	20	0	0	2	4
	30	0	0	1	3
C9 Channel Splice	10	0	0	2	8
	20	0	0	2	4
	30	0	0	1	3
C10 Welsbach	10	0	0	2	4
	20	0	0	2	3
	30	0	0	0	2

*Number Sections Damaged

Table 28. Cost Bases

TRUCK COSTS	Sections to Haul ≤4-30' ≤6-20' ≤12-10'	5-8 - 30' 7-12 - 20' 13-24-10'
Truck Use	42.00	84.00
Truck OPS Cost	22.00	44.00
Driver Cost	69.32	138.64
	$133.32	266.64

Drivers @ $17.33/hr.
Truck Use @ $42/½ day
Truck OPS @ $22/½ day

CRANE COSTS

Operator 21.50/hr X 4 = 86.00

Cherry Picker 165.00 for 4 hours = 165.00

$251.00

Plus transport to site and back to depot
Assume same as truck OPS cost 22.00

$283.00

PICKUP & PLACEMENT COSTS

Time Base: Empty transport to depot @ 20MPH = 30 min.
Transport to site @ 20MPH = 30 min.

2-Handlers - 1 hour in transit @ 16.54 = $33.08

Can handle 4 30' (no faster to do 20's or 10's)
in 10 minutes

So: MAX time at site 1 hour @ 16.54 = $33.08

DAMAGED SECTIONS - Transp. to depot @ 20 MPH = 30 min.
Back haul & drop @ 20 MPH = 30 min.

So: 2 hours just for xport

Handlers: 3 hours total X 2 X 16.54 = $99.24

Plus a super for 4 hours @ 21.50 = 86.00

So:	1 TRUCK	2 TRUCKS	
	133.32	266.00	Only differential cost then is joint hookup. (Negligible)
	283.00	283.00	
	99.24	99.24	
	86.00	86.00	
	$601.56 or $602.00	$734.00	

for a half-day maintenance activity (it could hardly be less, as the table shows) which basically involves men and equipment tied up for that length of time and the costs associated with such an activity. Since no cases involved more than one transport flatbed truck, a flat rate of $602 was taken for the cost of the maintenance activity associated with a single collision. If it is assumed that these sections must be replaced, then the cost associated with that replacement must be taken into account in estimating the total cost of maintenance. For the small numbers of joints that must be fastened in such maintenance jobs, the cost of that operation can be safely neglected. The per-section fabrication costs for each concept presented in Table 14, multiplied by the number of sections expected to be damaged in Table 27, plus $602 was taken for the cost of the maintenance activity associated with a single collision (Table 29). In this table, the total costs for a collision at a given level are presented for each joint concept for each of three section lengths, 10, 20 and 30 ft. In order to present these estimates in a perhaps more meaningful way, Figures 116 through 125 plot a curve for each section length of cost as a function of energy level of collision.

Most of these curves look much the same, with the exception of C1--Tongue and Groove, and C10--Welsbach, but even there, there is a convergence of costs for higher energy collisions, for 10 vs. 20 vs. 30 ft sections. Shorter sections maintain a cost advantage as far as maintenance and replacements costs over longer sections at a given level of energy for most concepts until the higher energy ranges are reached. Note that costs accelerate very rapidly for the lower two levels of energy.

A Hypothetical Case for PCB Cost Analysis

The foregoing section presents a picture of the costs associated with a collision, but the construction engineer needs a more complete perspective of the total costs that he is facing in using PCB for protection of a construction site; that is, cost of the barrier itself, costs for installation, and costs for maintaining the barrier once in place at any given place in his site for a period of time. How many collisions should he expect, and what will the consequences of these be on his total cost picture for construction protection?

In order to illustrate how such a costing estimate might be done, recourse was made to the AASHTO Guide, "Guide for Selecting, Locating, and

Table 29. $602 + Replacement Costs

CONCEPT	SECTION LENGTH	COLLISION LEVELS A	COLLISION LEVELS 1	COLLISION LEVELS 2A	COLLISION LEVELS 3	JOINT ASSY
C1 Tongue & Groove	10	765	928	1254	1906*	0
	20	925	1248	1571	1894*	0
	30	1085	1568	1568	2051*	0
C2 Dowel	10	766	930	1258	1914**	0
	20	926	1250	1574	1898**	0
	30	1086	1570	1570	2054**	0
C3 Grid Slot	10	769	936	1270	1938	.03
	20	929	1256	1585	1910	.03
	30	1089	1576	1576	2063	.03
C4 Top T-Lock	10	0	775	1294	1986	.11
	20	0	935	1268	1934	.11
	30	0	1098	1594	2090	.11
C5 Lapped Joint	10	772	772	1282	1962	.17
	20	932	932	1262	1922	.17
	30	1091	1091	1582	2072	.17
C6 Pin and Rebar	10	0	0	964	2050	.55
	20	0	0	1284	1966	.55
	30	0	0	1103	2105	.55
C7 Vert I-Beam	10	0	0	1000	2194	.03
	20	0	0	1320	2038	.03
	30	0	0	1121	2159	.03
C8 Bottom T-Lock	10	0	0	998	2186	0
	20	0	0	1318	2034	0
	30	0	0	1120	2156	0
C9 Channel Splice	10	0	0	1032	2322	2.00
	20	0	0	1352	2102	2.00
	30	0	0	1169	2302	2.00
C10 Welsbach	10	0	0	1096	2084**	0
	20	0	0	1416	1823**	0
	30	0	0	0	1736**	0

*May require moving undamaged PCB's to reconnect.

**Will require moving undamaged PCB's.

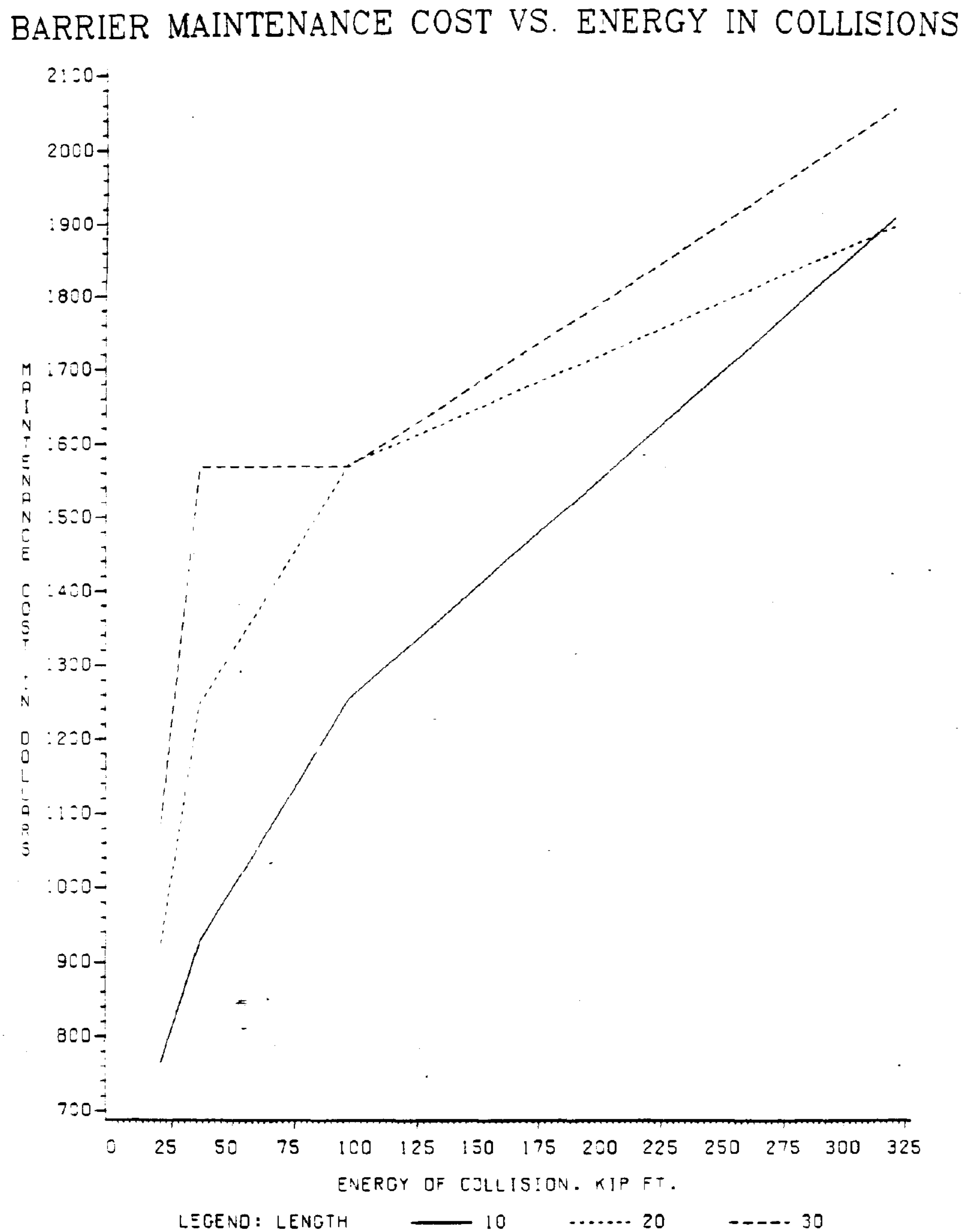

Figure 116. Barrier Maintenance Cost vs. Energy in Collisions--C1 Tongue and Groove.

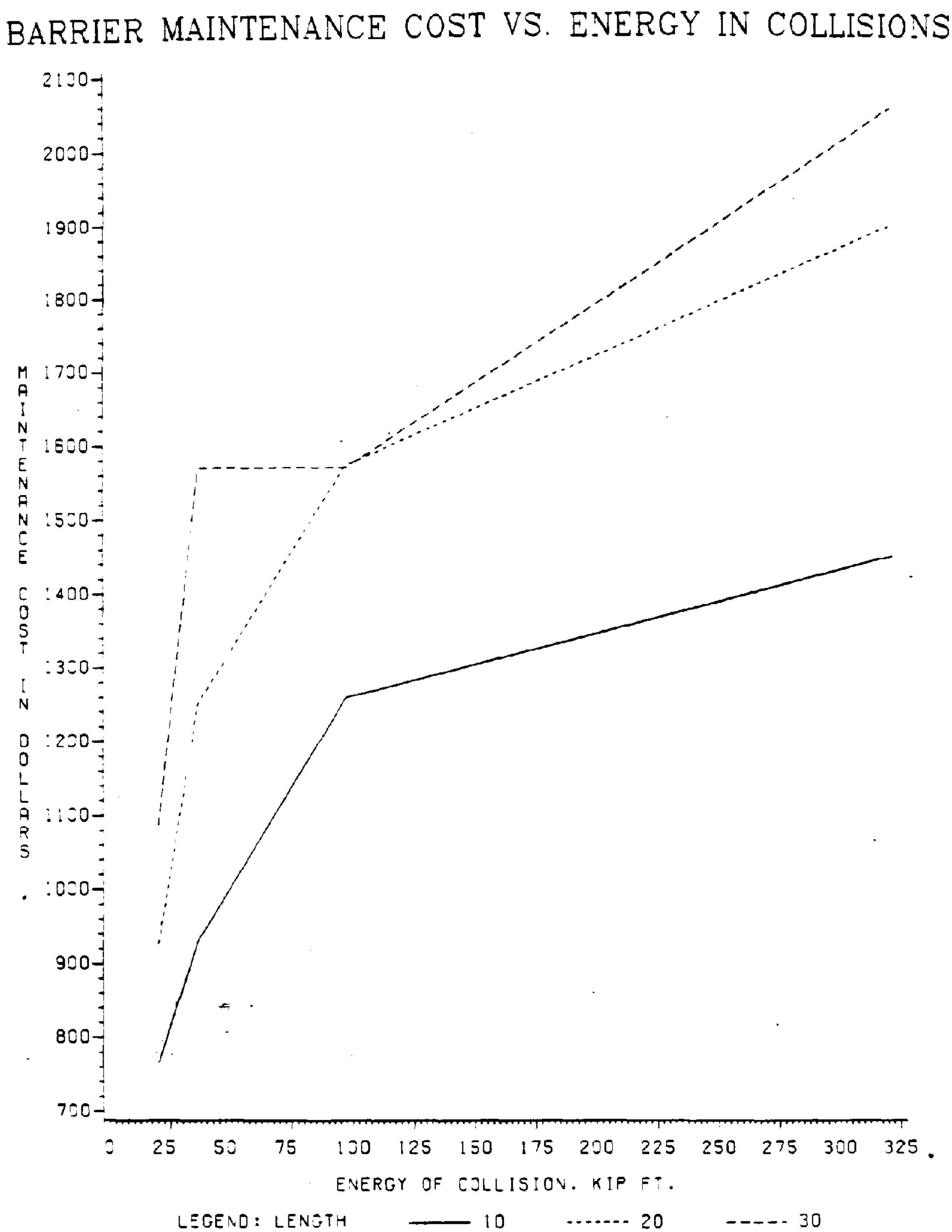

Figure 117. Barrier Maintenance Cost vs. Energy in Collisions--C2 Dowel.

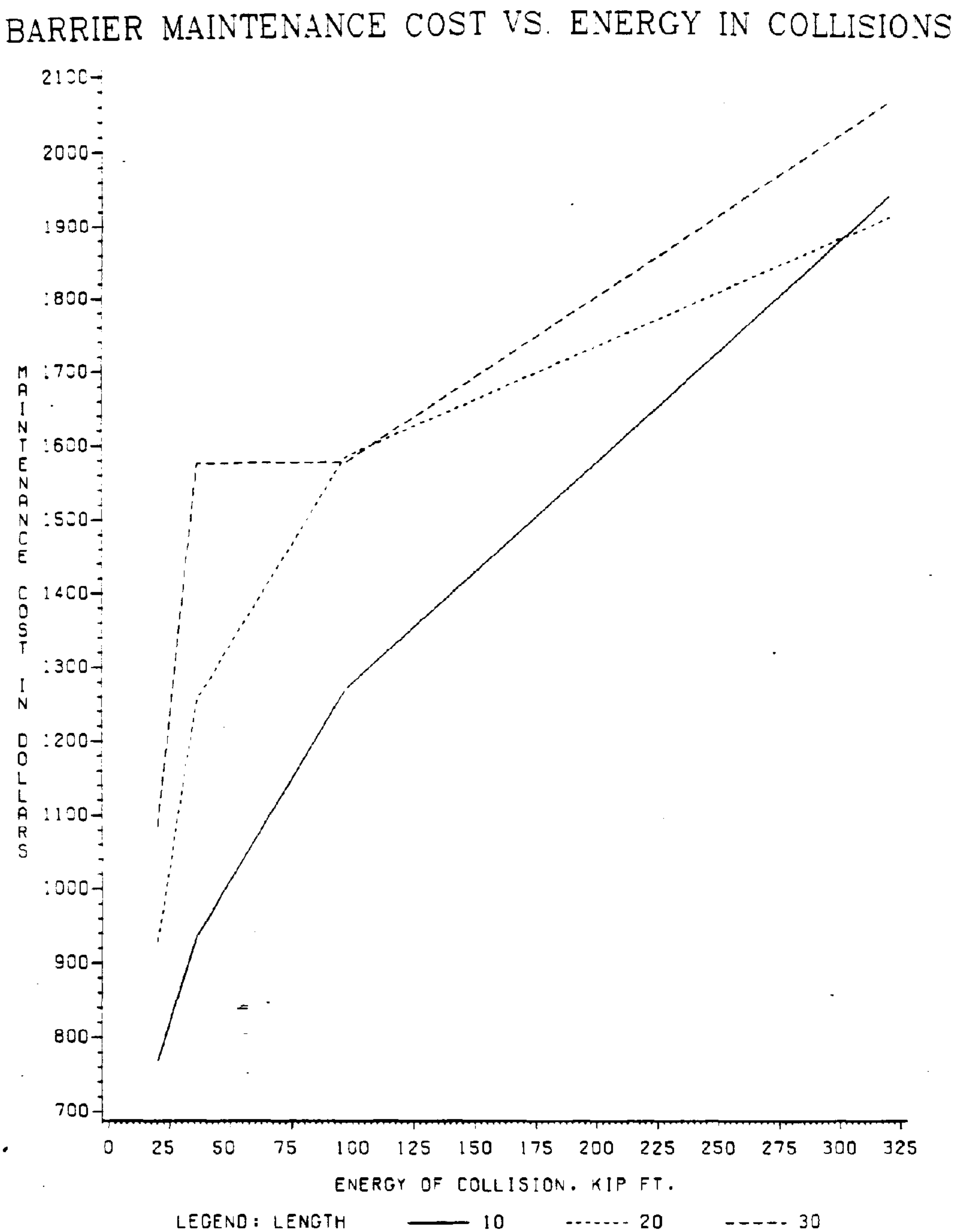

Figure 118. Barrier Maintenance Cost vs. Energy in Collisions--C3 Grid Slot.

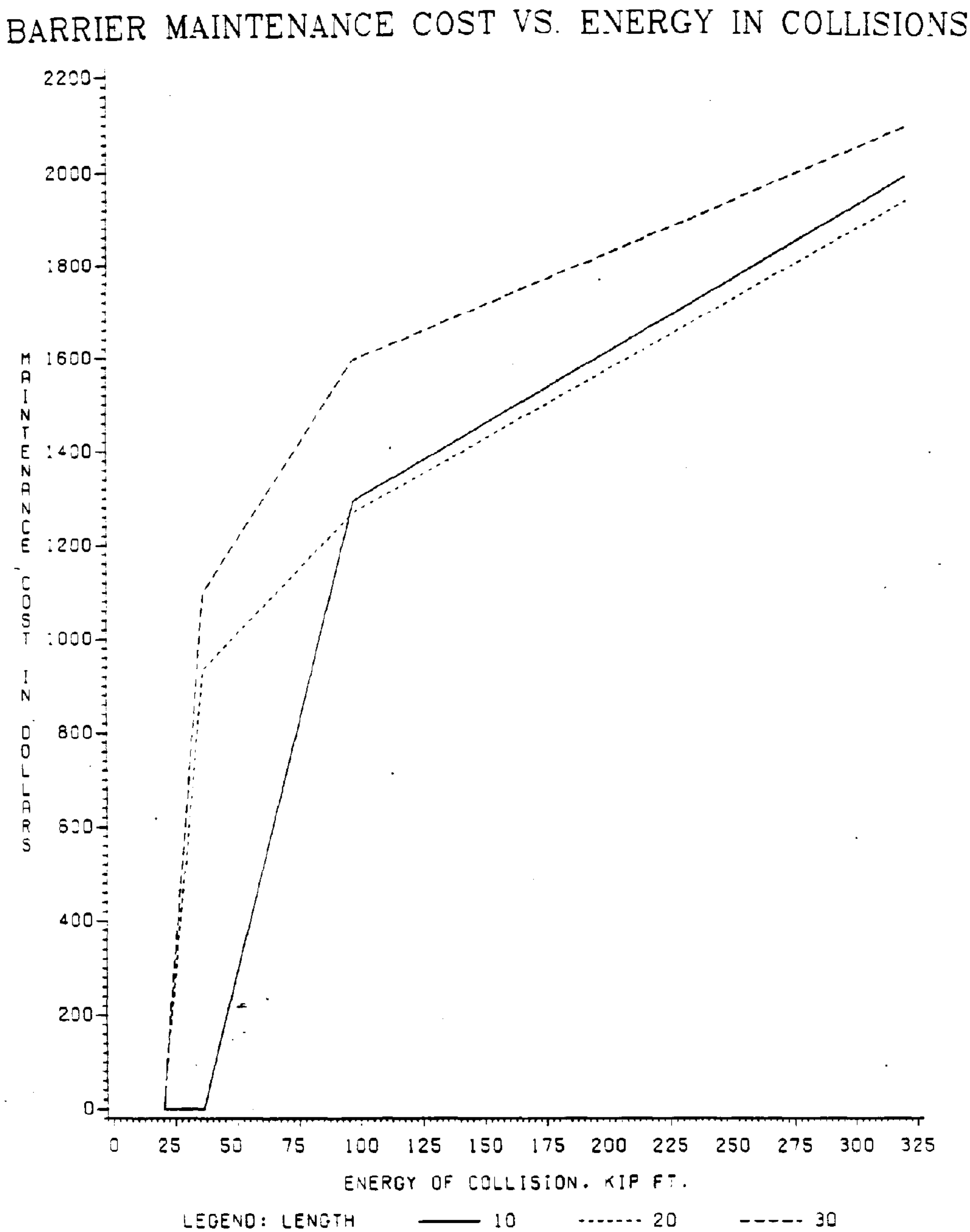

Figure 119. Barrier Maintenance Cost vs. Energy in Collisions--C4 Top T-Lock.

BARRIER MAINTENANCE COST VS. ENERGY IN COLLISIONS

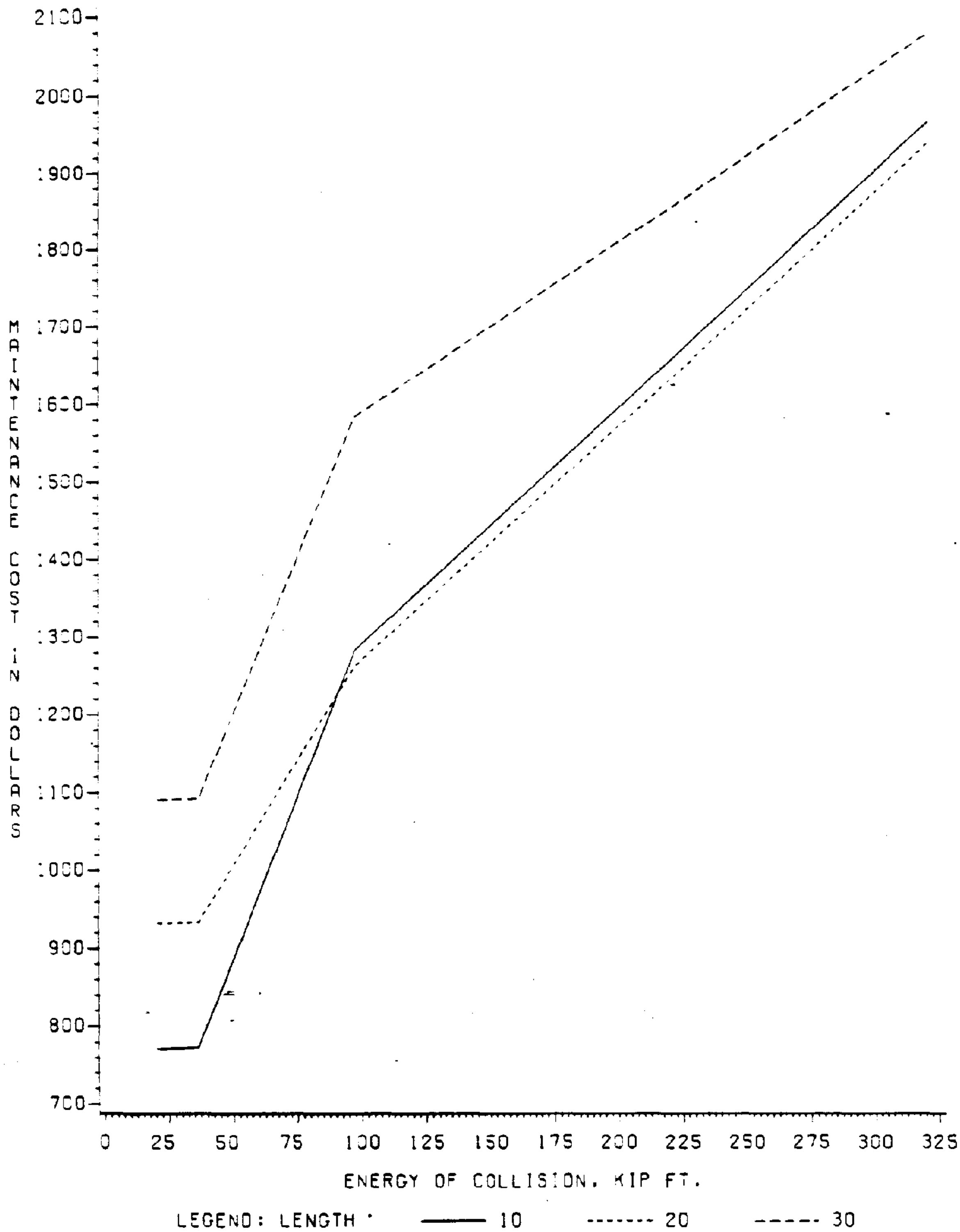

Figure 120. Barrier Maintenance Cost vs. Energy in Collisions--C5 Lapped Joint.

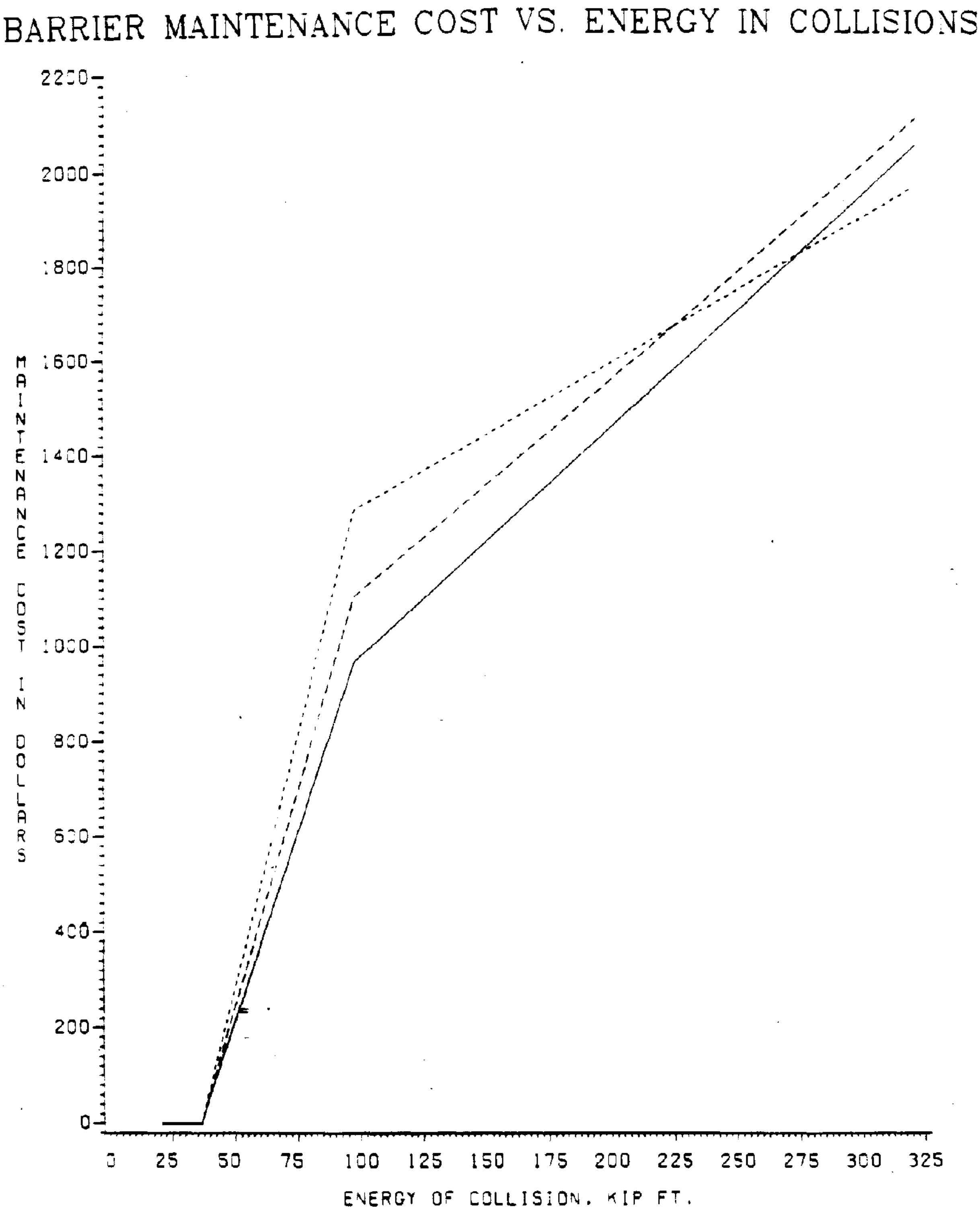

Figure 121. Barrier Maintenance Cost vs. Energy in Collisions--C6 Pin and Rebar.

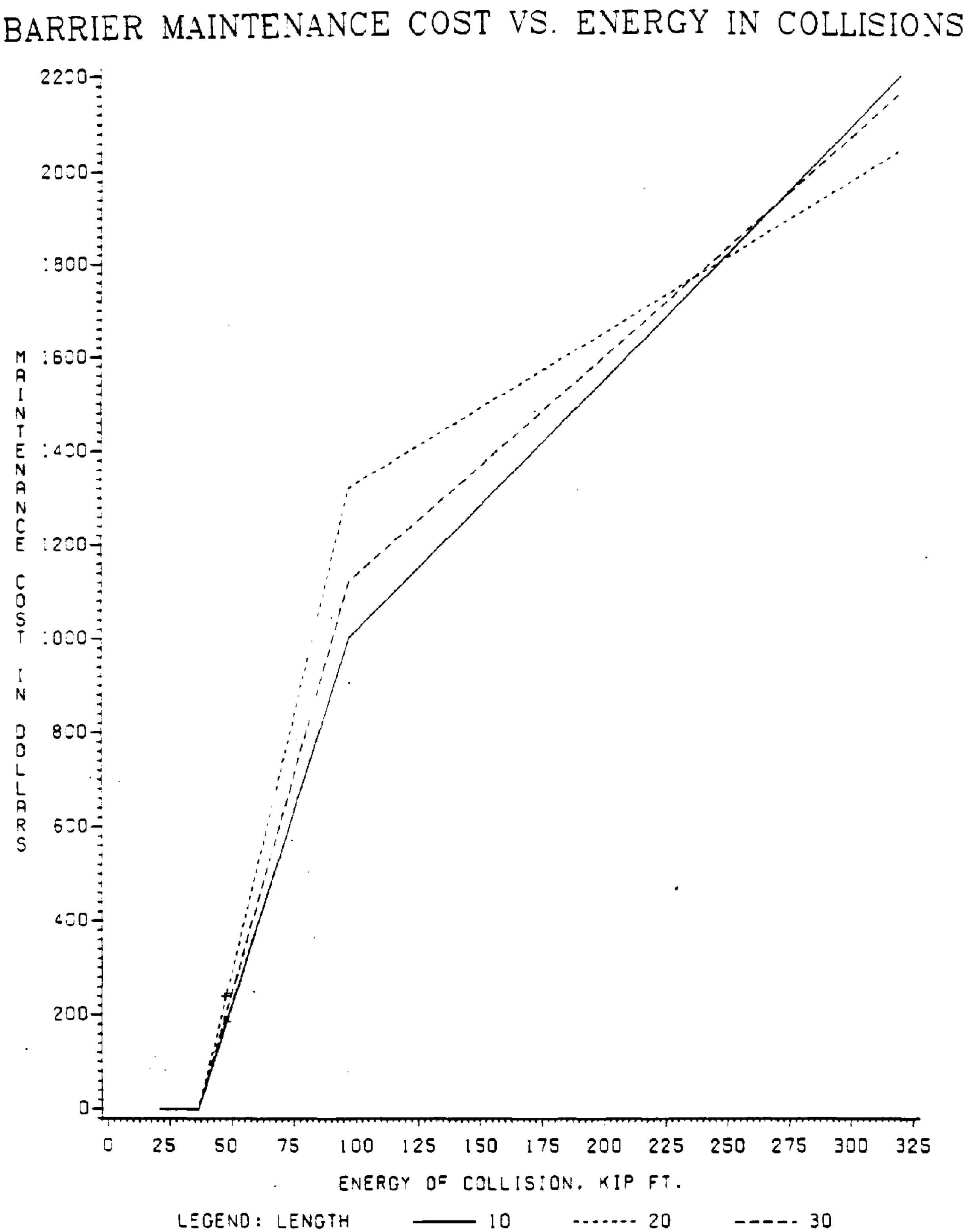

Figure 122. Barrier Maintenance Cost vs. Energy in Collisions--C7 Vertical I-Beam.

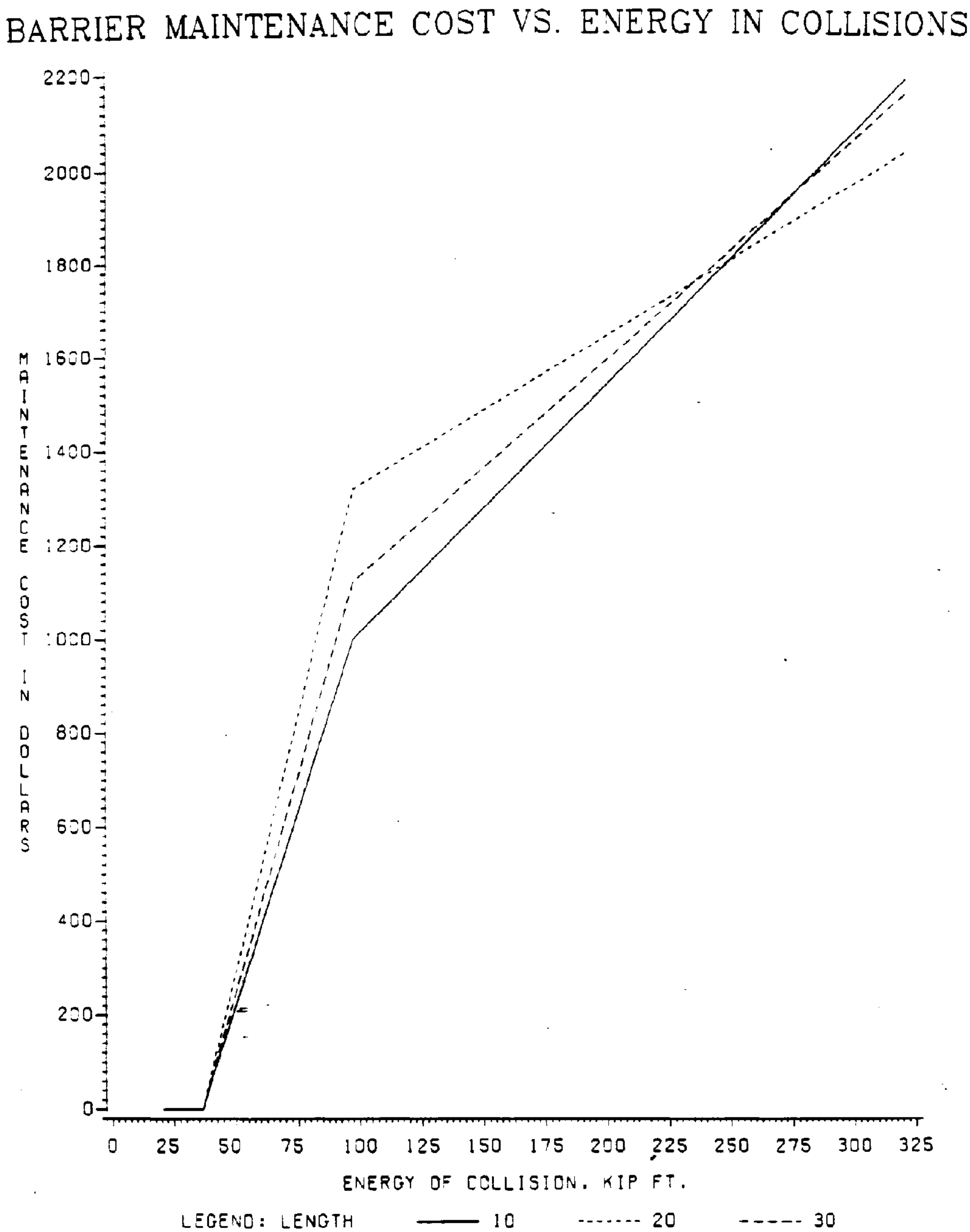

Figure 123. Barrier Maintenance Cost vs. Energy in Collisions--C8 Bottom T-Lock.

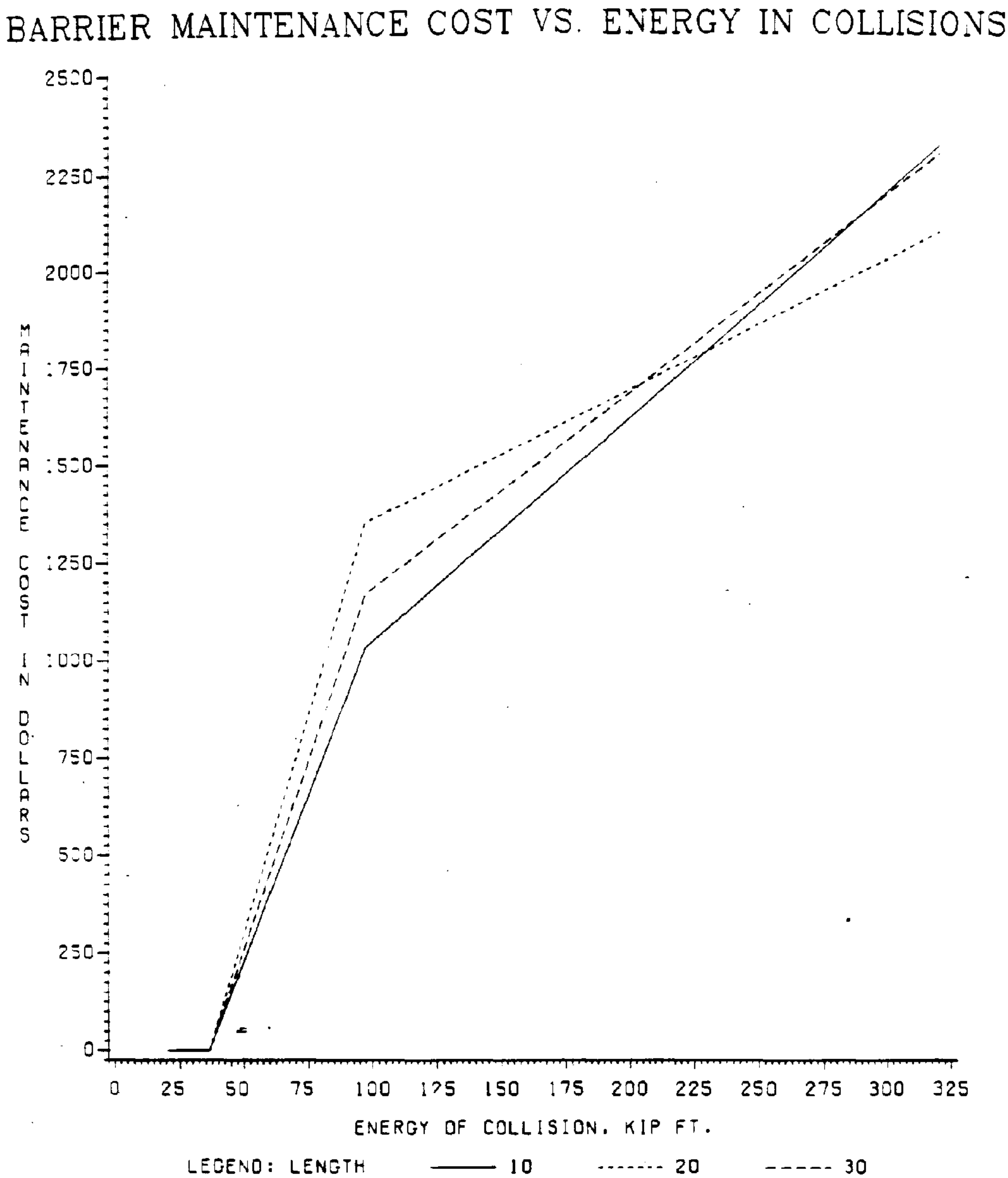

Figure 124. Barrier Maintenance Cost vs. Energy in Collisions--C9 Channel Splice.

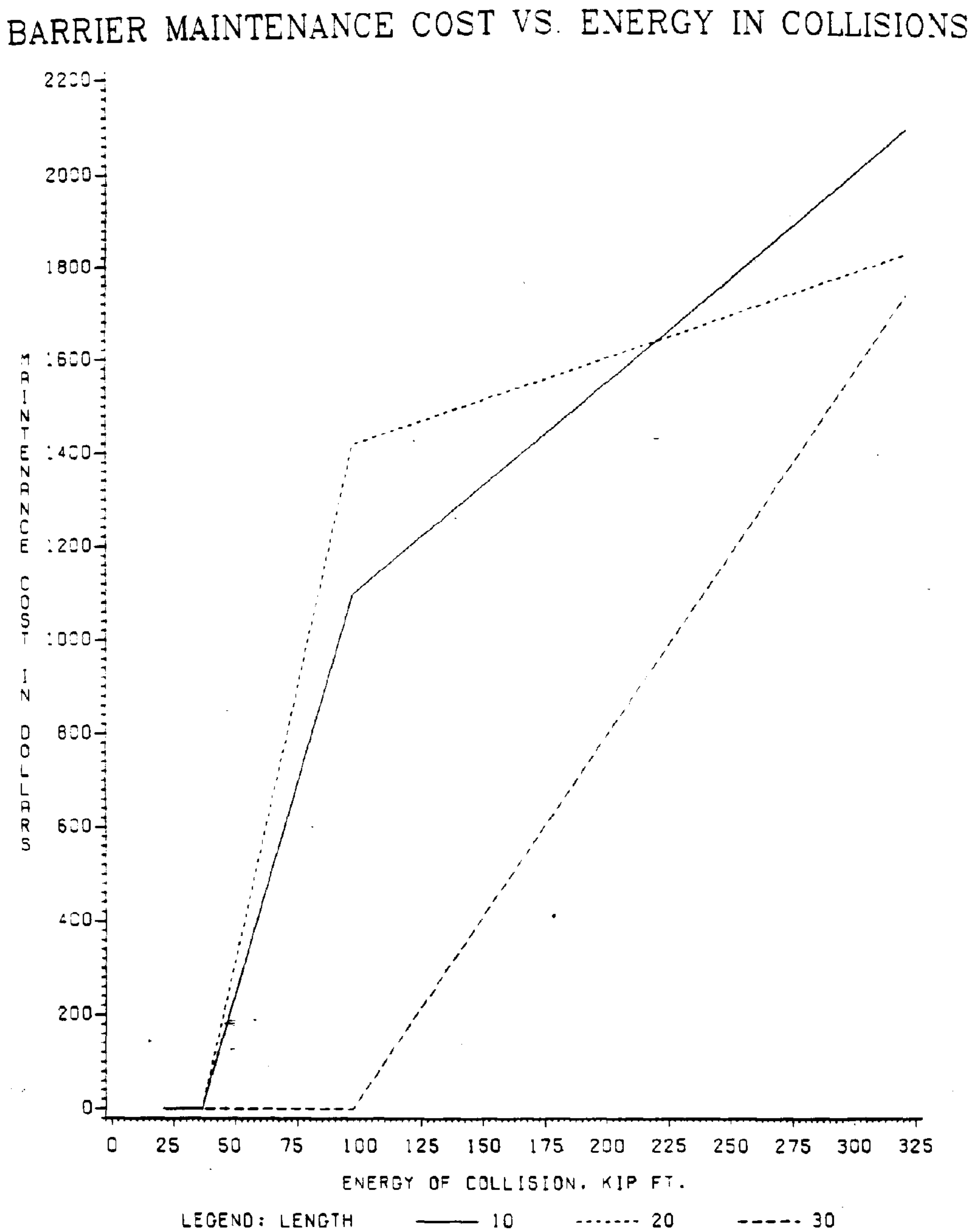

Figure 125. Barrier Maintenance Cost vs. Energy in Collisions--C10 Welsbach.

Designing Traffic Barrier"(13). The model in Section VII of the guide provides an estimate of collision frequency per year, given certain parameters about the highway and its geometrics with respect to a barrier or obstacle. This is to say,

- A = lateral placement from EOP of PCB line
- L = length of barrier array
- W = width of barrier
- ADT = 2-way volume flow
- E_f = vehicle encroachments per mile per year
- Y = lateral displacement of encroaching vehicle measured from edge of travelled way to longitudinal face of the barrier
- P{y>...} = probability of vehicle lateral displacement greater than some value
- J = no. of 1 ft increments of width of barrier, i.e. a 2 ft wide barrier would have a J-value of 2.

Obtain estimate of collision frequency per year C_f.

$$c_f = \frac{E_f}{10560} (L + 62.9) \cdot P \; [Y > A] + 5.14 \sum_{\upsilon}^{\omega} P \; [Y > A + 6.0 + \frac{2J-1}{2}]$$

Let us now adapt an actual site in Texas for the purpose of demonstrating this approach to cost analysis.

PLACE: Stemmons Fwy. I-35
w side of Dallas, Texas

ADT: 200,000 for all 8 lanes, divided median

A: 3 ft

L: 5,000 ft

W: 2.3 ft

P Y>A: 98%

E_f: 40%

$$C_f = \frac{E_f}{10560} (L+62.9) \cdot P\,[Y>A] + 5.14 \sum_{J=1}^{\omega} P\,\left[Y > A + 6 + \frac{2v-1}{2}\right]$$

$$= \frac{40}{10560} (5000+62.9) \cdot .98 + 5.14\,[.935 + .925]$$

$$\text{if } J=2;\; P\,\left[Y>3 + 6 + \frac{2-1}{2}\right] = [P\; Y>9.5 = 93.5]$$

$$P\,\left[Y>3 + 6 + \frac{4-1}{2}\right] = P\,[Y>10.5 = 92.5]$$

$$= .004\,[4961.6 + 9.56] = 19.88 \text{ collisions per year}$$

or approximately 20

Vehicle Mix:

Heavy Vehicles	16%	3.2 per year
Passenger Cars	84%	16.8 per year

Period of time barrier will be in place during construction: 1 Year

Since encroaching vehicles are "selected" randomly and might be distributed approximately normally, a good method of roughly estimating the energy of collision with the barrier might be the mean of energies associated with passenger vehicles at various speeds and angles of encroachment. This would be the mean of levels A, 1, and 2A, or 51.4 kip-ft.

By a similar argument, small trucks at 60 mph and 25 degrees encroachment expend the same energy as larger trucks at lower speeds/angle combinations, and distribute up to the extreme of 40,000 lb vehicles impacting at 15 degrees at 60 mph (322 kip-ft). An estimator of the energy associated with truck collisions would thus be the mean of level 2A and 3, which is 209.7 kip-ft.

Suppose (as was the case in this real-life example) the resident engineer is considering the C-3--Grid-Slot concept, but his contractor can supply the C-5--Lapped Joint. Which should be used on this busy freeway, and which length, 10, 20, or 30 ft?

For C3, the costs of maintenance for 1 year would be:

Length	Passenger Car Levels		Cost
10 ft	($ 992 x 16.8)	+	($1604 x 3.2) = $21798
20 ft	($1257 x 16.8)	+	($1748 x 3.2) = $26942
30 ft	($1413 x 16.8)	+	($1820 x 3.2) = $29562

For C5 the costs would be:

10 ft	($ 942 x 16.8)	+	($1622 x 3.2)	= $21016
20 ft	($1042 x 16.8)	+	($1592 x 3.2)	= $22600
30 ft	($1255 x 16.8)	+	($1827 x 3.2)	= $26930

From a maintenance standpoint, a 10 ft C5 is the most attractive in this example, however installation costs and relocation costs must also be considered from the previous sections. 5,000 ft of 10 ft C5 would cost:

Fabricate:	$17.00/ft x 5000 =	$85,000
Install :	$ 1.40/ft x 5000 =	$ 7,000
Maintain :		$21,016
	TOTAL COST	$113,016

whereas 30 ft sections of C5 would be:

Fabricate:	$16.33 x 5000 =	$81,650
Install:	$ 1.19 x 5000 =	$ 5,950
Maintain:		$29,562
	TOTAL COST	$117,160

The much simpler C3 concept, in comparison for 10 ft lengths would cost:

Fabricate:	$16.70/ft x 5000 =	$83,500
Install:	$ 1.41/ft x 5000 =	$ 7,050
Maintain:		$21,798
	TOTAL COST	$112,348

30 ft lengths would cost:

Fabricate:	$16.23/ft x 5000 =	$81,150
Install:	$ 1.21/ft x 5000 =	$ 6,050
Maintain:		$29,564
	TOTAL COST	$116,764

This rationale can be generalized into a summary table, Table 30, which assumes the nominal vehicle mix on the nation's highways of 16 per cent heavy truck, and 84 percent passenger or similarly sized vehicles. As a matter of determining how sensitive the relative total costs are to vehicle mix, the vehicle mix ratio was changed from 16-84 to 50-50 (an extremely high ratio of trucks, really unrealistic) and Table 31 was generated. Then from these figures, the histogram of Figure 126 was constructed showing the ten least

Table 30. Total 1 Year Costs With Maintenance for Trucks 16% - Passenger Cars 84%.

Concept	Length	Fabricate	Install	Level A	Level 1	Level 2A	Level 3	Main Cost	Total Cost
C1 Tongue	10	$ 81,500	$ 6,900	$ 765	$ 928	$ 1,254	$ 1,906	$ 21,559	$ 109,959
C1 Tongue	20	80,750	6,400	925	1,248	1,571	1,894	26,510	113,660
C1 Tongue	30	80,900	5,900	1,085	1,568	1,568	2,051	29,428	116,228
C2 Dowel	10	82,000	6,900	766	930	1,258	1,914	21,618	110,518
C2 Dowel	20	81,000	6,400	926	1,250	1,574	1,898	26,555	113,955
C2 Dowel	30	80,650	5,900	1,086	1,570	1,570	2,054	29,464	116,014
C3 Grid	10	83,500	7,050	769	936	1,270	1,938	21,793	112,343
C3 Grid	20	81,750	6,550	929	1,256	1,585	1,910	26,704	115,004
C3 Grid	30	81,150	6,050	1,089	1,576	1,576	2,063	29,572	116,772
C4 Top T	10	86,500	7,100	0	775	1,294	1,986	16,834	110,434
C4 Top T	20	83,250	6,600	0	935	1,268	1,934	17,460	107,310
C4 Top T	30	82,650	6,050	0	1,098	1,594	2,090	20,970	109,670
C5 Lapped	10	85,000	7,000	772	772	1,282	1,962	21,016	113,016
C5 Lapped	20	82,500	6,500	932	932	1,262	1,922	22,600	111,600
C5 Lapped	30	81,650	5,950	1,091	1,091	1,582	2,072	26,925	114,525
C6 Vert P	10	90,500	7,350	0	0	964	2,050	10,221	108,071
C6 Vert P	20	85,250	6,750	0	0	1,284	1,966	12,390	104,390
C6 Vert P	30	83,500	6,150	0	0	1,103	2,105	11,310	100,960
C7 Vert I	10	99,500	7,050	0	0	1,000	2,194	10,710	117,260
C7 Vert I	20	89,750	6,550	0	0	1,320	2,038	12,765	109,065
C7 Vert I	30	86,500	6,050	0	0	1,121	2,159	11,526	104,076
C8 Bottom	10	99,000	7,050	0	0	998	2,186	10,683	116,733
C8 Bottom	20	89,500	6,550	0	0	1,318	2,034	12,744	108,794
C8 Bottom	30	86,350	6,050	0	0	1,120	2,156	11,514	103,914
C9 Splice	10	107,500	8,050	0	0	1,032	2,322	11,146	126,696
C9 Splice	20	93,750	7,200	0	0	1,352	2,102	13,098	114,048
C9 Splice	30	89,150	6,350	0	0	1,169	2,302	12,100	107,600
C10 Welsb	10	123,500	7,050	0	0	1,096	2,084	11,226	141,776
C10 Welsb	20	101,750	6,550	0	0	1,416	1,823	13,112	121,412
C10 Welsb	30	94,500	6,050	0	0	0	1,736	2,778	103,328

Factor for Cars = 6.00
Factor for Trucks = 2.00

Table 31. Total 7 Year Costs With Maintenance for Trucks 50% - Passenger Cars 50%.

Concept	Length	Fabricate	Install	Level A	Level 1	Level 2A	Level 3	Main Cost	Total Cost
C1 Tongue	10	$ 81,500	$ 6,900	$ 765	$ 928	$ 1,254	$ 1,906	$ 25,614	$ 114,014
C1 Tongue	20	80,750	6,400	926	1,248	1,571	1,894	29,793	116,943
C1 Tongue	30	80,900	5,900	1,085	1,568	1,568	2,051	32,151	118,951
C2 Dowel	10	82,000	6,900	766	930	1,258	1,914	25,697	114,597
C2 Dowel	20	81,000	6,400	926	1,250	1,574	1,898	29,848	117,248
C2 Dowel	30	80,650	5,900	1,086	1,570	1,570	2,054	32,193	118,743
C3 Grid	10	83,500	7,050	769	936	1,270	1,938	25,947	116,497
C3 Grid	20	81,750	6,550	929	1,256	1,585	1,910	30,029	118,329
C3 Grid	30	81,150	6,050	1,089	1,576	1,576	2,063	32,318	119,518
C4 Top T	10	86,500	7,100	0	775	1,294	1,986	23,290	116,890
C4 Top T	20	83,250	6,600	0	935	1,268	1,934	23,346	113,196
C4 Top T	30	82,650	6,050	0	1,098	1,594	2,090	27,384	116,084
C5 Lapped	10	85,000	7,000	772	772	1,282	1,962	25,631	117,631
C5 Lapped	20	82,500	6,500	932	932	1,262	1,922	26,330	115,330
C5 Lapped	30	81,650	5,950	1,091	1,091	1,582	2,072	30,804	118,404
C6 Vert P	10	90,500	7,350	0	0	964	2,050	18,280	116,130
C6 Vert P	20	85,250	6,750	0	0	1,284	1,966	20,526	112,526
C6 Vert P	30	83,500	6,150	0	0	1,103	2,105	19,713	109,363
C7 Vert I	10	99,500	7,050	0	0	1,000	2,194	19,300	125,850
C7 Vert I	20	89,750	6,550	0	0	1,320	2,038	21,186	117,486
C7 Vert I	30	86,500	6,050	0	0	1,121	2,159	20,133	112,683
C8 Bottom	10	99,000	7,050	0	0	998	2,186	19,243	125,293
C8 Bottom	20	89,500	6,550	0	0	1,318	2,034	21,149	117,199
C8 Bottom	30	86,350	6,050	0	0	1,120	2,156	20,110	112,510
C9 Splice	10	107,500	8,050	0	0	1,032	2,322	20,207	135,757
C9 Splice	20	93,750	7,200	0	0	1,352	2,102	21,772	122,722
C9 Splice	30	89,150	6,350	0	0	1,169	2,302	21,248	116,748
C10 Welsb	10	123,500	7,050	0	0	1,096	2,084	19,550	150,100
C10 Welsb	20	101,750	6,550	0	0	1,416	1,823	20,910	129,210
C10 Welsb	30	94,500	6,050	0	0	0	1,736	8,680	109,230

Factor for Cars = 3.33
Factor for Trucks = 5.00

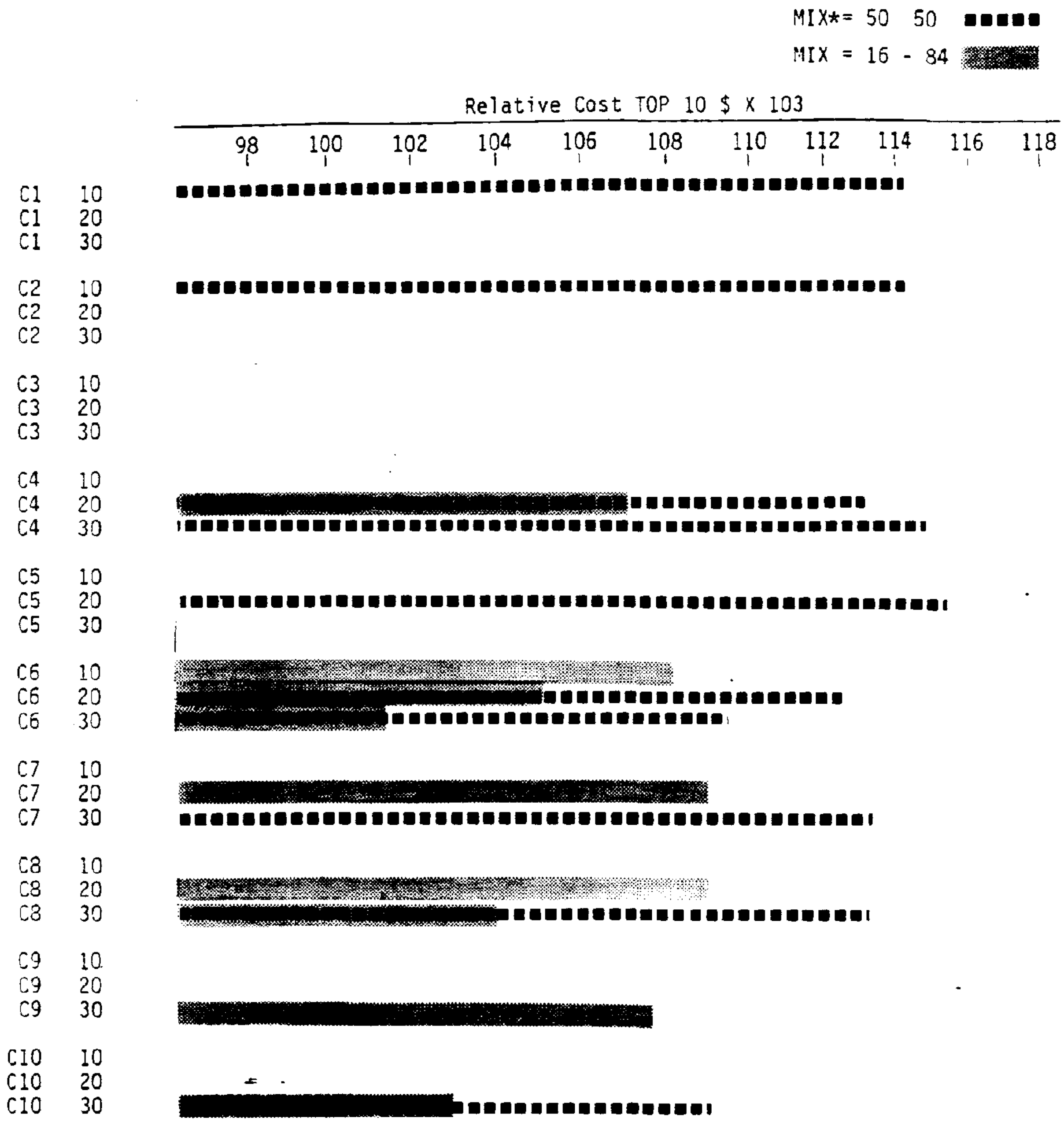

*Percentage of trucks and passenger cars respectively.

Figure 126. Comparison of Ten Least Expensive PCB Concepts.

expensive concepts for a vehicle mix of 16-84 trucks: cars (realistic) and the worst-case 50-50 mix. All costs, of course, go up for this worst case, but the relative standing of most of the barrier joint concepts for the three lengths of interest do not change a great deal. The least costly concept for both traffic mix cases is the familiar vertical pin with rebar, C6 concept, at a length of 30 ft, with C8, the Bottom T-Lock at 30 ft the next least expensive (tied with C7--Vertical I-Beam) for the heavy truck mix case. Others in the ten least expensive can be seen by studying this figure. Note that the longer lengths predominate in overall costs, and positive joints appear to have an advantage in cost over those less positive, although this relationship is not completely straightforward.

Analyses such as that presented above can be generated for a wide variety of different traffic situations at proposed construction sites to assist the construction engineer in choosing an appropriate design of PCB for his particular needs.

BARRIERS IN CONSTRUCTION ZONES

APPENDIX F

Conceptual Drawings

Prepared for
Contract DOT-FH-11-9458
Office of Research

Federal Highway Administration

U. S. Department of Transportation

Appendix F
by
Project Staff

Texas A&M Research Foundation

Texas Transportation Institute

The Texas A&M University System

April 1985

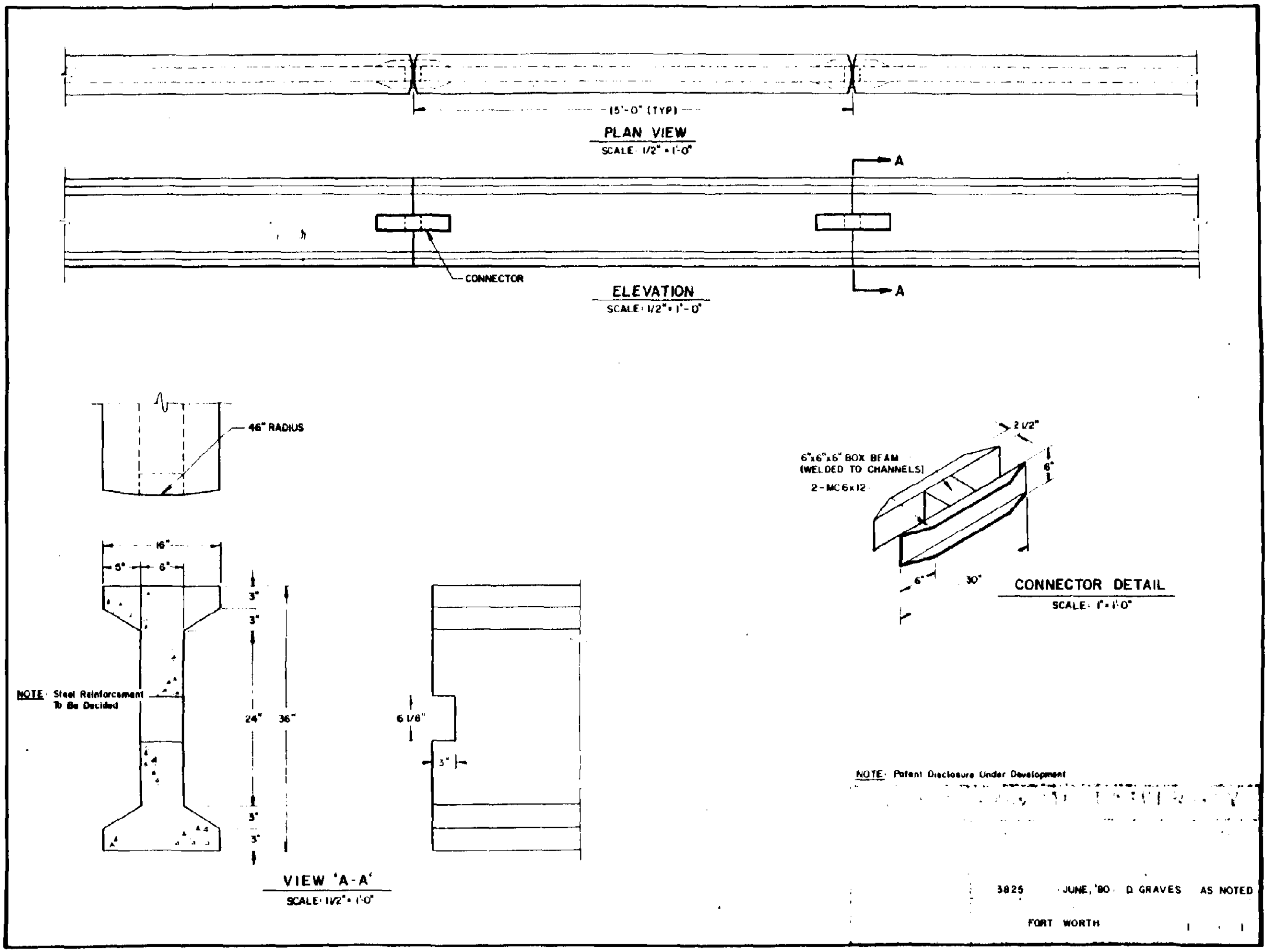

15'-0" (TYP)
PLAN VIEW
SCALE: 1/2" = 1'-0"
A
CONNECTOR
ELEVATION
SCALE: 1/2" = 1'-0"
46" RADIUS
16"
5"
6"
3"
24"
36"
6 1/8"
3"
NOTE: Steel Reinforcement To Be Decided
VIEW 'A-A'
SCALE: 1/2" = 1'-0"
2 1/2"
6"x6"x6" BOX BEAM (WELDED TO CHANNELS)
2-MC6x12
6"
30°
CONNECTOR DETAIL
SCALE: 1" = 1'-0"
NOTE: Patent Disclosure Under Development
3825
JUNE, '80
D. GRAVES
AS NOTED
FORT WORTH

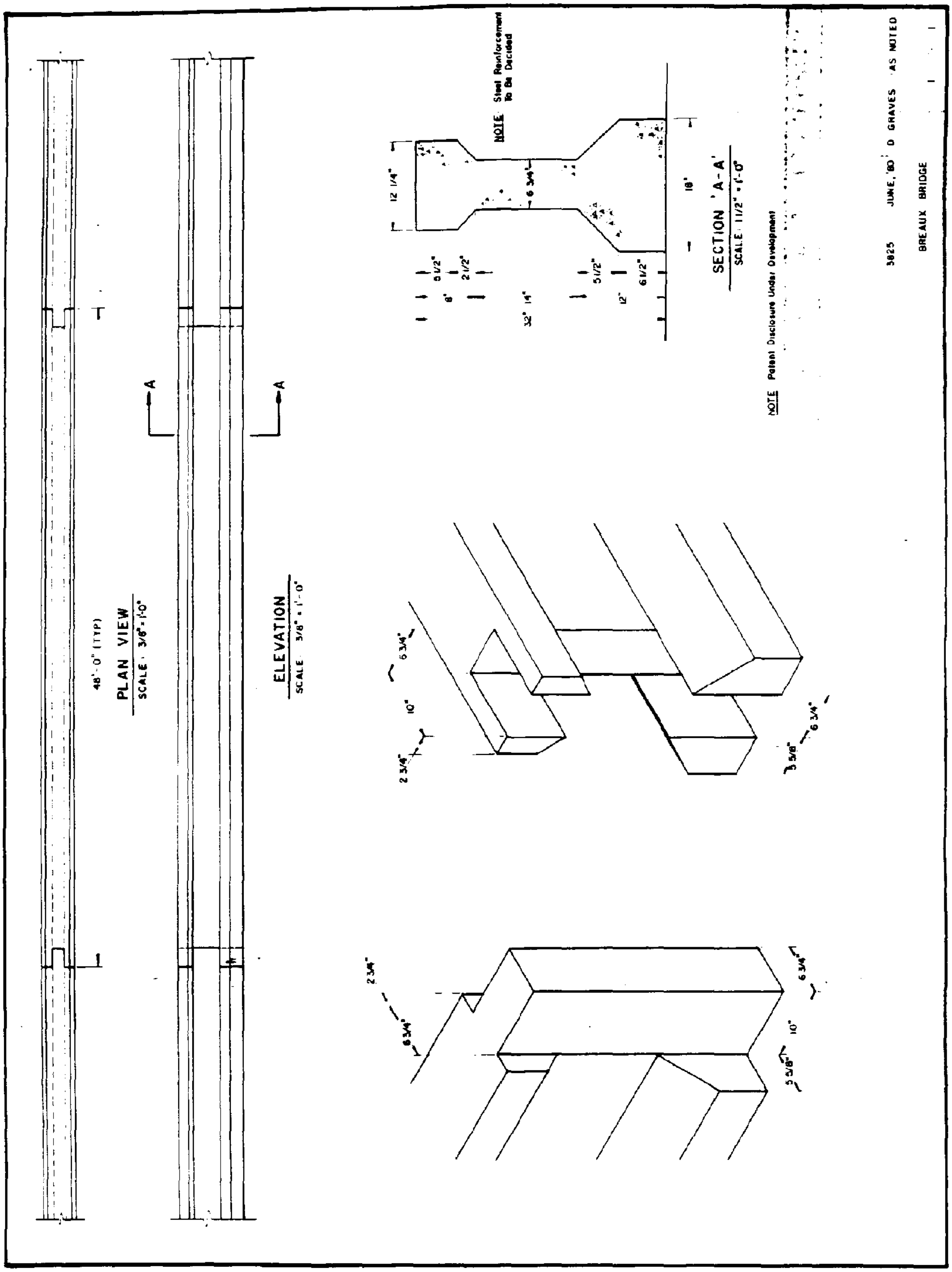

48'-0" (TYP)
PLAN VIEW
SCALE: 3/8" = 1'-0"
A
ELEVATION
SCALE: 3/8" = 1'-0"
A
2 3/4"
6 3/4"
5 5/8"
10"
6 3/4"
2 3/4"
10"
6 3/4"
5 5/8"
6 3/4"
12 1/4"
5 1/2"
8"
2 1/2"
32"
14"
6 3/4"
5 1/2"
12"
6 1/2"
18"
NOTE: Steel Reinforcement To Be Decided
SECTION 'A-A'
SCALE: 1 1/2" = 1'-0"
NOTE: Patent Disclosure Under Development
3825
JUNE, '80
D GRAVES
AS NOTED
BREAUX BRIDGE

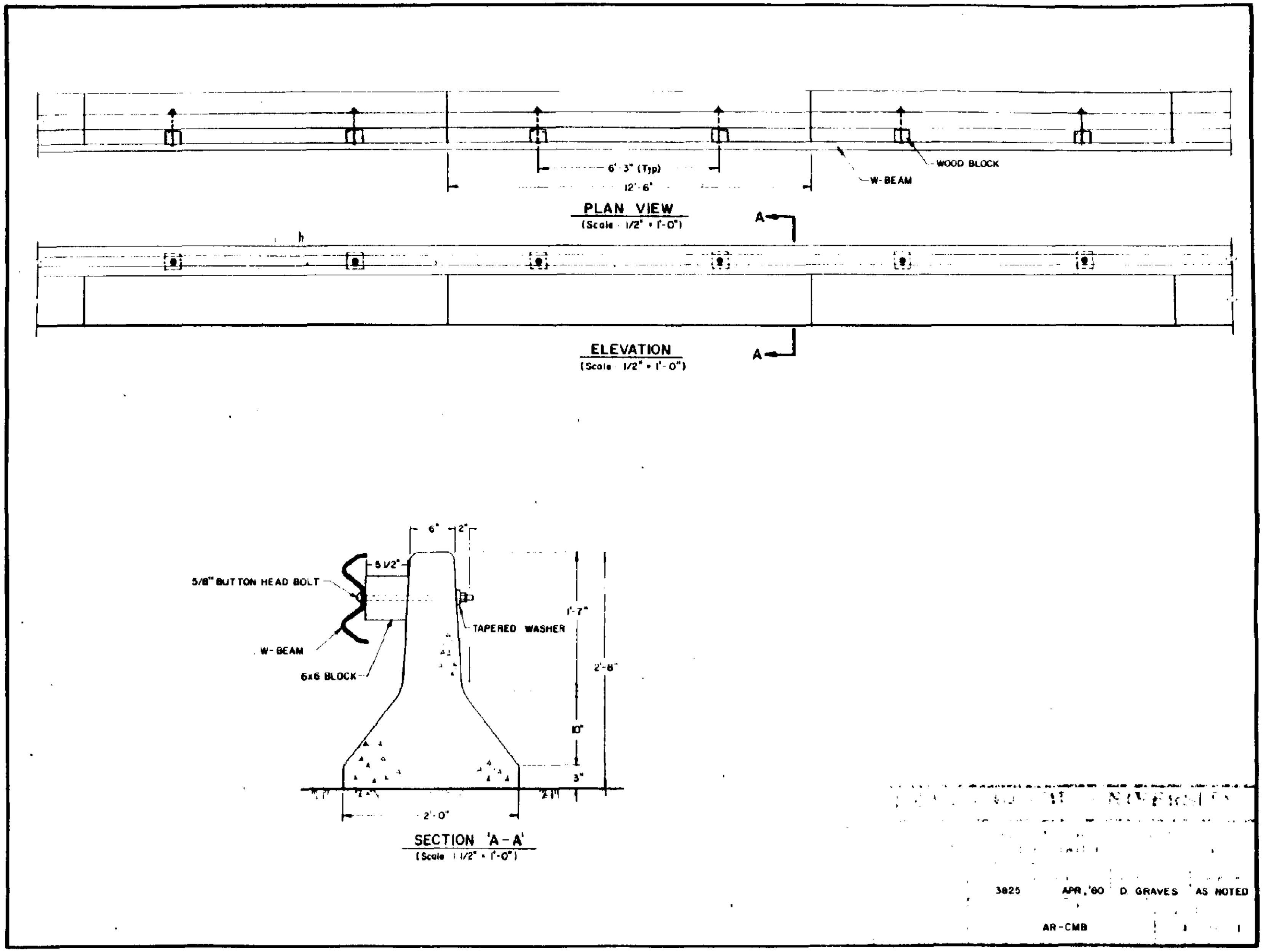
WOOD BLOCK
W-BEAM
6'-3" (Typ)
12'-6"
PLAN VIEW
(Scale: 1/2" = 1'-0")
A
ELEVATION
(Scale: 1/2" = 1'-0")
A
6"
2"
5 1/2"
5/8" BUTTON HEAD BOLT
TAPERED WASHER
W-BEAM
6x6 BLOCK
1'-7"
2'-8"
10"
3"
2'-0"
SECTION 'A-A'
(Scale: 1 1/2" = 1'-0")
3825
APR. '80
D. GRAVES
AS NOTED
AR-CMB

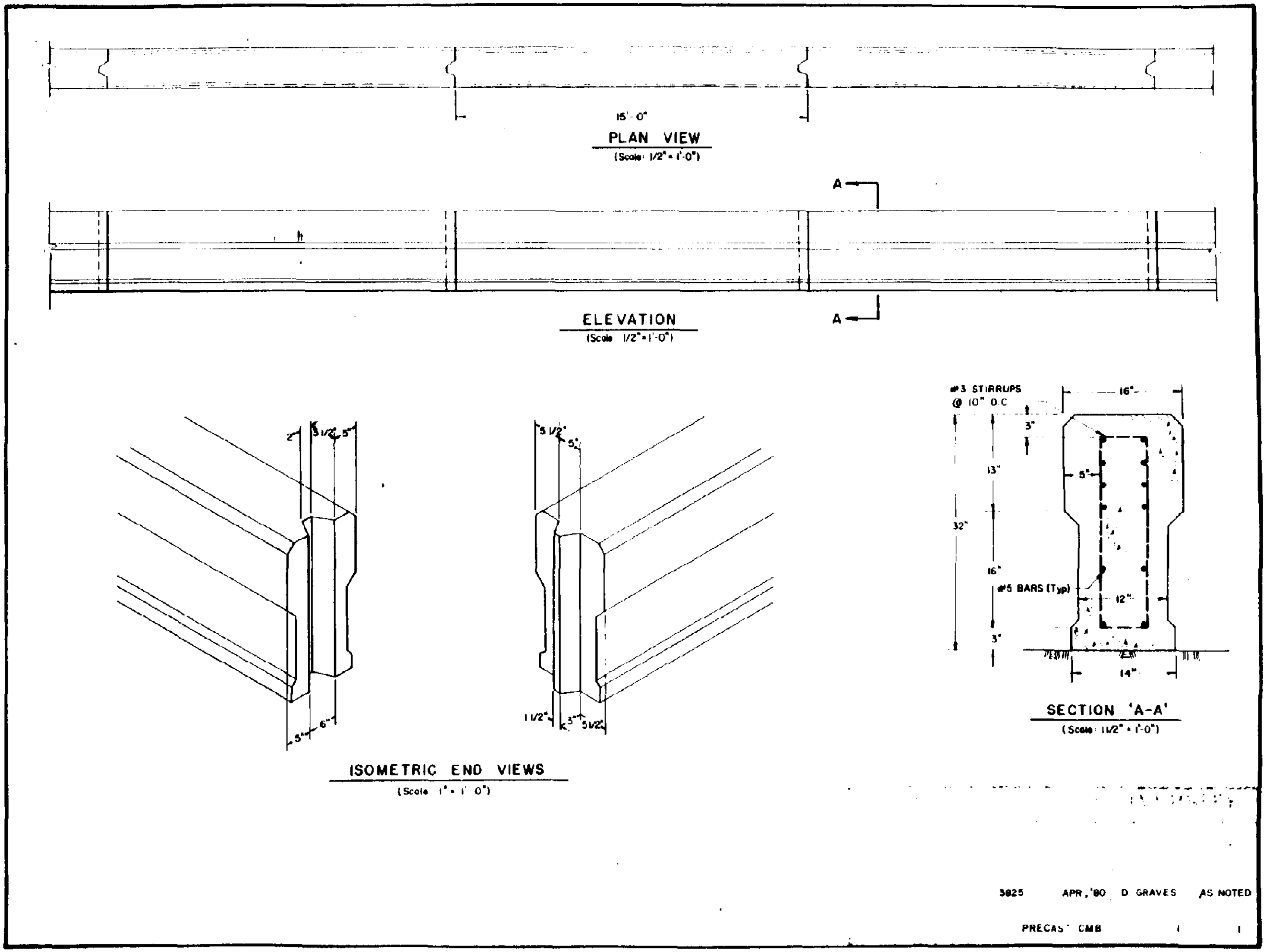

15'-0"
PLAN VIEW
(Scale: 1/2" = 1'-0")
A
A
ELEVATION
(Scale 1/2" = 1'-0")
#3 STIRRUPS
@ 10" O.C.
16"
3"
13"
5"
32"
16"
#5 BARS (Typ)
12"
3"
14"
SECTION 'A-A'
(Scale: 1 1/2" = 1'-0")
2"
3 1/2"
5"
5 1/2"
5"
5"
6"
1 1/2"
3"
5 1/2"
ISOMETRIC END VIEWS
(Scale 1" = 1'-0")
3825
APR. '80
D. GRAVES
AS NOTED
PRECAST CMB

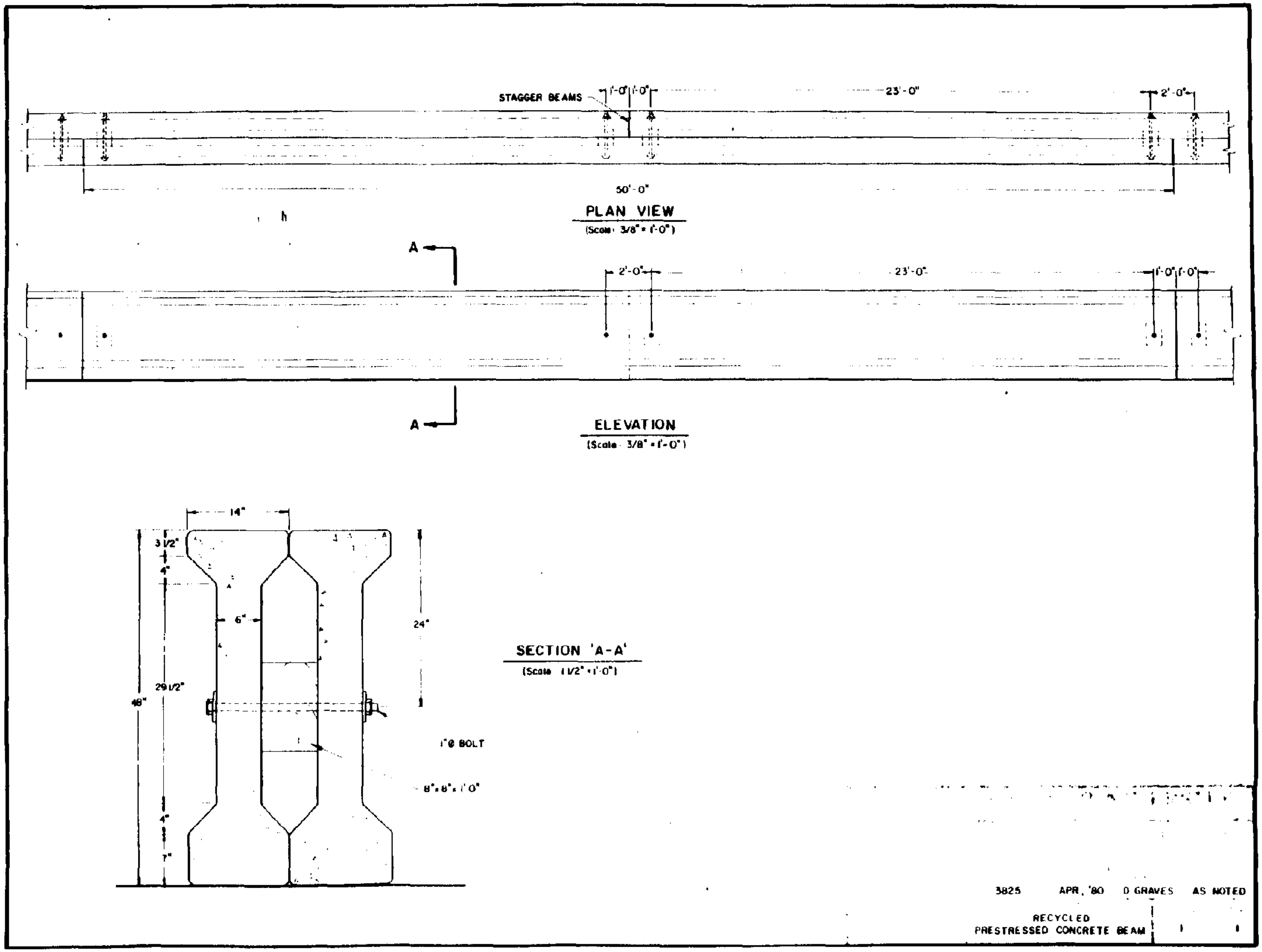
STAGGER BEAMS
1'-0"
1'-0"
23'-0"
2'-0"
50'-0"
PLAN VIEW
(Scale 3/8" = 1'-0")
A
2'-0"
23'-0"
1'-0"
1'-0"
A
ELEVATION
(Scale 3/8" = 1'-0")
14"
3 1/2"
4"
6"
29 1/2"
48"
4"
7"
24"
SECTION 'A-A'
(Scale 1 1/2" = 1'-0")
1"Ø BOLT
8" x 8" x 1'-0"
3825
APR. '80
D GRAVES
AS NOTED
RECYCLED
PRESTRESSED CONCRETE BEAM

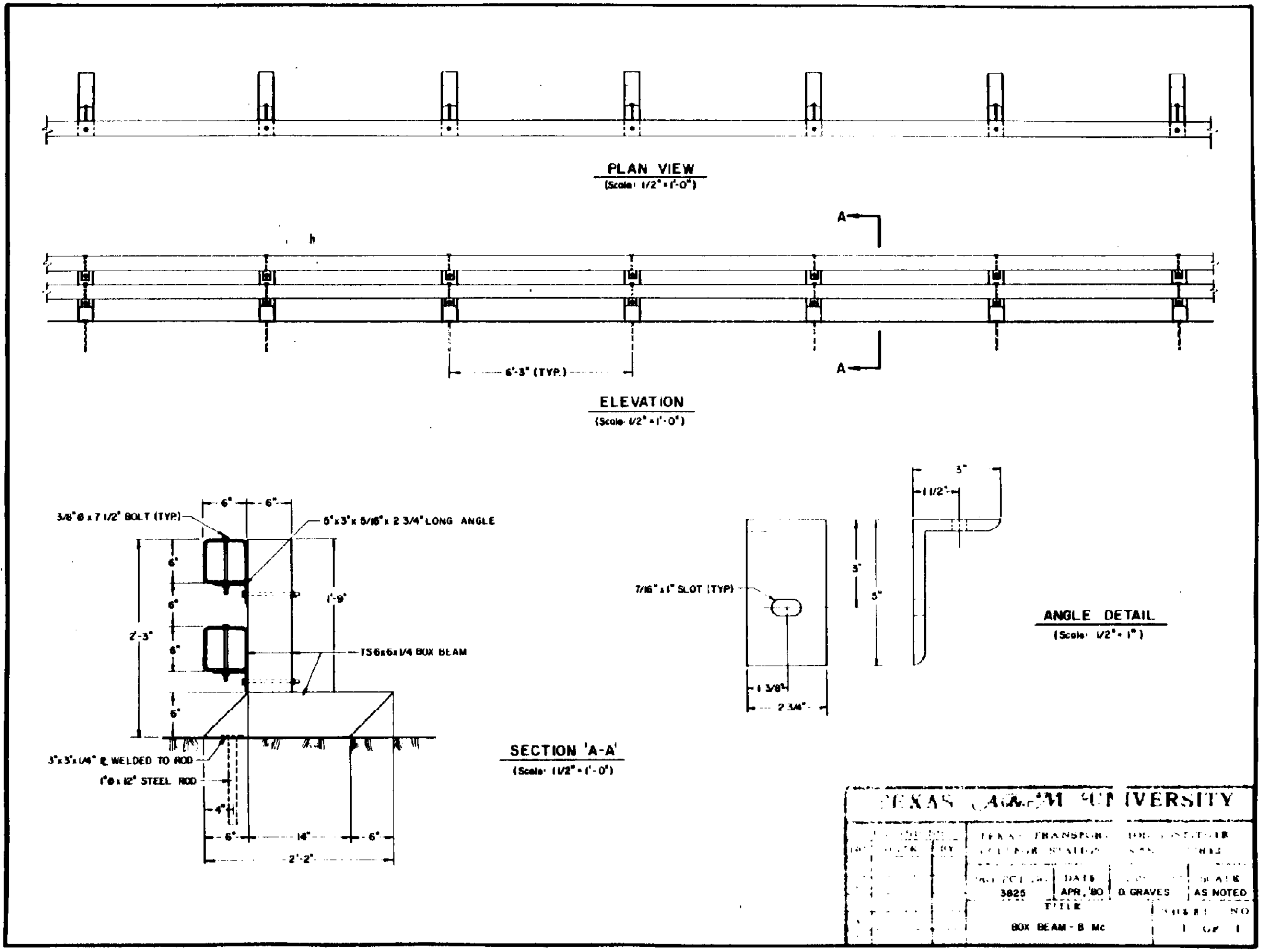

PLAN VIEW
(Scale: 1/2" = 1'-0")
A
A
6'-3" (TYP.)
ELEVATION
(Scale: 1/2" = 1'-0")
3/8" Ø x 7 1/2" BOLT (TYP)
6"
6"
5"x3"x 5/16"x 2 3/4" LONG ANGLE
6"
6"
6"
6"
2'-3"
1'-9"
TS6x6x1/4 BOX BEAM
3"x3"x1/4" ℞ WELDED TO ROD
1"Ø x 12" STEEL ROD
4"
6"
14"
6"
2'-2"
SECTION 'A-A'
(Scale: 1 1/2" = 1'-0")
7/16" x 1" SLOT (TYP)
3"
5"
1 3/8"
2 3/4"
3"
1 1/2"
ANGLE DETAIL
(Scale: 1/2" = 1")
TEXAS A&M UNIVERSITY
TEXAS TRANSPORTATION INSTITUTE
COLLEGE STATION, TEXAS
3825
DATE
APR. '80
D. GRAVES
SCALE
AS NOTED
TITLE
BOX BEAM - B Mc
SHEET NO
1 OF 1

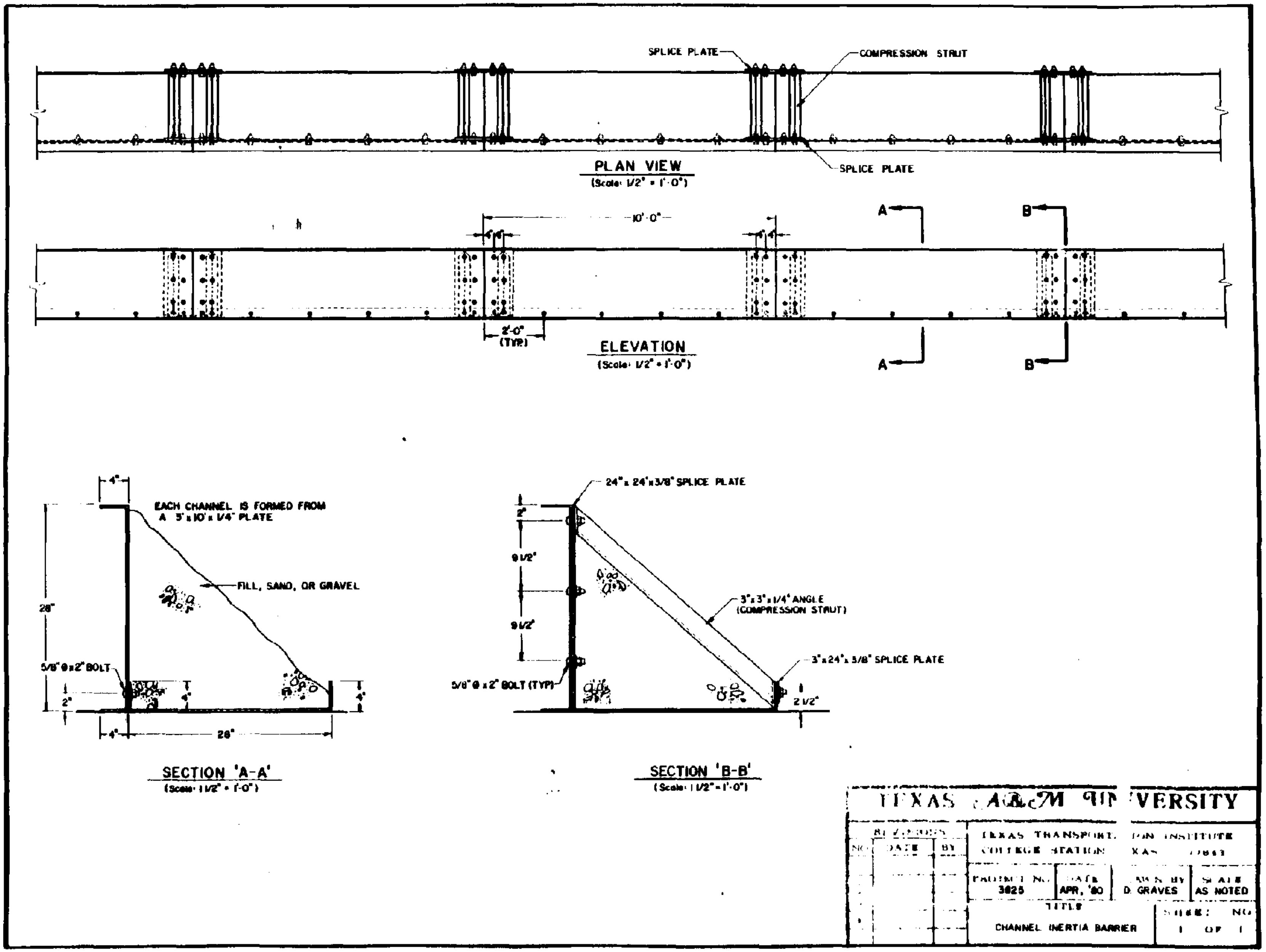
SPLICE PLATE
COMPRESSION STRUT
SPLICE PLATE
PLAN VIEW
(Scale: 1/2" = 1'-0")
10'-0"
4"
2'-0" (TYP)
ELEVATION
(Scale: 1/2" = 1'-0")
A
B
EACH CHANNEL IS FORMED FROM A 3'x10'x1/4" PLATE
FILL, SAND, OR GRAVEL
28"
5/8"Ø x 2" BOLT
2"
4"
28"
SECTION 'A-A'
(Scale: 1 1/2" = 1'-0")
24" x 24" x 3/8" SPLICE PLATE
9 1/2"
3"x3"x1/4" ANGLE (COMPRESSION STRUT)
3"x24"x3/8" SPLICE PLATE
5/8"Ø x 2" BOLT (TYP)
2 1/2"
SECTION 'B-B'
(Scale: 1 1/2" = 1'-0")
TEXAS A&M UNIVERSITY
REVISIONS
NO. DATE BY
TEXAS TRANSPORTATION INSTITUTE
COLLEGE STATION TEXAS
PROJECT No. 3825
DATE APR. '80
DWN. BY D. GRAVES
SCALE AS NOTED
TITLE CHANNEL INERTIA BARRIER
SHEET NO. 1 OF 1

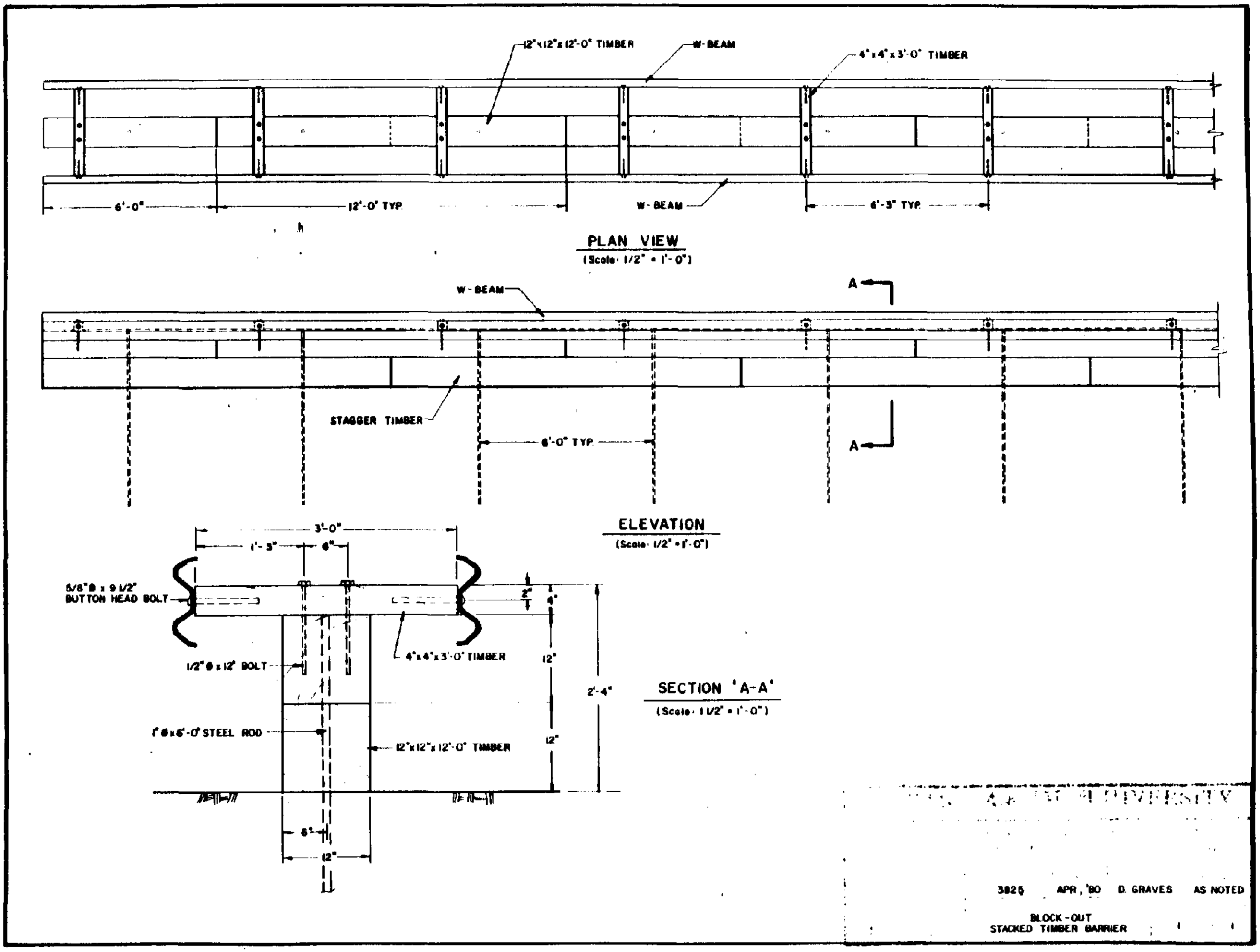
12"x12"x12'-0" TIMBER
W-BEAM
4"x4"x3'-0" TIMBER
6'-0"
12'-0" TYP.
W-BEAM
6'-3" TYP.
PLAN VIEW
(Scale: 1/2" = 1'-0")
W-BEAM
A
STAGGER TIMBER
6'-0" TYP.
A
ELEVATION
(Scale: 1/2" = 1'-0")
3'-0"
1'-3"
6"
5/8"Ø x 9 1/2" BUTTON HEAD BOLT
2"
4"
4"x4"x3'-0" TIMBER
1/2"Ø x 12" BOLT
12"
2'-4"
1"Ø x 6'-0" STEEL ROD
12"x12"x12'-0" TIMBER
12"
6"
12"
SECTION 'A-A'
(Scale: 1 1/2" = 1'-0")
3825
APR, '80
D. GRAVES
AS NOTED
BLOCK-OUT
STACKED TIMBER BARRIER

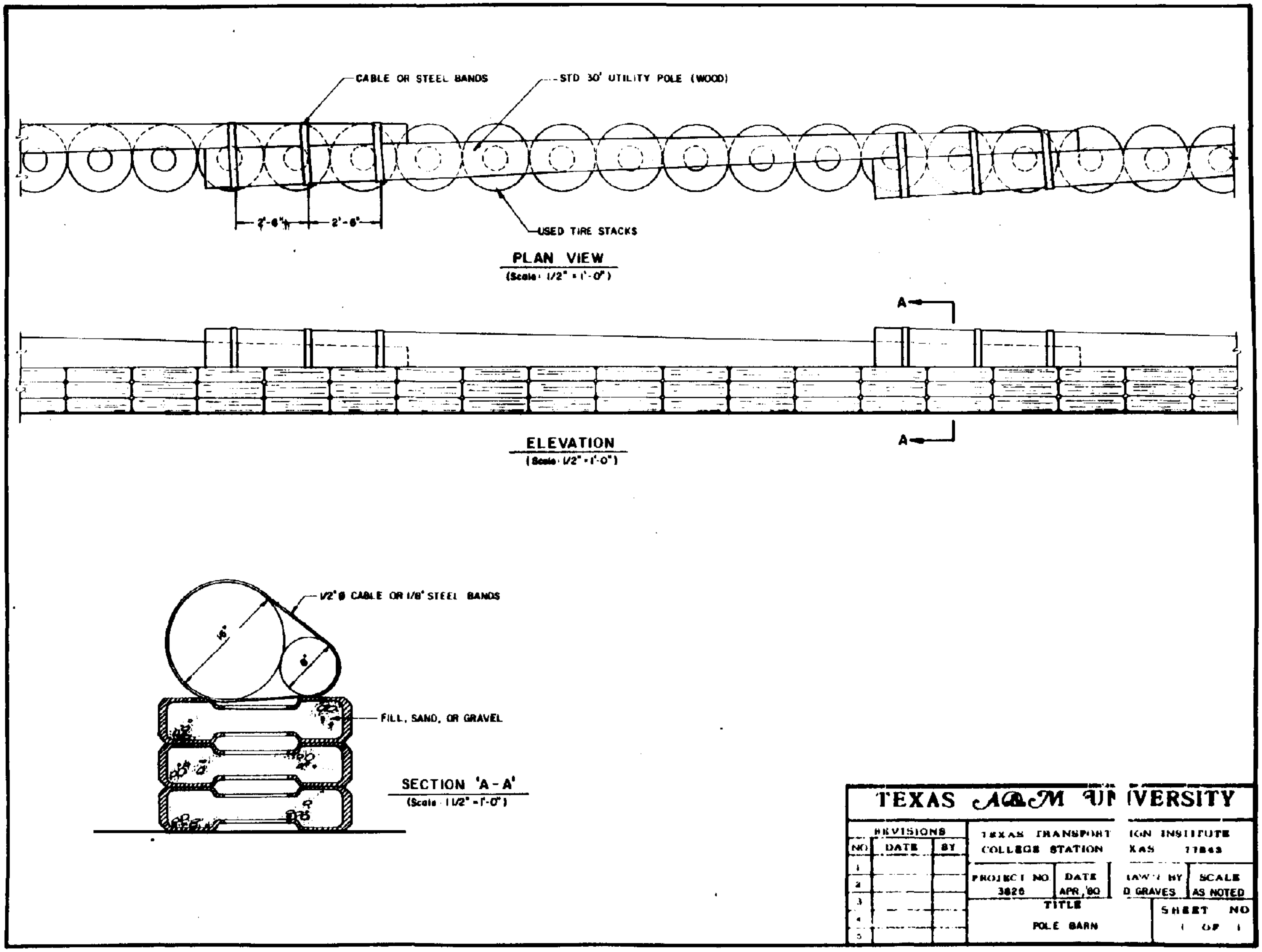

CABLE OR STEEL BANDS
STD 30' UTILITY POLE (WOOD)
2'-6"
2'-6"
USED TIRE STACKS
PLAN VIEW
(Scale: 1/2" = 1'-0")
A
A
ELEVATION
(Scale: 1/2" = 1'-0")
1/2" Ø CABLE OR 1/8" STEEL BANDS
FILL, SAND, OR GRAVEL
SECTION 'A-A'
(Scale: 1 1/2" = 1'-0")
TEXAS A&M UNIVERSITY
REVISIONS
NO
DATE
BY
1
2
3
4
5
TEXAS TRANSPORTATION INSTITUTE
COLLEGE STATION, TEXAS 77843
PROJECT NO.
3826
DATE
APR. '80
DRAWN BY
D. GRAVES
SCALE
AS NOTED
TITLE
POLE BARN
SHEET NO
1 OF 1

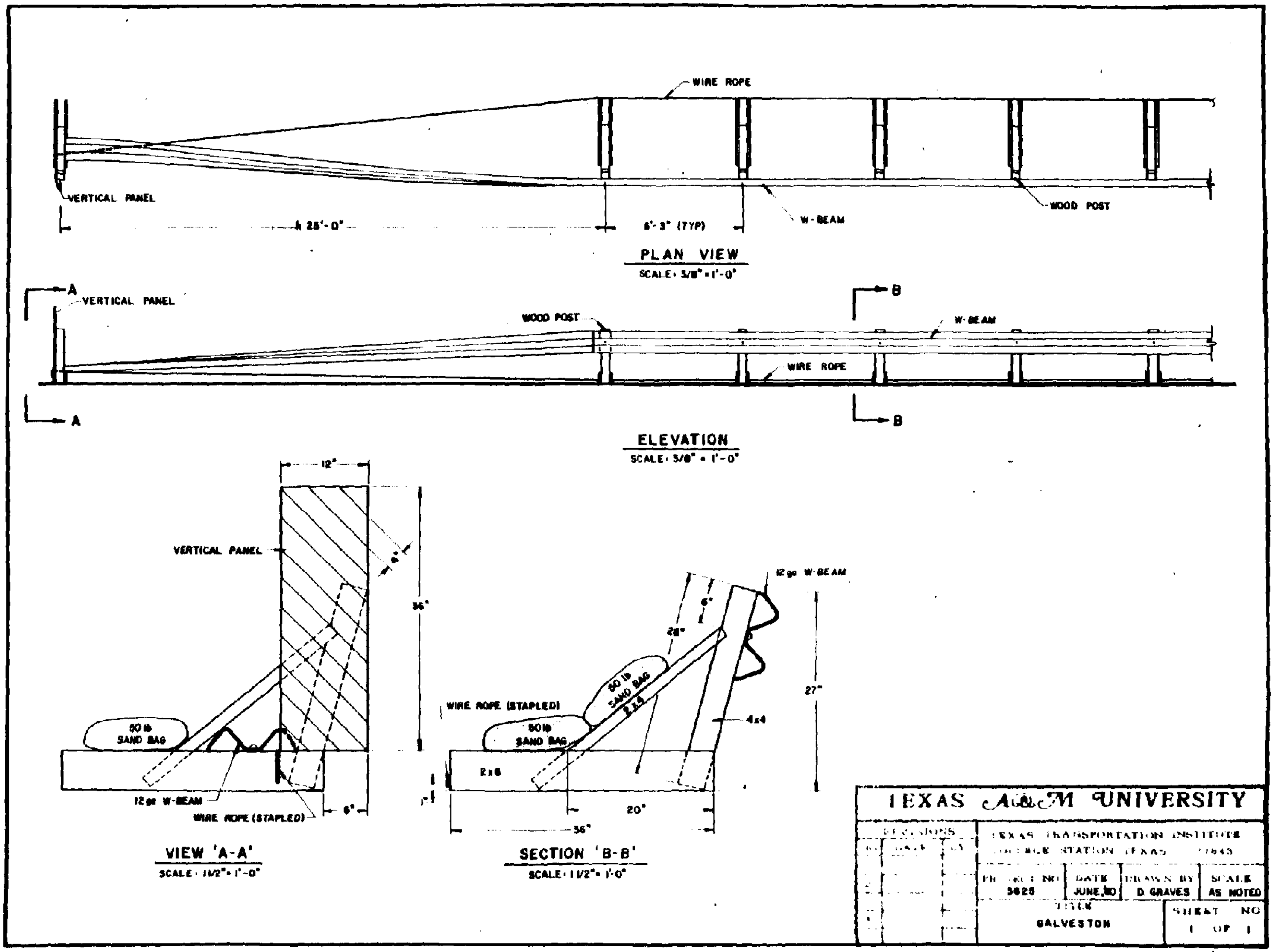
WIRE ROPE
VERTICAL PANEL
25'-0"
6'-3" (TYP)
W-BEAM
WOOD POST
PLAN VIEW
SCALE: 3/8" = 1'-0"
A
B
VERTICAL PANEL
WOOD POST
W-BEAM
WIRE ROPE
ELEVATION
SCALE: 3/8" = 1'-0"
12"
VERTICAL PANEL
36"
6"
50 lb SAND BAG
12 ga W-BEAM
WIRE ROPE (STAPLED)
VIEW 'A-A'
SCALE: 1 1/2" = 1'-0"
12 ga W-BEAM
6"
28"
50 lb SAND BAG
2x4
27"
WIRE ROPE (STAPLED)
50 lb SAND BAG
2x6
4x4
20"
SECTION 'B-B'
SCALE: 1 1/2" = 1'-0"
TEXAS A&M UNIVERSITY
REVISIONS
TEXAS TRANSPORTATION INSTITUTE
COLLEGE STATION, TEXAS
PROJECT NO
DATE
JUNE, 80
DRAWN BY
D. GRAVES
SCALE
AS NOTED
TITLE
GALVESTON
SHEET NO
1 OF 1

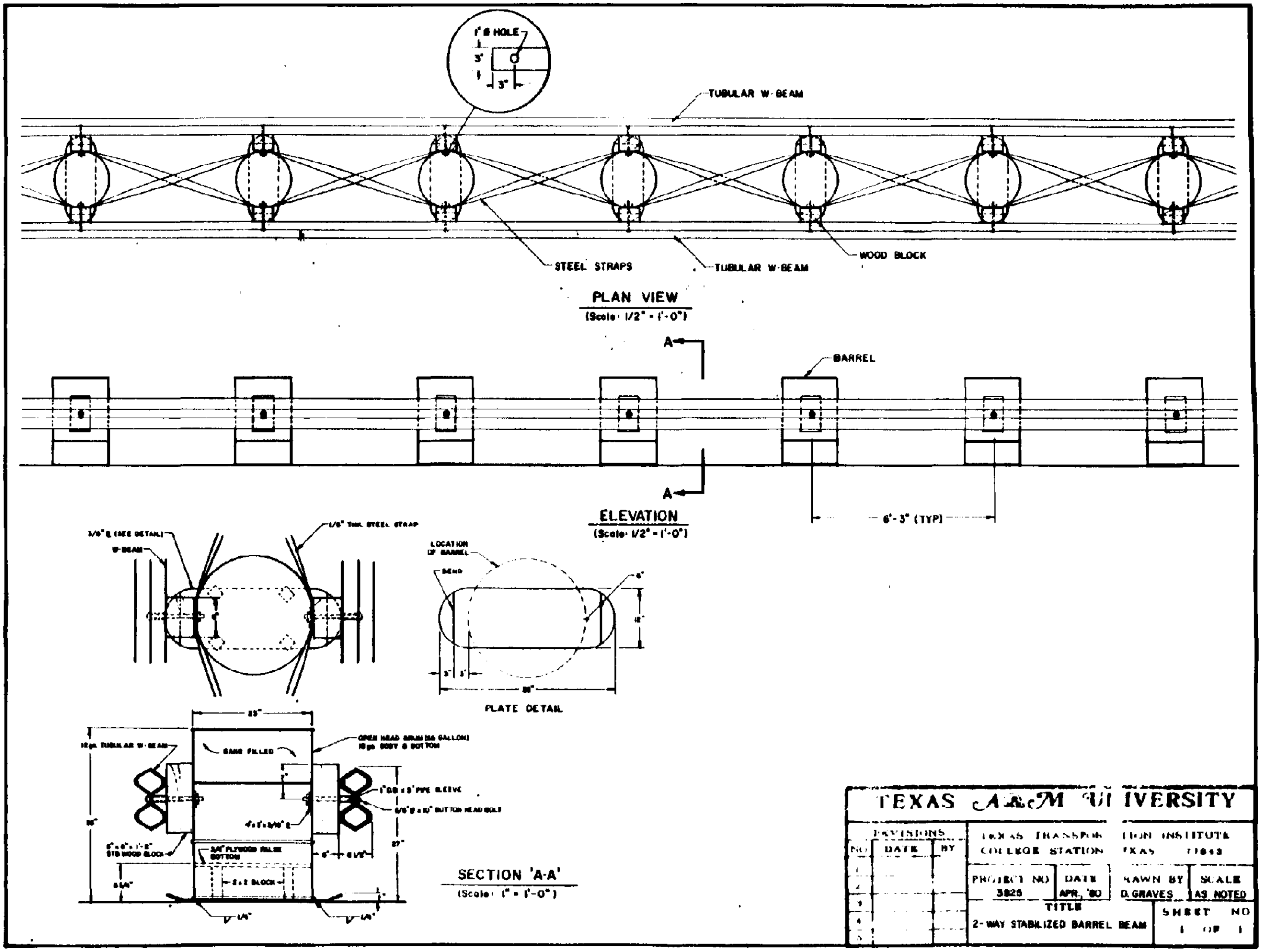
1" Ø HOLE
3"
3"
TUBULAR W-BEAM
STEEL STRAPS
TUBULAR W-BEAM
WOOD BLOCK
PLAN VIEW
(Scale: 1/2" = 1'-0")
A
BARREL
A
ELEVATION
(Scale: 1/2" = 1'-0")
6'-3" (TYP)
1/8" THK. STEEL STRAP
W-BEAM
LOCATION OF BARREL
PLATE DETAIL
SAND FILLED
SECTION 'A-A'
(Scale: 1" = 1'-0")
TEXAS A&M UNIVERSITY
REVISIONS
NO.
DATE
BY
TEXAS TRANSPORTATION INSTITUTE
COLLEGE STATION TEXAS 77843
PROJECT NO.
3825
DATE
APR. '80
DRAWN BY
D. GRAVES
SCALE
AS NOTED
TITLE
2-WAY STABILIZED BARREL BEAM
SHEET NO.
1 OF 1

REFERENCES

1. McCormick, J. M., and Salvadori, M. G., Numerical Methods in FORTRAN, Prentice Hall, Inc., Englewood Cliffs, New Jersey, 1965, pp. 100-102.

2. Hirsch, T. J., and Marquis, E. L., "Crash Test and Evaluation of a Precast Concrete Median Barrier," Report No. TTI-2-10-75-223-1, Texas Transportation Institute, Texas A&M University, College Station, Texas, October, 1975.

3. Ivey, D. L., and Marquis, E. L., "Portable Barriers for Construction and Maintenance Zones - Analysis and Redesign of Current Systems," Interim Report for Contract DOT-FH-11-9458, Texas Transportation Institute, Texas A&M Research Foundation, Texas A&M University, College Station, Texas, April, 1979.

4. Parks, D. M., Stoughton, R. L., Parker, J. R., and Nordlin, E. F., "Vehicular Crash Tests of Unanchored Safety-Shaped Precast Concrete Median Barriers with Pinned End Connections," Final Report CA-DOTOTL-6624-1-76-52, August 1976.

5. Stoughton, R. L., Parks, D. M., Stocker, J. R., and Nordlin, E. F., "Vehicluar Impact Tests of Precast Concrete Median Barriers with Corrugated Ends and Tensioned Cables," Report No. FHWA-CA-TL-78-13, Office of Transportation Laboratory, California Department of Transportation, Sacramento, California, June, 1978.

6. "Recommended Procedures for Vehicle Crash Testing of Highway Appurtenances," Transportation Research Circular No. 191, February, 1978.

7. Bronstad, M. E., and Kimball, C. E., "Crash Test Evaluation of a Precast Interlocked Median Barrier," Project No. 03-3777-002, Southwest Research Institute, San Antonio, Texas, August, 1974.

8. 1982 Dodge Manual for Building Construction Pricing and Scheduling, 8.McGraw-Hill, Princeton, N.J., 1981.

9. Engelsman, C., Heavy Construction Cost File, N.Y. Van Vostrand Reinhold Co., 1981.

10. Neibel, B.W., Motion and Time Study, Richard D. Irwin, Homewood, Ill., 1976.

11. Carmichael, C. (ed.), Kent's Mechanical Engineer's Handbook (Design and Production Volume) 12th Edition, John Wiley and Sons, New York, 1950.

12. FHWA Contract DOT-FH-11-9688, "Use and Delineation of Traffic Barriers in Work Zones."

13. "Guide for Selecting, Locating, and Designing Traffic Barriers," American Association of State Highway and Transportation Officials, 1977.